PHYSICO - CHEMICAL STUDIES ON SELECTED ASPECTS OF THE POLYMERIZATION OF WATER SOLUBLE VINYL MONOMERS ON PHYLLOSILICATES

THESIS SUBMITTED FOR THE DEGREE OF DOCTOR OF PHILOSOPHY (SCIENCE) OF THE UNIVERSITY OF NORTH BENGAL

1999

by

Palas Bera M.Sc.

DEPARTMENT OF CHEMISTRY
University of North Bengal
Raja Rammohanpur
Darjeeling - 734 430
West Bengal, India

STOCK TAKING - 2011

Dedicated to my parents

Contents

Acknowledgements

I take this opportunity to express my profound sense of gratitude to my supervisor, Dr S. K. Saha, Reader and Head of the Department of Chemistry, University of North Bengal for his wise guidance, continued interest and incessant encouragement throughout my investigation.

I would like to extend my thanks to the Council of Scientific and Industrial Research, for providing financial support and appreciate the authority of the University of North Bengal for extending the required laboratory and other facilities.

I also acknowledge the help extended to me by the Director, Regional Sophisticated Instrumentation Centre, Chandigarh and the Director, Central Glass and Ceramics Research Institute, Calcutta by providing elemental analysis facilities and recording of XRD data of polymers and copolymer samples.

Thanks are also due to all teachers, officers, research fellows and other staff members of the Department of Chemistry, University of North Bengal for their generous help.

I am specially thankful to Dr S. Ahmed and Mr R. Adhikary, of our laboratory and to Mr S. K. Giri, Senior Research Fellow of the Department of Physics, University of North Bengal for their good gesture and helpful co-operation.

My best regards are reserved for my parents, elder brother and other family members for their constant inspiration and patience. Without their love, understanding and emotional the work would not have been completed.

Palas Bera.

Date: University of North Bengal (Palas Bera)

CHAPTER - 1

INTRODUCTION

1. INTRODUCTION

A recent report put a value of nearly six billion dollars for the total world wide market in water soluble synthetic polymers (WSSP) reflecting their wide use in numerious products and processes. The wide field of application of these WSSP includes areas from adhesives to cosmetics, from explosives to medical products and from oil technology to paper technology[1]. Industrially, clay minerals are used as fillers and reinforcers in polymer systems such as elastromers, polyethylene, polyvinyl chloride and other thermoplastics and as coating agents for various types of paper.[2,3] All things being equal the efficiency of a filler in improving the physico-chemical properties of a polymer system is primarily determined by the degree of its dispersion in the polymer matrix.

The most effective way of achieving such compability is to graft a suitable polymer onto the filler surface and/or to encapsulate the mineral particles with the polymer layer.[2] Indeed, clay minerals specially those of phyllosilicates themselves are known to catalyze a variety of organic reactions including those which lead to polymer formation. The enormous success that has been achieved in the field of catalysis by molecular sieve zeolites has stimulated chemists to develop sophisticated ways of using clay as catalysts, for example, pillard clay catalysts.[4] Research on the intercalation chemistry of phyllosilicates is gaining momentum rapidly to transform these abundant minerals into new classes of selective heterogeneous catalysts. For example, the assymmetric synthesis of certain α-amino acrylates can be achieved with chiral rhodium complexes immobilized in smectite interlayers without sacrificing the high optical yields typified by the same complexes under homogeneous conditions.[4] The formation of stereoregular poly (acrylonitrile) and poly (acrylic acid) in the interlayer space of montmorillonite had been claimed[2].

1.1 POLYMERS OF ACRYLAMIDE

Acrylamide is a versatile, highly reactive monomer which readily undergoes vinyl polymerization to yield a broad spectrum of homopolymers and copolymers of controlled molecular weight and performance characteristics.[5] It is assuming increasing industrial importance as a chemical intermediate and as a monomer. Acrylamide is highly water soluble and tends to impart this same property to polymers and copolymers. Polyacrylamide is a very effective flocculant, a thickening agent and a pigment retension aid in paper making. It has found wide application in the treatment of ores, mineral and metal particles, sewage, industrial wastes etc. Polyacrylamide is usually fed as very dilute solutions which cause rapid agglomeration and sedimentation.

Extremely high molecular weight polyacrylamides have been found to be exceptionally effective flucculants.[6] Mixtures of acrylamide with small proportions of N, N^{l}-methylenebisacrylamide have been finding increasing application as chemical grouts. They are available commercially under the trademark "AM-9" (ref.7). Aqueous solutions of the monomer together with a redox catalyst are injected into soil formation. Copolymers of acrylamide and acrylic acid are being used as stock additives for improving the dry strength of paper.[8] These are particularly useful in the manufacture of printing papers. High molecular weight acrylamide copolymers have also shown considerable promises for increasing the retention of mineral fillers in paper making. Improvement in drawing rate and wet strength have also been obtained.

Copolymers of acrylamide and acrylic acid have been found to control the loss of fluid from oil well cements in hydraulic cementing operations.[9] Polyacrylamide with high molecular weight has been claimed to be useful as a thickening agent for water used in a secondary oil recovery method called water flooding. The thickened water is used to drive oil through the formation to a producing well[10]. Interpolymers of acrylamide and other monomers are useful for commercially important surface coatings[11-14].

On the other hand, a recent communication also describes a new series of antitumor agents which are derivatives of acrylamide, among which N-[(3-bromopropionamide) methyl] acrylamide was particularly effective[15].

1.2 MONTMORILLONITE

Montmorillonite possesses a layered structure and has strong sorptive properties due to expandability of the mineral layer. It is a 2:1 type or trimorphic layered phyllosilicate in which the central octahedral aluminium is surrounded by two tetrahedral silica sheets. The structure of montmorillonite was first given by Hoffmann, Endell and Wilm on the basis of its similarity with that of pyrophyllite[16]. This basic structure into which modifications by Marshall,[17] Maegdefrau and Hoffmann[18] and Hendricks[19] were subsequently incorporated, is now generally accepted[20,21]. The montmorillonite layer differs from that of pyrophyllite in that the substitution of Al (III) for other cations (e.g., Mg(II), Fe(II)) in octahedral positions, and less frequently of Si(IV) and Al(III) in the tetrahedral sheet always occurs. Although some internal compensating substitution may occur, the final result of the isomorphous replacement in the pyrophyllite structure is a layer which carries a permanent negative charge. The positive charge deficiency is balanced by sorption of exchangeable cation which, apart from those associated with external crystal surfaces are positioned between the randomly superposed layers within a crystals[18]. Water is also readily absorbed in the interlayer space. These concepts are illustrated in Figure 1. Water appears to enter the interlayer region as an integral number of complete layers of molecules, this number depends on the nature of the exchangeable cation.[21-23]

The d(001) spacing of montmorillonite can vary over a wide range, the minimum corresponding to the fully colapsed state being 0.96 nm with large monovalent and divalent cations occupying interlayer exchangeable sites. Interlayer (or intercrystalline) swelling is limited to a d(001) spacing of about 1.9 nm. On the other hand, montmorillonite samples saturated with small

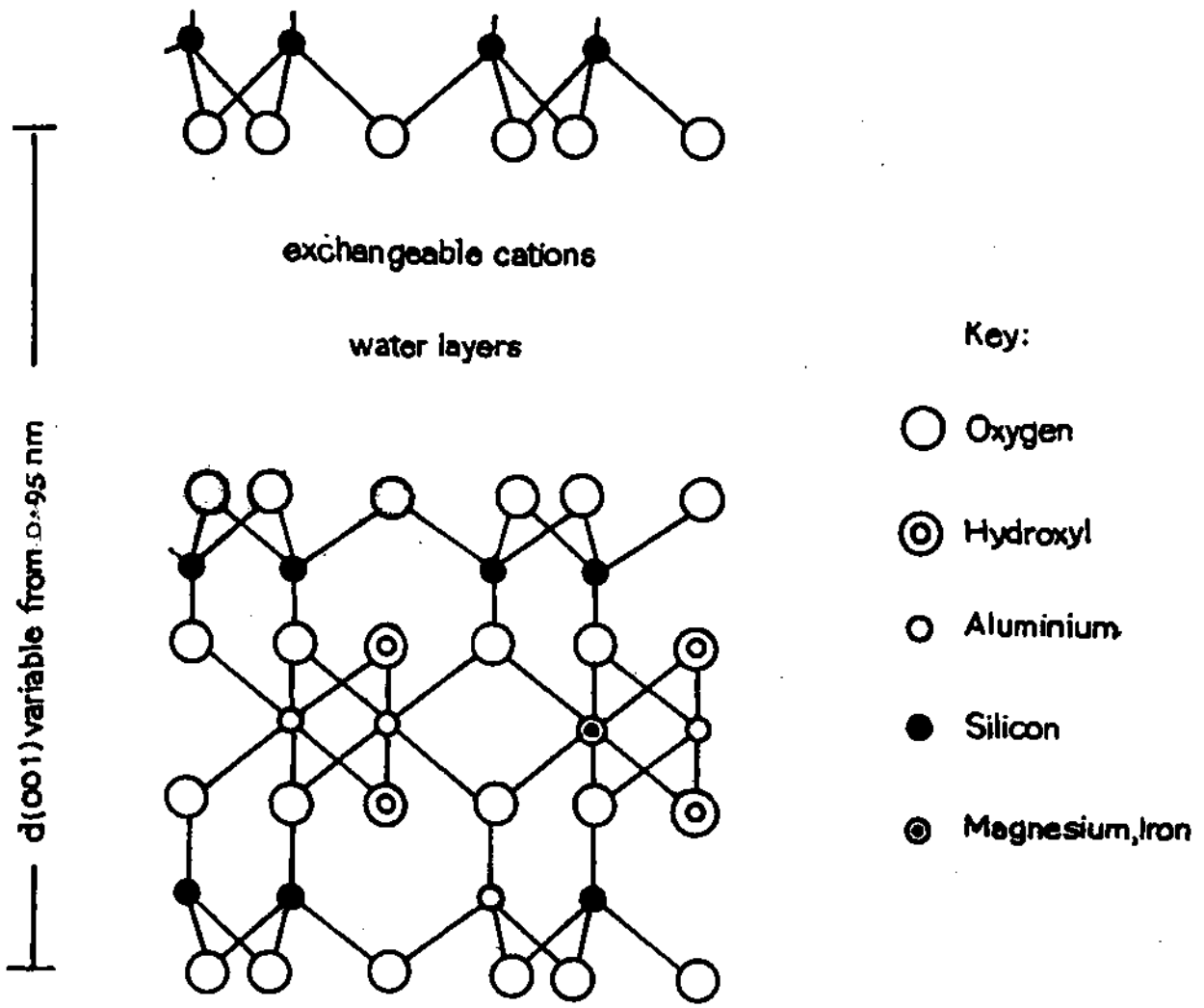

Fig. 1 The structure of a montmorillonite layer viewed along the a axis. The basal spacing is giving in nanometer units.

monovalent cations (Li^+, Na^+) may show extensive interlayer expansion in dilute aqueous solutions (0.3N) of their respective cation salt and in water, and under optimum conditioins the layers can dissociate completely.[23] The charge density of the clay surface as well as the nature of the exchangeable cation has a profound influence on the hydration properties of this 2:1 type phyllosilicates and obviously the hydration properties are affected more by the interlayer cation than by the silicate surface. Since uncharged polar organic molecules are absorbed essentially by replacement of the interlayer water, the behaviour of such molecules is likewise strongly influenced by the exchangeable cation. Evidence has accumulated to show that, at least at low water contents, cation-dipole interactions are of paramount importance in their effect on the absorption of polar molecules by clay minerals. Montmorillonite acquires its charge by the replacement of octahedral Al by Mg atoms. The structural formula is written as :

$$[Si_8]^{IV}\,[Al_{4-x}Mg_x]^{VI}\,O_{20}\,[OH_4]$$
$$\downarrow$$
$$M_x$$

(1)

This formula gives the composition of the planner unit cell. The number IV and VI indicate tetrahedral and octahedral positions respectively. The symbol M_x indicates the presence of compensator cations totalling x valencies per cell. The charge x is generally between 0.5 and 0.9 . Formula (1) is idealized. Fe(III) replaces a part of the Al's, Fe(II) replaces a part of the Mg's. Extensive chemical studies especially on the changes in composition of smectites by base exchange and the swelling effects in their geometrical significance, were made by M.D.Foster[24]. Swelling decreases with increasing octahedral replacement. In this respect the introduction of Fe(II) into the octahedral layers has greater depressing effect than that of Fe(III) which in turn appeared to have the same depressing effect as Mg(II).

An alternative and completely different structure (Figure 2) for

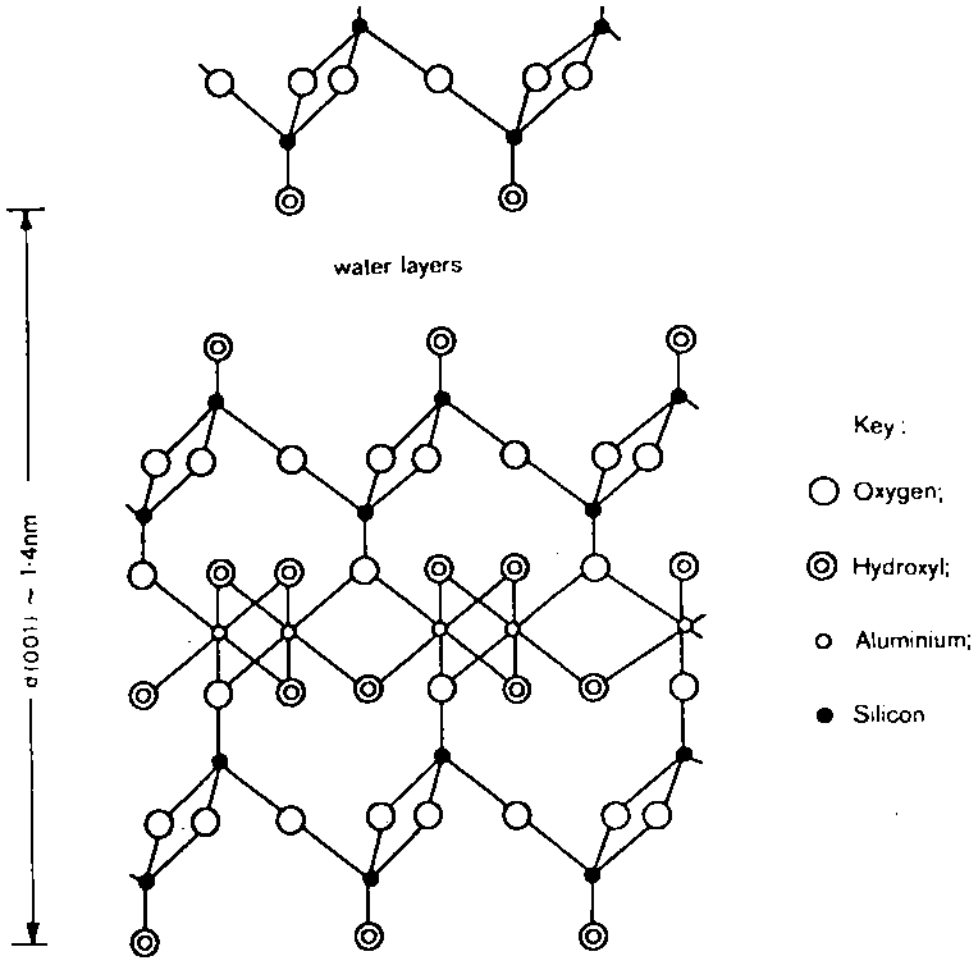

Fig. 2 The montmorillonite layer structure viewed along the axis according to Edelman and Favejee.

montmorillonite has been suggested by Edelmen and Favejee.[25] The main aspect of this structure is that every alternative SiO_4 tetrahedron in the tetrahedral sheet is inverted. The apical oxygens of such inverted tetrahedra, now pointed away from the surface, are replaced by hydroxyl groups which also fills the gaps left in the octahedral sheet. No isomorphous replacement within the structure is envisaged and the observed cation exchange capacity being solely ascribed to the dissociation of apical hydroxyl groups. Somewhat similar structure in which excess hydroxyl groups are present due to the replacement of some Si(IV) ions by $4H^+$ or $Al(III)H^+$ ions in the tetrahedral sheet has been suggested by McConnell.[26] On the other hand, Grim and Kulbicki postulated the existence of two types of montmorillonite, one confirming to the Hofmann-Endell-Wilm-Marshall-Maegdefrau-Hendricks structure and the other to the Edelman-Favajee structure.[27]

Because of the poorly crystalline nature of the clay mineral, X-ray diffraction patterns are generally broad and diffuse. Moreover, obtaining homogeneous and uncontaminated samples is not an easy task. These facts make it difficult to discriminate between the various possibilities using X-ray analysis alone. By a combination of X-ray, DTA, TGA and chemical analysis, it has been possible to distinguish between various types of montmorillonite samples.

1.3 CLAY-ORGANIC INTERACTION

Involvement of clay minerals in affecting organic reactions have now been well established by the contributions of Smith, Gieseking and co-workers[28-30], Hendricks[31], Jordon[32], Bradley[33], Mac.Dwan[34], and others. Excellent reviews of recent studies are available in books and journals (Grim[35], Eitel[36], Theng[2], Mc Ewan[34], Greenland and Hayes[37], Sposito[38], Bringley and Brown[39], Mortland[40] and others). Extensive studies on interaction of organic compounds with clay systems have also been the subject matter of research of different Indian scientists. In this context the noteworthy contribution of

Mukherjee[41,42], Chakravarty[43-48], Mukherjee and co-workers[49,50]. De and co-workers[51-54], deserve special mention.

On the basis of the above it has been abundantly clear that clays interact with many organic compounds to form complexes of varying stabilities and properties. Organic derivatives especially of montmorillonite have so far been obtained either by (a) ion-exchange reactions or (b) by direct introduction of the Si-C linkage.

The pronounced change in the physical properties of organo-clay complexes, particularly in relation to the development of organophilic characteristics, water proofness, exchange and other surface phenomena has been revealed by the work of Jordon[32], Gieseking[28-30], Mukherji[41], Chakravarty[47,48] and others. In the above studies some attempts have also been made to ascertain the nature of the bond in the clay organic complexes.

The absorption behaviour of quaternary ammonium compounds of varying chain length on surfaces of montmorillonite, soil colloids and clay mixtures has been critically studied by Chakravarty with the help of electrochemical, viscometric, electrophoretic and sedimentation volume techniques.[43-48]

The complicated process of interaction of larger ions with clays is accompanied by significant variation of exchangers, namely, charge reversal as shown by electrophoretic and sedimentation volume measurements.[43,49,51] In the formation of the clay organic complexes and for their stability the involvement of Van der Waals and hydrophobic bonds in addition to columbic bond has been reported by the authors.[44-47]

While most of these studies are on the interaction between clays and defined organic molecules of known structure, another interesting area of study that has gained importance in the recent past is "Clay polymer complexes".

Theng summarises the development in this area and the immense possibilities of studying interactions of clays with synthetic and naturally occuring polymers.[55] The contributions of Mortland, Boyd and Morland in this context are very significant.[56-59]

Hofmann and Brindley reported appreciable adsorption of non ionic aliphatic compounds having chain length C_5-C_{10} on Calcium montmorillonite[61]. But little or no adsorption of short chain organic compounds on montmorillonite from dilute solution (less than 0.5 M) occurred. However, German and Harding have reported that calcium and sodium montmorillonite adsorbed adequate amounts of primary n-alcohols viz, ethanol, propanol and butanol.[62] This deviation from chain length rule of Hofmann and Brindley has been supported by Bradley for adsorption of some aliphatic amines.[33] Larger molecules with more than five units – both aliphatic and aromatic may be adsorbed to an appreciable extent by montmorillonite in the presence of excess water.[61-64] That is, they can displace the water molecules associated with the exchangeable cations. The increase in affinity with molecular size or chain length can be generally applied to the adsorption of organic compounds of clays and is attributed to the increased contribution of Van der Waals forces to the adsorption energy.[60] As the size of the molecule increases, Van der Waals interactions become important because these forces are essentially additive and tend to orient the molecule so that the maximum number of contact points is established.[65,66]. The adsorption of one organic molecule is accompanied by the desorption of a number of water molecules initially co-ordinated to the cation, an appreciable amount of entropy is gained by the system, favouring adsorption.

Thus, entropy effects arising from multiple bond formation between the organic compound and the water molecules in the primary hydration shell contribute to the strong adsorption of some uncharged linear polymers by montmorillonite[67,68]. Besides chain length (molecular size), the chemical character of the organic molecule influences adsorption behaviour. For many

aliphatic compounds, a useful index of character is their "CH activity" arising from the activation of methylene groups by neighbouring electron withdrawing substituents like $\rangle C{=}O$ and $-C{\equiv}N$. At equilibrium concentration, the amount of $C_6 - C_7$ organic compounds of different functional group adsorbed on the clay mineral is in the order :

α-methoxy - acetyl acetone > acetoacetic ethyl ester > β-ethoxy propionitrile hexanedione - 2,5 > hexane diol - 1,6 > 2,4 - hexadiyne diol - 1, 6 (ref. 61).

Complex formation with polar organic compounds is profoundly affected by the nature of exchangeable cation and by the water content (hydration status) of the clay. Apparently, hydration of the clay facilitates acetone uptake presumably due to the expansion of mineral interlayers. In an attempt to prepare acetone complex, it was found that dehydrated calcium montmorillonite invariably yielded as double layer complex whereas the corresponding sodium clay gave either a single or a double layer complex.[69] This difference between calcium and sodium montmorillonite in their behaviour towards polar organic liquids accords with later findings of German, Harding, Bissada and co-workers for ethanol–montmorillonite and acetone–montmorillonite systems is ascribable to the greater solvation energy of the calcium ion compared to that of sodium ion.[62,70] The formation of double layer complexes of montmorillonite with some ethers and polyethers has been reported[33,69]. From X-ray data the basal spacings of 1.31 – 1.34 and 1.57 – 1.76 nm were suggested for both single and double layer complexes respectively.[61]

The complex formation between aliphatic or aromatic amines and 2:1 type clay minerals has received much attention. The basic information available are (i) the amines can exist in the cationic form like the corresponding alkyl ammonium ions which can replace the inorganic cation occupying exchange sites at the clay surface (ii) adsorption of some primary n-amines by hydrogen

montmorillonite is influenced by the pH of the system and by the size (chain length) of the organic molecule.

In acidic media, amides may accept a proton on either the oxygen or the nitrogen atom. However, the weight of evidence from both spectroscopic and solution studies lies on the side of the former alternative.[2] From infrared studies of acetamide, Tahoun and Morland have confirmed that amides predominantly protonate on the oxygen atom in acidic montmorillonite system.[71] In acidic montmorillonite system, hemisalt formation is observed when excess amide is present, i.e. two amide molecules share a proton through a symmetrical hydrogen bond.

Weismiller has examined the interlayer expansion of montmorillonite crystals in N-ethyl acetamide.[72] Irrespective of the kind of interlayer cation present, montmorillonite apparently expands to a basal spacing of about 2.05 nm which is interpreted in terms of the intercalation of three layers of N-ethyl acetamide molecules with the exchangeable cations occupying positions midway between two opposing silicate layers. In the initial stage of adsorption, the amide molecule co-ordinates to the interlayer cation through the oxygen atom, but as the amount present increase the "excess" amide may form hydrogen bond of the cation-linked species and/or to the oxygen ion of the silicate surface.

Weil-Malherbe and Weiss showed that both acid-base interaction and oxidation-reduction reactions were involved in the formation of coloured clay complexes with certain aromatic amines.[73] Briegleb showed that the association between clays and organic compounds may be termed 'electron donar-acceptor complexes.[74] Solomon and coworkers proposed a model based on charge transfer between the mineral and the absorbed organic species.[75] Toth and Szepvolgyi and co-workers studied the thermal decomposition of complexes produced from bentonite and a linear polyacrylamide (PAM) by using TG - mass spectroscopy[76]. Thermal behaviour of bentonite-PAM

complexes was mainly determined by PAM degradation and the decomposition of bentonite complexes above a temperature of 580°C proved to the formation of strong bonding between the constituents of the complexes.

Ogawa, Kuroda and co-workers suggested that acrylamide (AM) was intercalated in the interlayer spaces of montmorillonite through hydrogen bonds and co-ordination complexes in the Cu-montmorillonite-AM and Na-montmorillonite -AM intercalation compounds and that the molecular plane of AM was perpendicular to the silicate sheet[77]. Intercalated AM was polymerized to form montmorillonite - PAM intercalation compounds which adsorbed more water than raw montmorillonite .

The adsorption and polymerization of AM in the complex composite films which were prepared by adding acrylamide and water to Na-fluorterasilicic mica were investigated by Nagal and co-workers.[78] From X-ray diffraction it was observed that the interlayer spacing of the film was 9.6 Å for the Na-montmorillonite complex and 8.8 Å for the Na-fluortetrasilicic mica. From the DSC technique the quantity of uncrystaled AM was measured to be equal to that of AM intercalated into the interlayer space. AM in the films was polymerized upon irradiation. The extent of polymerization increased almost linearly with the irradiation time. The interlayer space of the polymered film did not change from that of the inirradiated film.

1.4 CLAY CATALYZED POLYMERIZATION

Synthetic and naturally occurring clay minerals due to their favourable structures, are used in a number of widely diversified roles in the chemical industry as catalyst for cracking or depolymerization[79], alkylation[80] isomerization[81], polymerization[82] etc. In 1960's and earlier clay initiated polymerizations of vinyl monomers emphasised on the use of dry clay minerals and non-polar solvents.[83-85] Butadiene, trans and cis-butene-2 was found to be

spontaneously polymerized on the external surface of neutral and acidic montmorillonite at room temperature and atmospheric pressure without additional catalysts.[83] The olefins were adsorbed on dry clay from systems like (i) solid-gas at reduced pressure and at various temperatures, (ii) solid-gas at room temperature and (iii) solid-liquid at –78° or 0°C for neat monomer or monomer dissolved in solvent.

Although the carbocationic polymerizations of vinyl monomers have been investigated extensively with Lewis acid such as $AlCl_3$, $TiCl_4$, BF_3, Et_2O, BCl_3 alkyl aluminiums etc.[86-92], the first report on such polymerization of styrene with acid clays[84] came in 1964. Almost 100% yield of polystyrene of molecular weights 500 to 2000 was achieved. The catalytic activity of the clay has been shown to be due to active protons associated with tetrahedral (due to dehydration of the mineral) aluminium.[93,94] The formation of carbonium ion following surface absorption of olefins on acid sites caused subsequent polymerization. Proton accepting contaminants such as water, amines etc., being preferentially absorbed over styrene suppressed the polymerization. Styrene polymerized on the surface of the homoionic clays.[95] It is thought that an electron transfer from adsorbed styrene to the aluminium produced radical cations which rapidly dimerized. Both radical cations and dimers are involved in the initiation step but the propagation being cationic. Using activated clay minerals, however, styrene did not polymerize in the presence of ethanol, dioxane, ethyl acetate and methyl methacrylate (MMA) within 30 minutes of the reaction. All these data lead to postulate that the active sites are the octahedral aluminium at the crystal edges. The aluminium acts as electron acceptors.

Matsumoto, Sakai and Arihara preferred the concept of Bronsted acidity rather than Lewis acidity to be responsible for the initiation of the polymerization of styrene by montmorillonite[96]. The inconsistency in their experiments, however, is in the reduction of polymer yield in the presence of trityl chloride which selectively absorbs on Lewis acid sites. They argued in favour of the Bronsted acidity on the ground that the replacement of exchangeable hydrogen

ions by sodium or ammonium ions almost completely inhibited the polymerization. On reacidifying the mineral, however, the activity to polymerize styrene was restored. Since the degree of polymerization increased with the dielectric constant of the medium and was almost independent of the initial concentration, cationic mechanism for the initiation process was favoured.[97]

This would apply equally well to the propagating process and therefore, the initiation by a radical ion mechanism cannot be ruled out.[95] The possibility of proton transfer to monomer leading to decreased average degree of polymerization, as in conventional cationic mechanism, has also been discussed.[93] The work of Matsumoto and coworkers along with Solomon and Rosser lead one to the conclusion that acidity of the clay can not be solely ascribed to either Bronsted acidity or Lewis acidity.[95-96] It is to be understood that dry mineral surface is very acidic due to the polarization of residual water molecules by the exchangeable cations. Such acidity is influenced by the solvent as evident from the blue colouration of aqueous benzidine in the presence of oxidized montmorillonite. Instead a yellow colour appeared when a benzene solution of benzidine was treated with dry clay mineral.[95,98] Solomon and Rosser failed to find evidence of styrene interacting with the clay mineral which lead them to assure that styrene is either incapable of moving into the interlayer space or capable of doing so with difficulty.

The polymerization of MMA on such clay minerals has not yet received much attention. The failure of MMA to polymerize can be accounted for in the light of well accepted mechanism of charge transfer from the monomer to the clay mineral to produce a radical cation which is a non-propagating species for the polymerization of MMA. However, Dekking could prepare MMA-montmorillonite complex using the conventional free radical initiator, 2-2^{l} azo-bis-isobutyramidine (AIBA).[105] The polymerization of MMA and methyl acrylate in montmorillonite interlayer induced by γ-radiation has been studied by Blumstein and co-workers.[99-102] The interlayer polymers were difficult to isolate by the usual solvent extraction and could only be isolated by treating the clay-

polymer complex with hydrofluoric acid which damaged most polymers. Glavati and co-workers found that polymerization of acrylonitrile / montmorillonite complex by γ-radiation produced stereospecific polymers.[103]

Thermal polymerization of number of vinyl monomers e.g. MMA, acrylamide, vinyl acetate, 4-vinyl pyridine could be induced by montmorillonite if AIBA was previously introduced to the clay mineral.[104] The cationic form of AIBA goes to the exchange sites in montmorillonite to form AIBA-clay complex which decomposes thermally to generate free radicals. The complex has high initiating efficiency. The rate of polymerization with the AIBA-montmorillonite complex initiator was greater than for AIBA alone.[105] It has been proposed that free radicals remain attached to the adjacent planes of AIBA-montmorillonite dispersed in water, and on heating these planes move away from each other allowing more water to penetrate. This situation is represented in Figure 3 and 4.

From X-ray studies it was concluded that type 'c' and 'd' radicals do not recombine but move apart due to driving force of water. Once the radicals are separated some 30 Å, they can initiate the polymerization of the three types of free radicals formed during the decomposition of AIBA-clay complex, only type 'a' (Figure 4) can form homopolymer, and type 'a' radicals are free to be deactivated through recombination with type 'b'. Figure 4 also explains how the formation of homopolymer may be greatly decreased while the formation of graft polymer (from clay) is increased by decomposing the AIBA-montmorillonite complex. If the clay is dispersed in methanol, the later surrounds the intercalated free radicals inhibiting their separation and thus facilitating the graft polymer formation. From X-ray studies, Solomon and Loft suggested an interlamellar complex formation between a series of acrylate and methacrylate monomers and montmorillonite[106], as illustrated by Figure 5.

Only type III (Figure 5) is responsible for spontaneous polymerization of acrylic monomers in presence of peroxide initiator[106]. The polymerization of

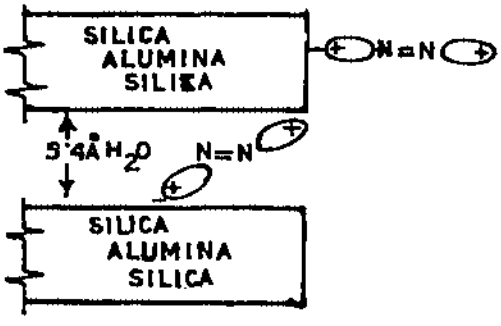
SILICA
ALUMINA
SILICA
N=N
5·4Å H2O
N=N
SILICA
ALUMINA
SILICA

FIG- 3

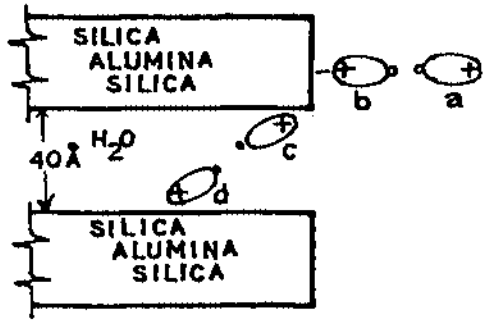
SILICA
ALUMINA
SILICA
b
a
40Å H2O
c
d
SILICA
ALUMINA
SILICA

FIG - 4

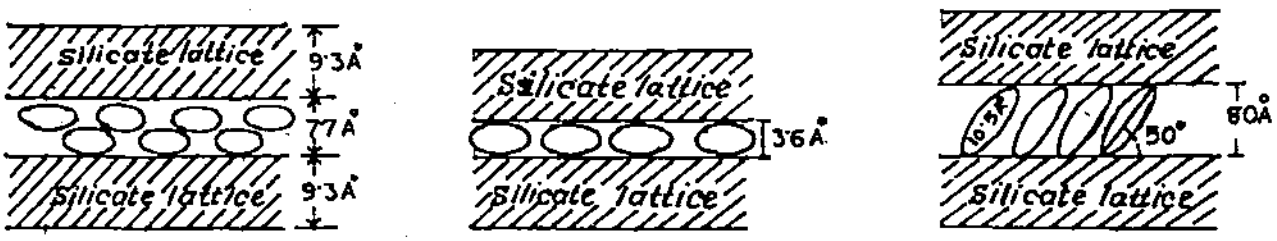

TYPE I

TYPE II

TYPE III

Fig. 5 Two monomer layers lying flat. (Spacing shown is for methyl methacrylate)

One monomer layer lying flat (Spacing shown is for dimethyl amino ethyl methacrylate)

One layer of inclined molecules. (Spacing shown is for hydroxyethyl methacrylate)

hydroxy methacrylates has been suggested to be due to the presence of electron donating sites within the silicate layers. The inclined orientation of the hydroxyl groups gave a favourable orientation for initiator, and the propagation involved radical anions. The following mechanisms have been forwarded.

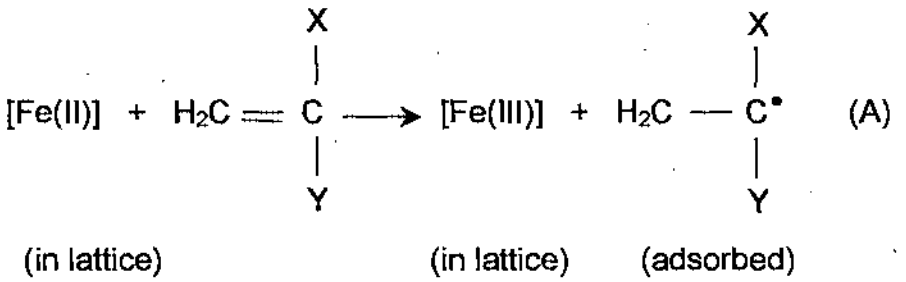

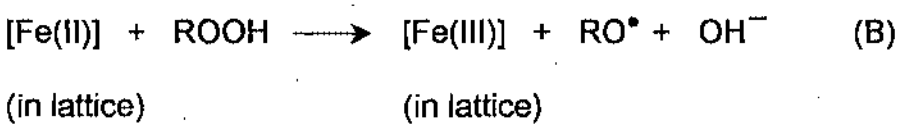

Iron is shown as a oxidizable atom in the silicate lattice although other transition metals may be present. In mechanism (A), the radical anion is formed via electron transfer from the mineral to the double bond. The mechanism is similar to that proposed for the polymerization of olefins by transition metal catalysts.

The influence of aluminosilicates and magnesium silicates on the free radical polymerization of MMA has been studied in terms of termination reaction and supported by studies of the reaction of stable free radicals with the minerals. In the absence of clay mineral the yield of PMMA was 3.68% (mol.wt. 1.36×10^6) whereas with montmorillonite the yield was 0.68% (mol.wt. 3.05×10^6). That the decreased amount of polymer in the presence of the mineral is not due to the depolymerization has been established by heating PMMA with montmorillonite and determining the viscosity average molecular weight before and after the treatment. A recent work involved ESR study to assess the state of iron in montmorillonite.[109] The absorbtion bands in the weak field as 'G' values

7.6, 4.2 and 3.9 were assigned to Fe(III) ions in the octahedral layer of montmorillonite. The intensities of the wide bands of the spectra remain unchange when the cations were altered as the exchanging sites. This indicated that the montmorillonite had particularly no iron in the ion exchangeable positions.

Studies on the structural properties of the polymers from clay catalyzed polymerizations of vinyl monomers have been made by several workers. Blumstein and co-workers studied dilute solution properties of the polymers prepared in the presence of clay minerals which differed significantly from those obtained using conventional free radical technique and suggested that the interlayer PMMA developed a two-dimensional sheet structure in the presence of a cross linking agent during the polymerization.[99-102] Analysing the n.m.r. data they concluded that PMMA probably consisted predominantly of short isotactic sequences. Small scale stereo-regularity of this kind could be ascribed to the orientation induced in the intercalated monomer by ion-dipole and the ester carbonyl group of the monomer. Earlier, Glavati and co-workers obtained oriented stereo-regular poly (acrylonitrile) and poly (acrylic acid) using similar procedures.[104]

Theng reported that the influence of clay minerals on the polymerization reactions extends beyond direct action on the monomers.[107-108] The chemical compounds used as polymerization initiators may also be modified by the minerals. It has been observed that clay mineral could affect both the rate and products of decomposition of initiators.

Uskov and co-workers reported that PVC or a vinyl acetate-vinyl chloride copolymer modified by a latex of Butyl acrylate-methylmethacrylate copolymer, Butadiene-styrene co-polymer, PMMA or a similar polymer was prepared by adding the latex to the reactor during the suspension polymerization.[109] The addition was made after 30-95% conversion of monomers. If inorganic compounds such as silica, montmorillonite or calcium phosphate was added

before or during the polymerization, the polymers with satisfactory particle size separated out from the aqueous suspension.

Recently, Talapatra and co-workers reported that bentonite in conjuction with alcohols or thiols effectively initiate the aqueous polymerization of vinyl monomers on the surface of the mineral[110-114]. A granular soil amendment was formulated from acrylamide polymers, silicic acid or silicate and one or more of phosphates, nitrates and sulfates, or free form of urea, guanidine, dicynidiamide, and amidinothiourea.[115] The product markedly improved aggregation of clay containing soils. T. Ono and co-workers, however, polymerized MMA in H_2O containing phyllosilicates such as montmorillonite in presence of water and azo- initiators.[116]

Powder minerals encapsulated with PMMA were formed when the montmorillonite-encapsulated minerals were extracted with hot benzene or methyl acetate, a fraction remained unextractable. The PMMA encapsulated mineral composites had good processability and charpy impact strength. The polymerization of formaldehyde with o- and p- cresol in the presence of Na-montmorillonite results in the formation of linear, short copolymer chains (oriented parallel to the silicate group) in the interlamellar spaces of Na-montmorillonite.[117] The polymerization of HCHO with m-cresol did not result in copolymer formation in interlamellar spaces i.e., the high reactivity of the m-cresol resulted in the formation of 3-dimensional copolymers.

CHAPTER -2

SCOPE AND OBJECT

SCOPE AND OBJECT

Water soluble synthetic polymers are extensively used in the industry in numerous products and processes from adhesives to cosmetics, from explosives to medical products and from oil technology to paper technology. Among the water soluble synthetic polymers, polyacrylamide is one which is a very effective flocculant for finely divided solids in aqueous suspensions. These polymers are used in acid, neutral or alkaline systems even in the presence of high concentration of electrolytes. They have found wide applications in the treatment of ores, particularly acid-leached uranium ore, minerals and metal particles, sewage, industrial waste and chemical precipitants as already mentioned. Extremely high molecular weight polyacrylamide have been found to be exceptionally effective flocculants. Aqueous solutions of acrylamide monomer together with a redox catalyst are injected into soil formations. In a predetermined period of time, which may be controlled, the monomers polymerize giving a cross linked rigid gel which prevents the passage of water through the mass and also binds the soil particles together. They are also used to seal off the flow of water into oil wells, drill holes, basements, tunnels, mineshafts, caissons and dams.

In view of the above, redox polymerization technique for the acrylamide polymerization is of great importance. However, usually redox polymerization of acrylamide in aqueous medium yields polymers having not so high molecular weight primarily because of fast termination process via transfer to the oxidant of the redox couple (e.g., metal ions at the higher oxidation states). Many potential redox catalysts involving metal ions as the oxidants viz., Fe(III)/Thiourea (TU), Ce(IV)/EDTA, Ce(IV)/Nitriloacetic acid etc. have been shown to be very promising free radical initiators in respect of high reaction rate, small induction period, low activation energy and above all their simple experimental procedures. Even these systems yield polymers having low molecular weights only, due to the fast termination process as mentioned

above. An appropriate redox polymerization technique which yields very high molecular weight polyacrylamide would, therefore, be an ideal procedure for many purposes.

Industrially, clay minerals are used as fillers and reinforcers in polymer systems such as elastomers, polyethylene, polyvinylchloride and other thermoplastics. All things being equal the efficiency of a filler in improving the physico-chemical properties of a polymer system is primarily determined by the degree of its dispersion in the polymer matrix. The most effective way of achieving such compatibility is to graft a suitable polymer on to the filler surface and/or to encapsulate the mineral particles with polymer layer. Indeed, clay minerals specially those of phyllosilicates (e.g., montmorillonite) themselves are known to catalyse a variety of organic reactions including those which lead to polymer formation. Moreover, research on the intercalation chemistry of phyllosilicates is gaining momentum rapidly to transform these abundant minerals into new classes of selective heterogeneous catalysts. These aspects have already been mentioned in the introduction. Interestingly, when metallic cations are adsorbed by montmorillonite, they are trapped between the interlayer spaces at the negatively charged sites of the minerals. If polymerization reaction could be initiated in the interlayer spaces of the mineral by redox couples involving the trapped metal ions, one may expect a controlled linear termination process because the growing polymer chain may not be able to transfer to these metals in the constrained spaces. This technique may also be proved useful for acrylamide polymerization in view of previous claim of stereoregular polymerization of acrylonitrile and acrylic acid monomers on smectite clays.

Therefore, one major objective of the present investigation is to perform the polymerization reaction of acrylamide monomer on the montmorillonite surfaces by redox initiators (Fe(III)/Thiourea) involving the trapped metal ions with a view to enhance the chain growth of the polymer. A detail solution phase reaction will also be performed involving the same redox couple ($FeCl_3$ /

Thiourea) in order to check what modifications pertaining to kinetics and mechanism have been achieved by the mineral phase reaction. A detail aspect of kinetics and mechanism of the reaction of both the procedures will be looked into. The technique of interlayer polymerization will be applied to other redox systems (viz., Ce(IV)/EDTA) to examine the scope of the proposed technique of controlling the termination process.

In addition, copolymers of acrylamide have shown a number of properties leading themselves to a variety of industrial applications. Of growing importances are those related to use as water soluble viscofiers and displacement fluid in enhanced oil recovery. Two of the critical limitations of polyelectrolytes including those derived from hydrolysing homopolyacrylamide, are the loss of viscosity in the presence of mono and multivalent electrolytes (NaCl, $CaCl_2$ etc.) and ion binding to the porous reservoir rock substrate. Some attempts have been made including that of preparing copolymers of acrylamide with diacetone acrylamide (N (1, 1 - Dimethyl - 3 - oxylbutyl) acrylamide) having large hydrodynamic dimensions in electrolyte solutions. Another objective of the present investigation is, therefore, to attempt to prepare this (viz., poly (acrylamide - co - N - (1,1 - Dimethyl - 3 - oxylbutyl) acrylamide)) and other copolymers (viz., poly (acrylamide - co - N - tert - butyl acrylamide)) on the montmorillonite surface with a view to have copolymers with higher molecular weights and intrinsic viscosities. Composition of copolymers, reactivity ratios of monomers and also the microstructure of copolymers would be examined.

In view of the use of polyacrylamide for preparing highly viscous solution in the secondary oil recovery process, the understanding of the role of charged groups on different factors which govern the efficiency in their use is important. A complete molecular characterization including the knowledge of their unperturbed dimensions is also necessary. A detail study of solution properties of polyacrylamide in water and water-organic solvent will be carried out for this purpose.

CHAPTER - 3

STUDIES ON REDOX POLYMERIZATION OF ACRYLAMIDE IN AQUEOUS AND AQUEOUS - MONTMORILLONITE MEDIA

3.1 REVIEW OF PREVIOUS WORK

Acrylamide is readily polymerized in aqueous solution at elevated temperatures with free radical initiators. Polymerization of acrylamide (AM) in aqueous solution with different free radical initiators have been reported by several workers[118-145]. Gnansundaram and co-workers observed that for the initiator, bis [2-[(2-hydroxy-ethyl)amino] ethoxo] copper (II) at pH 1.8, the polymerization rate was first order with respect to acrylamide monomer and 0.5 with respect to catalyst[120]. Faster polymerization and high molecular weight polymers were obtained using 2,2' - azobis [2-(N,N^{l} -ethylenamidino)] propane initiator than $K_2S_2O_8$ - Mohr's salt initiating system[121]. The rate of polymerization (R_p) of acrylamide by peroxydiphosphate in H_2SO_4, was decreased when the temperature raised from 30^0 to 50^{0}c but increased above that temperature, which was independent of pH[122].

Kinetics of polymerization in aqueous acetic acid (ACOH) using Pb $(OAC)_4$ as initiator was studied by Balakrishnan who found that polymerization rate was first order with respect to AM[127]. The propagation and termination reactions of the $K_2S_2O_8$ - initiated polymerization of AM in water were not influenced by the anionic emulsifier Dowfax 2 Al[128]. The induction of polymerization was affected by manganous salts while the polymerization rate and polymer molecular weight were not affected to a detectable degree, as was observed by Xuanchi[129]. Using trigol and polyethylene glycol initiators, it was found that the yield and the molecular weight of the polymer decreased with increasing chain length of substituted AM[131]. Cvetkovsha and co-workers explained the kinetic model by the formation of a monomer-initiator complex and inhibiting effect of the Mn(II) acetylacetonate formed by the reduction of Mn(III) acetylacetonate[132]. The polymerization rate of AM in H_2SO_4 or ACOH by Co(III) system showed similar mechanism as that of $Pb(OAC)_4$ initiator in ACOH[133]. Vaskova and co-workers found that in mixtures of water and aliphatic alcohols, in the presence and absence of inhibitor, the rate of polymerization

and molecular weight were reduced depending upon the length and character of the aliphatic chain[134]. Yinghai Liu and co-workers observed that the polymerization rate depended on the catalyst concentration, and pH of the solution[135, 137]. Using (2,2' - bipyridine) cobalt (II) complex initiator, Takahashi and co-workers found that the average molecular weight of polymer was (1-7) x 10^4. (Ref. 139). Bhanu and co-workers observed that co-ordinately unsaturated Co(II) complexes significantly inhibited the thermal polymerization of AM but they imparted a significant induction period during AIBN - initiated polymerization of AM[142]. High molecular weight polyacrylamide could be obtained by using heptane as the organic phase, $K_2S_2O_8$ as catalyst and sorbital-s-20 system as the emulsifier[144]. The author also reported that polymer molecular weight can be increased with increased concentration of AM and emulsifier and also by decreasing catalyst concentration[144]. Redox catalyst systems were frequently employed for polymerization at comparatively lower temperatures. Bajpai, Mishra and Behari and co-workers investigated the polymerization of AM initiated by $KMnO_4$ / various amino acids and unsaturated acids redox couples[145-157]. A value of $KMnO_4$ catalyst exponent of unity in the rate equation confirmed a unimolecular chain termination process by the redox system[145,146,151]. However, a bimolecular chain termination was observed by other redox systems[148,150,153-155]. The same result was observed in the case of $KMnO_4$ / glyceric acid in H_2O-DMF also[157]. The rate of polymerization was first order for the monomer in all the above systems. Bajpai, Mishra and co-workers suggested that polymer-molecular weight was directly proportional to initial monomer concentration and inversely proportional to the rate of initiation.

With the increase in temperature, the molecular weight of polymer was decreased in most of the cases. The effect of various additives (alcohols, neutral salts, complexing agents) on the polymerization rate were also inverstigated. Polymerization was initiated by radicals generated in the decomposition of the oxidant-reductant complex. A numbers of workers studied the mechanism and kinetics of aqueous polymerization of AM in acidic medium

initiated by Ce (IV) / reductant couples[158-174]. The rate of polymerization was first order in monomer and half order with respect to Ce(IV) ion in cases where the initiator was either Ce(IV) / thioglycolic acid or Ce(IV) / L-cysteine[162, 161]. In the polymerization of AM initiated by Ce (IV) / thiourea in water, the polymerization rate is governed by the relation $R_p = k_p [AM]^{1.20} [Ce(IV)]^{0.5} [TU]^{0.5}$. Presence of alkyl phenylcarbonate or alkyl-4-toly-carbonate increased the polymerization rate of AM initiated by Ce(IV) in H_2O-MeCN and H_2O-$HCONH_2$ and decreased the activation energy of polymerization compared to the system where Ce(IV) was used alone[172]. The rate of polymerization was derived as $R_p = k [AM]^{1.5} [Ce]^{0.39}$ [alkyl phenylcarbonate]. The overall rate of polymerization was faster and activation energy was lower with Ce(IV) / p-acetotoluidide system compared to Mn(III) / p-acetotoluidide system[171].

The effects of various aliphatic diamines on vinyl polymerization using persulfate as initiator were studied by different workers[175-176]. They suggested that the promoting activities of diamines on vinyl polymerization were of the order :

t - diamine > s - diamine > p - diamine.

In a reversible redox initiating systems involving metals and porphyrin, the aqueous polymerization rate depended on the types of metal (Fe(III), Cu(II), Ce(IV), Ti(IV), Mn(II)) in the porphyrin complex, polymerization temperature and concentration of AM[177].

The presence of carboxylic acids promoted and enhanced the polymerization rate of AM initiated by $Mn(OAC)_4$ (Ref. 179). The kinetics and mechanism of aqueous polymerization of AM initiated by the persulphate catalyst in the presence of different activators were studied by several workers[180-187]. Kurenkov and co-workers observed that, higher molecular weight polymers could be obtained with higher conversions using $K_2S_2O_8$ / $Na_2S_2O_3$ redox system during adiabatic polymerization of AM in comparison to the

$K_2S_2O_8$ / $Na_2S_2O_5$ - $CuSO_4$ system[180,182]. Molecular weight of the polymer was increased with increasing monomer concentration but decreasing catalyst concentration.

Akopyan and co-workers obtained polymers having molecular weight of 8 x 10^5 at 25°C by a three component catalyst system comprising of $K_2S_2O_8$, triethanolamine and amino-acetic acid[184]. The overall polymerization rate was increased in presence of Cu(II) ions for the polymerization initiated by persulfate-(dimethylamino)ethylmethacrylate-Cu(II) catalyst[183]. Voronova, shaglaeva and co-workers observed that the polymers having molecular weight (20-5) x 10^6 could be obtained in the presence of $K_2S_2O_8$ / urea as catalyst[185]. The polymerization kinetics, mechanism, polymer molecular weight and effect of additive were examined by several workers for various redox polymerization involving chelate complexes[186-209]. For a radical polymerization of AM initiated by Mn(III) - acetylacetonate in aqueous solution of pH 2.0, Cvetkovska explained the deviation of the kinetics from the conventional kinetic model via the formation of a monomer-initiator complex[189]. Smith obtained polymers having molecular weight as high as 40 x 10^6 by Fe(II) / hydroperoxide redox initiator at the temperature range between - 20°C and +40°C (Ref. 190). Wu and He obtained polyacrylamide having average molecular weight of 10^7 at room temperature by $NaHSO_3$-O-$MnSO_4$ catalyst[191]. They also pointed out that the presence of $MnSO_4$ would only affect the catalytic activity of the system but it did not involve in chain propagation or termination. Electrochemical study of the redox initiating systems, Fe(III)-EDTA / N_2H_4-H_2O_2 and Fe(III)-EDTA / NH_2OH-H_2O_2, in alkaline aqueous media (pH 9-11) showed that the former redox system was more effective than the later[194]. Peng pointed out that in the case of Mn(II) / $K_2S_2O_8$ initiating system, the induction of polymer molecular weights were not affected at all[196]. Lenka, Nayak and co-workers observed that the polymer rate was decreased with increasing thiosulfate concentration and was first order with respect to AM during aqueous polymerization of AM initiated by potassium peroxydiphosphate / Na-thiosulphate redox system[198]. The kinetics were

examined for the thermal polymerization of AM in the presence of CCl_4 and a bis amino acid chelate of Cu(II) with glutamic acid, serine or valine by Namasivayan and Natarajan[200]. The activation energy of polymerization reaction decreased from 18.7 to 4.5 KCal / mole on addition of 1.0 ppm Fe during the polymerization by H_2O_2/NH_2OH•HCL redox couple[201]. From the observation, it was concluded that the predominant reaction appeared to be Fe-catalysed decomposition of the peroxide in presence of small amount of NH_2OH•HCL. Sur and Choi found that the reaction rate in presence of $CoCl_2$ and N-N-dimethylaniline was proportional to $[AM]^{1.08}$ and $[Co(II)]^{0.53}$ indicating bimolecular termination process to be involved[206,209]. The rate of polymerization and the maximum yield decreased when the temperature was raised above 40°C. Chshmarityan and Beileryan observed that the polymerization of AM in aqueous solution initiated by $K_2S_2O_8$ - Ag (aminoacetate) chelate system was first order in monomer and 0.5 order in initiator[211].

3.2 EXPERIMENTAL

3.2.1 Materials and Purification

Montmorillonite

An aqueous suspension of 25 lit, was prepared by stirring continuously 100 gms of the mineral (Bentonite, Evans Medical Co, England) in double distilled water. The suspension was maintained at pH nearly to 8.0 by adding NaOH solution. After every 24 hours, 10 cm. layer of the suspension (from the top) was siphoned out and each time the original volume was restored by adding water. This process gives sample having particle size less than 2 micron[48]. The clay suspension was collected after acidification with HCl to pH nearly 4 and allowing to settle at the bottom of the container or by centrifugation. This coagulated clay was washed repeatedly with double distilled water and centrifuged. The free oxide of iron has been removed by the dithionite-citrate method[212]. The suspended mineral was washed throughly after each treatment. Organic matters have been freed by gently heating at 80°C with 30% (V/V) H_2O_2 (2ml per 3 lit. clay suspension) in a large beaker on a water bath for a long time with occasional stirring to ensure complete removal of H_2O_2. The montmorillonite suspension so obtained has been extensively dialyzed and stored. H^+ - montmorillonite (HM) was prepared by shaking the stock of the mineral (3% w/v) in presence of 0.5 M HCl for about 6 hours followed by repeated centrifugation (20,000 r.p.m.) and washing with double distilled water. The cation exchange capacity (CEC) of montmorillonite was determined by potentiometric titrations with standard KOH solution under nitrogen atmosphere and was found to be 0.91 meq/g. The hydrogen montmorillonite (HM) suspension thus obtained, was stored at 5-10°C. Fe(III) - montmorillonite (FeM) was prepared by shaking HM suspension (3% w/v) in presence of 0.5 M $FeCl_3$ (reagent grade) at pH 2.5 for 6 hrs. followed by purification by repeated centrifugation and washing with distilled water until the test of Fe(III) ions in the

supernatent was negative. A separate experiment on the sorption of Fe(III) on the montmorillonite shows that the maximum intake by Fe(III) ions by HM samples slightly exceeds the CEC value viz., 0.98 meq/g. Ce(IV) montmorillonite (CeM) was prepared by shaking HM suspension (3% w/v) in presence of 0.5M $(NH_4)_2[Ce(NO_3)_6]$ (reagent grade) at pH 2.5 for 5 hours followed by purification by repeated centrifugation and washing with distilled water until the test of Ce(IV) ions in the supernatent was negative. The colloid content of clay minerals in each case was determined by evaporating a known volume to complete dryness. The FeM and CeM suspensions were stored at 5-10°C temperature.

Monomers

Acrylamide (AM, reagent grade, Fluka) was purified by recrystallization from methanol (two times) and dried in vacuum oven at 45°C overnight.

Solvents and Reagents

Rectified spirit (C.P) was treated with proportional amount of freshly burnt quicklime and kept overnight. Absolute ethanol was obtained on distillation and the middle fraction (78°C) was stored in a sealed brown bottle. N,N'-dimethylformamide (DMF, Merck) was stored over P_2O_5 for nearly 10 hours and distilled. 1,4-Dioxan (Merck) was stored over P_2O_5 for nearly 10 hours and distilled. Dimethyl sulphoxide (DMSO, Merck) was treated with proportional amount of freshly burnt quicklime and kept overnight. Absolute DMSO was obtained on distillation at reduced pressure and the middle fraction was stored. Thiourea (TU, Merck) was used after recrystallization three times from distilled water (m.p. 180°C). Ferric chloride (reagent grade), Triton-x-100 (R) (sigma), Cetyl trimethyl ammonium bromide (CTAB, Aldrich) were used as received. Double distilled water has been used throughout.

Nitrogen

The commercial grade nitrogen was passed through a series of bubblers containing Fiesser's solution[213]. The oxygen free nitrogen was dried by passing through two bubblers containing conc. H_2SO_4.

Polymerization

Measured quantity of AM was added to the TU solution of known concentration under nitrogen atmosphere in a 100 ml stoppered pyrex bottle. In another bottle, known volume of aqueous suspension of Fe(III) - montmorillonite (FeM) was degassed and finally added to the former bottle under nitrogen. The pH of the reaction mixture was then adjusted to desired value by adding dil HCl/NaOH solutions under nitrogen (pH measured by a Systronics, India pH meter equipped with a combined glass electrode). The mixture was well shaken and immediately placed in a thermostated waterbath in the dark to attain polymerization temperature. The reactions were carried out for desired time with intermittent shaking. Control runs were carried out side by side by $FeCl_3$/TU initiating system instead of Fe(III) montmorillonite/TU. The bottles were withdrawn from the thermostat and the polymerization reactions were stopped by diluting the mixture with chilled water keeping the reaction vessels in ice bath. Similar procedure was followed in polymerization of AM with Ce(IV)-montmorillonite (CeM)/EDTA initiating system also.

Polymer Separation

The reaction mixtures were centrifuged (20,000 r.p.m.) to remove mineral clay montmorillonite after the completion of the reaction. The polyacrylamide (PAM) was precipitated out by adding excess of acetone to the supernatent, washed repeatedly with acetone and PAM was dried at 40°C for 48 hours under vacuum. The centrifuged clay mineral was also washed and dried at 60°C for 48

hours under vacuum. The dried samples of polymer as well as clay mineral were weighed to determine the polymer yields and non-extractable polymers in the clay minerals respectively.

Evaluation of Molecular Weight of Polymer by Solution Viscosity Method

A series of PAM solutions of different concentrations in aqueous 0.1M NaCl solution were prepared. The time of flow of the solutions and of distilled water were recorded by Ubbelohde Viscometer placed in thermostatic water bath at 30°C (± 0.2°C). Specific viscosity (η_{sp}) was calculated from the time of flow. The intrinsic viscosity ([η]) value was obtained from the intercept of the plot of η_{sp}/C versus C following the relation.

$$[\eta] = \eta_{sp}/C, \text{ Lim } C \rightarrow 0$$

Where C stands for concentration of polymer solution. The molecular weights (M_v) of the prepared PAM were calculated using the Mark-Houwink relationship[214-215].

$$[\eta] = 9.33 \times 10^{-3} M_v^{0.75} \text{ cm}^3/\text{g}.$$

Sorption of TU and AM onto montmorillonite

10 ml portions of a 0.5% suspension of HM were placed in a number of pyrex bottles and different amounts of either thiourea or acrylamide were added followed by pH adjustment at 2.0 by dilute HCl solution. The total volume of the suspension was made upto 15 ml in each case by adding the requisite amount of water and was shaken at 30° C for 4 hours to attain equilibrium. The suspernatent solutions were then centrifuged (20,000 r.p.m.) and analysed for TU or AM by a Shimadzu (Japan) double beam UV-VIS spectrophotometer (Model UV-240) at 235 nm and 195 nm respectively.

Potentiometric measurements

The redox behaviour of Fe(III)/TU and FeM/TU systems were examined by potentiometric titration of either $FeCl_3$ solution or FeM suspension with TU. The electrochemical cells were simple, as shown below :

pt / Fe(III) (or Fe(III) M), Fe(II) (or Fe(II) M)/ / KCl, $HgCl_2$, Hg/Pt

A stoppered pyrex beaker fitted with nitrogen gas inlet-outlet tubes, pt-electrode, salt bridge and mechanical stirring arrangements was placed in a thermostat at 50°C. 20 ml $FeCl_3$ solution or FeM suspension was then titrated at pH 2.0 with standard thiourea solution under nitrogen atmosphere.

XRD and Spectroscopic Measurements

ESR spectra were recorded at room temperature with a Varian V4502 spectrometer using 100 KHz magnetic field modulation. In Spin-trapping experiments, the ESR spectra recording was started from 5 minutes after mixing the solution with the spin trap, methyl nitrosopropane (MNP) (aldrich, U.K.). The microwave power level was maintained at 10 mW or lower to avoid saturation. A typical spectrometer setting was as follows : Modulation amplitude 0.2 mT, signal level 2.0 x 10^2, sweep time 5 min, response 1s, and microwave frequency 9.53 MHz (measured by cavity wavemeter). The magnetic field sweep was calibrated using a purposebuilt marginal oscillator to measure the corresponding ^1H n.m.r frequency, read by digital frequency meter. ^1H and ^{13}C n.m.r. spectra were recorded on a varian XL-300 Spectrometer in D_20. Chemical shifts were measured with reference to dioxane at $\delta = 67.40$ ppm. The X-ray powder diffraction patterns of solid mineral were recorded with a Philips PW 1730 machine using Ni-filtered Cuk_α radiation. X-ray generator was operated at 40 KV/20 mA. Other characteristics are as follows : slit assemble - $1^0 > 0.2^0 > 1^0$, Range - $2E_3$.

3.3 AQUEOUS POLYMERIZATION OF ACRYLAMIDE BY $FeCl_3$- TU REDOX COUPLE

3.3.1 Introduction

Ability of clay minerals to intercalate various molecules and their catalytic properties are long known. The clay-polymer interaction has found many and varied applications[3]. Montmorillionite, a smectite clay has been shown to catalyse the polymerization of some unsaturated organic compounds such as styrene and hydroxyethylmethacrylate and yet to inhibit polymer formation from other structurally related monomers such as methyl methacrylate[112]. This behaviour is believed to be due to electron accepting or electron donating sites on the clay minerals. However, it has been shown recently that montmorillonite can be used in conjunction with organic substances, viz., alcohols, thioureas etc. to polymerize methyl methacrylate in aqueous medium[112,110]. In this system, the lattice substituted Fe(III) of the mineral is probably involved in forming initiating radicals in presence of TU[216]. Over the last 20 years, the use of thiourea and N-substituted thiourea as redox components for the initiation of aqueous vinyl polymerization has been examined[217]. These experiments applied various oxidents, viz., metallic salts, organic and inorganic peroxides, persulphate, permanganate, bromate to name a few. A number of articles have also appeared in the literature on graft polymerization of various monomers using the above initiators[217,218]. The special features of these systems are a very short induction period, a relatively low energy of activation and the low temperature required. However, no report on the polymerization of water soluble monomers viz., acrylamide, by Fe(III)/TU redox system is available. In view of increasing industrial applications of water soluble acrylamide polymers, clay minerals, and their combinations in various fields including the use of polyacrylamide as water soluble viscofier in enhanced oil recovery as mentioned earlier, present scheme of study is undertaken[219]. High molecular weight polyacrylamide have such other applications as effective flocculants and

chemical grouts. Redox initiated polymerization of acrylamide is one of the most common techniques applied for aqueous polymerization because of the simplicity of technique as well as high yield and reaction rates. Moreover, the above technique is uniquely applied for *in situ* polymerization of AM, where aqueous solutions of the monomer together with a redox catalyst are injected into soil formation. However, one major difficulty of such a technique is the fast termination by oxidant of the redox couple. In an attempt to increase the chain length of polyacrylamide (PAM) formation initiated by Fe(III)/TU redox couple via trapping the potential electron acceptor, viz., Fe(III), into the interlayer space of montmorillonite, polymerization experiments have been performed and the results are presented in section 3.4.3. In view of this, it may be argued that the effect of montmorillonite microenvironment should not be confined in controlling the termination process only, rather the overall polymerization mechanism and kinetics may also be modified to a great extent. A prior study on the detail polymerization mechanism and kinetics of solution phase reaction in absence of any mineral, applying the same redox initiator is, therefore, justified. Above reasons have prompted us to undertake a detail study on the polymerization of acrylamide by Fe(III)/TU redox couple in aqueous solution. The result of such study, which includes among others, kinetics and mechanism of the polymerization are presented in this section.

3.3.2 Experimental

Experimental procedure has been discussed in section 3.2.

3.3.3 Results and Discussion

Table 1-3 show data pertaining to the aqueous homogeneous polymerization of acrylamide by $FeCl_3$/TU redox initiator. The molecular weights of the polymer were ranged between (0.2 - 3.6) x 10^5. The initial rate of polymerization R_p's, were moderately high and ranged between (3 - 17) x 10^{-5} $mol.L^{-1}s^{-1}$. At a fixed TU and AM concentrations, all the parameters viz., R_p, X_L

and M_v were decreased with the increase in Fe(III) concentration of the initiating redox couple. The rate of polymerization, R_p, as well as the polymer yield, X_L, decreased from 17.17 x 10^{-5} to 4.16 x 10^{-5} mol.L^{-1}.s^{-1} and 73% to 26% respectively with the increase in the Fe(III) ion concentrations in the range of (1.5 - 8.0) x 10^{-3} mol.L^{-1}. The percent conversion of polymerization has been plotted as a function of time interval at different AM, TU and Fe(III) concentrations in Figures 6 -8. No induction period is observed in any set of polymerization experiment. The initial rate, R_p, decreases significantly with the increase in $FeCl_3$ concentration. This clearly shows the involvement of the linear termination process in the present polymerization reaction via transfer to the metal ion. The value of metal ion exponent, obtained from the slope of the double logarithmic plot of R_p versus metal concentration is found to be 0.90 (Figure 9). Thus, the rate is inversely proportional to nearly first power of metal concentration. On the other hand, R_p increases with increased concentrations of thiourea. Thiourea alone is incapable of initiating polymerization. Increasing concentrations of the activator, thiourea, in the range (0.01 - 0.04) mol.L^{-1} increases the concentrations of the initiating radical and consequently the number of propagating polymer chains and hence the rate of polymerization increases with increased TU concentration. However at still higher concentrations of TU, R_p as well as X_L tend to decrease considerably due to increase in the rate of termination via dimerization of isothiocarbamido primary radicals $(TU^{\bullet})$[114]. The value of TU exponent obtained from the slope of the double logarithmic plot of R_p versus TU concentration, is 1.8 (Figure 10). Thus, the rate of polymerization shows a nearly second order dependence on the TU concentration. The dependence of R_p on the monomer concentration is, however, interesting. The initial rate and polymer yield increases with the increase of monomer concentration as expected. The slope of logarithmic plot R_p versus concentration of AM is nearly 2.0 (Figure 11) in the range of AM concentration of (0.25 - 0.40) mol.L^{-1}, but tends to decrease (the value becomes1.0, experimental points shown in Figure 11) in the higher concentration range of (0.4 - 0.6) mol.L^{-1}. The $[\eta]$ as well as M_v are also

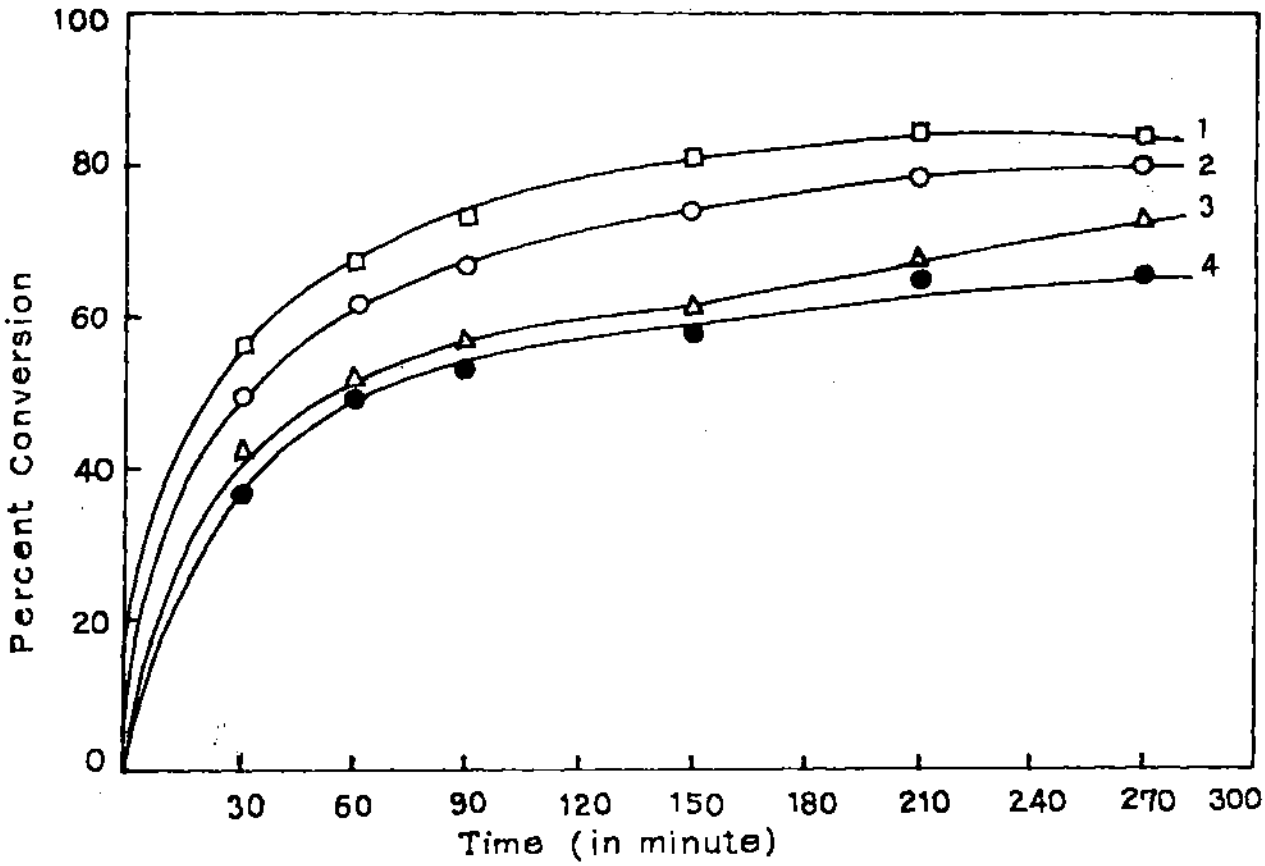

Fig. 6 Time - conversion plots for the aqueous polymerization of AM at 50°c with $FeCl_3$/TU.; [$FeCl_3$] = 1.5 x 10^{-3} M; [TU] = 0.04 M and [AM] = 0.3 M (1); 0.4 M (2); 0.5 M (3) and 0.6 M (4).

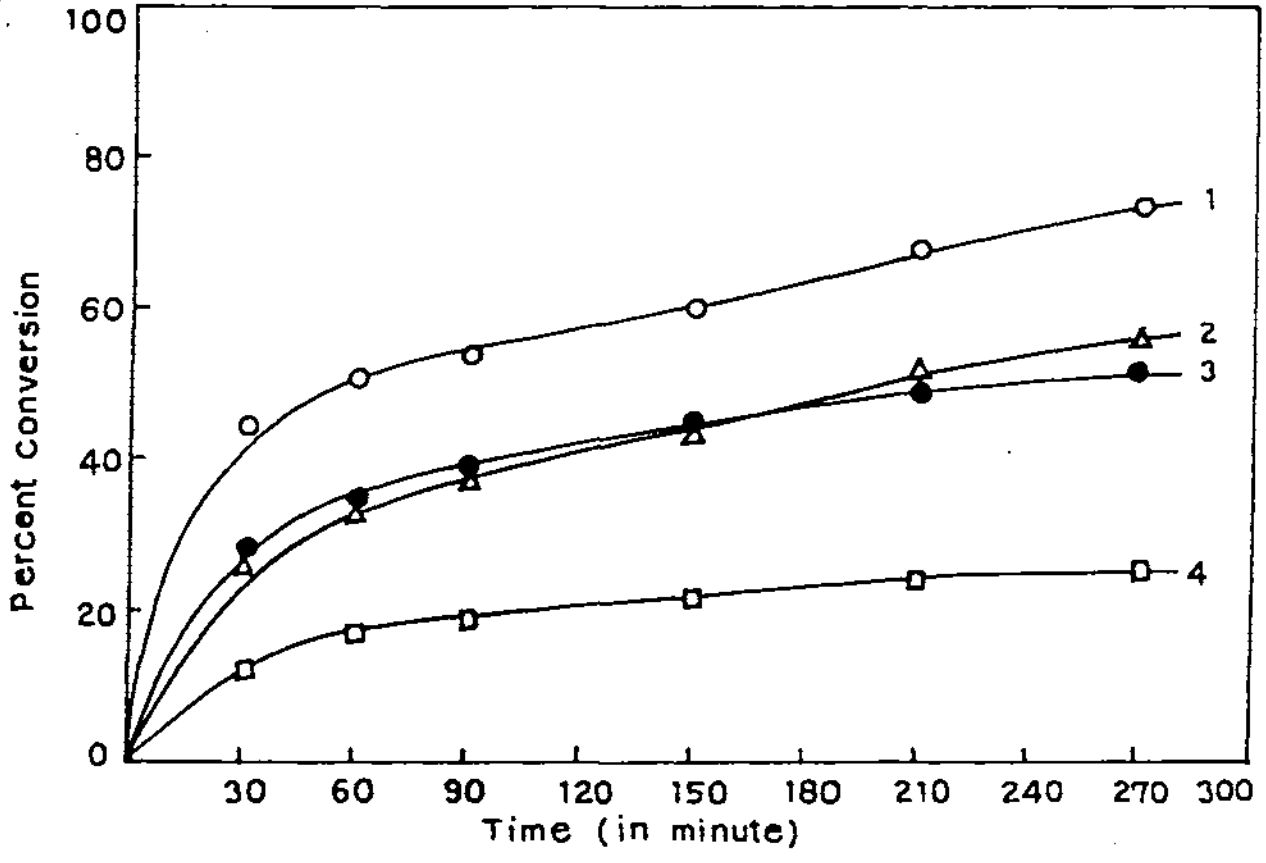

Fig. 7 Time - conversion plots for the aqueous polymerization of AM at 50°c with $FeCl_3$/TU.; [AM] = 0.4 M; [TU] = 0.04 M and [$FeCl_3$] = 1.5 x 10^{-3} M (1); 3 x10^{-3} M (2); 4 x 10^{-3} M (3) and 8 x 10^{-3} M (4).

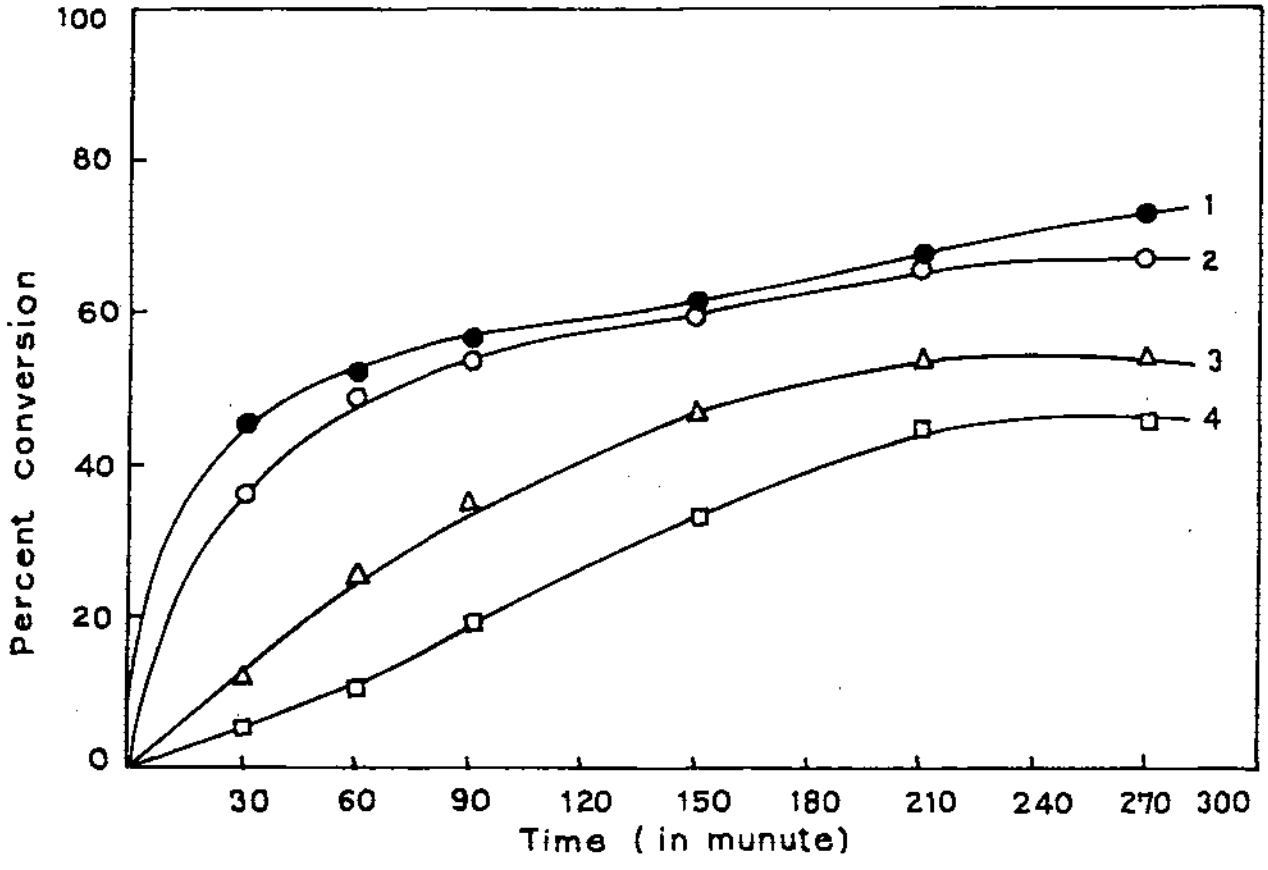

Fig. 8 Time - conversion plots for the aqueous polymerization of AM at 50°c with $FeCl_3$/TU.; [AM] [$FeCl_3$] = 1.5 x 10^{-3} M and [TU] = 0.04 (1); 0.03 M (2); 0.02 (3) and 0.01 M (4).

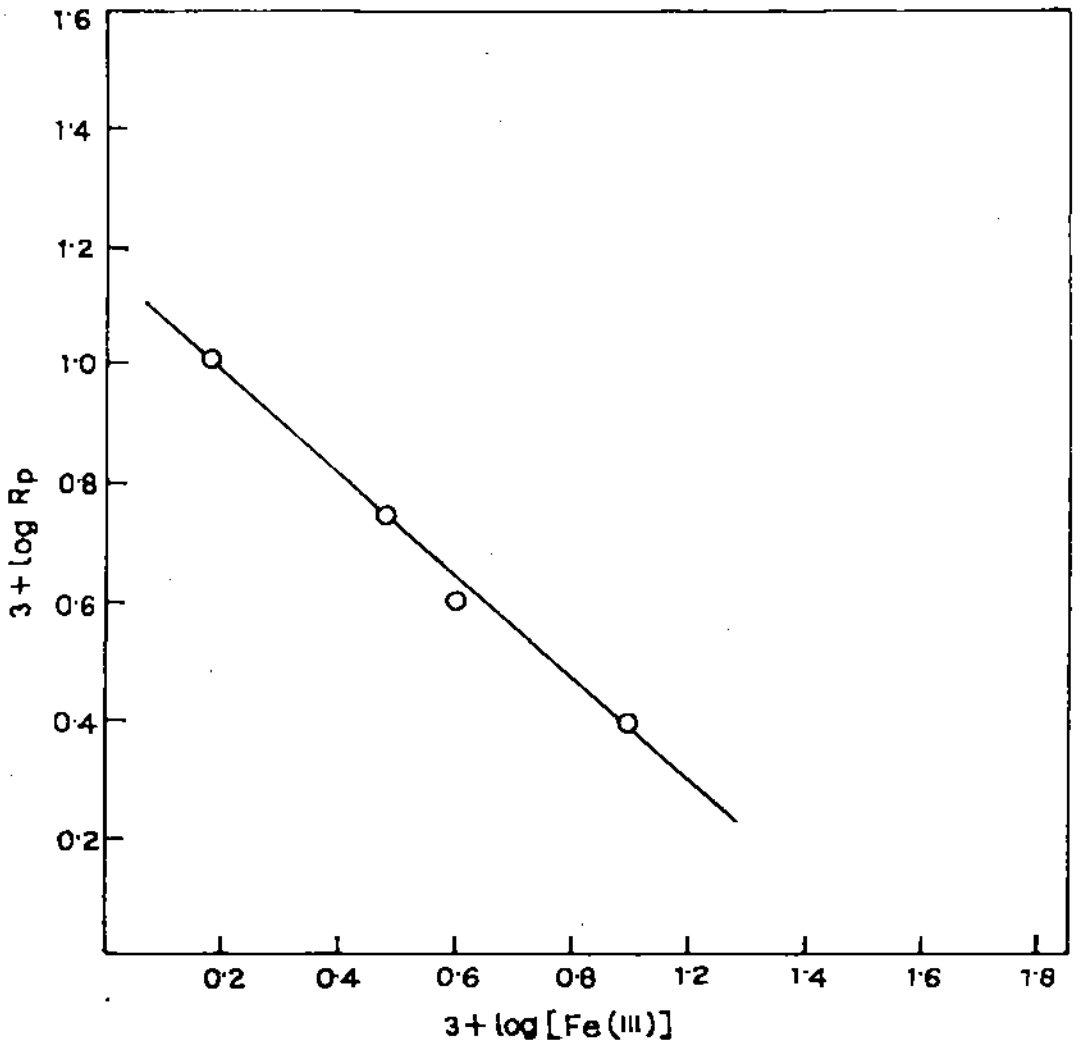

Fig. 9 Logarithm plot of Rp versus [$FeCl_3$] :
[AM] = 0.4 M and [TU] = 0.04 M.

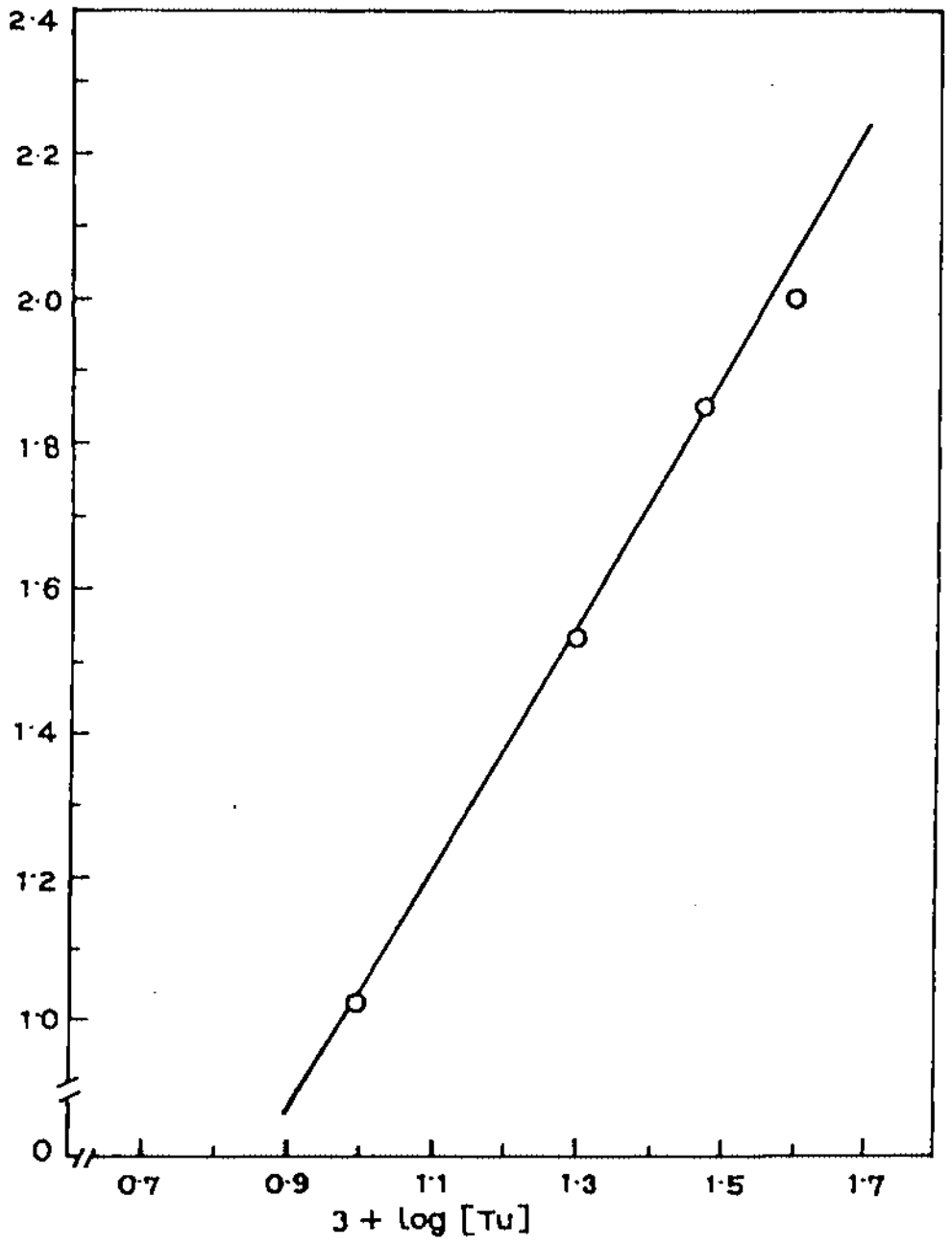

Fig. 10 Logarithm plot of Rp versus [TU] :
[AM] = 0.4 M and [$FeCl_3$] = 1.5 x 10^{-3} M.

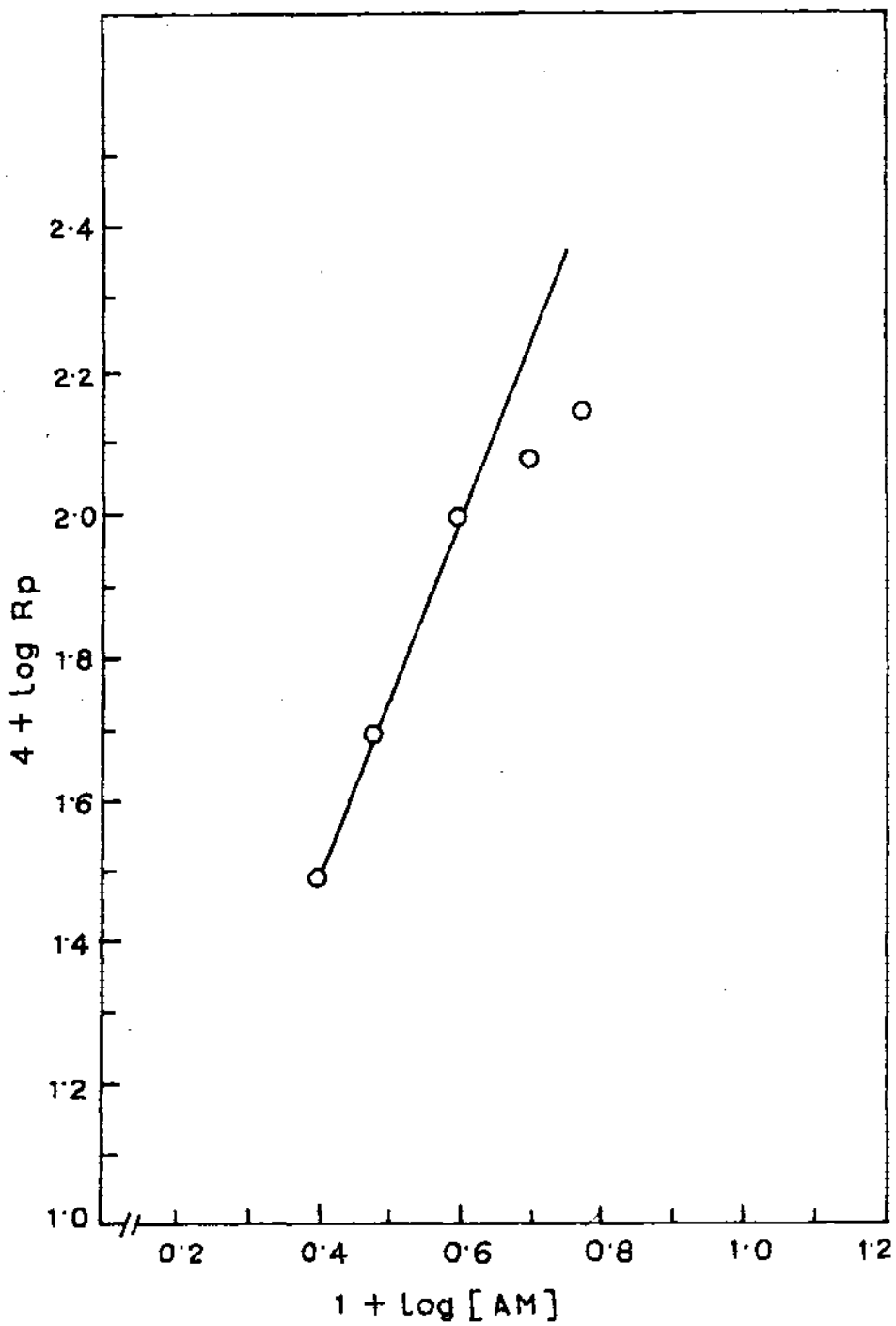

Fig. 11 Logarithm plot of Rp versus [AM] :
[$FeCl_3$] = 1.5 x 10-3 M and [TU] = 0.04 M.

Table - 1

Polymerization of 0.4 AM (0.7108 g) in aqueous medium (25 ml.) in presence of 0.04 M TU at 50°C and varying $FeCl_3$ concentrations (pH ~ 2.0).

[$FeCl_3$] m.mol.L^{-1}	$R_p^a \times 10^5$ mol.L^{-1}.s^{-1}	X_L^b %	$[\eta]^c$ ml.g^{-1}	$M_v \times 10^{-5}$
1.5	17.17	73	64	1.3
3.0	9.37	56	73	1.5
4.0	6.68	40	61	1.2
8.0	4.16	26	45	0.8

[a]Initial polymerization rate, [b]Yield after 4.5 hrs. and [c]Intrinsic viscosity

Table - 2

Polymerization of AM in aqueous medium (25 ml.) in presence of 0.04 M TU and 0.0015 M $FeCl_3$ at 50°C and varying AM concentrations (pH ~ 2.0).

[AM] mol.L^{-1}	$R_p \times 10^5$ mol.L^{-1}.s^{-1}	X_L %	$[\eta]$ ml.g^{-1}	$M_v \times 10^{-5}$
0.3	8.33	62	14	0.2
0.4	17.17	73	68	1.4
0.5	20.00	81	96	2.2
0.6	22.91	77	108	2.6

Table - 3

Polymerization of 0.4 AM (0.7108 g) in aqueous medium (25 ml.) in presence of TU and 0.0015 M $FeCl_3$ at 50°C and varying TU concentrations (pH ~ 2.0).

[TU] mol.L^{-1}	$R_p \times 10^5$ mol.$L^{-1}.s^{-1}$	X_L %	[η] ml.g^{-1}	$M_v \times 10^{-5}$
0.01	2.90	40	14	0.2
0.02	5.70	53	68	1.4
0.03	11.94	68	73	1.6
0.04	17.17	73	64	1.3

Table - 4

Polymerization of 0.4 AM (0.7108 g) in aqueous medium (25 ml.) in presence of 0.04 M TU and 0.0015 M $FeCl_3$ at different temperatures and varying $FeCl_3$ concentrations (pH ~ 2.0).

[$FeCl_3$] m.mol.L^{-1}	Temp. °C	$R_p \times 10^5$ mol.$L^{-1}.s^{-1}$	X_L %	[η] ml.g^{-1}	$M_v \times 10^{-5}$
1.5	70	19.20	86	137	3.60
	60	27.80	65	74	1.60
	50	17.17	73	65	1.30
	45	12.60	75	75	1.22
4	70	7.81	56	76	1.63
	60	7.56	57	59	1.17
	50	6.63	52	41.5	0.72
	45	6.41	50	23	0.33

increased with increasing monomer and TU concentrations.

Effect of Temperature

The study of the effect of temperature on the polymerization of AM with $FeCl_3$/TU initiating system is important. Table 4 represents the data pertaining to the R_p, X_L, $[\eta]$ and M_v of the polymer formed as functions of the concentration of $FeCl_3$ in the temperature range from 45° to 70°C. The R_p as well as X_L increase with increasing polymerization temperature (Figure 12). However, R_p decreases with decreasing polymerization temperature. The overall energy of activation as calculated from the Arrhenius plot (Figure 13) has been found to be 12.93 kcal.mol^{-1} within the temperature range 45° - 70°C.

^1H and ^{13}C - NMR Spectra of PAM

^1H and ^{13}C - NMR spectra of polyacrylamide samples obtained in the present study by $FeCl_3$/TU initiator in solution at 50° and 70°C are shown in Figures 14 - 16. In the case of ^1H as well as ^{13}C NMR, spectra obtained from polymers prepared at above two temperatures are identical. The ^1H NMR spectra of PAM are not usually well resolved spectra and no special feature is apparent in the present spectra also except that of overlapping of a sharp line with chemical shift of 2.12 ppm near the $CHCONH_2$ position. This line in all probability represents the hydrogens from the isothiocarbamido end groups of thiourea terminated PAM. The ^{13}C NMR of PAM obtained in solution phase reaction by $FeCl_3$/TU initiator is important because the idea of polymer tacticity it provides may be compared with those obtained in the montmorillonite phase reaction (discussed in section 3.4.3) in the light of the possibility of stereoregular polymer formation in the later case. The expanded ^{13}C NMR spectra show methylene, methine and carbonyl carbons of head - to - tail polymer of AM. No monomeric acrylamide was seen indicating purity of the

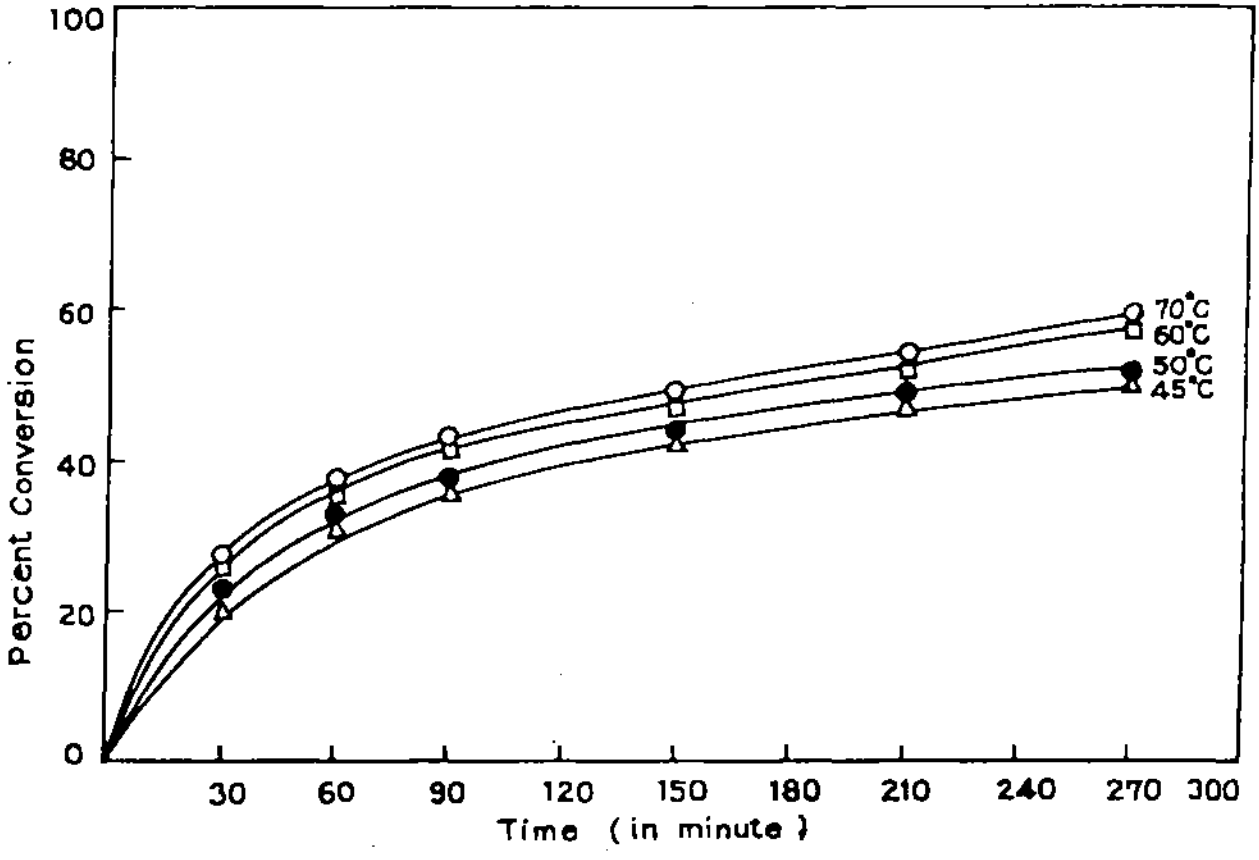

Fig. 12 Time-conversion plots for the aqueous polymerization of AM with $FeCl_3$/TU at various temperatures: [AM] = 0.4 M; [TU] = 0.04 M and [$FeCl_3$] = 1.5 x 10^{-3} M

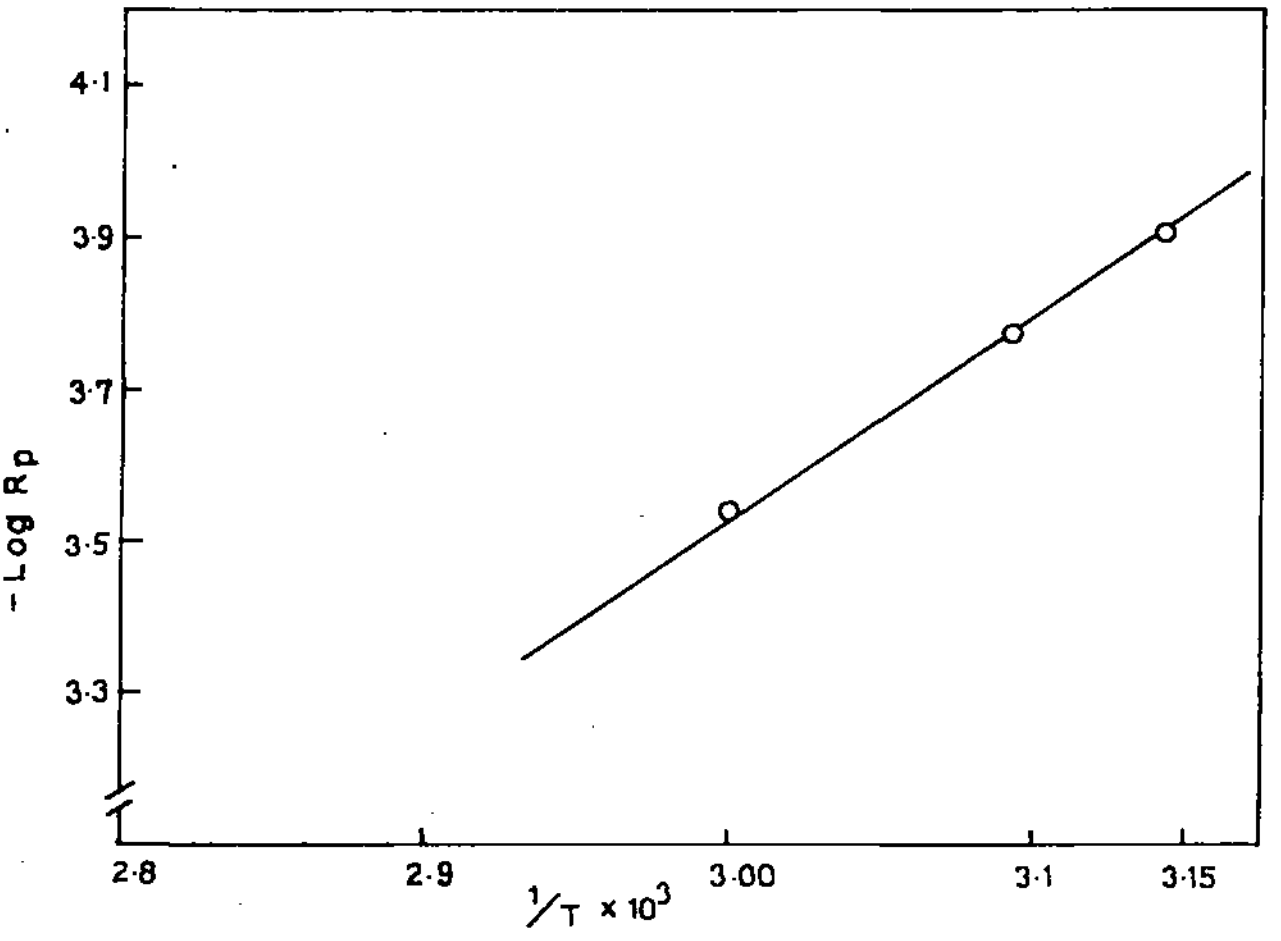

Fig. 13 Plot of - Log Rp versus I/T for 0.4 M AM with 0.04 M TU and 4×10^{-3} M $FeCl_3$.

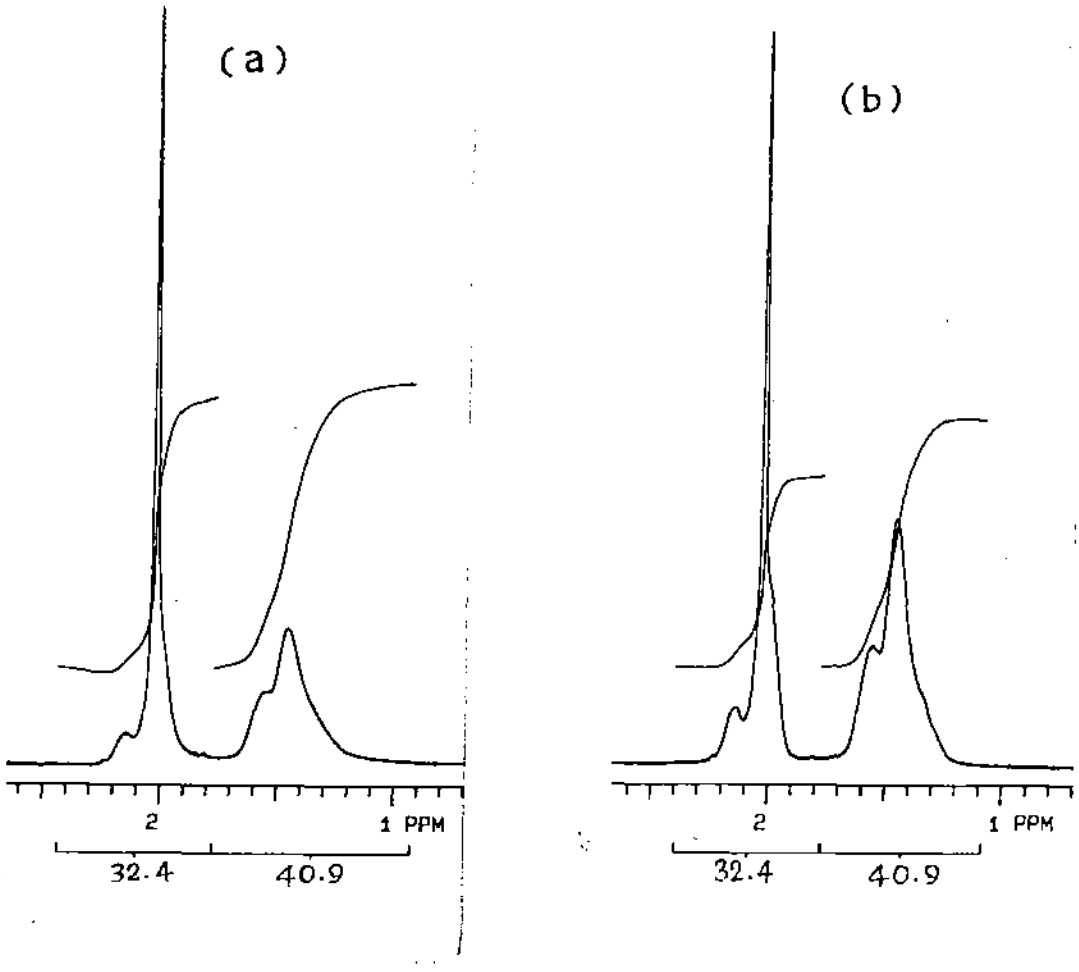

Fig. 14 ^{1}H spectra of thiourea terminated polyacrylamide formed in solution phase : (a) 70°c; (b) 50°c.

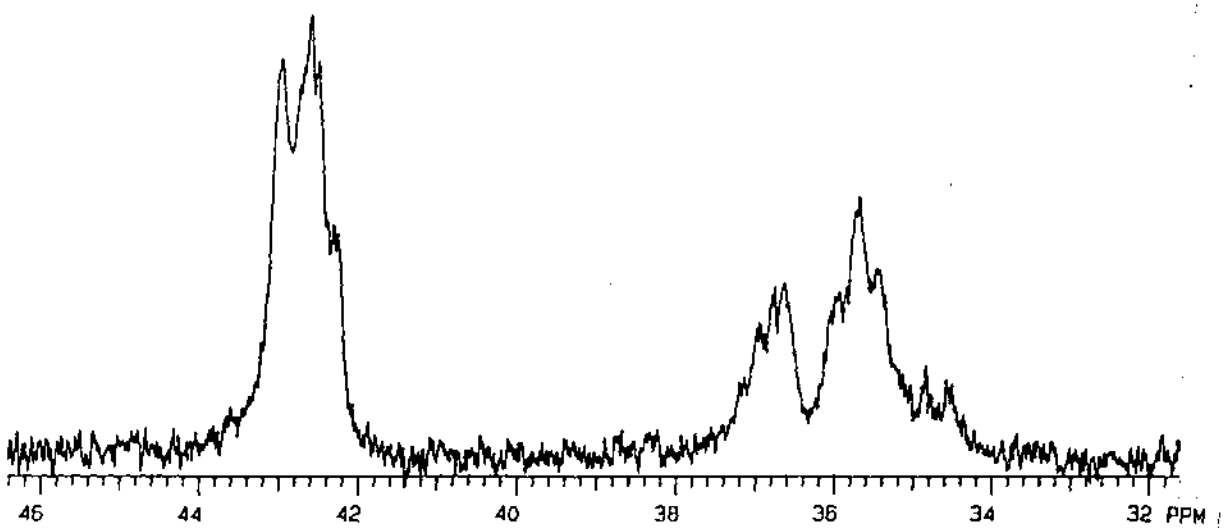

Fig. 15 ^{13}C n. m. r. spectra of thiourea terminated polyacrylamide formed in solution phase at 70°c.

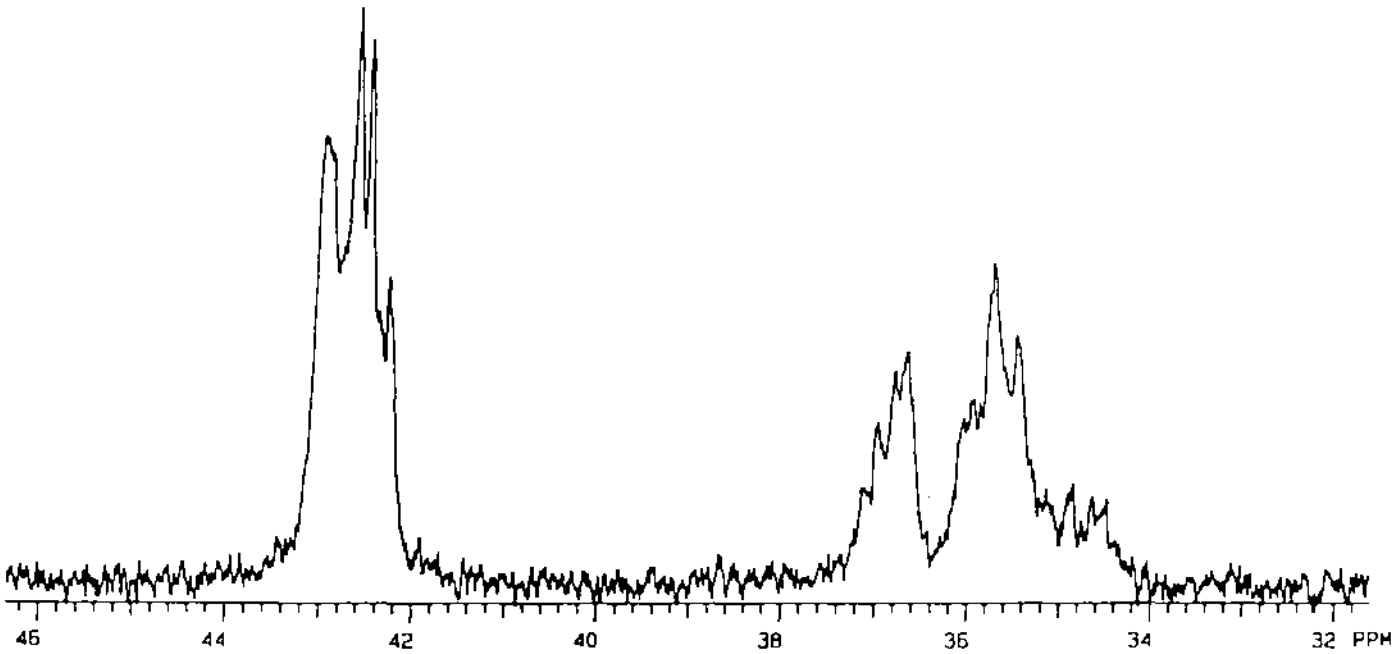

Fig. 16 ^{13}C n. m. r. spectra of thiourea terminated polyacrylamide formed in solution phase at 50°c.

polymeric sample. The carbonyl carbon splittings are generally small and not as readily interpreted as backbone carbon absorptions (not shown in figure). The methine resonance (42.2 - 43.5 ppm) is a triplet (triad sensitivity) which is further split, showing pentade sensitivity. The low field and high field triplet peaks are assigned to rr (syndiotactic) and mm (isotactic) sequences, respectively. The central peak corresponds to heterotactic sequences (mr + rm). The methylene carbon lines (34 - 37.4 ppm) fall into three fairly well separated groups with almost all the 20 lines required by hexad sensitivity resolved. The resemblance of the spectra to those obtained by Lancaster and O'connor suggests that Bernoulli statistics are followed, which are common in vinyl polymers[220].

Kinetics and Mechanism

In the polymerization reactions initiated by redox couple involving TU, a free radical mechanism has already been assumed involving the isothiocarbamido radicals (i.e., amido-sulfenyl radicals, NH_2–C(=NH)S radical), as the primary radical[113]. The kinetics of oxidation reaction of thiourea by Fe(III) ions was studied by Pustelnik and Soloniewiez[221]. It is believed that the reaction proceeds via the intermediate complex $[Fe(SC(NH_2)_2]^{+3}$, the stability constant of which is approximately 2.0. The decomposition of the complex involves a second order reaction, producing two isothiocarbamido radicals, which dimerize further in the presence of ferric ions. In order to rationalize the results of polymerization experiments following assumptions are made to predict the mechanism of aqueous homogeneous polymerization of acrylamide by $FeCl_3$/TU system. The rationale behind the approach adopted herein has been found to be equally applicable in explaining the kinetic behaviour of the seemingly complicated montmorillonite gel phase polymerization reaction initiated by either Fe(III)/TU or Ce(IV)/EDTA system (discussed in sections 3.4.3 and 3.5.3 respectively).

(1) Isothiocarbamido ($TU^{\bullet}$) primary radicals are formed via an intermediate complex between Fe(III) ions and TU. The decomposition of the complex is the rate determining step[221,222].

$$Fe(III) + TU \underset{}{\overset{K}{\rightleftharpoons}} \underset{\text{complex}}{Fe(III) - TU} \qquad (1)$$

$$Fe(III) - TU + TU \xrightarrow{k_d} Fe(II) + (2TU^{\bullet}) + H^{+} \qquad (2)$$

(2) Since the reactive TU radicals are formed as pairs, assumption of 'cage effect' seems to be conceptually appropriate[223,224]. The 'cage effect' suggests that when an initiator decomposes into two radicals, there is a formation of a potential barrier by the surrounding solvent molecules which prevent their immediate diffusion and favours their destruction by mutual recombination. The initiation step involves collision of acrylamide molecules with caged TU radicals at the wall of the cage and random diffusions of the radicals from the cage and their secondary recombination are less significant.

Initiation

$$(TU^{\bullet}) + M \xrightarrow{k_i} M_1^{\bullet} \qquad (3)$$

Propagation

$$M_1^{\bullet} + M \xrightarrow{k_p} M_2^{\bullet}$$

$$M_{n-1}^{\bullet} + M \xrightarrow{k_p} M_n^{\bullet} \quad \ldots\ldots\ldots \text{ etc.} \qquad (4)$$

Termination

$$M_n^{\bullet} + Fe(III) \xrightarrow{k_t} M_n^{\bullet} + Fe(II) \qquad (5)$$

$$(TU^{\bullet}) + Fe(III) \xrightarrow{k_t'} TU + Fe(II) \qquad (6)$$

$$(2TU^{\bullet}) \xrightarrow{k_t''} TU - TU \qquad (7)$$

(caged species are enclosed in brackets)

At the rate controlling step i.e.,

$$-\frac{d}{dt}[Fe(III)] = k_d [C][TU]$$

([C] denotes concentration of the complex)

Considering the above equilibrium and material balance on the [Fe(III)] i.e.,

$$[C] = K [Fe(III)]_f [TU]$$

(suffix 'f' stands for 'free')

and
$$\begin{aligned}[Fe(III)] &= [C] + [Fe(III)]_f \\ &= K [Fe(III)]_f [TU] + [Fe(III)]_f \\ &= [Fe(III)]_f (1 + K [TU])\end{aligned}$$

$$[Fe(III)]_f = \frac{[Fe(III)]}{1+K[TU]}$$

$$[C] = \frac{[Fe(III)][TU]}{1+K[TU]} \qquad (8)$$

Assuming that the rate of formation of TU radicals is exactly equal to the rate of disappearing Fe(III) ions, we obtain, (considering the steady state of $TU^{\bullet}$)

$$\frac{k_d K[Fe(III)]\left[TU^{\bullet}\right]^2}{1+K[TU]} = k_i\left[TU^{\bullet}\right][M] + k_t'\left[TU^{\bullet}\right][Fe(III)] + k_t''\left[TU^{\bullet}\right]$$

$$\left[TU^{\bullet}\right] = \frac{k_d K[Fe(III)][TU]^2}{\left(k_i[M] + k_t'[Fe(III)] + k_t''\right)(1+K[TU])} \qquad (9)$$

Again, considering the steady state of $M_n^{\bullet}$

$$k_i\left[TU^{\bullet}\right][M] = k_t\left[M_n^{\bullet}\right][Fe(III)]$$

$$\left[TU^{\bullet}\right] = \frac{k_t\left[M_n^{\bullet}\right][Fe(III)]}{k_i[M]} \qquad (10)$$

Equating RHS of the equations (9) and (10)

$$\frac{k_t\left[M_n^{\bullet}\right][Fe(III)]}{k_i[M]} = \frac{k_d K[Fe(III)][TU]^2}{\left(k_i[M] + k_t^{'}[Fe(III)] + k_t^{''}\right)(1+K[TU])}$$

$$\left[M_n^{\bullet}\right] = \frac{k_i k_d K[M][TU]^2}{k_t\left(k_i[M] + k_t^{'}[Fe(III)] + k_t^{''}\right)(1+K[TU])}$$

$$R_p = k_p\left[M_n^{\bullet}\right][M]$$

$$R_p = \frac{k_p k_i k_d K[M]^2[TU]^2}{k_t\left(k_i[M] + k_t^{'}[Fe(III)] + k_t^{''}\right)(1+K[TU])} \qquad (11)$$

Since the concentration of TU throughout the experiment is low and the value of the equilibrium constant, K, is only of the order of 2 $L.mol^{-1}$(ref 221), the quantity (1 + K [TU]) in the denominator may approximately be equated to unity. Hence the equation (11) is reduced to

$$R_p = \frac{k_p k_i k_d K[M]^2[TU]^2}{k_t\left(k_i[M] + k_t^{'}[Fe(III)] + k_t^{''}\right)} \qquad (12)$$

Plot of $[TU]^2[M]^2 / R_p$ versus [M] at constant Fe(III) ion concentration is a straight line. Similar plot of $[TU]^2[M]^2 / R_p$ as a function of [Fe(III)] at constant [M] is also a straight line (Figure 17). Moreover, the slopes and intercepts of the above two plots yield the same values of $k_t / k_p k_d$ and $k_t^{'}/k_i$ as 4.70 and 2.80×10^2 respectively. Reviewing the experimental results it seems apparent

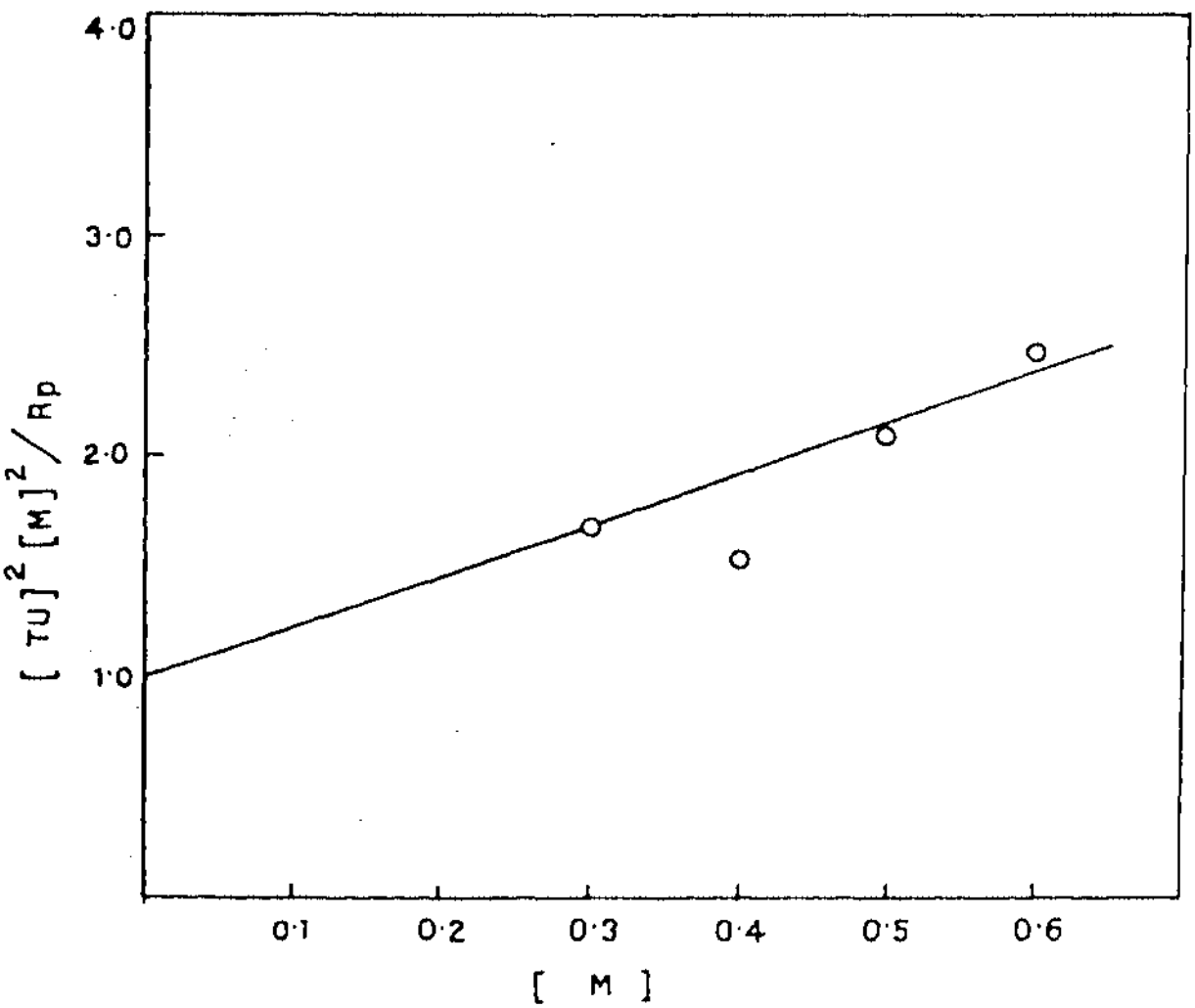

Fig. 17a Plot of $[TU]^2$ $[M]^2$ / R_p versus [M] for the polymerization of AM by $FeCl_3$ / TU system.

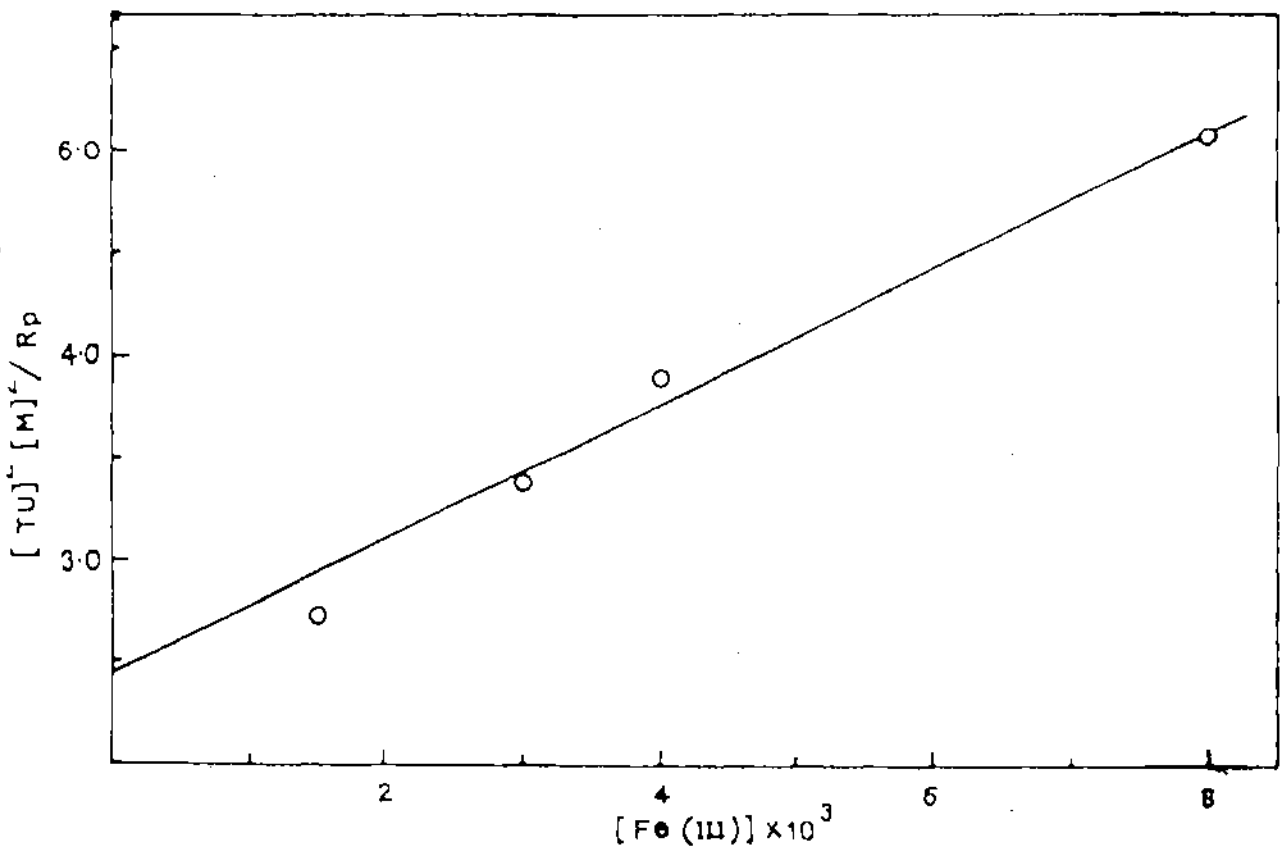

Fig. 17b Plot of $[TU]^2\,[M]^2 / R_p$ versus [Fe(III)] for the polymerization of AM by $FeCl_3$/TU system.

that k_t'' in the present homogeneous polymerization is not significant enough, specially in the presence of the monomer, in comparison to other terms in the denominator of equation (12). High value of k_t'/k_i ratio ensures that k_i [M] is also insignificant at low [M] in comparison to the second term in the bracket of the denominator. Thus, equation (12) could satisfactorily take account the high monomer exponent as is observed in Figure 11. Deviation of the points from the straight line in the Figure 11 as the consequence of high monomer concentration is, however, the manifestation of the dominance of the first term of denominator over the other.

3.4 REDOX POLYMERIZATION OF ACRYLAMIDE ON AQUEOUS MONTMORILLONITE SURFACE

3.4.1 Introduction

In the present section of the thesis, the results of polymerization of acrylamide in the montmorillonite microenvironment has been presented. The major objective of such a study was two folds viz., to examine the catalytic activity of clay mineral in the present aqueous polymerization process of water soluble polymer (PAM) and to prepare polymers having high molecular weight with high rate of formation under ordinary condition. However, in the present study, attempts to polymerize water soluble acrylamide monomers by lattice Fe(III)/TU combination were unsuccessful at a wide range of tempertature[113]. This is probably due to efficient inhibition of radical polymerization of acrylamide by montmorillonite via electron transfer from initiating or propagating radicals to the Lewis acid sites. On the other hand, montmorillonite microenvironment seems to have a dramatic effect on the redox polymerization of acrylamide by Fe(III)/TU combination in aqueous medium. This results in the slow termination due to inability of a growing polymer chain to transfer to the oxidant trapped inside the layered space. High molecular weight polymers may be expected with high intrinsic viscosities. A detailed study concerning the kinetic and mechanistic aspects has been made for the aqueous polymerization of acrylamide with ferric montmorillonite (FeM) / thiourea (TU) initiating system. X-ray diffraction, spectroscopy and other analytical data have been taken into consideration to determine the pathways involved in the reaction.

3.4.2 Experimental

Experimental procedure has been discussed in section 3.2.

3.4.3 Results and Discussion

The polymer yield (X_L), rate of polymerization (R_p) as well as molecular weight (M_v) and non-extractable polymer conversion data at different AM, TU and $\overline{Fe}$(III) concentrations, keeping other reaction parameters fixed, at 50°C are given in Tables 5 - 7.

Present technique increases the degree of polymerization and the intrinsic viscosity of the polymers dramatically by decreasing the rate of linear termination process. The method seems to be a promising technique for achieving high molecular weights and intrinsic viscosities of polymer for redox initiated reactions, where low molecular weight polymers are normally obtained. The corresponding experimental results in the absence of montmorillonite i.e., reaction in homogeneous solutions are presented in section 3.3.3.

The M_v values as calculated from viscosity data of present experiments are ranged from 0.70×10^6 to 2.5×10^6. The initial rate of polymerization, R_p's are ranged between $(0.92 - 9.26) \times 10^{-5}$ mol.L^{-1}.s^{-1}. The [η] values displayed by polymers formed in the presence of montmorillonite are found to vary from 247 to 600 ml.g^{-1}. At a fixed TU and $\overline{Fe}$(III) concentrations (concentration of Fe(III) being moles of interlayer metal ions per 1000 ml. of the reaction mixture), all the parameters viz., R_p, X_L, [η] and M_v are increased with the increase in AM concentration. The values of [η] and R_p varied from 363 to 480 ml.g^{-1} and 1.8×10^{-5} to 9.26×10^{-5} mol.L^{-1}.s^{-1} respectively for the variation of AM concentration from 0.3 to 0.6 mol.L^{-1} (Table 5). Amount of non-extractable PAM increases (0.09% to 0.4%) with increasing AM, TU and $\overline{Fe}$(III) concentrations. The percent conversions of the monomer have been plotted as a function of time of reaction at different AM, TU and $\overline{Fe}$(III) concentrations in Figures 18 - 20. No induction period is observed in the present system also. Although R_p and the X_L decreased with decreasing TU concentrations, molecular weight of the polymer

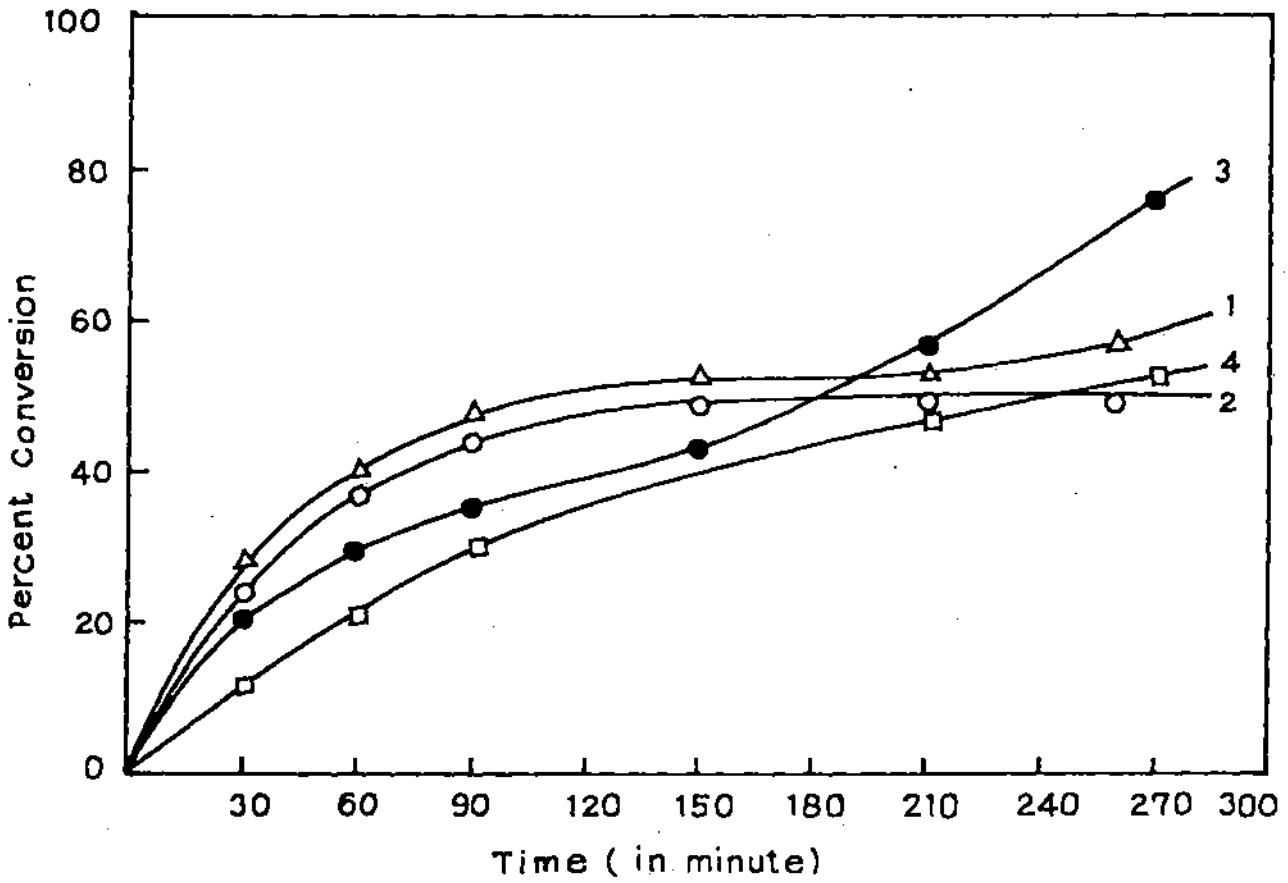

Fig. 18 Time-conversion plots for the aqueous polymerization of AM at 50°c with FeM / TU : [$\overline{Fe}$ (III)] = 1.5 x 10^{-3} M; [TU] = 0.04 M; [MO] = 0.5% (w/v) and [AM] = 0.6 M (1), 0.5 M (2), 0.4 M (3) and 0.3 M (4).

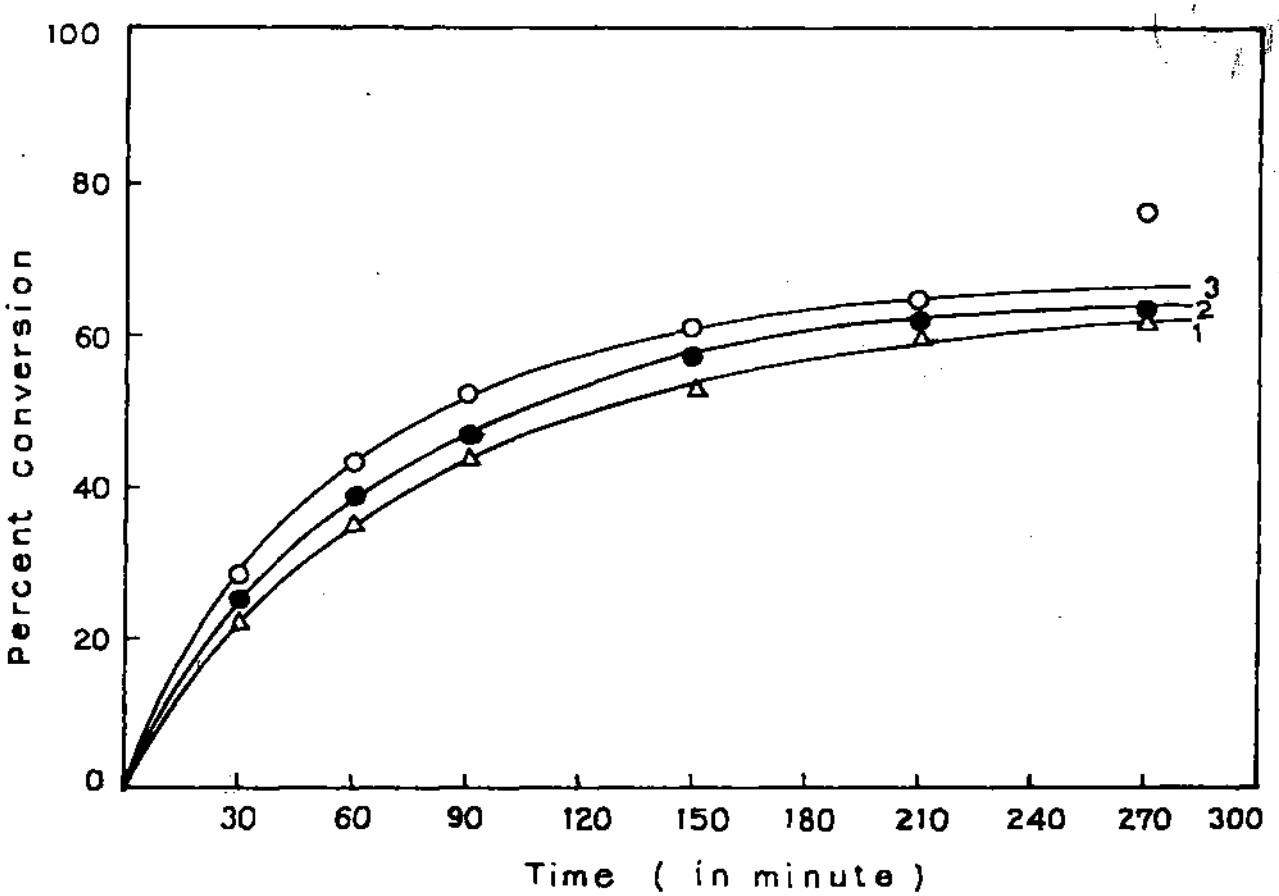

Fig. 19a Time-conversion plots for the aqueous polymerization of AM at 50°c with FeM / TU : [AM] = 0.4 M; [TU] = 0.04 M and [FeM] in w/v = 0.20% (1); 0.30% (2) and 0.69% (3).

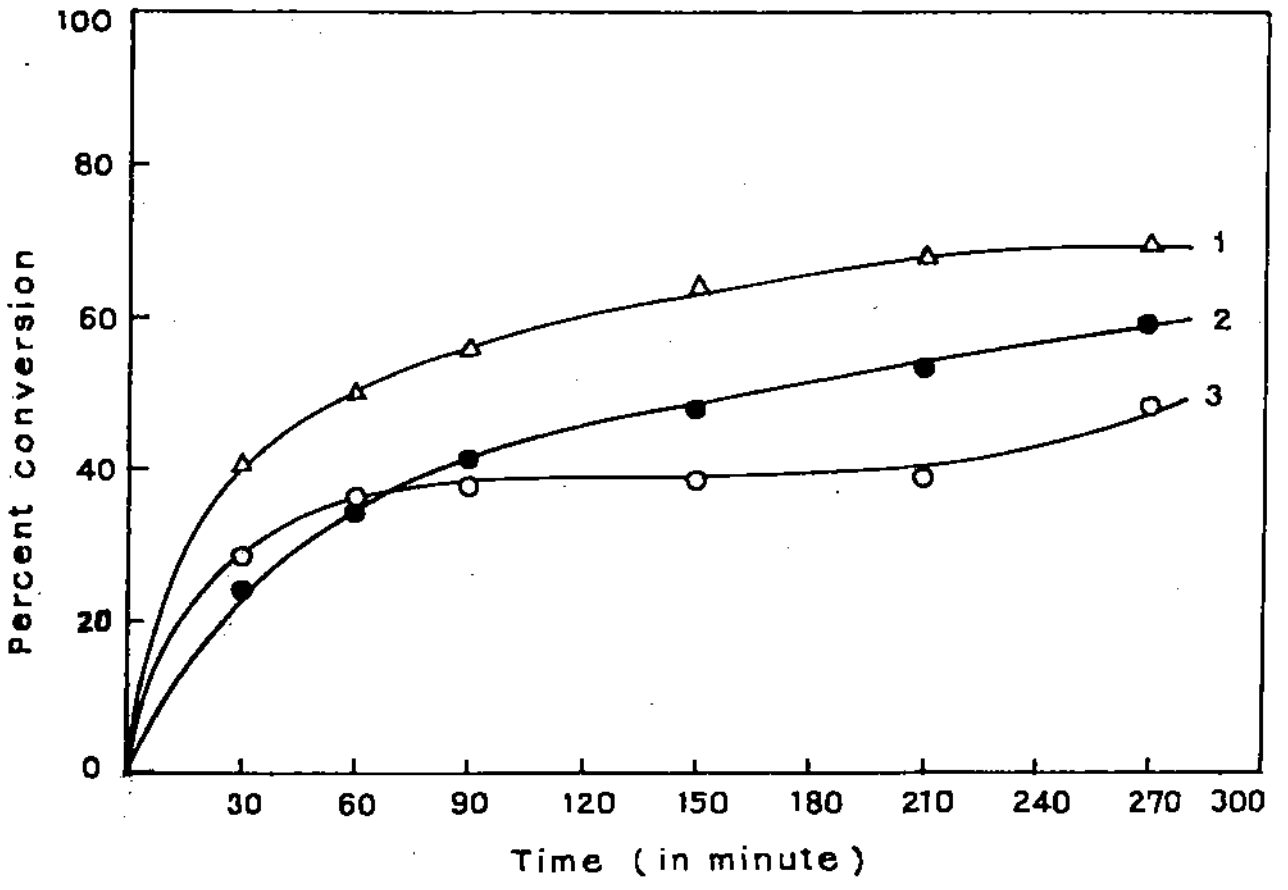

Fig. 19b Time-conversion plots for the aqueous polymerization of AM at 50°c with FeM / TU : [AM] = 0.4 M; [TU] = 0.04 M and [FeM] in w/v = 0.40% (1); 0.89% (2) and 1.33% (3).

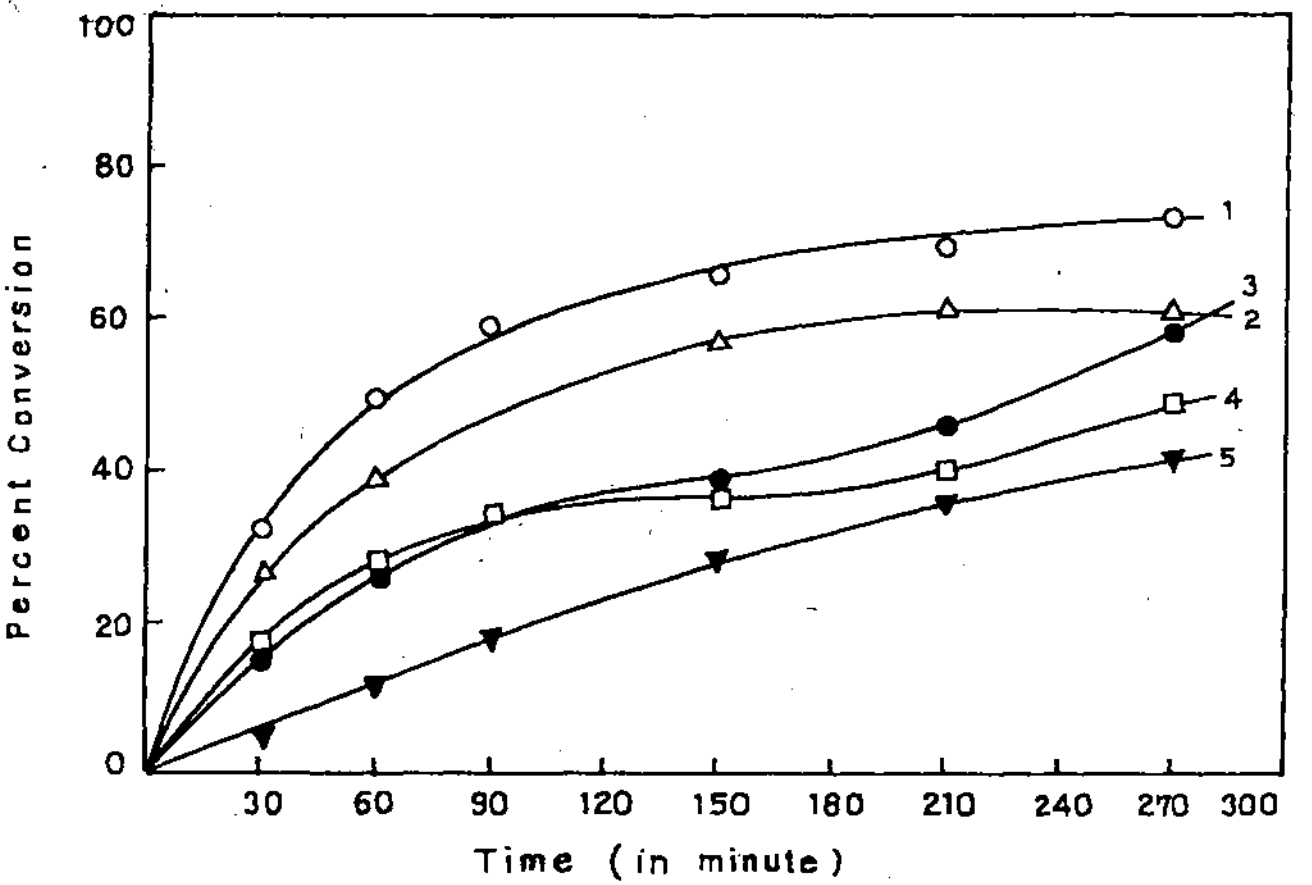

Fig. 20 Time-conversion plots for the aqueous polymerization of AM at 50°c with FeM / TU : [AM] = 0.4 M; $\overline{[Fe\ (III)]}$ = 1.5 x10^{-3} M; [MO] = 0.5% (w/v) and [TU] = 0.08 M (1); 0.06 M (2); 0.03 M (3); 0.02 M (4) and 0.01 (5).

Table - 5

Polymerization of AM in aqueous medium (25 ml.) in presence of 0.04 M TU and 0.50% (w/v) FeM at 50°C and varying monomer concentrations (pH ~ 2.01)

[AM] mol.L^{-1}	$R_p^a \times 10^5$ mol.$L^{-1}.s^{-1}$	X_L^b %	$[\eta]^c$ ml.g^{-1}	$M_v \times 10^{-5}$	Non-extractable PAM (wt%)
0.3	1.80	63	363	12.2	0.050
0.4	5.51	76	369	12.5	0.135
0.5	6.00	48	397	14.9	0.133
0.6	9.26	57	480	19.1	0.163

[a]Initial polymerization rate, [b]Yield after 4.5 hrs., [c]Intrinsic viscosity.

Table - 6

Polymerization of 0.4 M AM (0.7108 g) in aqueous medium (25 ml.) in presence of 0.04 M TU and 0.50% (w/v) FeM at 50°C and varying TU concentrations (pH ~ 2.01)

[TU] mol.L^{-1}	$R_p \times 10^5$ mol.$L^{-1}.s^{-1}$	X_L %	$[\eta]$ ml.g^{-1}	$M_v \times 10^{-5}$	Non-extractable PAM (wt%)
0.005	0.92	20	270	8.9	0.138
0.010	1.73	42	487	19.5	0.106
0.015	1.90	45	300	10.3	0.126
0.020	4.26	50	595	25.0	0.136
0.030	4.33	55	560	23.0	0.118
0.040	5.51	76	369	12.5	0.135
0.060	6.01	62	325	11.4	0.135
0.080	7.22	74	230	7.2	0.178

Table - 7

Polymerization of 0.4 M AM (0.7108 g) in aqueous medium (25 ml.) in presence of 0.04 M TU at 50°C and varying amounts of FeM (pH ~ 2.01)

[Fe(III)][a] m.mol.L^{-1}	[Mo][b] g.L^{-1}	$R_p \times 10^5$ mol.$L^{-1}.s^{-1}$	X_L %	[η] ml.g^{-1}	$M_v \times 10^{-5}$	Non-extractable PAM (wt%)
0.60	2.0	4.76	61	340	12.0	0.09
0.90	3.0	5.55	62	364	12.2	0.06
1.20	4.0	5.56	66	325	11.4	0.14
1.50	5.0	5.51	76	369	12.5	0.13
2.07	7.0	6.61	77	284	9.5	0.21
2.67	9.0	6.50	60	291	9.8	0.25
3.93	13.3	6.43	48	230	7.2	0.39

[a]Concentration of interlayer Fe(III) in m.mol. per litre of the reaction mixture; corresponding concentrations in montmorillonite gel phase is 0.03 m.mol.L^{-1}, [b]Montmorillonite content.

Table - 8

Polymerization of 0.4 M AM (0.7108 g) in aqueous medium (25 ml.) in presence of 0.04 M TU and mixtures of 0.50% (w/v) montmorillonite (FeM and HM) at 50°C and varying Fe(III) concentration in gel phase (pH ~ 2.01)

[Fe(III)][a] m.mol.L^{-1}	$R_p \times 10^5$ mol.$L^{-1}.s^{-1}$	X_L %	[η] ml.g^{-1}	$M_v \times 10^{-5}$	Non-extractable PAM (wt%)
0.38 (0.008[f])	2.05	36	290	9.8	0.102
0.75 (0.015[f])	3.31	43	360	13.0	0.125
1.13 (0.023[f])	3.70	45	355	12.8	0.128
1.50 (0.030[f])	3.70	76	369	12.5	0.135

[f]Moles of interlayer Fe(III) in 1000 ml. of montmorillonite gel phase.

was higher at lower TU concentrations. The R_p increases (0.92 $x10^{-5}$ to 7.2 x 0^{-5} $mol.L^{-1}.s^{-1}$) with increased TU concentration (5 x 10^{-3} to 8 x 10^{-2} $mol.L^{-1}$). Hence on increasing the concentration of catalyst more thiourea is oxidized to generate relatively more isothiocarbamido radicals. Consequently, the number of propagating polymer chains and hence the rate of polymerization increases. At concentrations lower than 5.0 x 10^{-3} mol. L^{-1}, the polymer yield was too insignificant to be detected. At such a low concentration of TU, formation of the initiating species is obviously too small to initiate the polymerization reaction. The M_v of polymer reached its maximum value viz., 2.5 x 10^6 at 2.0 $x10^{-2}$ $mol.L^{-1}$ of TU and a lowest value of 7.2 x 10^5 at 8.0 x 10^{-2} $mol.L^{-1}$ concentration (Table 6). Unlike solution phase reaction as shown in previous section, R_p increased from 4.76 x 10^5 to 6.61 x 10^5 $mol.L^{-1}.s^{-1}$ as the $\overline{Fe}$(III) concentration increased from 0.60 x 10^{-3} to 2.07 x 10^{-3} $mol.L^{-1}.s^{-1}$ (Table 7). At more high concentration of $\overline{Fe}$(III), however, R_p tends to decrease. Conversion efficiencies were also increased regularly with increasing $\overline{Fe}$(III) concentration upto 2.07 x 10^{-3} $mol.L^{-1}$. Although [η] and molecular weights increased significantly due to montmorillonite phase reaction, the value of [η] and M_v were found to increase only slightly (from 340 to 369 $ml.g^{-1}$) for the increase in $\overline{Fe}$(III) concentration upto 1.50 x 10^{-3} $mol.L^{-1}$ and at more higher concentrations of $\overline{Fe}$(III), however, [η] value tends to decrease (Table 7) again.

Effect of Temperature

Tables 9 -11 represent the data pertaining the R_p, X_L, [η], M_v and non-extractable polymer yield as functions of the concentration of $\overline{Fe}$(III), TU, AM in the temperature range from 45° to 70°C. The R_p as well as X_L increase with increasing polymerization temperature (Figure 21). The effect of temperature on the polymer viscosity and molecular weight are interesting. Upto a certain temperature these are increased but above that temperature the values ([η] and

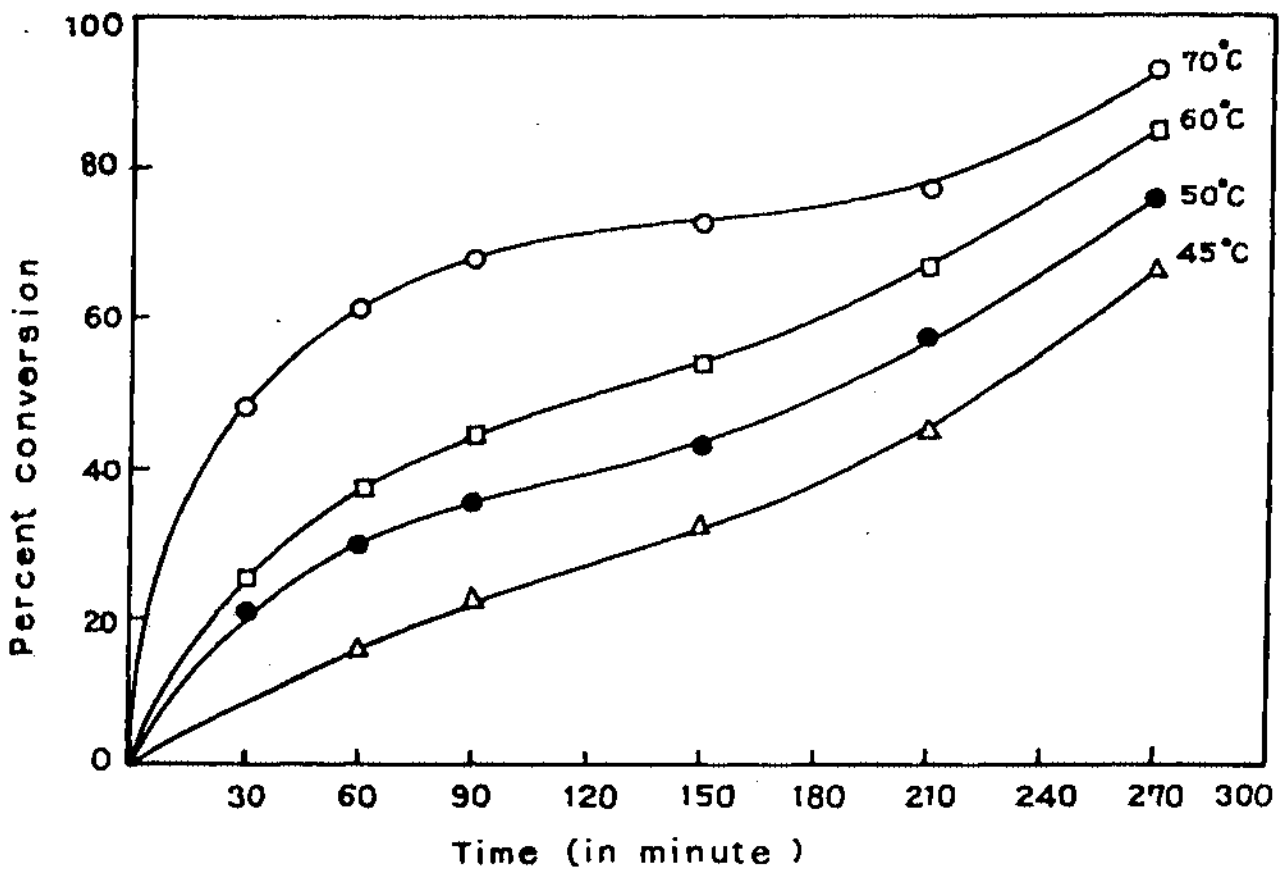

Fig. 21 Time-conversion plots for the aqueous polymerization of AM at 70°c, 60°c, 50°c and 45°c; [AM] = 0.4 M; [TU] =0.04 M; [$\overline{Fe}$ (III)] = 1.5 x 10^{-3} M and [MO] = 0.50% (w/v).

Table - 9

Polymerization of 0.4 M AM (0.7108 g) in aqueous medium (25 ml.) in presence of 0.04 M TU and varying amounts of FeM and different temperatures (pH ~ 2.01)

[Fe(III)][a] m.mol.L^{-1}	[Mo][b] g.L^{-1}	Temp. °C	$R_p \times 10^5$ mol.$L^{-1}.s^{-1}$	X_L %	[η] ml.g^{-1}	$M_v \times 10^{-5}$	Non-extractable PAM (wt%)
0.60	2.0		8.23	62	362	13.20	0.105
0.90	3.0		11.74	63	275	9.10	0.097
1.20	4.0		11.11	70	210	6.35	0.126
1.50	5.0	70	10.51	93	260	8.45	0.120
2.07	7.0		13.90	86	160	4.40	0.210
2.67	9.0		14.80	75	135	3.53	0.260
3.93	13.3		8.55	49	100	2.40	0.387
0.60	2.0		9.72	75	275	9.10	0.060
0.90	3.0		11.94	80	235	7.40	0.105
1.20	4.0		12.65	90	225	6.97	0.118
1.50	5.0	60	6.20	85	425	16.20	0.143
2.07	7.0		8.73	82	225	6.97	0.180
2.67	9.0		9.25	69	220	6.76	0.248
3.93	13.3		7.22	47	200	5.95	0.405
1.50	5.0		1.70	66	208	6.30	0.08
2.07	7.0		5.95	53	280	9.33	0.137
2.67	9.0	45	3.75	48	198	5.90	0.228
3.93	13.3		6.25	36	180	5.18	0.342

[a]Concentration of interlayer Fe(III) in m.mol. per litre of the reaction mixture; corresponding concentrations in montmorillonite gel phase is 0.03 m.mol.L^{-1},
[b]Montmorillonite content.

Table - 10

Polymerization of 0.4 M AM (0.7108 g) in aqueous medium (25 ml.) in presence of 0.05% (w/v) FeM and varying TU concentrations and different temperatures (pH ~ 2.01)

[TU] $mol.L^{-1}$	Temp. °C	$R_p \times 10^5$ $mol.L^{-1}.s^{-1}$	X_L %	[η] $ml.g^{-1}$	$M_v \times 10^{-5}$	Non-extractable PAM (wt%)
0.005		1.83	46	150	4.06	0.13
0.010		6.50	42	563	23.67	0.12
0.015		6.94	57	265	8.70	0.14
0.020	70	9.60	49	535	22.12	0.13
0.030		10.41	46	400	15.01	0.09
0.040		10.51	93	260	8.45	0.12
0.060		13.67	78	265	8.66	0.21
0.080		15.87	84	200	5.95	0.18
0.005		1.64	36	115	2.85	0.18
0.010		2.77	48	447	17.40	0.13
0.015		3.81	61	235	7.40	0.19
0.020		5.55	53	443	17.20	0.12
0.030	60	6.01	59	575	24.34	0.17
0.040		6.20	85	400	15.02	0.14
0.060		8.02	71	260	8.45	0.21
0.080		12.82	77	250	8.01	0.29
0.01		1.88	41	500	20.20	0.13
0.02		2.29	36	505	20.50	0.07
0.03	45	3.00	48	580	24.62	0.15
0.04		1.70	66	208	6.30	0.08

Table - 11

Polymerization of AM in aqueous medium (25 ml.) in presence of 0.04 M TU and 0.05% (w/v) FeM and varying AM concentrations at different temperatures (pH ~ 2.01)

[AM] $mol.L^{-1}$	Temp. °C	$R_p \times 10^5$ $mol.L^{-1}.s^{-1}$	X_L %	$[\eta]$ $ml.g^{-1}$	$M_v \times 10^{-5}$	Non-extractable PAM (wt%)
0.3		6.10	64	342	12.17	0.03
0.4		10.15	93	260	8.45	0.12
0.5	70	15.84	65	355	12.86	0.07
0.6		28.18	72	370	13.52	0.13
0.3		3.60	60	317	11.03	0.030
0.4		6.20	85	400	15.00	0.143
0.5	60	7.90	67	435	16.80	0.102
0.6		17.09	73	425	16.30	0.172
0.3		0.38	15	110	2.70	0.070
0.4		1.70	66	208	6.30	0.080
0.5	45	3.01	36	350	12.55	0.076
0.6		5.20	57	343	12.20	0.184

M_v) decreased. However, the optimum temperature upto which chain growth is enhanced, strongly depended on the reaction conditions. Significant 'gel effect' is observed, which is more prominent at lower temperature (Figure 21). The variation of the molecular weight of the polymer as a function of AM, TU and $\overline{Fe}$(III) concentrations at different temperatures are shown in Figures 22 - 24. From the Figure 22 it is observed that the variation of molecular weight with AM concentration is significant upto 0.5 $mol.L^{-1}$ of AM above which the molecular weights are almost constant. Several sets of polymerization experiments with four different monomer concentrations at four different temperatures were

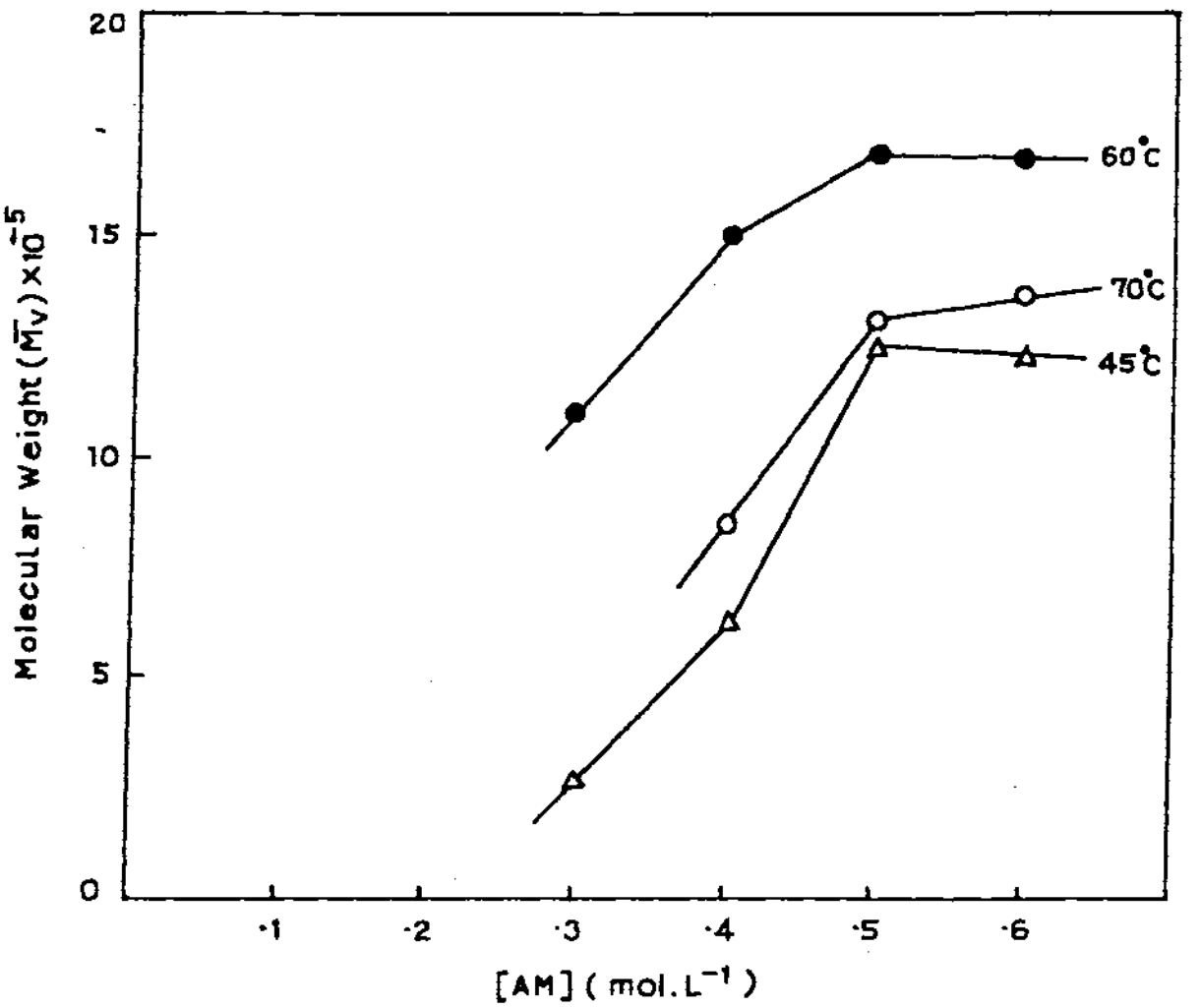

Fig. 22 Plots of Molecular weight versus [AM] for aqueous polymerization of AM with FeM/TU at 70°, 60° and 45°C: [TU] = 0.04 M; FeM = 0.50% (w/v).

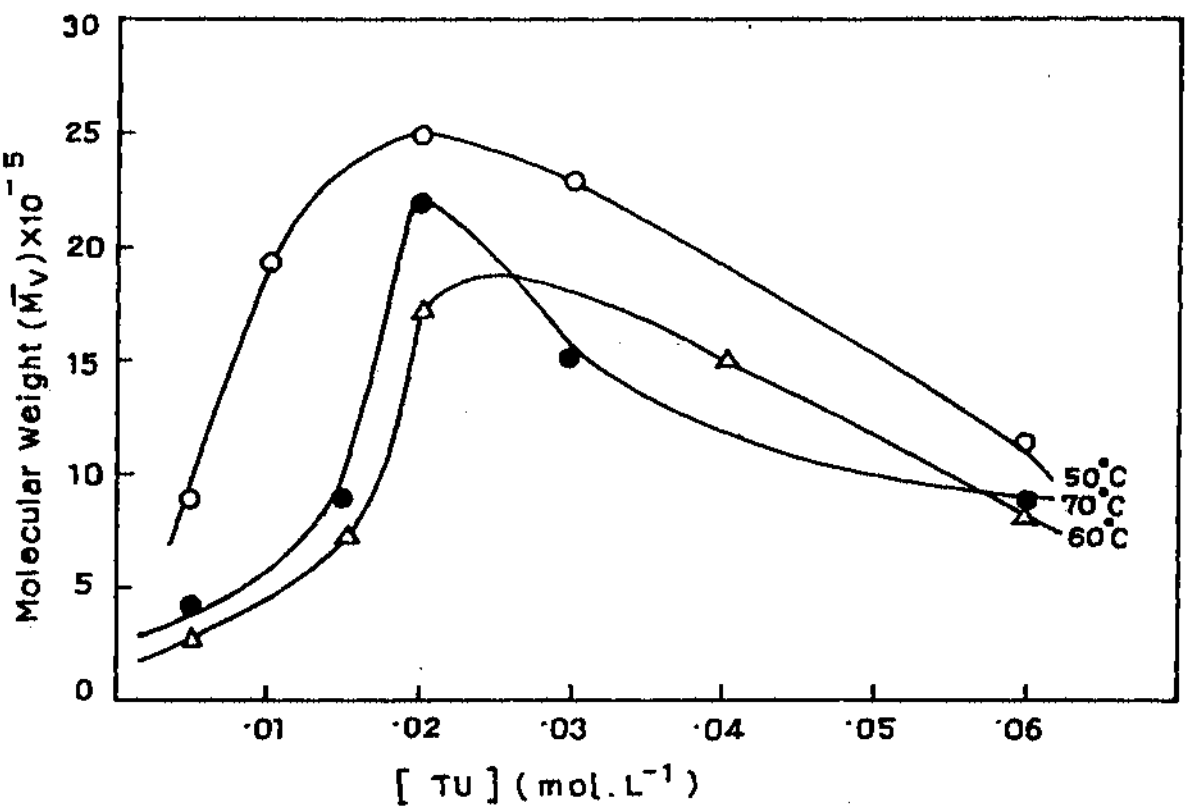

Fig. 23 Plots of Molecular weight versus [$\overline{Fe}$(III)] for aqueous polymerization of AM with FeM/TU at 70°, 60°, and 45°C: [AM] = 0.4 M; [TU] = 0.04 M.

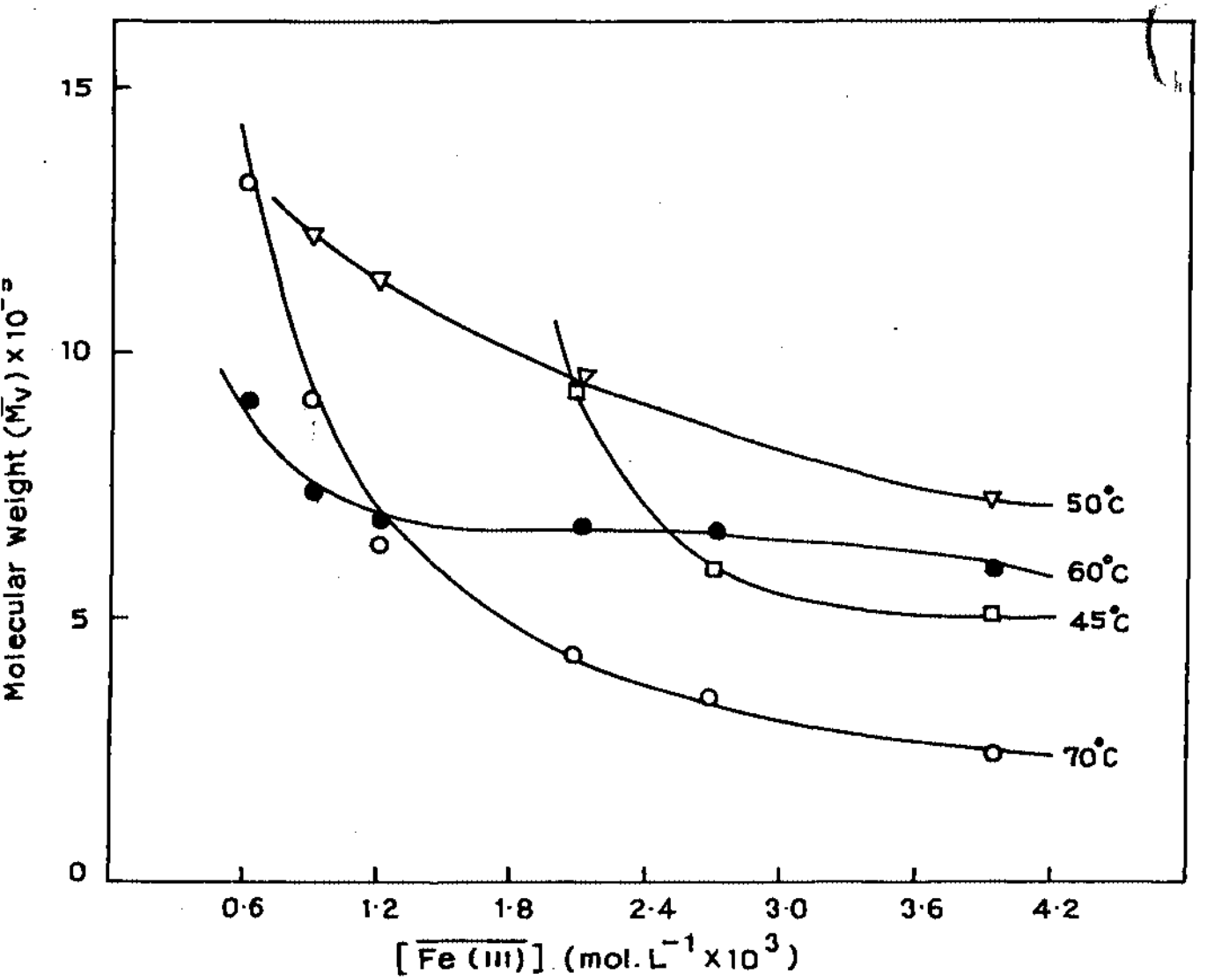

Fig. 24 Plots of Molecular weight versus [TU] for aqueous polymerization of AM with FeM / TU at 70°c, 60°c and 50°c : [TU] = 0.04 M; FeM = 0.50% (w/v).

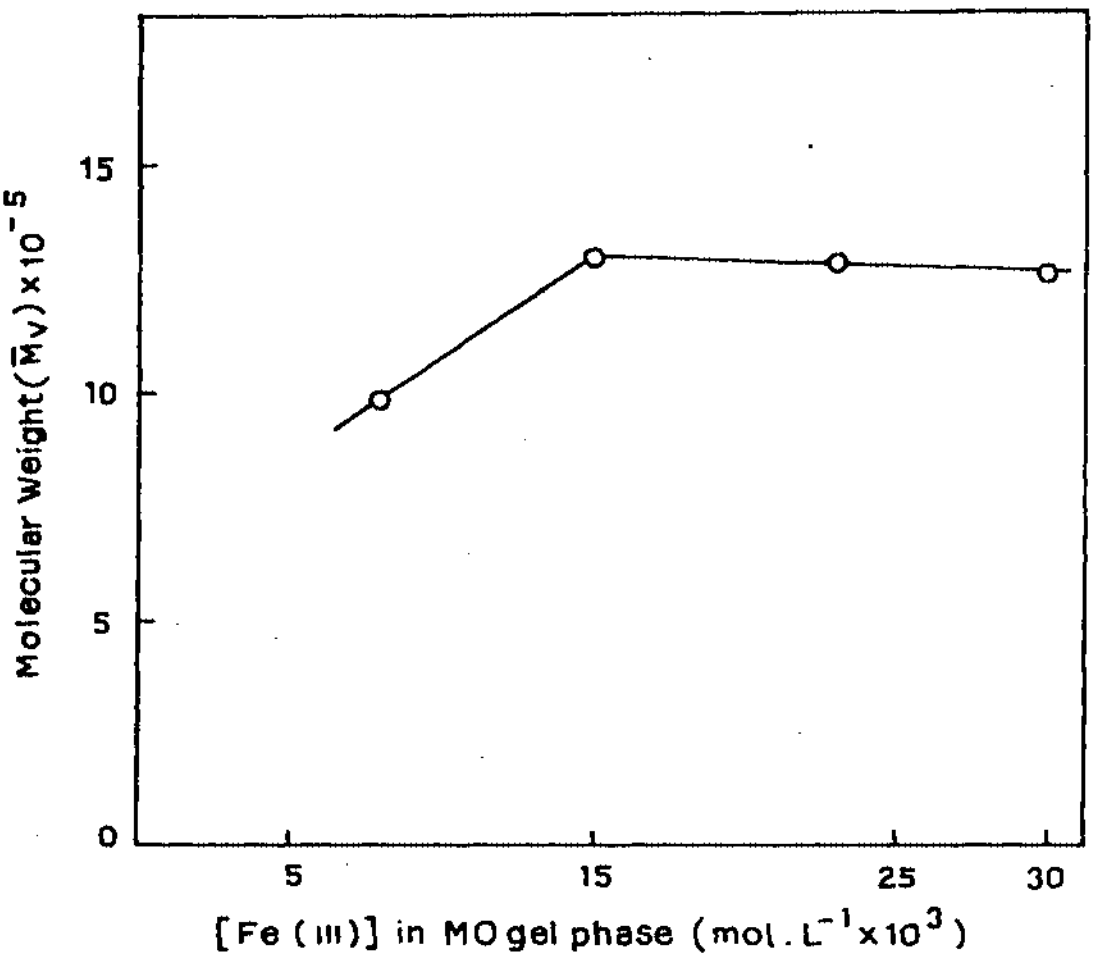

Fig. 25 Plots of Molecular weight versus [$\overline{Fe}$ (III)] in MO gel phase at 50°c
[AM] = 0.4; [TU] = 0.04 M

carried out keeping the TU (0.04 $mol.L^{-1}$) and $\overline{Fe}$(III) (1.5 x 10^{-3} $mol.L^{-1}$) concentration fixed. Arrhenius plot of - log (R_p) versus 1/T (in the temperature range 45° - 70°C) as shown in the Figure 26 leads to an average value of 14.9 $kcal.mol^{-1}$ for the activation energy, E_a, of the overall polymerization reaction. The activation energy was increased from 10.2 to 14.9 $kcal.mol^{-1}$ as the $\overline{Fe}$(III) concentration increased from 0.90 x 10^{-3} to 1.50 x 10^{-3} $mol.L^{-1}$ (Figure 27). At a higher concentration of $\overline{Fe}$(III) (3.93 x 10^{-3} $mol.L^{-1}$), however, E_a decreased significantly (4.57 $kcal.mol^{-1}$).

^1H and ^{13}C NMR Spectra of PAM

^1H and ^{13}NMR spectra of polyacrylamide samples obtained from the polymerization on the montmorillonite surface by FeM/TU initiator are shown in Figure 28. The ^1H and as well as ^{13}C NMR spectral patterns of PAM obtained in the montmorillonite phase reaction are almost identical with those obtained in solution phase reaction in absence of montmorillonite (discussed in section 3.3.3). In Figure 28a, the overlapping of a sharp line with chemical shift of 2.12 ppm, represents the hydrogens from the isothiocarbamido end groups of thiourea terminated PAM. The expanded ^{13}C NMR spectrum (Figure 28b) showed methylene, methine and carbonyl carbons of head - to - tail polymer of AM. The carbonyl carbon (at 180.2 ppm) splittings were small. Similar to the spectrum of PAM obtained from solution phase reaction (discussed in section 3.3.3) the methine resonance (42.2 - 43.5 ppm) is a triplet (tried sensitivity) which is further split, showing pentade sensitivity. The low field and high field triplet peaks may be assigned to rr (syndiotactic) and mm (isotactic) sequences, respectively. The central peak corresponds to heterotactic sequences (mr + rm). The methylene carbon lines (34 - 37.4 ppm) also fall into three well separated groups with all 20 lines required by hexad sensitivity resolved. It seems apparent from the ^{13}C spectrum that just like the spectrum of PAM obtained in homogeneous solution, Bernoulli statistics are followed and stereo-regularity has not been observed in the present case also. However, the PAM trapped

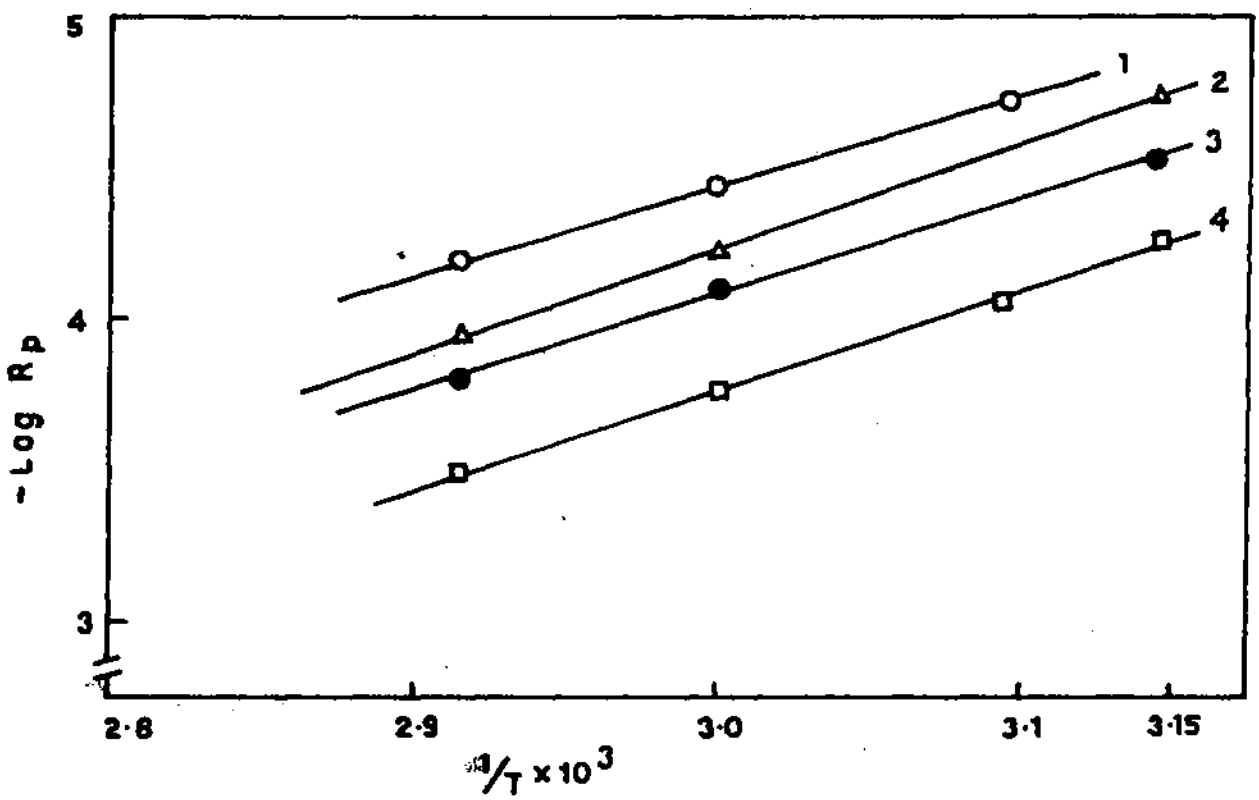

Fig. 26 Plots of - Log Rp versus 1/T with var ious amounts of AM with FeM / TU : [TU] = 0.04 M; [FeM] = 0.50% (w/v) and [AM] = 0.3 M (1); 0.4 M (2); 0.5 M (3) and 0.6 M (4).

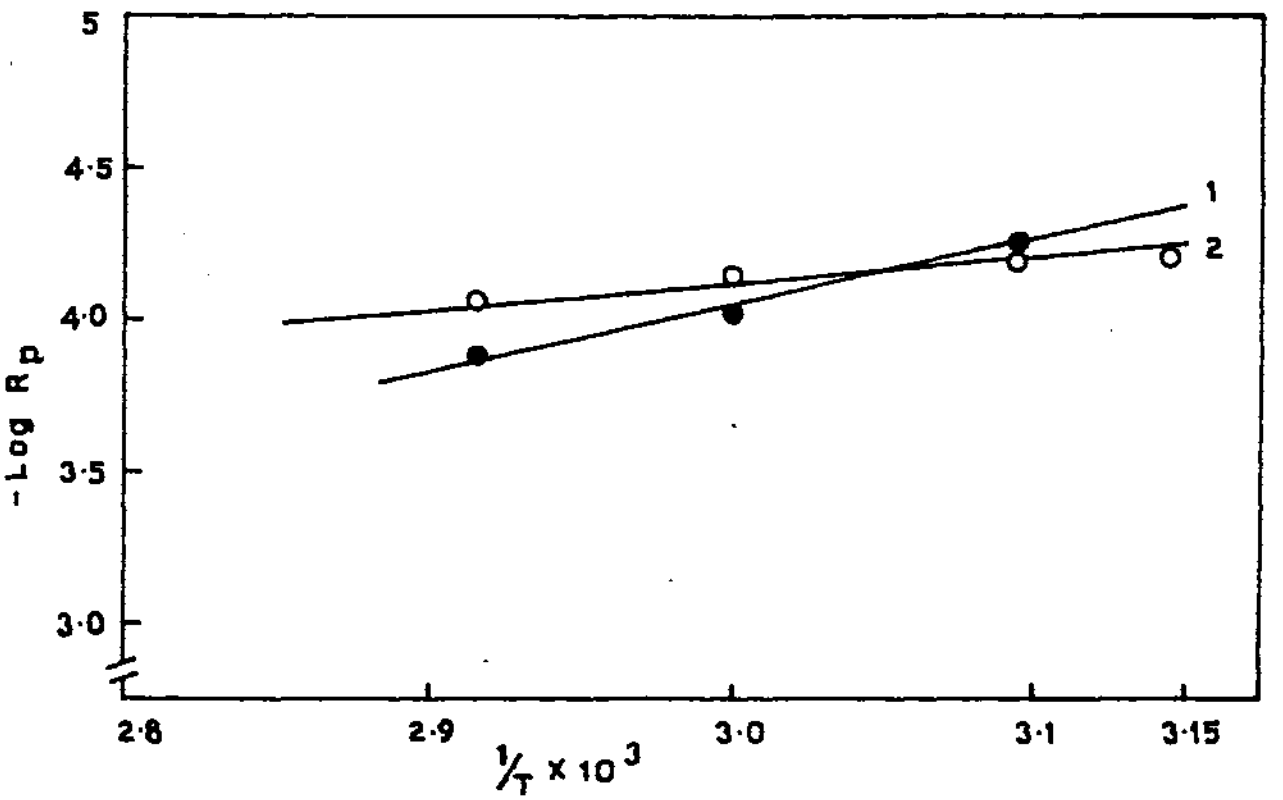

Fig. 27 Plots of - Log Rp versus I/T with AM usuing various amounts of FeM in presence of TU.
[AM] = 0.4; [TU] = 0.4 M and
[FeM] in w/v = 0.30% (1); 1.33% (2).

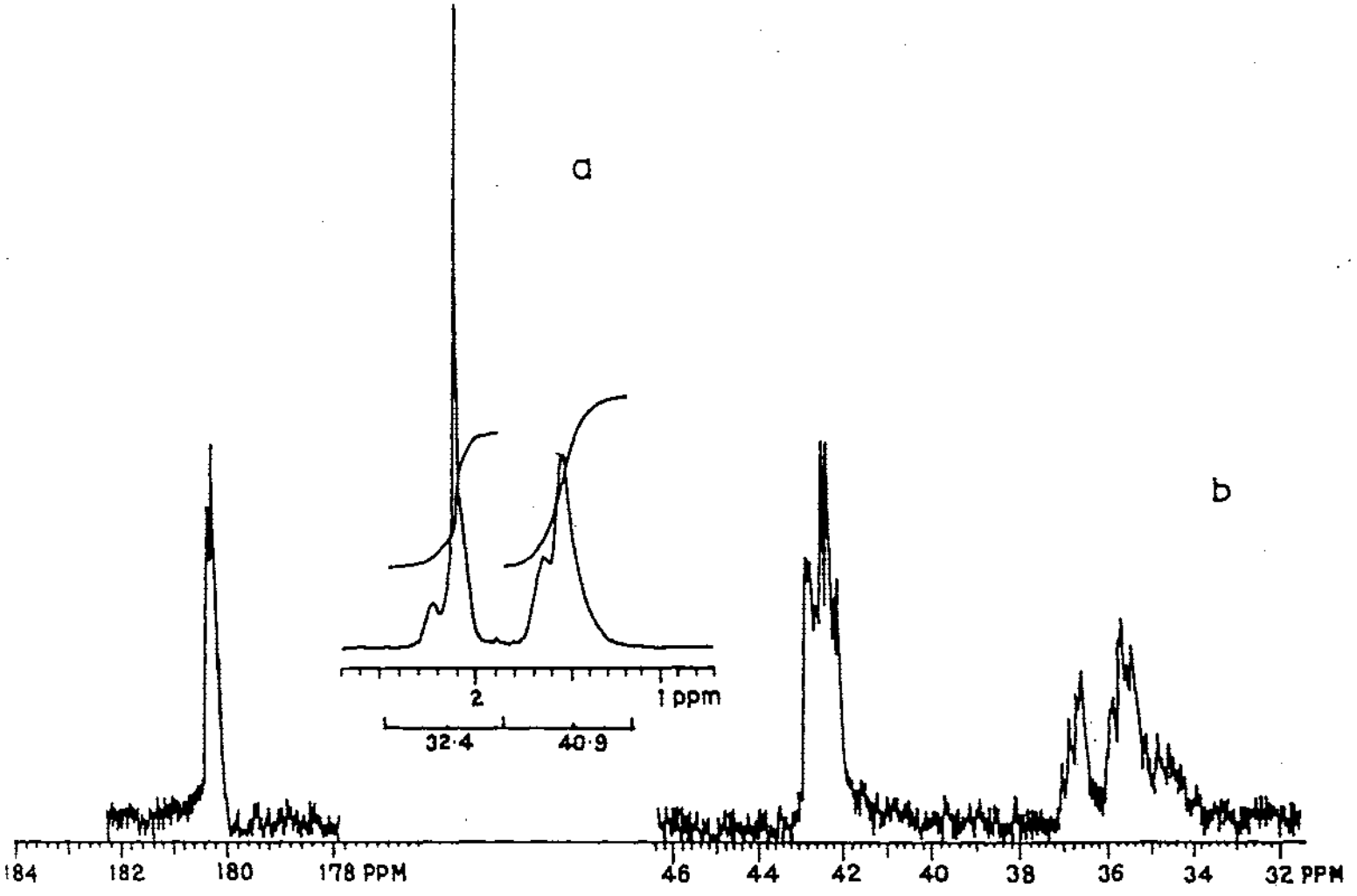

Fig. 28 ^{1}H and ^{13}n.m.r. spectra of thiourea terminated polyacrylamide formed on montmorillonite surface:
(a) ^{1}H n.m.r. spectrum; (b) ^{13}C n.m.r. spectrum.

inside the interlayer spaces of montmorillonite, which could not be extracted by washing with water may have such possibility of showing stereo-regularity. Attempts are being made to extract these polymers in mild condition for further study.

Effect of pH

Aqueous polymerization of AM is also dependent significantly on the pH of the solution. Previous report showed that low-moisture content clay minerals promote the spontaneous cationic polymerization of styrene but interfere with the free radical polymerization. Both Brönsted and Lewis acidity have been involved in the cationic polymerization initiated by dry clay minerals. The acidity of the clay mineral increases on drying[225-227]. In the present study, the reaction is carried out in aqueous medium and the surface acidity is less as compared to the dry mineral. In the pH range from 1.52 to 2.10, the polymerization is carried out with FeM/TU initiating system. Above pH 2.10, no significant polymerization takes place. The X_L, R_p and $[\eta]$ as well as M_v of the polymer are shown as a function of pH in Table 12. The transition metal (Fe(III)) in interlayer space of montmorillonite reacted with isothiourea, the tautomeric form of thiourea, generating amidosulfenyl radical to initiate polymerization[2116].

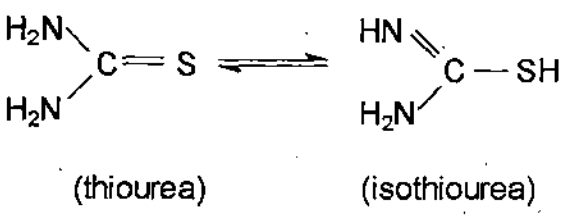

(thiourea) (isothiourea)

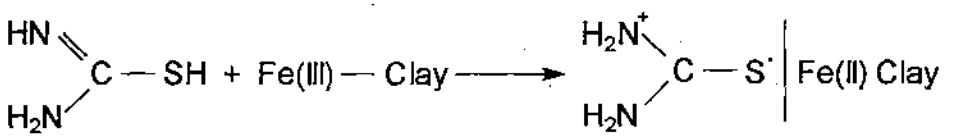

(amidosulfenyl radical)

Table - 12

Polymerization of 0.4 M AM (0.7108 g) in aqueous medium (25 ml.) in presence of 0.04 M TU and 0.50% (w/v) FeM at 50°C and varying pH.

pH	$R_p \times 10^5$ $mol.L^{-1}.s^{-1}$	X_L %	$[\eta]$ $ml.g^{-1}$	$M_v \times 10^{-5}$	Non-extractable PAM (wt%)
1.52	4.41	63	300	10.0	0.080
2.10	5.51	40	369	12.5	0.135
2.52[a]	—	—	—	—	—
2.95[a]	—	—	—	—	—

a = no polymer formed

At low pH the tautomeric equilibrium of TU in aqueous solution a shifted towards isothiocarbamido form facilitating the formation of primary radical. Moreover, the protonated form of the amidosulfenyl radical at low pH is more stable than the radical itself and consequently the dimerization process is less favourable[114].

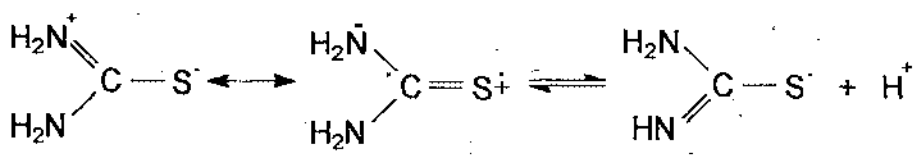

Previous studies have also shown that the intensity of E.S.R. signal of the spin trap-radical adduct was maximum at low pH[114].

Effect of Organic Solvents

It has been found that the use of additives like different

solvents[149,162,164,230], surfactants[150], neutral salts[229,210,157], complexing agents[154], retarders[228] and catalyst influenced the polymerization process and the properties of the resulting polymers. Different solvents were added to the polymerization medium and their effect on the polymer yield were studied. From the Table 13, it is found that some water miscible organic solvents viz., ethanol, DMSO and DMF depressed the polymer yield increasingly as the concentration of such solvents was increased from 2 to 40% (v/v). But in case of dioxan, the polymer yield increased with increasing the concentration upto 20% (v/v) but decreased at higher concentrations. The decrease in polymer yield on addition of such solvents was due to decrease in the area of a shielding of a strong hydration layer in aqueous medium resulting in the termination of radical end of the growing chain. Similar observations were made on addition of such solvents, namely DMF and alcohols to the polymerization medium by Misra and Bhattacharya[130,164]. Following factors[131] may considered for the observed increase in the polymer yield upto 20% dioxan solvent.

(i) Capability of the solvent to dissolve the monomer in the polymerization medium,

(ii) Formation of the solvent radicals from the primary radical species of the initiating system,

(iii) Contribution of the solvent radical in the activation of the monomer.

At a particular composition (20% v/v) of organic aqueous mixtures, the efficiency of solvents in promoting the polymerization of AM follows the order;

Dioxan > Ethanol >DMSO > DMF

The effect of concentration of different solvents on molecular weight are depicted in Table 13. The decrease in molecular weight with increasing concentration of the organic solvents is probably due to premature termination of the growing polymer chains by transfer to solvents[164].

Table -13

Effect of organic solvents on polymerization of 0.4 M AM (0.7108 g) in aqueous medium (25 ml.) in presence of 0.04 M TU and 0.50% (w/v) FeM at 50°C (pH ~ 2.01)

% of organic solvents (v/v)	Ethanol		DMSO		Dioxan		DMF		Water	
	X_L %	M_v x 10^{-5}	X_L %	M_v x 10^{-5}	X_L %	M_v x 10^{-5}	X_L %	M_v x 10^{-5}	X_L %	M_v x 10^{-5}
0	—	—	—	—	—	—	—	—	76	12.5
2	65.99	5.75	63.51	11.37	20.71	6.23	71.04	3.10	—	—
5	65.10	—	61.64	—	60.65	—	51.88	—	—	—
10	64.32	—	59.00	—	76.49	—	46.86	—	—	—
20	61.16	0.05	44.56	3.18	94.36	0.90	24.86	0.48	—	—
40	31.63	—	23.77	—	44.97	—	1.96	—	—	—

Effect of Surfactants

The effect of cationic (CTAB) and non ionic (Triton-x-100 (R)) surfactants on the polymerization of AM with FeM/TU initiating systems have been studied. The rate of polymerization as well as percent conversion are found to increase with cationic micelle concentration of CATB (Table 14). However, the effect of non ionic micelles on the polymerization rate and yield is reverse.

FeM/TU redox couple brings about 76% conversion in aqueous medium at 50°C but 98% conversion is observed in presence of CTAB under identical conditions. The hydrophobic interaction and the electrostatic attraction are possibly responsible for the spectacular rate enhancement or retardation

exhibited by the micelles of surfactants[231,233]. The molecular weight of the resulting polymer are found to decrease for both CTAB and Triton-X-100 (R).

Table -14

Effect of surfactants on polymerization of 0.4 M AM (0.7108 g) in aqueous medium (25 ml.) in presence of 0.04 M TU and 0.50% (w/v) FeM at 50°C (pH ~ 2.01)

Medium	Concentration $mol.L^{-1} \times 10^3$	$R_p \times 10^5$ $mol.L^{-1}.s^{-1}$	X_L %	$[\eta]$ $ml.g^{-1}$	$M_v \times 10^{-5}$	Non-extractable PAM (wt%)
Water	—	5.51	76	369	12.50	0.13
CATB	5	10.31	98	20	0.27	0.16
Triton-X-100 (R)	5	6.82	63	245	7.80	0.22

Kinetics and Mechanism

Polymerization mechanism and kinetics both are affected to a great extent due to the occurrence of the reaction in the mineral microenvironment resulting in the significant increase in the molecular weights and intrinsic viscosities of the polymers. The variation of the initial rate of polymerization as a function of monomer concentration in the presence of montmorillonite is shown (double logarithm plot) in Figure 29. Not all the points fell on a linear line. If it is assumed to be linear, the slope could be estimated as about 2.3. (The proposed mechanism, however, predicts an exponent of 2.0, the error in the experimental data may be introduced from the inherent coarseness in following the kinetics of

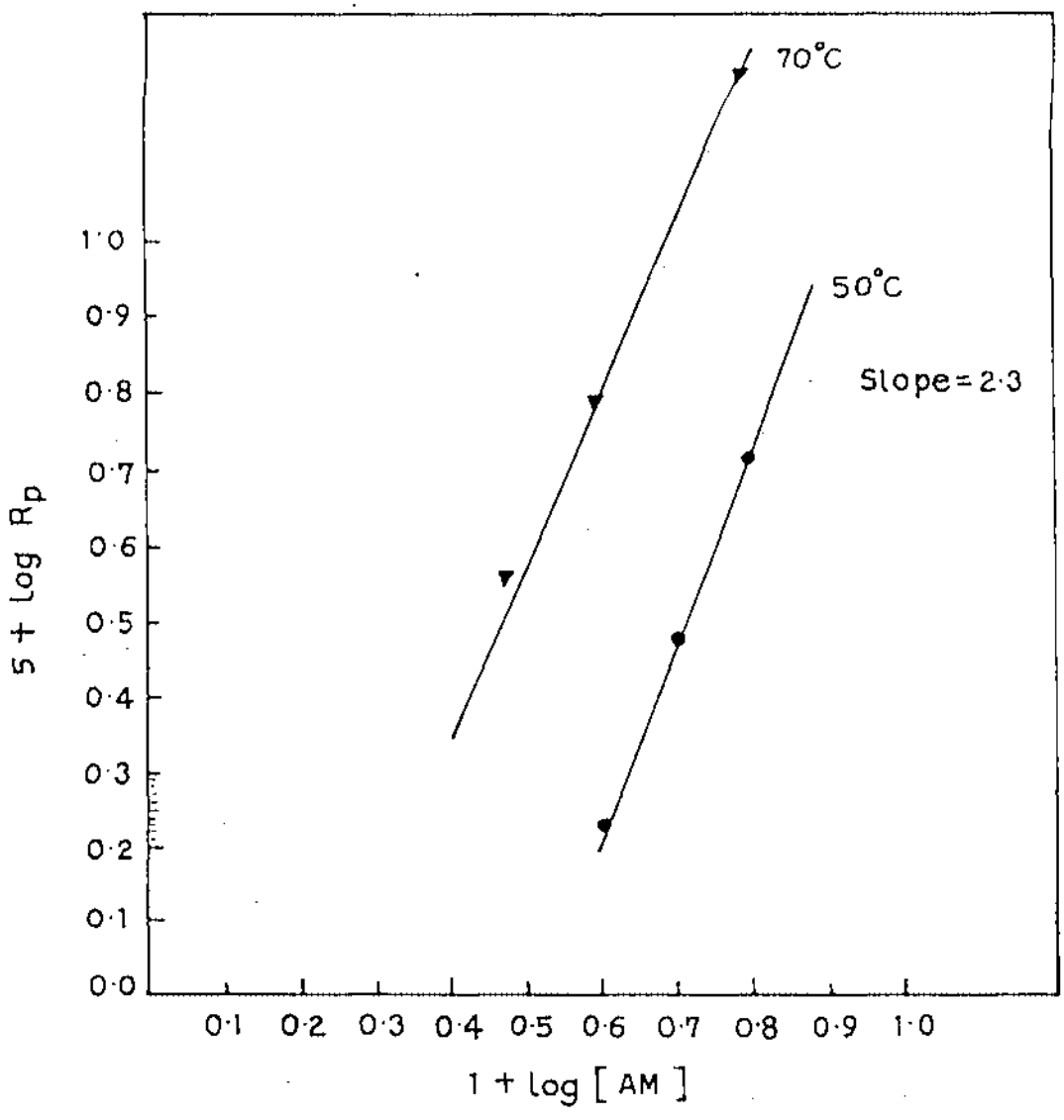

Fig. 29 Logarithmic plot of R_p versus [AM] for polymerization of AM by FeM / TU system.

a heterogeneous system.) The significant change in the monomer exponent due to occurrence of the reaction on the montmorillonite surface indicates that the polymerization mechanism is greatly affected by the mineral microenvironment. A rate dependence of second order and above on monomer concentration was also observed earlier in heterogeneous and precipitation polymerization of acrylamide and various interpretations, including 'cage effect' and 'complex theory' were proposed to account for the significant departure from first order kinetics[223,224]. The 'cage effect' suggests that when an initiator decomposes into two radicals, there is a formation of a potential barrier by the surrounding solvent molecules which prevent their immediate diffusion and favours their destruction by mutual recombination (already discussed). The 'complex theory' is based on the formation of a complex between the initiator and the monomer, the rate of initiation then being determined by the rate of decomposition of the complex. The 'cage effect' seems to be a good conceptual starting point in explaining the high monomer exponent which have been observed in the present system. To examine the dependence of rate on the montmorillonite content and $\overline{Fe}$(III) concentrations, the initial rate of polymerization is plotted as a function of $\overline{Fe}$(III) ion concentration (Figure 30). R_p is increased with the montmorillonite and $\overline{Fe}$(III) contents of the reaction mixture but the slope of the logarithm plot varied from 0.25 to 0.40 as a result of raising the reaction temperature from 50° to 70°C. However, if the locus of polymerization is assumed to be the interlayer space of montmorillonite, above slopes cannot be regarded as metal ion exponents because increasing addition of $\overline{Fe}$(III)-saturated mineral does not increase $\overline{Fe}$(III) ion concentration in the mineral phase but, on the contrary, only adds to the total metal ion and adsorbent contents of the reaction mixture. This, in tern, increases monomer and TU contents of the intercalate position, which result in the high rates of polymer yield. In order to measure the actual metal exponent for the reaction in the mineral phase, R_p values were plotted as a function of Fe(III) ion concentration in the montmorillonite gel. The concentrations of Fe(III) in the montmorillonite gel were varied by adding calculated quantities of HM in the reaction mixture

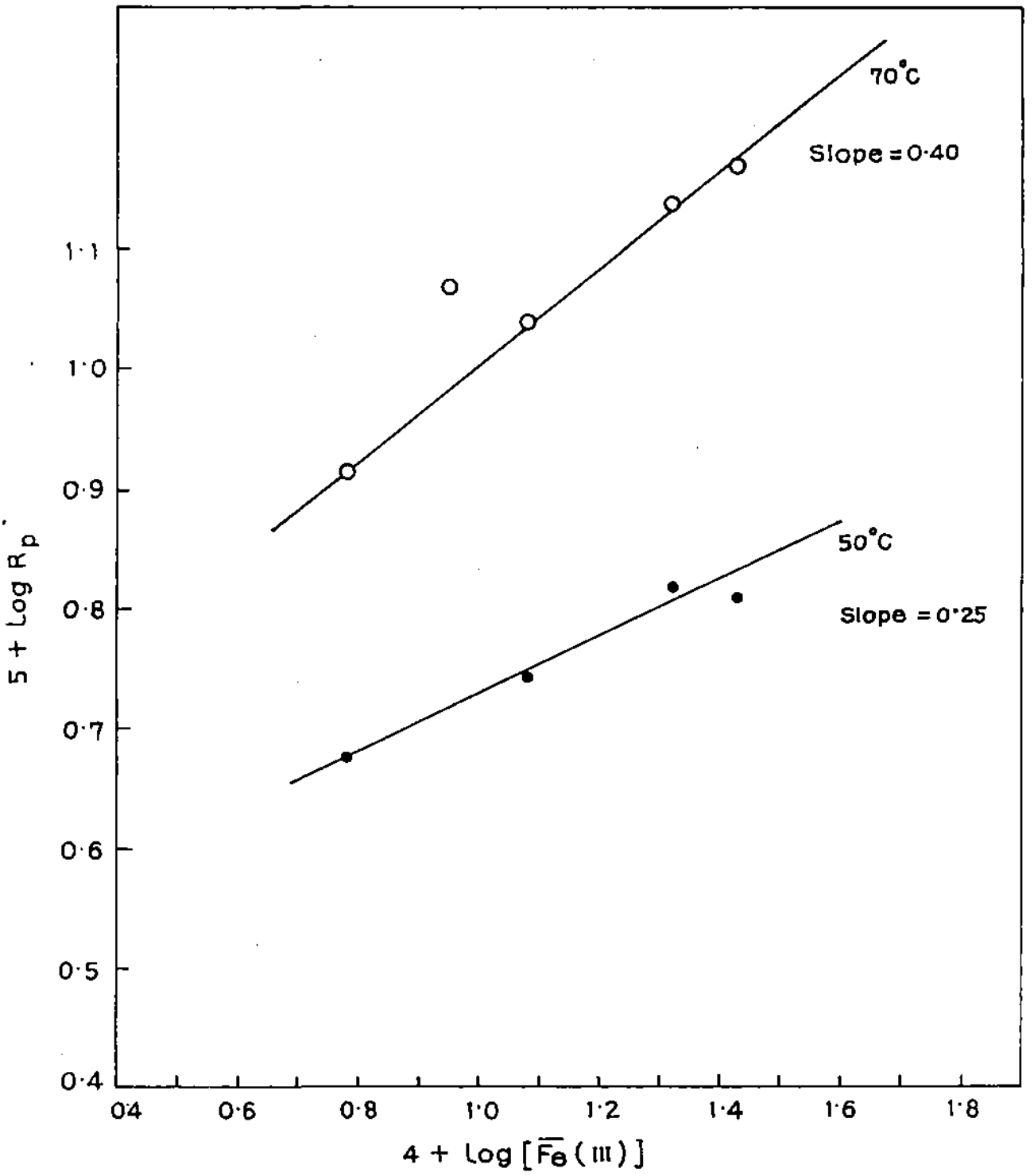

Fig. 30 Logarithm plot of Rp versus [$\overline{Fe}$ (III)] : [AM] = 0.4 M; [TU] = 0.04 M and[MO] = 0.5%

(Table 8). The slope of such logarithm plot (Figure 31) has been estimated as 0.50 at 50°C. (The concentration of Fe(III) now being moles of interlayer Fe(III) ions per 1000 ml. montmorillonite gel; the water content of montmorillonite sample was measured following the method described by Marinsky and co-workers and found to be 10 $ml.g^{-1}$)[234]. Figure 32 shows the dependence of R_p on TU concentrations. Since the isothiocarbamido primary radicals have strong tendency to dimerize above 0.05 $mol.L^{-1}$, present study was confined below that concentration only[114]. Again not all the points fell on the linear line (in the logarithm plot) owing to the heterogeneous reaction mixture. However, the slopes of the average line drawn through the points at two different temperatures indicate that the reaction is first order with respect to TU concentrations. To rationalize the experimental results and to predicts a possible mechanism for the seemingly complex polymerization reaction occurring in the mineral microenvironment, the following assumptions are made[221,222].

(1) Intercalated TU reacts fast with $\overline{Fe(III)}$ ions of montmorillonite layered spaces to form the reactive $TU^{\bullet}$ (isothiocarbamido radicals) via an intermediate complex. The decomposition of the complex is the rate controlling step.

(2) In the acidic and metal ion exchanged aqueous montmorillonite system, a fraction of the intercalated acrylamide molecules are present near reacting sites as pairs either through hemisalts formation, where two amide molecules share a proton by means of symmetrical hydrogen bond or/and through weak coordination to the exchanged cations[2]. The protonated as well as the complexed amide pairs are at first equilibrium with unprotonated and free amide molecules, respectively, which are defined by a protonation constant or a formation constant. In view of high monomer exponent, it is certain that it must have resulted in part from the involvment of monomer in the initiation step, where such monomer pairs are entailed.

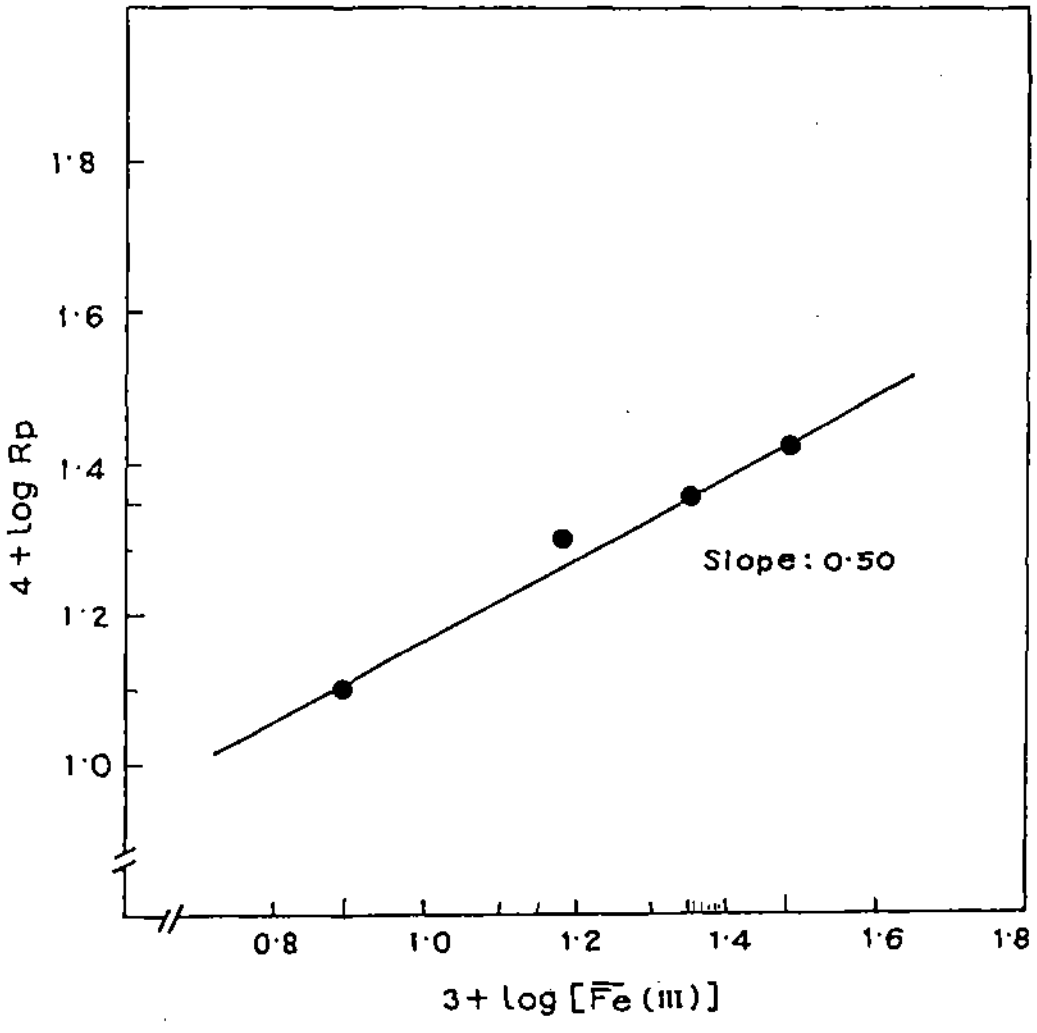

Fig. 31 Logarithm plot of Rp versus [$\overline{Fe}$(III)] : [AM] = 0.4 M; [TU] = 0.04 M and[MO] = 0.5% ([Fe (III)] represents moles of ferric ions in the montmorillonite gel phase).

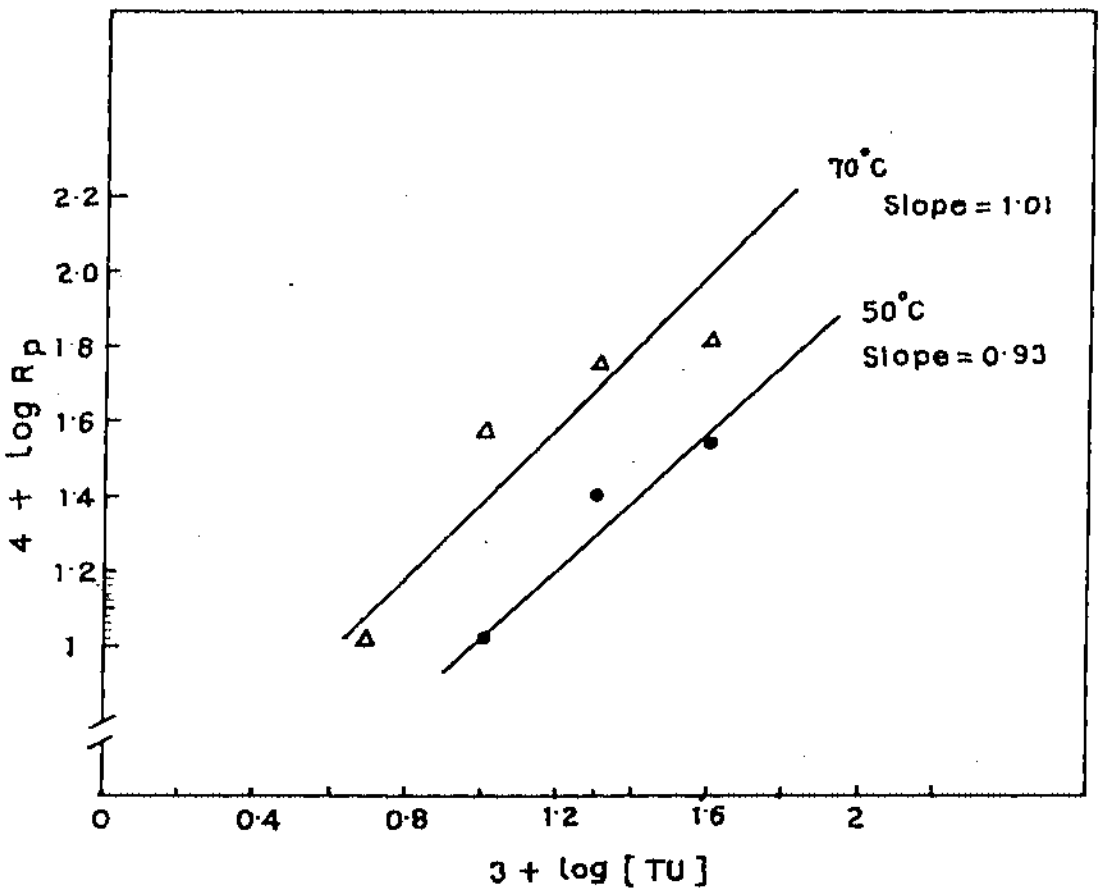

Fig. 32 Logarithm plot of Rp versus [TU] : [$\overline{Fe}$ (III)] = 1.5 x 10^{-3} M; [AM] = 0.4 M and [MO] = 0.5%.

(3) Since the reactive TU radicals are formed as pairs, assumption of the 'cage effect' seems to be conceptually appropriate. The initiation step involves collision of the 'amide pairs' with caged TU radicals at the wall of the cage and random diffusion of the radicals from the cage and their secondary recombination are less significant in comparison to the rate of dimerization of caged radicals or their reaction with acrylamide.

Initiation

$$\overline{Fe}(III) + TU \underset{}{\overset{K}{\rightleftharpoons}} \underset{\text{complex}}{\overline{Fe}(III) - TU} \qquad (13)$$

$$\overline{Fe}(III) - TU + TU \xrightarrow{k_d} \overline{Fe}(II) + \left(2TU^{\bullet}\right) + H^{+} \qquad (14)$$

$$\left(TU^{\bullet}\right) + M_2H^{+} \xrightarrow{k_i} M_1^{\bullet} + M + H^{+} \qquad (15)$$

Propagation

$$M_1^{\bullet} + M \xrightarrow{k_p} M_2^{\bullet} \qquad (16)$$

$$M_{n-1}^{\bullet} + M \xrightarrow{k_p} M_n^{\bullet} \quad \ldots\ldots\ldots \text{ etc.}$$

Termination

$$M_n^{\bullet} + M_n^{\bullet} \xrightarrow{k_t} M_n - M_n \qquad (17)$$

$$\left(TU^{\bullet}\right) + \overline{Fe}(III) \xrightarrow{k_t'} TU + \overline{Fe}(II) \qquad (18)$$

$$\left(2TU^{\bullet}\right) \xrightarrow{k_t''} TU - TU \qquad (19)$$

(caged species are enclosed in brackets)

Utilising the equation (13) and (14), the consumption rate of Fe(III) concentration as shown in previous section 3.3.3, is given below:

$$-\frac{d}{dt}\left[\overline{Fe}(III)\right] = \frac{k_d K\left[\overline{Fe}(III)\right][TU]^2}{1+K[TU]} \qquad (20)$$

Now, assuming that the rate of formation of TU radicals is exactly equal to the rate of disappearing $\overline{Fe}$(III) ions we obtain, (considering the steady state of $TU^{\bullet}$).

$$\frac{k_d K\left[\overline{Fe}(III)\right][TU]^2}{1+K[TU]} = k_i K^{I}\left[TU^{\bullet}\right][M]^2 + \frac{k_t^{'}\left[TU^{\bullet}\right]\left[\overline{Fe}(III)\right]}{1+K[TU]} + k_t^{''}\left[TU^{\bullet}\right]$$

($K^{I} = [M_2H^{+}] / [M]^2$ is the apparent protonation constant at a fixed pH (or a formation constant))

$$\left[TU^{\bullet}\right] = \frac{k_d K\left[\overline{Fe}(III)\right][TU]^2}{\left(k_i K^{I}[M]^2 + \frac{k_t^{'}\left[\overline{Fe}(III)\right] + k_t^{''}}{1+K[TU]}\right)(1+K[TU])} \qquad (21)$$

Again, considering the steady state of $M_n^{\bullet}$

$$k_i K^{I}\left[TU^{\bullet}\right][M]^2 = k_t\left[M_n^{\bullet}\right]^2$$

$$\left[TU^{\bullet}\right] = \frac{k_t\left[M_n^{\bullet}\right]^2}{k_i K^{I}[M]^2} \qquad (22)$$

Equating RHS of equation (21) and (22)

$$\frac{k_t\left[M_n^{\bullet}\right]^2}{k_i K^{I}[M]^2} = \frac{k_d K\left[\overline{Fe}(III)\right][TU]^2}{k_i K^{I}[M]^2 + k_i K^{I} K[M]^2[TU] + k_t^{'}\left[\overline{Fe}(III)\right] + k_t^{''}(1+K[TU])}$$

$$\left[M_n^{\bullet}\right]^2 = \frac{k_i K^{I} K k_d\left[\overline{Fe}(III)\right][TU]^2[M]^2}{k_t\left(k_i K^{I}[M]^2 + k_i K^{I} K[M]^2[TU] + k_t^{'}\left[\overline{Fe}(III)\right] + k_t^{''}(1+K[TU])\right)}$$

$$\left[M_n^{\bullet}\right] = \frac{\left(k_i K^{l} K k_d\right)^{1/2} \left[\overline{Fe}(III)\right]^{1/2} [TU][M]}{k_t^{1/2}\left(k_i K^{l} [M]^2 + k_i K^{l} K [M]^2 [TU] + k_t^{'}\left[\overline{Fe}(III)\right] + k_t^{''}(1+K[TU])\right)^{1/2}}$$

$$R_p = k_p \left[M_n^{\bullet}\right][M]$$

$$R_p = \frac{k_p\left(k_i K^{l} K k_d\right)^{1/2} \left[\overline{Fe}(III)\right]^{1/2} [TU][M]^2}{k_t^{1/2}\left(k_i K^{l} [M]^2 + k_i K^{l} K [M]^2 [TU] + k_t^{'}\left[\overline{Fe}(III)\right] + k_t^{''}(1+K[TU])\right)^{1/2}} \qquad (23)$$

If the oxidative termination (step 18) is assumed to be insignificant in comparison with the dimerization rate of caged radicals, equation (23) reduces to:

$$R_p = \frac{k_p\left(k_i K^{l} K k_d\right)^{1/2} \left[\overline{Fe}(III)\right]^{1/2} [TU][M]^2}{k_t^{1/2}\left(k_i K^{l} [M]^2 + k_i K^{l} K [M]^2 [TU] + k_t^{''}(1+K[TU])\right)^{1/2}} \qquad (24)$$

The interpretation of high kinetic order of the monomer finally hinges on the dominance of a reaction between caged radicals and those of monomers with the radicals at the cage wall. Although the concentrations of the monomer and TU in solution phase were fixed mostly at 0.40 mol.L^{-1} and 0.04 mol.L^{-1} respectively, the concentration of intercalated species must be much lower, specially due to the presence of water molecules in the interlayer spaces.

Thus, while the concentrations, [M] and [TU], in the montmorillonite gel-phase should be

$$[M] = L_o^a \theta_m = \frac{L_o^a K_m^a [M]_s}{1 + K_{tu}^a [TU]_s + K_m^a [M]_s} \qquad (25)$$

and

$$[TU] = L_o^a \theta_m = \frac{L_o^a K_{tu}^a [TU]_s}{1 + K_{tu}^a [TU]_s + K_m^a [M]_s} \qquad (26)$$

(subscript 's' denotes solution)

(L_o^a and θ are the total active sides in units mass of montmorillonite and the fraction of total sites occupied by such species respectively; K_m^a and K_{tu}^a are the selectivity coefficients).

The denominators of equations (25) and (26) are nearly unity. By appropriate substitution of [M] and [TU] in equation (24) and considering the dominance of the last term of the denominator over others, the equation becomes

$$R_p = \frac{k_p \left(k_d k_i K K^1 / k_t k_t''\right)^{1/2} K_{tu}^a \left(K_m^a\right)^2 \left(L_o^a\right)^3 \left[\overline{Fe(III)}\right]^{1/2} [TU]_s [M]_s^2}{\left(1 + K L_o^a K_{tu}^a [TU]_s\right)^{1/2}} \qquad (27)$$

(Values of K_m^a (or K_{tu}^a), L_o^a and K are of the order of 10^{-2}, 2 m.mol.g^{-1} and 2 L.mol^{-1}, respectively[221]. Small values of above parameters including that of K^1, ensure that terms involving quadratic and above concentrations are very small in the present conditions[235,236]).

Further inspection of equation (27) shows that the value of $KL_o^a K_{tu}^a [TU]_s$ in the denominator varies from 10^{-5} to 10^{-6} for the variation of aqueous TU concentration from 0.05 to 0.005 mol.L^{-1}. This implies that the rate equation under the present condition is reduced to

$$R_p = k_p \left(k_d k_i K K^1 / k_t' k_t''\right)^{1/2} K_{tu}^a \left(K_m^a\right)^{1/2} \left(L_o^a\right)^3 \left[\overline{Fe(III)}\right]^{1/2} [TU]_s [M]_s^2 \qquad (28)$$

Reviewing the above result, it is found that equation (28) could satisfactorily account for the present behaviour of the $\overline{Fe}$(III)-TU initialised acrylamide polymerization exhibited in the aqueous montmorillonite layered space.

3.5 AQUEOUS POLYMERIZATION OF ACRYLAMIDE BY Ce(IV) - EDTA REDOX COUPLE ON MONTMORILLONITE SURFACE

3.5.1 Introduction

Redox initiators have been used extensively in homo and copolymerization reactions. Considerable amount of works are available in the literature on redox polymerization where metal ions viz., cerium (IV), vanadium (V), chromium (VI), cobalt (III) and iron (III) were used as oxidants[222,237]. The reducing agents in the above redox systems were alcohols, aldehydes, acids, thiols and amines. Although most of them showed low conversions and rates, some of them exhibited more promising results than others. However, a common feature of these systems is that almost all of them yield only low molecular weight polymers due to fast termination of polymer chain via transfer to the metal oxidant of the initiator couple. In the previous section of the present chapter a novel technique by which chain growth was enhanced by trapping the metal oxidants in the interlayer space of montmorillonite has been demonstrated. While the redox characteristics of the metal and its efficiency in activating redox polymerization of aqueous acrylamide molecules remain almost unaltered in the montmorillonite layered space, linear termination of growing polymer chain was sufficiently controlled. This is possible because polar organic activator (thiourea) as well as the monomer could intercalate between the layers of the mineral where the metal oxidants are already trapped. In this section, attempts have been made to extend the scope of the technique as described in section 3.4 by studying the effect of mineral microenvironment on Ce(IV)-EDTA initiated aqueous acrylamide polymerization with a view to generalise the adopted method for enhancing chain growth.

3.5.2 Experimental

Experimental procedure has been discussed in section 3.2.

3.5.3 Results and Discussion

Tables 15 - 17 represent the data pertaining to the initial rates (R_p), polymer yield (X_L), intrinsic viscosity [η] as well as molecular weight (M_v) and non-extractable polymer formed as functions of the concentration of $\overline{Ce}$(IV), EDTA, AM and temperature.

The molecular weights of the polymer are moderately high and ranged from 3.9×10^5 to 2.9×10^6. The initial rate of polymerization, R_p's obtained are ranged between (2.1 - 10.6) $\times 10^{-5}$ mol.L^{-1}.s^{-1} depending on various reaction parameters. Upto 95% of the polymers are formed at 50°C in the presence of 1.5×10^{-3} mol.L^{-1} of $\overline{Ce}$(IV) ions (EDTA = 0.01 mol.L^{-1} and AM = 0.4 mol.L^{-1}). At a fixed EDTA and $\overline{Ce}$(IV) concentrations, all the parameters, viz., R_p, X_L and M_v are increased with the increase in AM concentrations. The R_p and X_L also increase from 3.0×10^{-5} to 8.9×10^{-5} mol. $L^{-1}.s^{-1}$ and 16% to 50% respectively with the increase of AM concentrations in the range of (0.36-0.60) $\times 10^{-3}$ mol.L^{-1}. The value of [η] as well as M_v are also varied from 145 to 650 ml.g^{-1} and 3.9×10^5 to 2.87×10^6 respectively. On the other hand, R_p increases with increased concentration of EDTA. Higher concentration of the activator, EDTA, increases the concentration of initiating radicals and consequently the number of propagating polymer chain and the rate of polymerization increases. Higher the concentration of EDTA, higher is the polymer yield but lower is the molecular weights of the polymer. The value of [η] is also varied from 430 to 240 ml.g^{-1} with the variation of EDTA concentration between (2.5 to 10.0) $\times 10^{-3}$ mol.L^{-1}. At a fixed AM and EDTA concentrations, the R_P also increases with the increased concentration of $\overline{Ce}$(IV) ion. The concentration of $\overline{Ce}$(IV) in the montmorillonite gel phase was varied by adding calculated quantities of HM in the reaction mixture. Molecular weight of polymer and polymer yield as well as intrinsic viscosity decreased with increased Ce(IV) concentration in the gel phase.

Table - 15

Polymerization of AM in aqueous medium (25 ml.) in presence of 0.0025 M EDTA and 0.50% (w/v) CeM at 50°C and varying monomer concentrations (pH ~ 2.01). [Concentration of interlayer $\overline{Ce}$(IV) is 1.5 m.mol. per litre of the reaction mixture. Corresponding concentration in montmorillonite gel phase is 0.03 $m.mol.L^{-1}$]

[AM] $mol.L^{-1}$	$R_p^b \times 10^5$ $mol.L^{-1}.s^{-1}$	X_L^c %	$[\eta]^d$ $ml.g^{-1}$	$M_v \times 10^{-5}$	Non-extractable PAM (wt%)
0.36	3.0	16	145	3.9	0.01
0.40	4.5	44	430	16.5	0.06
0.50	7.9	40	620	26.9	0.23
0.60	8.9	50	650	28.7	0.70

[b]Initial polymerization rate, [c]Yield after 4.5 hrs., [d]Intrinsic viscosity.

Table - 16

Polymerization of 0.4 M AM (0.7108 g) in aqueous medium (25 ml.) in presence of EDTA and 0.50% (w/v) CeM at 50°C and varying EDTA concentrations (pH ~ 2.01).

[EDTA] $mol.L^{-1}$	$R_p^b \times 10^5$ $mol.L^{-1}.s^{-1}$	X_L^c %	$[\eta]^d$ $ml.g^{-1}$	$M_v \times 10^{-5}$	Non-extractable PAM (wt%)
0.0025	4.5	44	430	16.5	0.06
0.0050	7.0	86	300	10.2	0.20
0.0075	9.7	89	210	6.4	0.27
0.0100	10.6	95	240	7.6	0.30

Table - 17

Polymerization of 0.4 M AM (0.7108 g) in aqueous medium (25 ml.) in presence of 0.0025 M EDTA and 0.50% (w/v) montmorillonite (CeM + HM) at 50°C and varying Ce(IV) concentrations in gel phase (pH ~ 2.01).

$[\overline{Ce(IV)}]^a$ m.mol.L^{-1}	$R_p \times 10^5$ mol.$L^{-1}.s^{-1}$	X_L %	$[\eta]$ ml.g^{-1}	$M_v \times 10^{-5}$	Non-extractable PAM (wt%)
0.0125	2.1	68	600	25.7	0.25
0.0150	2.2	63	620	26.9	0.19
0.0188	2.6	61	325	11.3	0.04
0.0225	3.1	35	450	17.6	0.13

[a]Concentration of interlayer Ce(IV) in m.mol. per litre in montmorillonite gel.

Table - 18

Polymerization of 0.4 M AM (0.7108 g) in aqueous medium (25 ml.) in presence of 0.0025 M EDTA and 0.50% (w/v) CeM at different temperatures (pH ~ 2.01).

$[\overline{Ce(IV)}]^a$ m.mol.L^{-1}	Temp. °C	$R_p \times 10^5$ mol.$L^{-1}.s^{-1}$	X_L %	$[\eta]$ ml.g^{-1}	$M_v \times 10^{-5}$	Non-extractable PAM (wt%)
	70	22.2	85	315	10.9	0.11
	60	10.2	75	270	8.9	0.09
1.5	50	4.5	44	430	16.5	0.06
	45	2.0	40	500	20.0	0.17

[a]Concentration of interlayer Ce(IV) in m.mol per litre of the reaction mixture.

The percent conversion of polymerization has been plotted as a function of reaction time at different AM, EDTA and Ce(IV) concentrations in Figures 33 - 35. No induction period is observed in any set of the polymerization experiment. The increasing amount of non-extractable polymer has been observed with increasing concentration of AM, EDTA but the same is decreased with increase in concentration of Ce(IV) in gel phase.

Effect of Temperature

The effect of temperature on the polymerization rate of acrylamide was investigated over the range of 45° - 70°C (Table 18). The higher the temperature faster is the polymerization rate and higher the polymer yield (Figure 36). On the other hand, higher the temperature, lower is the molecular weight of the polyacrylamide formed. As shown in Figure 37 the temperature dependence of the polymerization rate almost followed the Arrhenius relations. The pseudo-overall activation energy might be estimated from the slope of the plot: it was 19.3 kcal.mol^{-1}, which is close to that usually observed for polymerization by redox systems[169,238].

Kinetics and Mechanism

Ce(IV)-EDTA pair is an effective initiator for the aqueous polymerization of acrylamide. The polymers formed by the above system should carry with EDTA at the terminal. In other words, the EDTA supported chelating polymers may be obtained, and they would be potentially used as catalyst for chemical reactions, chelating agents for metallic ions and functional polymers. Figure 38 shows the logarithm plot of R_p as a function of monomer concentration. The plot is linear with a slope of approximately unity. This indicates that the initial rate is approximately first order with respect to the monomer concentration. Small value of R_p below an acrylamide concentration of 0.4 mol.L^{-1}, which results in the marked deviation of the point from the straight line of Figure 38 is probably

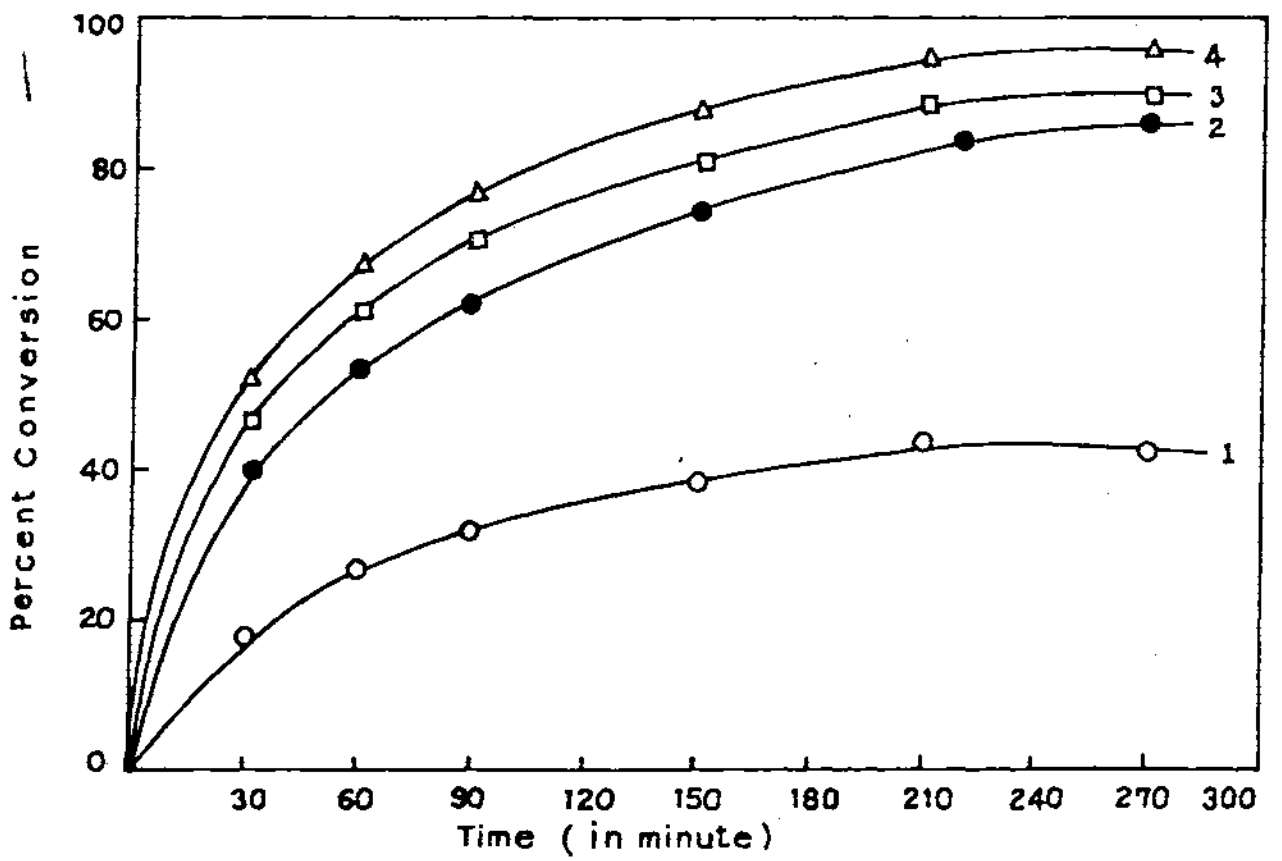

Fig. 33 Time-conversion plots for the aqueous polymerization of AM at 50°c with CeM/EDTA : [$\overline{Ce}$ (IV)] = 1.5 x 10^{-3} M; [MO] = 0.5% (w/v) and [AM = 0.36 M (1); 0.4 M (2); 0.5 M (3) and 0.6 (4).

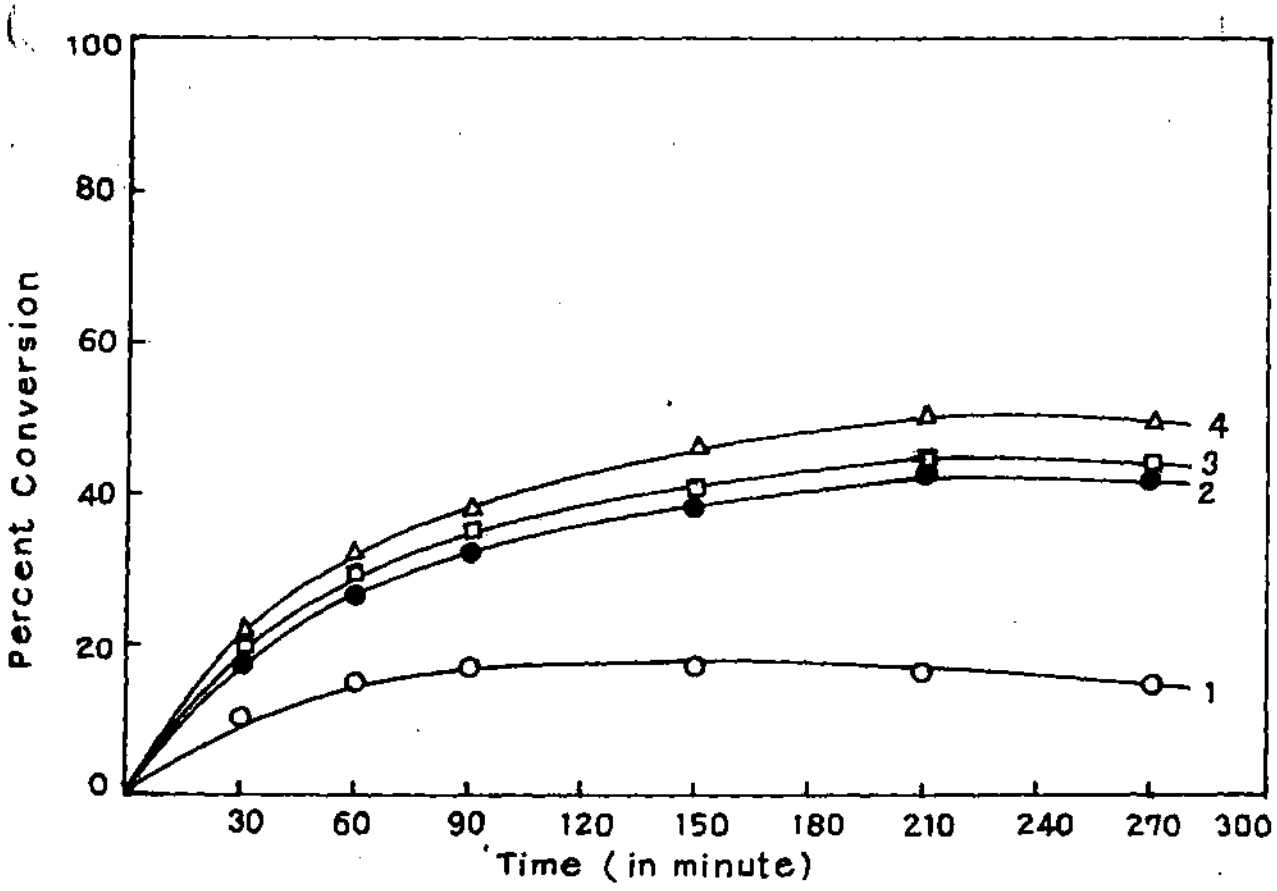

Fig. 34 Time-conversion plots for the aqueous polymerization of AM at 50°c with CeM/EDTA : [AM] = 0.4 M; [$\overline{Ce}$ (IV)] = 1.5 x 10^{-3} M; [MO] = 0.5% (w/v) and [EDTA] = 2.5 x 10^{-3} M; (1); 5 x 10^{-3} M (2); 7.5 x 10^{-3} M (3) and 1 x 10^{-2} M (4).

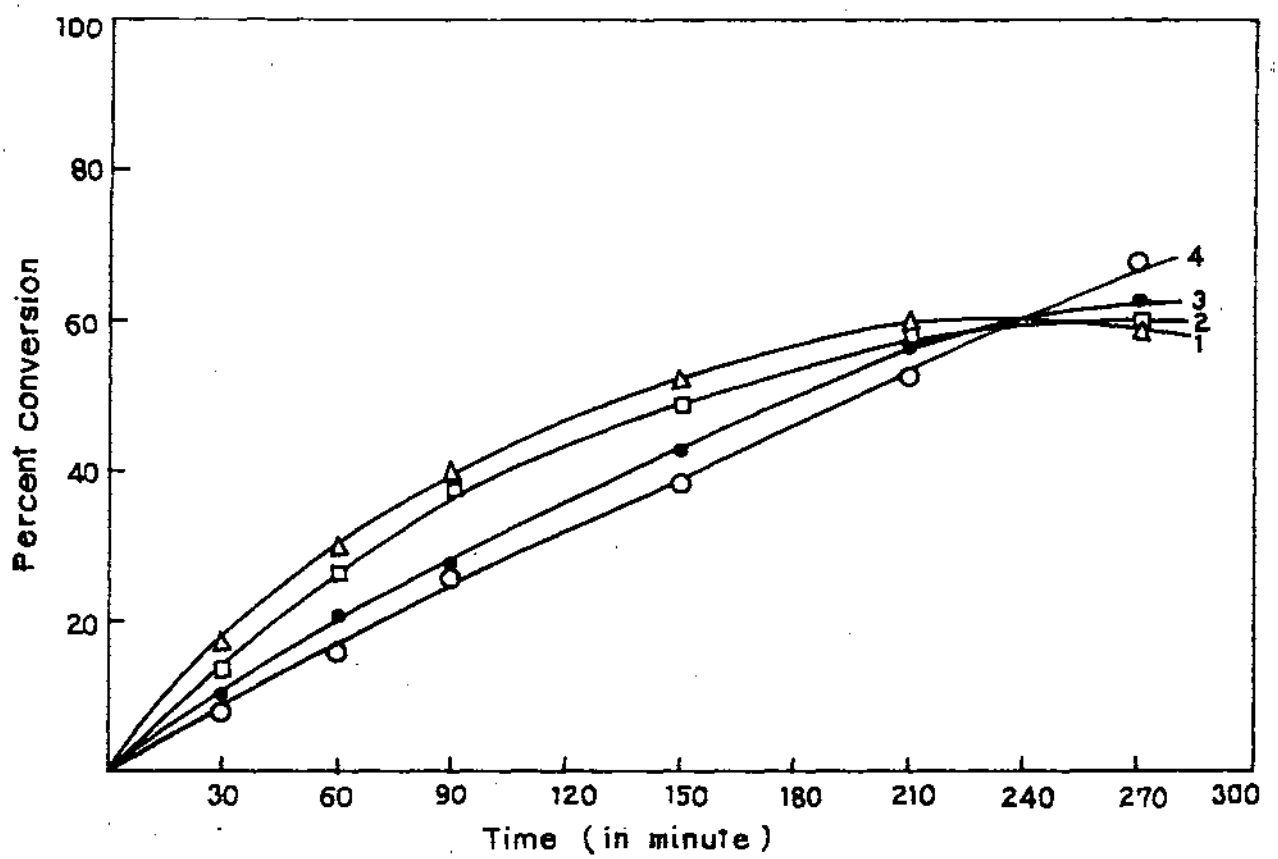

Fig. 35 Time-conversion plots for the aqueous polymerization of AM at 50°c with CeM/EDTA : [AM] = 0.4 M; [EDTA] = 2.5 x 10^{-3} M;[MO] = 0.5% (w/v) and [$\overline{Ce}$ (IV)] = 22.5 x 10^{-3} M (1); 18.8 x 10^{-3} M (1); 15.0 x 10^{-3} M (3) and 12.5 x 10^{-3} (4) ([$\overline{Ce}$ (IV)] represents moles of inter-layer Ce (IV) ions in 1000 ml of Mo gel phase).

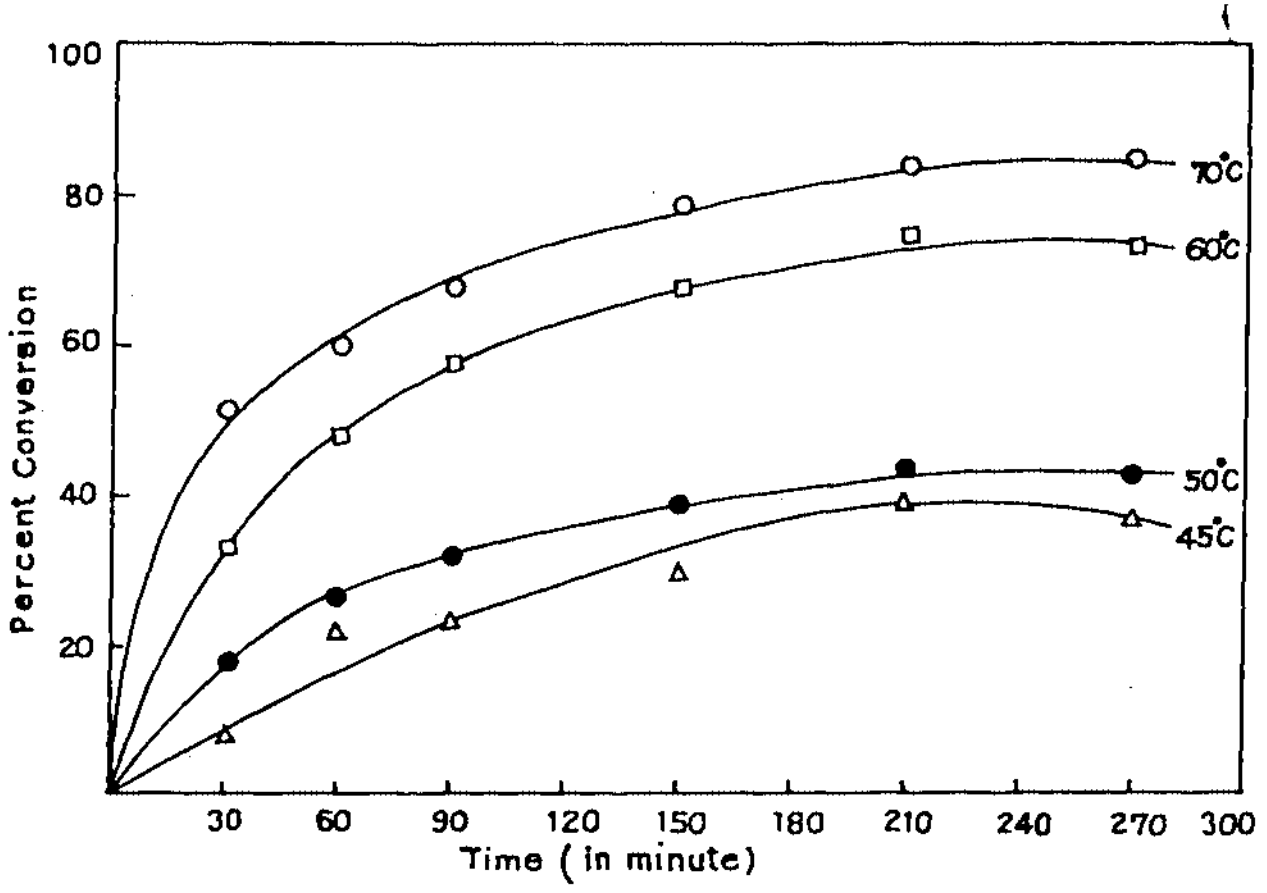

Fig. 36 Time-conversion plots for the aqueous polymerization of AM with Ce(IV)/EDTAat 70°c, 60°c, 50°c, and 45°c : [AM] = 0.45; [$\overline{Ce}$ (IV)] = 1.5 x 10^{-3} M; [MO] = 0.5% and [EDTA] = 2.5 x 10^{-3} M.

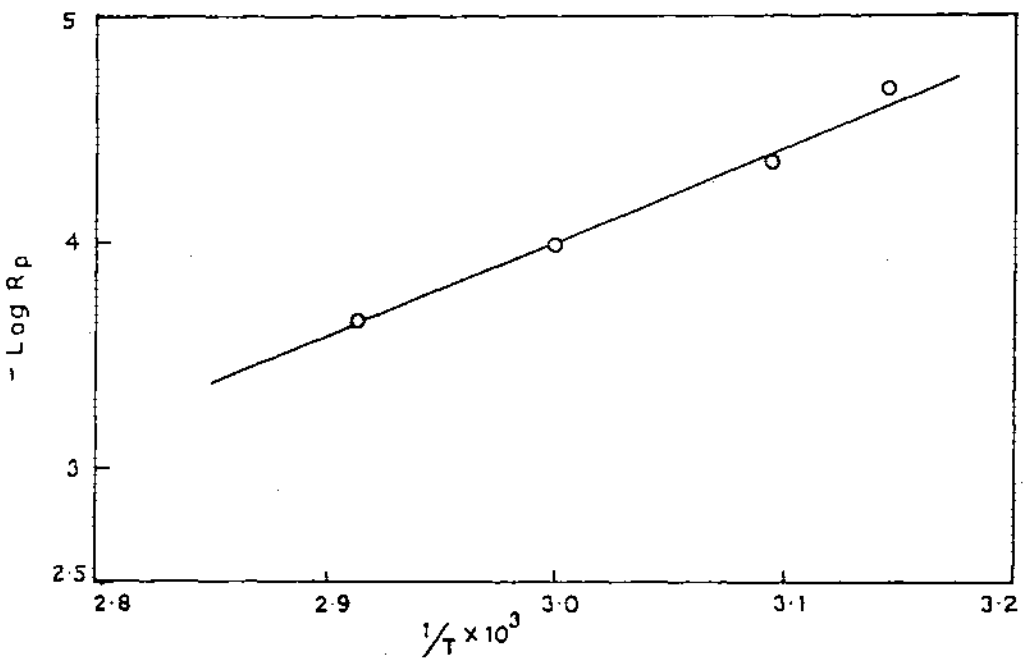

Fig. 37 Plot of - Log Rp versus 1/T for aqueous polymerization of AM with Ce M / EDTA. [AM] = 0.4 M; [EDTA] = 2.5 x 10^{-3} M; [$\overline{Ce}$ (IV)] = 1.5 x 10^{-3} M and [Mo] = 0.5%

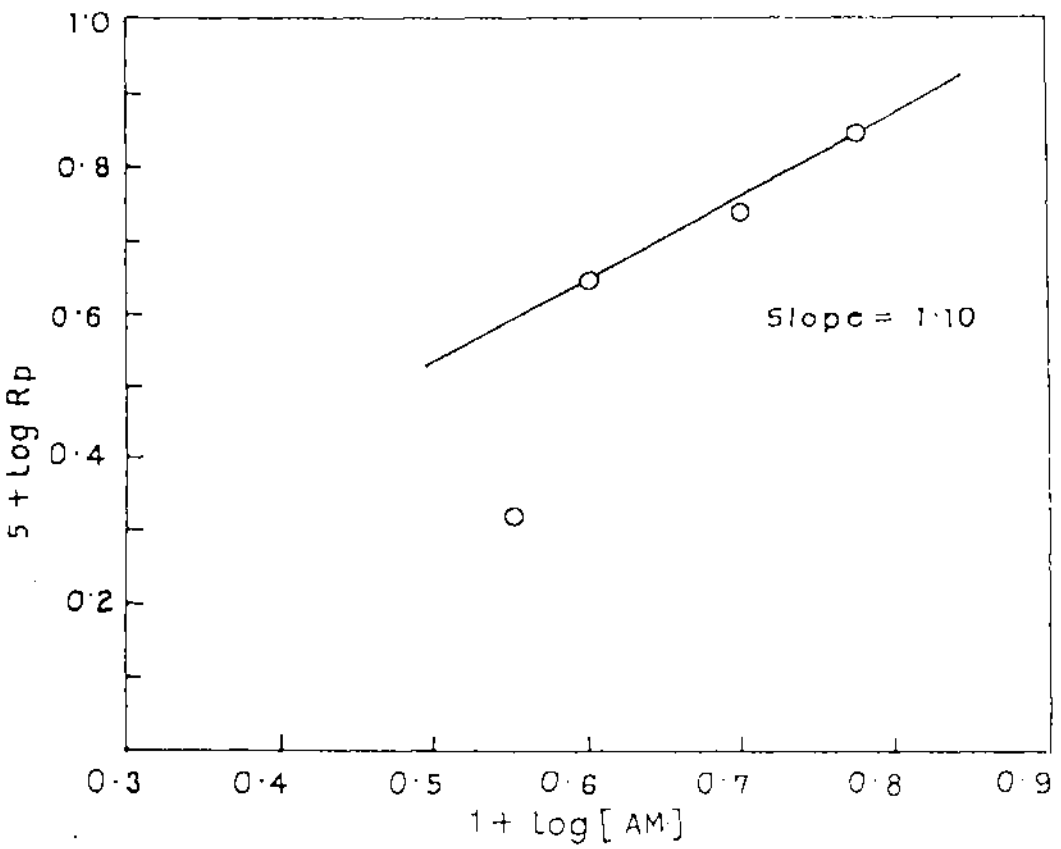

Fig. 38 Logarithmic plot of R_p versus [AM] for polymerization of AM by CeM / EDTA: [Ce(IV)] = 1.5×10^{-3} M; [EDTA] = 2.5×10^{-3} M and [Mo] = 0.50%.

an indication of low level of intercalated monomer in the interlayer space. The significant departure of monomer exponent from 2.0 (in absence of montmorillonite) to 1.0 in the presence of clay mineral demands that the polymerization mechanism be reconsidered for the present condition[222]. To examine the dependence of the rate of reaction on $\overline{Ce}$(IV) ion concentrations, the initial rate of polymerization is plotted as a function of $\overline{Ce}$(IV) concentrations in montmorillonite gel phase (water content of montmorillonite gel was 10 $ml.g^{-1}$ as already mentioned in section 3.4.3). The slope of such a logarithmic plot (Figure 39) has been estimated as 0.64 (proposed mechanism, however, predicts an exponent of 0.50, the error in the experimental data may be introduced from the inherent coarseness in following kinetics of a heterogeneous system). Figure 40 shows the dependence of R_p on EDTA concentration. Not all points fell on a linear line (in the logarithm plot) owing to the heterogeneous reaction mixture. However, the slope of the average line drawn through the points is found to be approximately 0.50. To rationalize the above experimental results and to predict a possible mechanism for the $\overline{Ce}$(IV)-EDTA initiated polymerization in presence of montmorillonite, following assumptions are made.

(1) Intercalated EDTA molecules react fast with $\overline{Ce}$(IV) ions of montmorillonite layered space to form reactive EDTA radicals via an intermediate complex. Due to restricted mobility of $\overline{Ce}$(IV) ions at the exchange sites of montmorillonite, the formation constant of the complex is small. The decomposition of the complex is the rate controlling step.

(2) Polymerization locus is the interlayer space of montmorillonite. The linear termination of growing polymer chain by $\overline{Ce}$(IV) ions is restricted due to the presence of metal ions in the layered space.

(3) In the acidic and metal ion exchanged aqueous montmorillonite system, a fraction of the intercalated acrylamide molecules is present near reacting

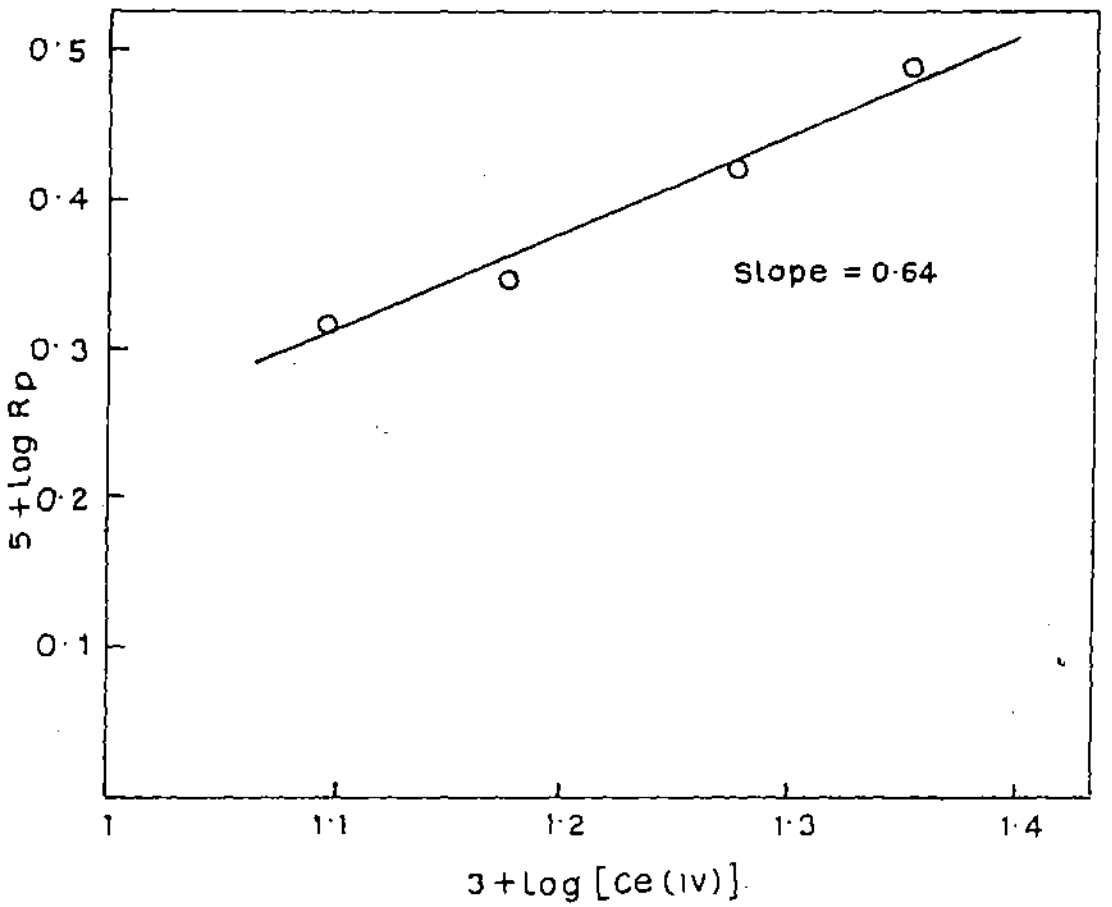

Fig. 39 Logarithm plot of Rp versus [$\overline{Ce}$ (IV)] : [AM] = 0.4 M; [EDTA] = 2.5 x 10^{-3} M; [MO] = 0.5% ([Ce (IV)] represents moles of inter-layer Ce(IV) ions in 1000 ml of MO gel phase).

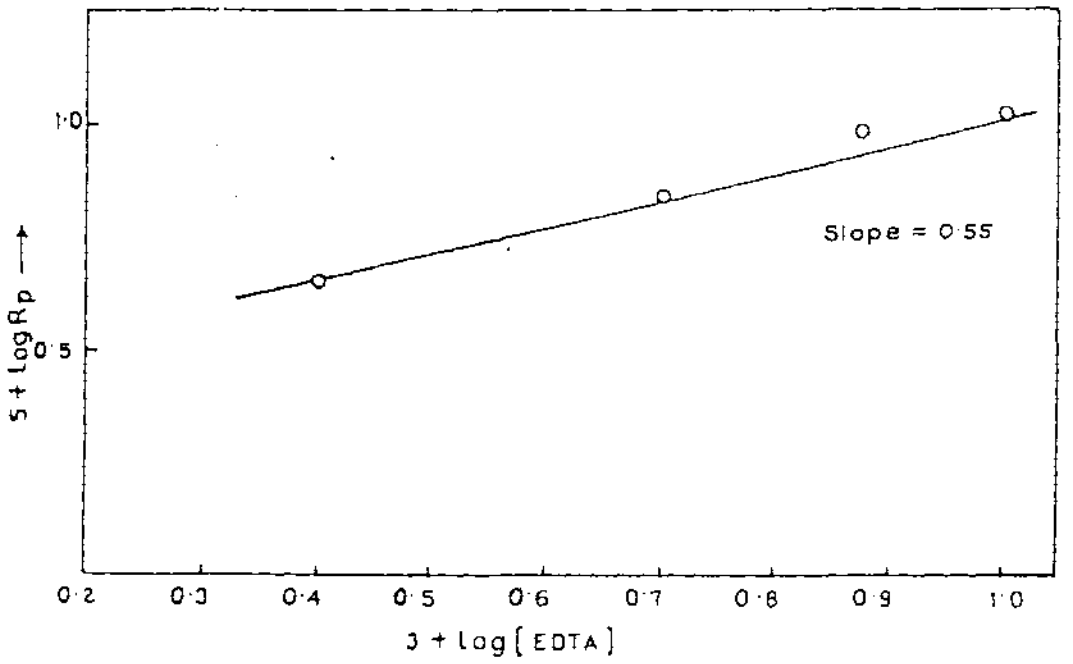

Fig. 40 Logarithmic plot of R_p versus [EDTA] for polymerization of AM by CeM / EDTA: [Ce(IV)] = 1.5×10^{-3} M; [AM] = 0.4 M and [Mo] = 0.50%.

sites as pairs either through hemisalts formation, where two amide molecules share a proton by means of symmetrical hydrogen bond or/and through weak coordination to the exchanged cations. The protonated as well as the complexed amide pairs are at first equilibrium with unprotonated and free amide molecules, respectively, which are defined by a protonation constant or a formation constant. The initiation step involve the collisions of acrylamide with EDTA radicals, where such monomer pairs are entailed.

Initiation

$$\overline{Ce}(IV) + EDTA(R) \overset{K}{\rightleftharpoons} \underset{\text{complex}}{\overline{Ce}(IV)-R} \qquad (29)$$

$$\overline{Ce}(IV) - R \xrightarrow{k_d} R^{\bullet} + \overline{Ce}(III) + H^{+} \qquad (30)$$

$$R^{\bullet} + M_2H^{+} \xrightarrow{k_i} M_1^{\bullet} + M + H^{+} \qquad (31)$$

Propagation

$$M_1^{\bullet} + M \xrightarrow{k_p} M_2^{\bullet} \qquad (32)$$

$$M_{n-1}^{\bullet} + M \xrightarrow{k_p} M_n^{\bullet} \quad \ldots\ldots\ldots \text{ etc.}$$

Termination

$$M_n^{\bullet} + M_n^{\bullet} \xrightarrow{k_t} M_n - M_n \qquad (33)$$

$$R^{\bullet} + \overline{Ce}(IV) \xrightarrow{k_t'} \text{Oxidative product} + \overline{Ce}(III) + H^{+} \qquad (34)$$

Using the above scheme and the pseudo steady state assumption we derive the rate expression as follows:

$$-\frac{d}{dt}\left[\overline{Ce}(IV)\right] = \frac{k_d K[R]\left[\overline{Ce}(IV)\right]}{1+K[R]} \qquad (35)$$

Now, assuming that the rate of formation of EDTA radicals is exactly equal to the rate of disappearing of $\overline{Ce}$(IV) ions, we obtain, (considering the steady state of EDTA$^{\bullet}$).

$$\frac{k_d K[R]\left[\overline{Ce}(IV)\right]}{1+K[R]} = k_i K^{l}\left[R^{\bullet}\right][M]^2 + \frac{k_t^{'}\left[R^{\bullet}\right]\left[\overline{Ce}(IV)\right]}{1+K[R]}$$

(K^{l} (= $[M_2H^{+}]$ / $[M]^2$) is the apparent protonation constant at a fixed pH (or a formation constant))

$$\left[R^{\bullet}\right] = \frac{k_d K[R]\left[\overline{Ce}(IV)\right]}{\left(k_i K^{l}[M]^2 + \frac{k_t^{'}\left[\overline{Ce}(IV)\right]}{1+K[R]}\right)(1+K[R])}$$

$$\left[R^{\bullet}\right] = \frac{k_d K[R]\left[\overline{Ce}(IV)\right]}{k_i K^{l}[M]^2 + K k_i K^{l}[M]^2[R] + k_t^{'}\left[\overline{Ce}(IV)\right]} \qquad (36)$$

Again, considering the steady state of $M_n^{\bullet}$

$$k_i K^{l}\left[R^{\bullet}\right][M]^2 = k_t\left[M_n^{\bullet}\right]^2$$

$$\left[R^{\bullet}\right] = \frac{k_t\left[M_n^{\bullet}\right]^2}{k_i K^{l}[M]^2} \qquad (37)$$

Equating RHS of equation (36) and (37)

$$\frac{k_t\left[M_n^{\bullet}\right]^2}{k_i K^{l}[M]^2} = \frac{k_d K[R]\left[\overline{Ce}(IV)\right]}{k_i K^{l}[M]^2 + k_i K^{l} K[M]^2[R] + k_t^{'}\left[\overline{Ce}(IV)\right]}$$

$$\left[M_n^{\bullet}\right]^2 = \frac{k_i K^l K k_d [M]^2 [R]\left[\overline{Ce}(IV)\right]}{k_t\left(k_i K^l [M]^2 + k_i K^l K [M]^2 [R] + k_t^{'}\left[\overline{Ce}(IV)\right]\right)}$$

$$\left[M_n^{\bullet}\right] = \frac{\left(k_i K^l K k_d\right)^{1/2} [M] [R]^{1/2} \left[\overline{Ce}(IV)\right]^{1/2}}{k_t^{1/2}\left(k_i K^l [M]^2 + k_i K^l K [M]^2 [R] + k_t^{'}\left[\overline{Ce}(IV)\right]\right)^{1/2}}$$

$$R_p = k_p \left[M_n^{\bullet}\right] [M]$$

$$R_p = \frac{k_p \left(k_i K^l K k_d\right)^{1/2} [R]^{1/2} [M]^2 \left[\overline{Ce}(IV)\right]^{1/2}}{k_t^{1/2}\left(k_i K^l [M]^2 + k_i K^l K [M]^2 [R] + k_t^{'}\left[\overline{Ce}(IV)\right]\right)^{1/2}} \qquad (38)$$

Careful analysis of the experimental result suggests that the rate of oxidative termination (step 34) is very slow in the restricted space of the mineral and the last term in the bracket of the denominator may be neglected. Above equation may thus be reduced to

$$R_p = \frac{\left(k_d^{1/2} K^{1/2} k_p / k_t^{1/2}\right) \left[\overline{Ce}(IV)\right]^{1/2} [R]^{1/2} [M]}{\left(1 + K[R]\right)^{1/2}} \qquad (39)$$

The concentrations, [M] and [R], in the montmorillonite gel-phase may be given by equations (40) and (41)

$$[M] = L_o^a \theta_m = \frac{L_o^a K_m^a [M]_s}{1 + K_R^a [R]_s + K_m^a [M]_s} \qquad (40)$$

and

$$[R] = L_o^a \theta_R = \frac{L_o^a K_R^a [R]_s}{1 + K_R^a [R]_s + K_m^a [M]_s} \qquad (41)$$

(subscript 's' denotes solution)

(L_o^a and θ are the total active sites in units mass of montmorillonite gel and the fraction of the total sites occupied by each species respectively; K_m^a and K_R^a are the selectivity coefficients).

Although the concentrations of the monomer and EDTA in solution phase were fixed mostly at 0.40 $mol.L^{-1}$ and 2.5 x 10^{-3} $mol.L^{-1}$ respectively, concentration of intercalated species must be low, due to the presence of water molecules in the interlayer spaces. Substituting [M] and [R] in equation (39) in terms of those of equations (40) and (41) (assuming the denominators to be approximately unity under present condition), R_p becomes,

$$R_p = \frac{k_p K_m^a \left(L_o^a\right)^{3/2} \left(k_d K K_R^a / k_t\right)^{1/2} \left[\overline{Ce}(IV)\right]^{1/2} [R]_s^{1/2} [M]_s}{\left(1 + K L_o^a K_R^a [R]_s\right)^{1/2}} \qquad (42)$$

The concentrations of EDTA used in the present study were low and ranged between 2.5 x 10^{-3} to 0.01 $mol.L^{-1}$. In view of the assumption that the complex formation constant, K, in the present condition is also small, the value of ($K L_o^a K_R^a [R]_s$) may be considered insignificant in comparison to unity. Equation (42) thus be reduced to

$$R_p = k_p K_m^a \left(L_o^a\right)^{3/2} \left(k_d K K_R^a / k_t\right)^{1/2} \left[\overline{Ce}(IV)\right]^{1/2} [R]_s^{1/2} [M]_s \qquad (43)$$

Reviewing the above result, we find that equation (43) could satisfactorily account for the present behaviour of the $\overline{Ce}$(IV)–EDTA initialized acrylamide polymerization exhibited in the aqueous montmorillonite layered space.

3.6 GENERAL DISCUSSION

Montmorillonite especially, and other clay minerals in general, give powder ESR spectra containing a multiplicity of lines which essentially fall into three zones. Figure 41a shows ESR spectra of the present montmorillonite sample containing 0.03% and 2.14% (w/w with respect to mineral wt.) iron in exchangeable and lattice position respectively. Signal near g = 4.3 due to paramagnetic Fe(III) cations may be attributed to cis and trans octahydral sites, having axial and rhombic symmetry. A very broad signal near g = 2.2 arises from exchange interactions between clusters of Fe(III) ions which may be present on the surfaces of the smectite as well as due to hydrated Fe(III) in the exchangeable sites[239]. A very small but sharp signal at g = 2.00 has been assigned to structural defects. Figure 41b shows the ESR spectrum that arises from the same montmorillonite sample but pretreated with excess TU at 50°C for 30 min. under nitrogen. Significant decrease of the intensity at g = 4.3 signal indicates that TU reacts with lattice Fe(III) and forms non-Kramers species which are ESR silent. Bhattacharya and co-workers put forward chemical and electrochemical evidences to show that isothiocarbamido radicals (I) in above reaction can activate radical polymerization of methyl methacrylate in aqueous medium[113]. However, in the present study attempts to polymerize water soluble acrylamide monomers by lattice Fe(III)/TU combination were unsuccessful at a wide range of temperature as already mentioned in section 3.4.1. On the other hand, polymerization initiated by the same redox couple but by loading Fe(III) ions in the interlayer spaces of montmorillonite influences the kinetics as well as the mechanism to a great extent than those of solution phase reraction.

Previous studies showed that polymerization of various water insoluble vinyl monomers by redox couples involving TU as the reductant, involved isothiocarbamido primary free radicals (I) in aqueous acid solution[113]. Owing to high 'g' anisotropy and a very short relaxation time, detection of this radical by ESR spectroscopy was not possible until recently, when ESR study of spin adducts of the radical was reported[114]. In the present system also it is believed

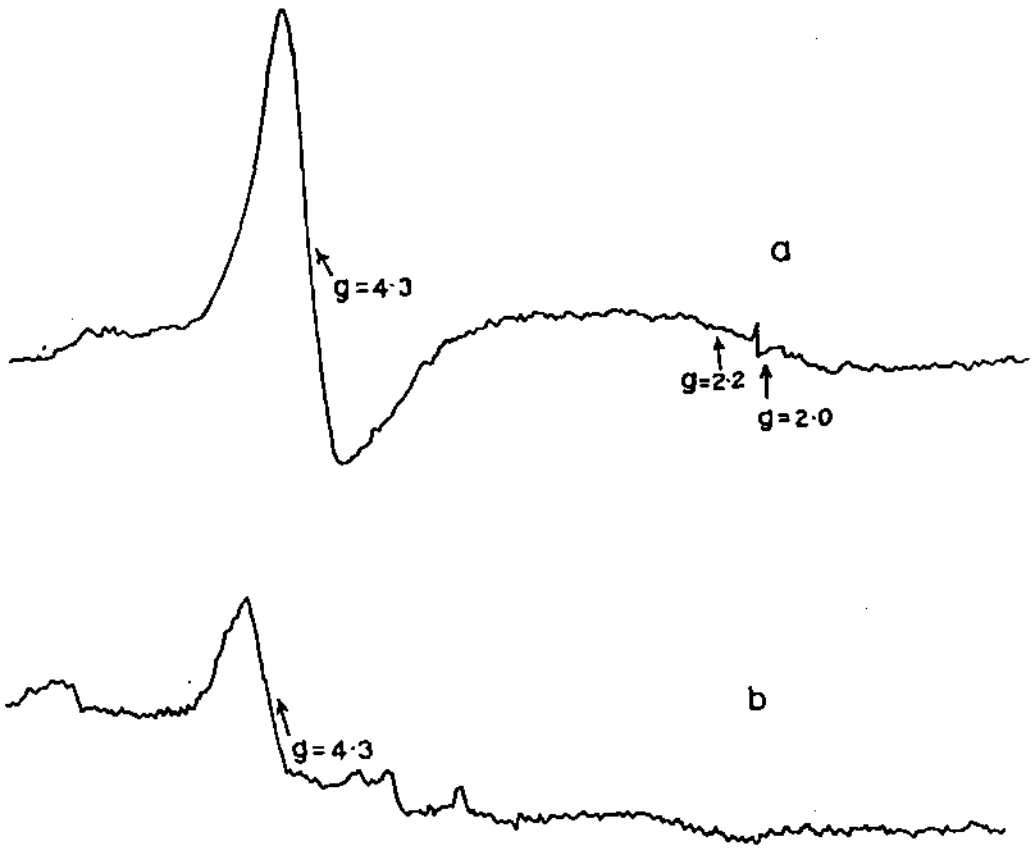

Fig. 41 E. s. r.. spectra of air dried powder montmorillonite sample at 20°c : (a) H+ exchanged; (b) pretreated with thiourea at 50°c under N_2

the same primary radicals (I) is formed and the propagating radicals from acrylamide are trapped by methyl nitrosopropane (MNP) spin trap. Figure 42 show the ESR spectrum of the MNP spin adduct of the radical (II).

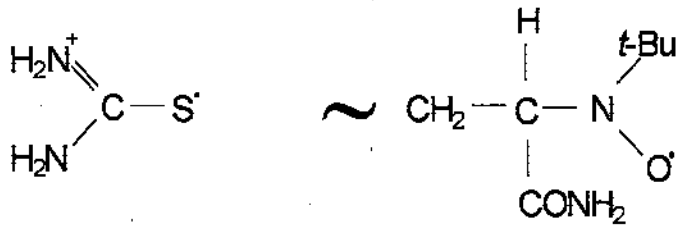

(I) (II)

The spectrum depicts a 1:1:1 triplet of doublets. The triplet is undoubtedly originated from the nitroxide radical (a_N = 1.45 mT) of MNP and the doublets are generated from H^β splitting (a_H = 0.31 mT). The isothiocarbamido radicals (I) are, however, not trapped by MNP under present condition.

X-ray diffractograms of unoriented powder samples of H^+-montmorillonite, TU treated Fe(III)-montmorillonite and Fe(III) -montmorillonite-polyacrylamide adduct before and after glycerol treatment are shown in Figures 43 - 45. The XRD pattern of the montmorillonite samples are consistent with published results[239]. After the polymerization reaction is carried out , the intensity of peak for montmorillonite sample at 2θ = 6.25° became much lower because of the presence of templates of polymer materials in the interlayer space. On the other hand, intensity of the peak at 2θ = 9.5 - 9.8 is increased due to polymerization as well as glycerol treatment. Basal spacing of the H^+ and Fe(III) exchanged minerals are increased from 14 to 17Å due to glycerol treatment for both untreated and TU treated samples respectively. Polymerization increases basal spacing from 14 to 15 Å. Glycerol does nor affect basal spacing at this stage. This indicates the presence of intercalated PAM in the interlayer space. Forgoing result indicates that Fe(III) ions and Tu

Fig. 42 E. s. r. spectra of MNP–PAM spin adduct

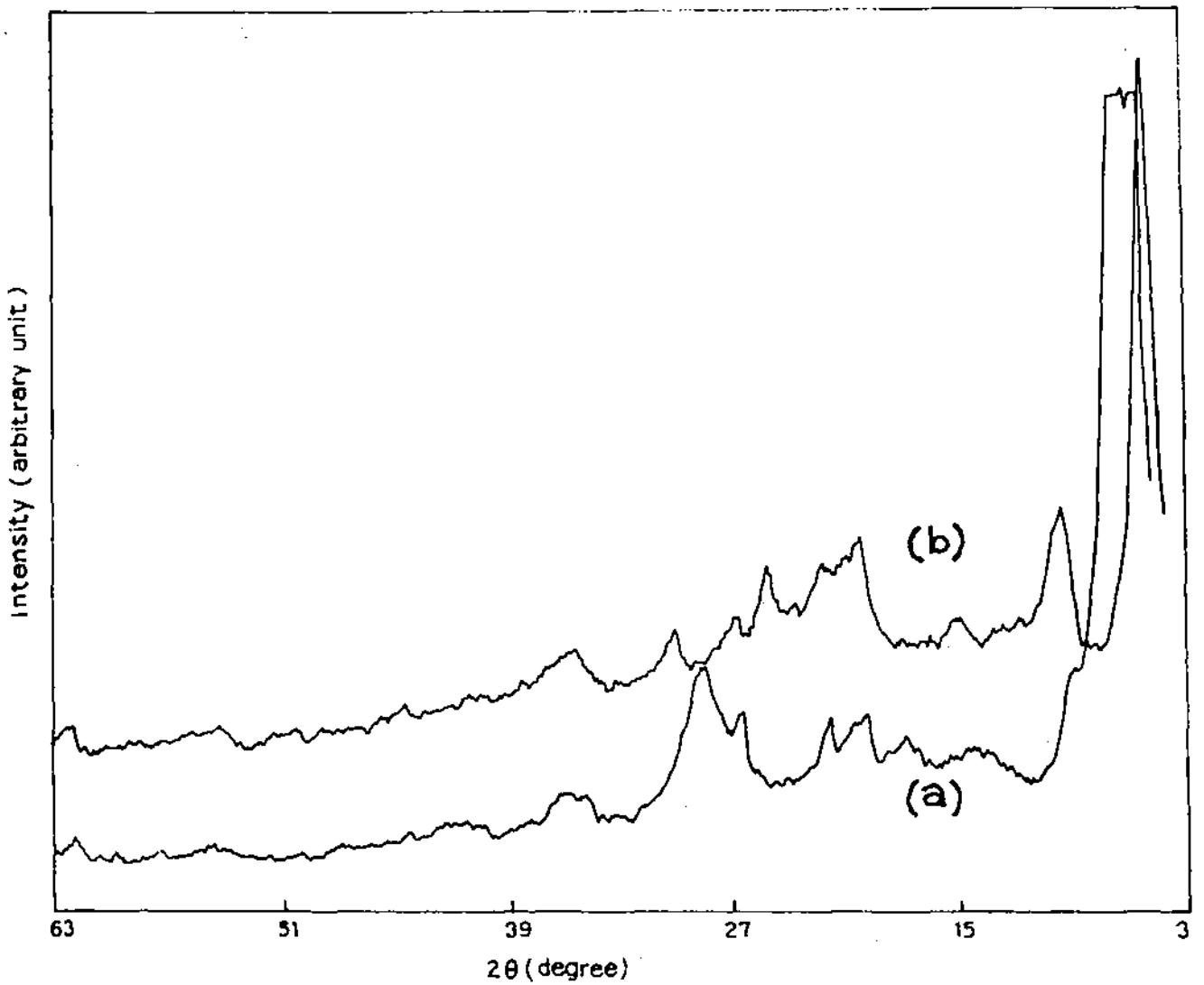

Fig. 43 X-ray diffractograms of dried hydrogen montmorillonite; (a) before glycerol treatment; (b) after glycerol treatment.

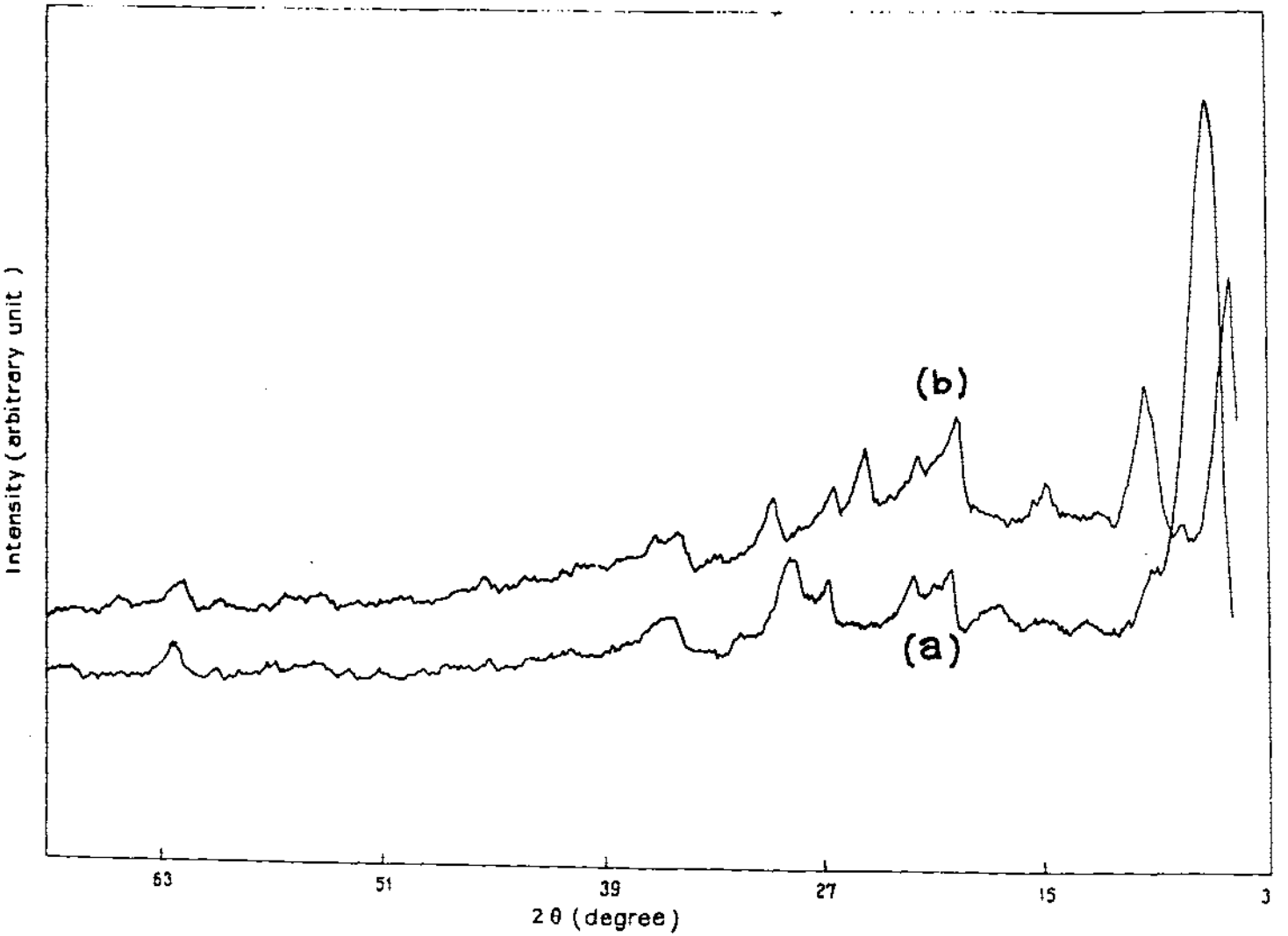

Fig. 44 X-ray diffractograms of dried ferric montmorillonite treated with thiourea: (a) before glycerol treatment; (b) after glycerol treatment.

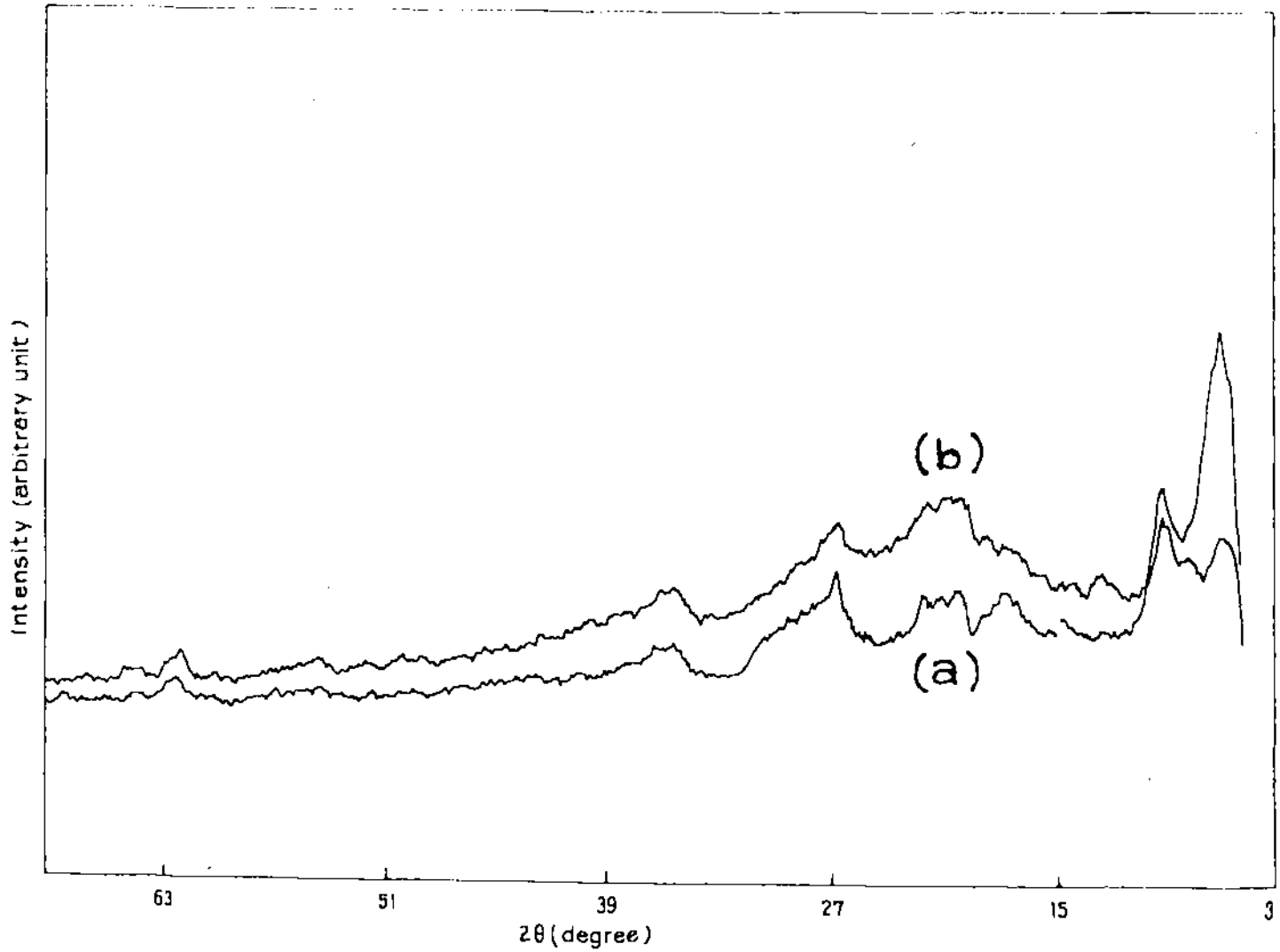

Fig.45 X-ray diffractograms of dried ferric montmorillonite - polyacrylamide adduct: (a) before glycerol treatment; (b) after glycerol treatment.

molecules are intercalated between the layers of the mineral without expanding the same but, as the polymers are formed in the interlayer space the basal spacing is increased. It further shows that the locus of the polymerization reaction is most probably the interlayer space of the mineral.

The redox characteristics of Fe(III) towards TU reductant remains almost unaltered even when Fe(III) ions are absorbed by the mineral clay montmorillonite. This is evident from the potentiometric titration data of Fe(III) and FeM by TU solution (Figure 46). It is thus believed that the same initiating radicals are also involved when Fe(III) ions are trapped between layer spaces of the mineral.

The adsorption isotherm for Fe(III) ion interaction with montmorillonite exhibit L-type nature, which suggests strong sorbate-sorbent interaction. The maximum saturation corresponds to 0.98 meg/g of the mineral. Figure 49 shows that the acrylamide molecules readily intercalate from the aqueous solution into the interlayer space of both forms of the mineral, viz., H^+ as well as Fe(III) forms. Both the isotherms are characterized by two plateau regions indicating two-stage intercalation of amide molecules. The first saturation value is nearly 1.25 $m.mol.g^{-1}$ whereas the second one is just nearly double. The bilayer of acrylamide in the internal surface of the mineral seems to play pivotal role in affecting the initiation of polymerization and its mechanism in the layered space as compared to the homogeneous polymerization. In acidic medium, amides may apriori accept a proton on either the oxygen or the nitrogen atom. However, spectroscopic as well as solution studies support the possibility of coming about of the former alternative[2]. Using infrared spectroscopy, Tahaun and Morland have confirmed that amides predominantly protonate on the oxygen atom in acidic montmorillonite system[71]. In acidic montmorillonite system, hemisalt formation is observed when excess amide is present, that is two amide molecules share a proton through a symmetrical hydrogen bond. On the other hand, thiourea is absorbed in the mineral layer from the aqueous solution giving rise to the isotherm as shown in Figure 50. The process of

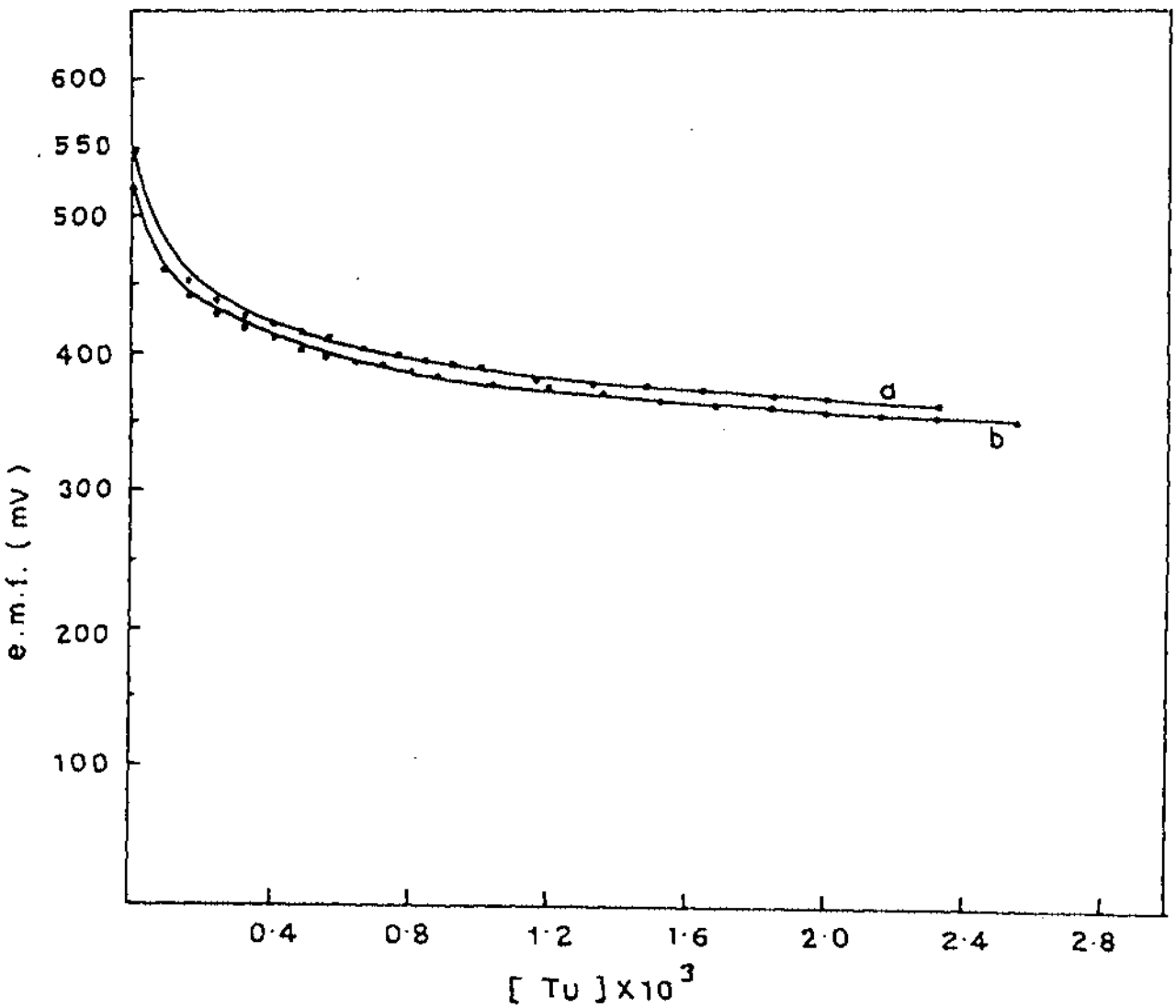

Fig. 46 Potentiometric titrations of (a) FeM (1.3×10^{-3} M in terms of exchanged Fe (III) per 1000 ml of suspension) versus TU; (b) $FeCl_3$ (1.2×10^{-3} M) versus TU.

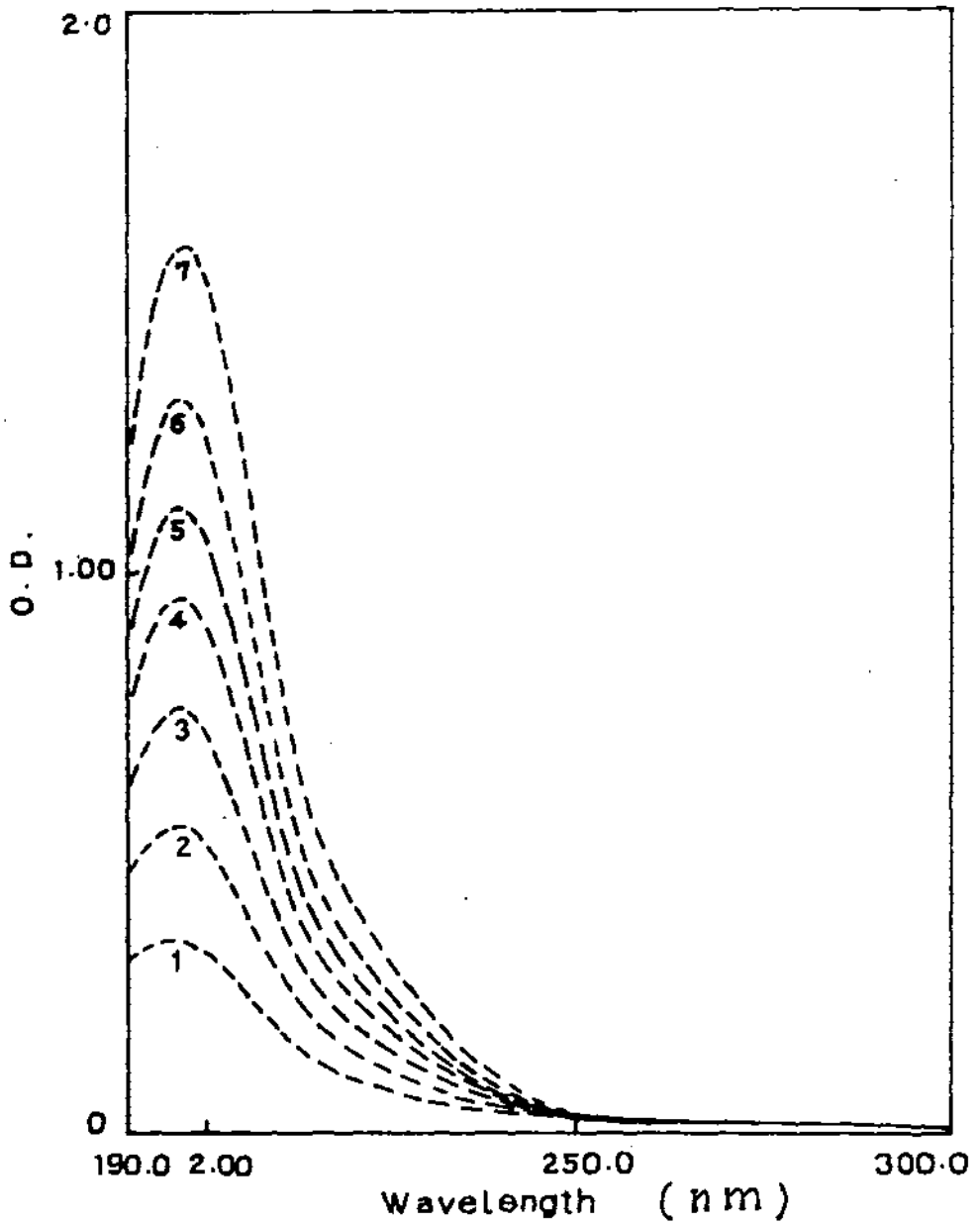

Fig. 47 Visible adsorption spectra of AM at different concentrations. [AM] = 1.48 x 10^{-5} M(1); 2.29 x 10^{-5} M (2); 4.44 x 10^{-5} M (3); 5.92 x 10^{-5} M(4); 7.40 x 10^{-5} M(5); 8.80 x 10^{-5} M(6); 11.10 x 10^{-5} M(7).

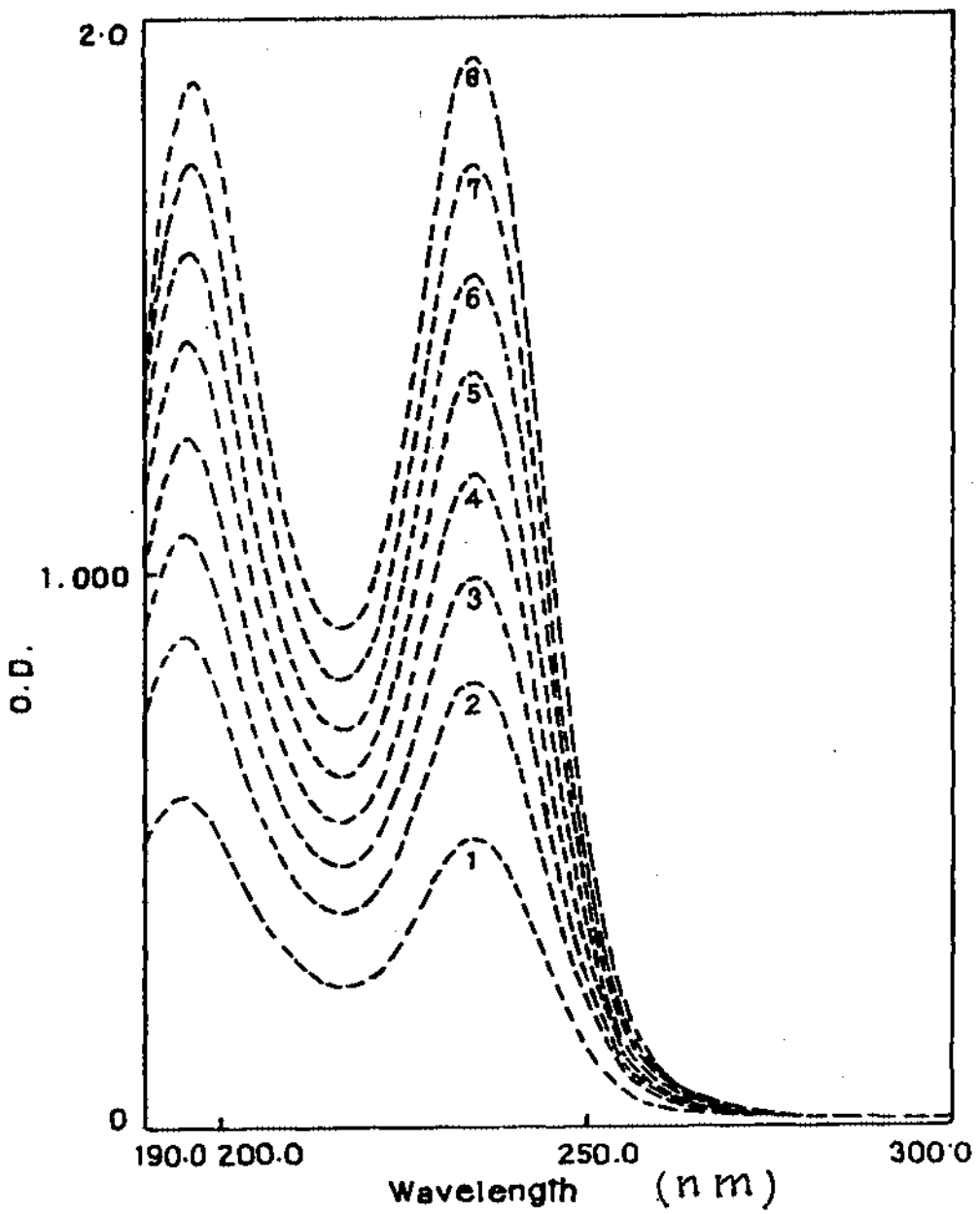

Fig. 48 Visible adsorption spectra of TU at different concentrations. [TU] = 3.80 x 10^{-5} M(1); 6.07 x 10^{-5} M (2); 7.60 x 10^{-5} M (3); 9.11 x 10^{-5} M(4); 10.63 x 10^{-5} M(5); 12.15 x 10^{-5} M(6); 13.67 x 10^{-5} M(7); 15.19 x 10^{-5} M(8).

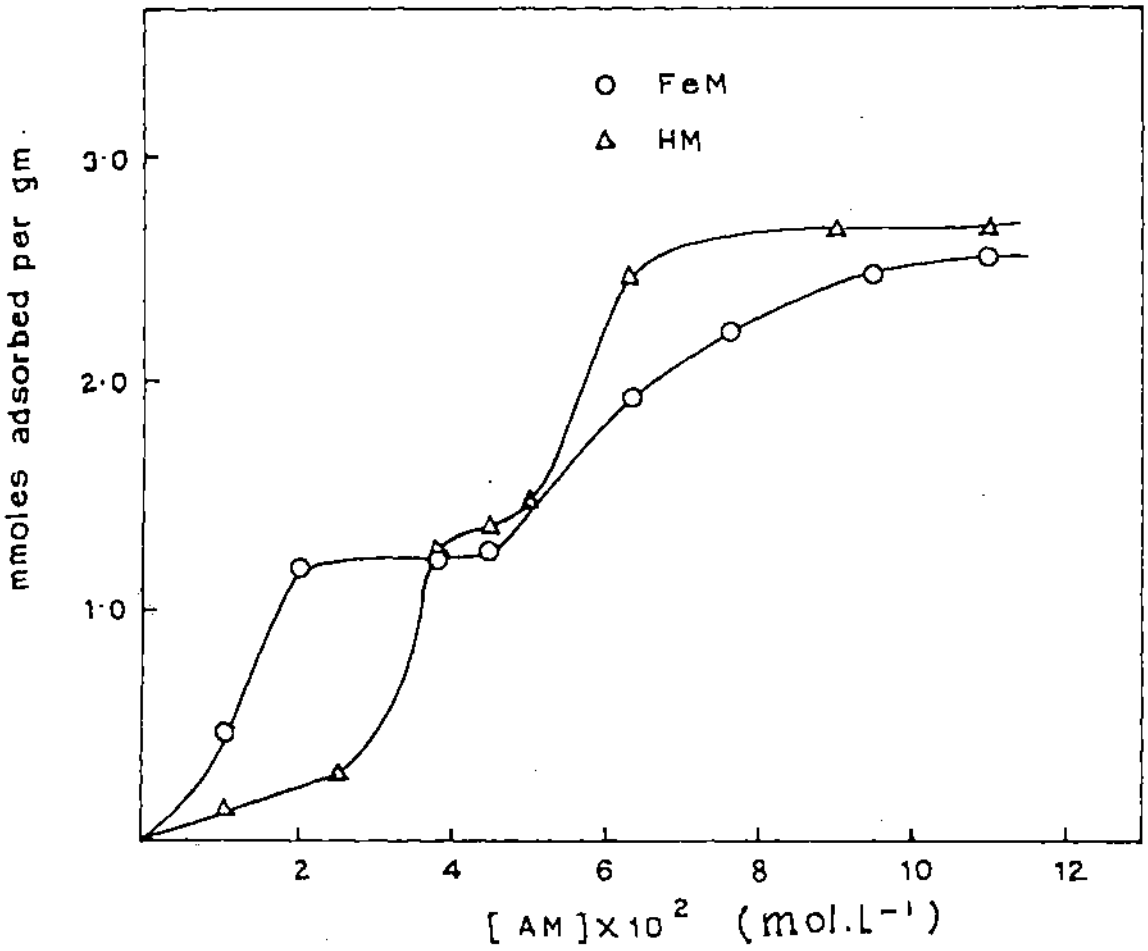

Fig. 49 Adsorption isotherms of acrylamide on Fe– and H– montmorillonite.

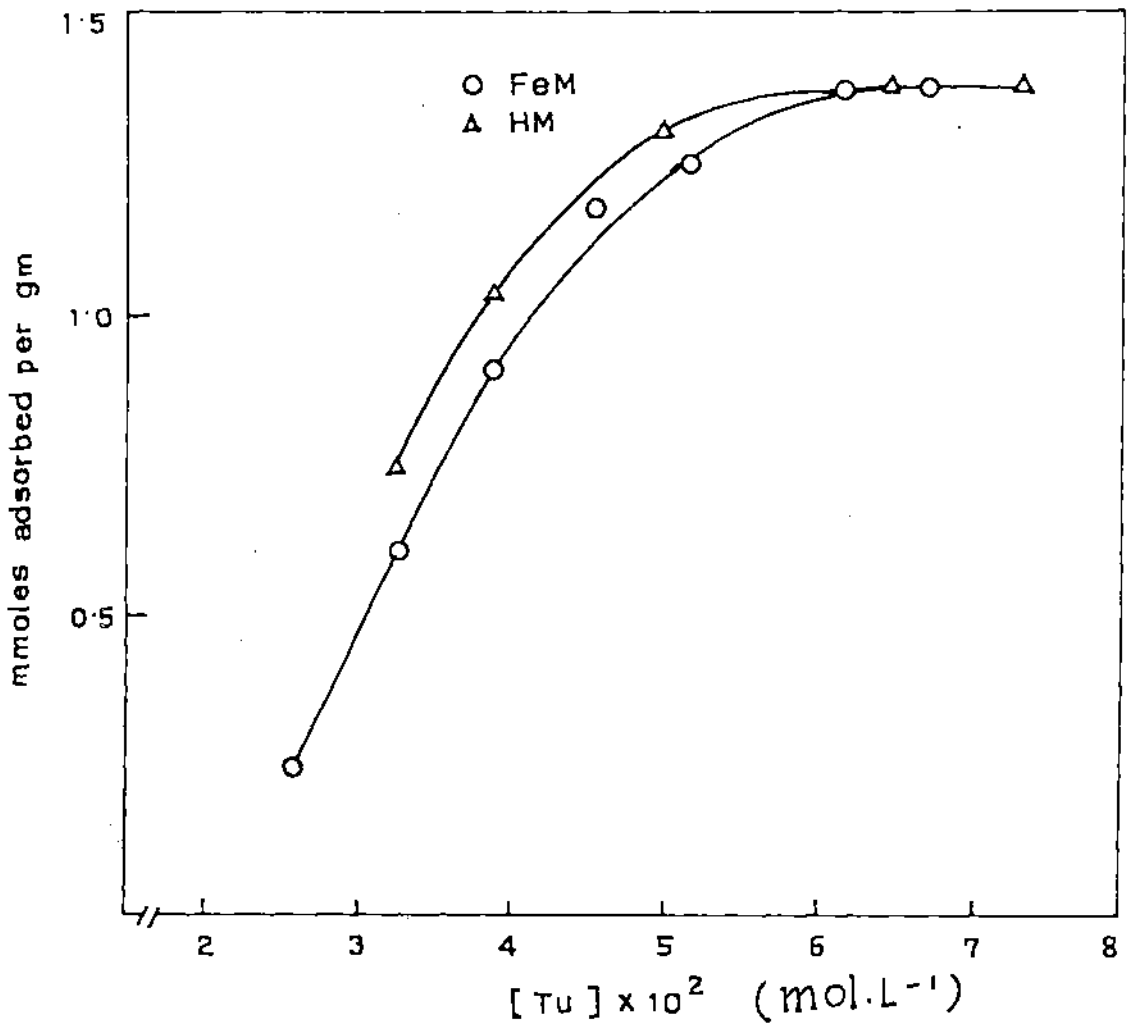

Fig. 50 Adsorption isotherms of thiourea on Fe– and H– montmorillonite.

removal of water molecules either from the H^+-clay or Fe(III)-clay to intercalate TU seems almost identical. Unlike acrylamide, the thiourea leads to the monolayer formation only and maximum capacity is found to be 1.37 m.mol.g^{-1}, which is consistent with that of monolayer of acrylamide. Tables (19 and 20) give an idea of the strength of intercalation of AM and TU molecules in both HM and FeM interlayer spaces. The distribution coefficient (K_D) values are low and of the order of 10^{-2} in the concentration range of AM and TU used for polymerization experiments. The distribution coefficients have been calculated according to the relation;

$$K_D = \frac{\overline{m_i}}{m_i}$$

where $\overline{m_i}$ and m_i are the concentrations of the species in the solid and liquid phase respectively. As is expected from their very nature, the adsorption isotherms (Figure 40 and 41) do not obey the Langmuir relation:

$$\frac{C}{(x/m)} = \frac{1}{K_L (x/m)_{max}} + \frac{C}{(x/m)_{max}}$$

where, C = equilibrium concentration of the adsorbate
x/m = moles adsorbed per gm of adsorbent
K_L = Langmuir constant

The plots of C/(x/m) vs. C are not linear over a range of adsorbate concentrations (Figure 51). However, from the slopes and intercepts of the average line drawn through the points over a short range of concentration of the adsorbates [(4.0 - 6.0) x 10^{-2} mol.L^{-1} for TU and (6.0 - 9.0) x 10^{-2} mol.L^{-1} for AM] give a rough idea of the K_L value in the above concentration range. The values are low; they are 12.0 and 9.2 for TU and AM respectively in the case of FeM.

In general, the R_p's are somewhat lower in presence of montmorillonite than those obtained in homogeneous polymerization maintaining the polymer

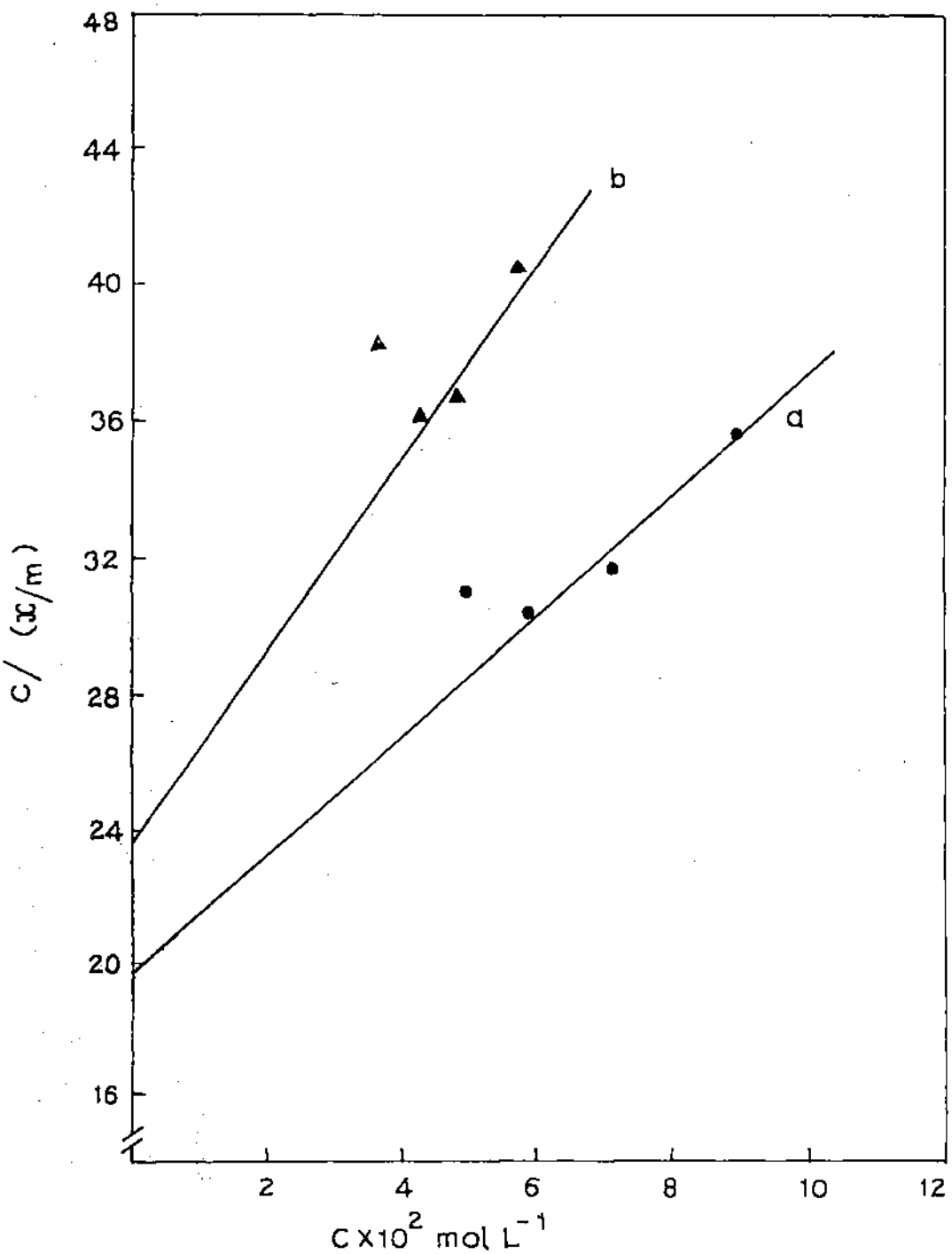

Fig. 51 Langmuir plots of FeM–AM(a) and FeM–TU(b) systems.

yield (X_L) almost same. In the absence of clay minerals, as the concentration of $FeCl_3$ is decreased, X_L as well as R_p are increased significantly (already shown in section 3.3.3), which indicates that Fe(III) ions are involved in the termination

Table - 19

Intercalation of acrylamide (AM) molecules in Hydrogen-montmorillonite (HM) and Ferric-montmorillonite (FeM) interlayer spaces.

Mineral %	Conc. of added AM $(mol.L^{-1}) \times 10^2$	Conc. of adsorbed AM $(mol.L^{-1}) \times 10^3$	Conc. of free AM $(mol.L^{-1}) \times 10^2$	Distribution coefficient K_D
	1.00	1.52	0.85	0.18
	1.50	2.83	1.22	0.23
	2.00	3.91	1.61	0.24
FeM	5.50	5.33	4.97	0.11
(0.33)	6.50	6.41	5.86	0.11
	7.80	7.39	7.06	0.10
	9.70	8.26	8.87	0.09
	11.00	8.37	10.16	0.08
	1.00	0.49	0.95	0.05
	2.00	0.82	1.92	0.04
	3.00	1.63	2.84	0.06
HM	4.00	4.46	3.55	0.13
(0.33)	5.00	5.11	4.49	0.11
	6.00	5.98	5.40	0.11
	7.00	8.70	6.13	0.14
	8.00	8.91	7.11	0.12
	9.00	9.02	8.09	0.11

Table - 20

Intercalation of thiourea (TU) molecules in Hydrogen-montmorillonite (HM) and Ferric-montmorillonite (FeM) interlayer spaces.

Mineral %	Conc. of added TU ($mol.L^{-1}$) x 10^2	Conc. of adsorbed TU ($mol.L^{-1}$) x 10^3	Conc. of free TU ($mol.L^{-1}$) x 10^2	Distribution coefficient K_D
	2.60	0.83	2.52	0.03
	3.25	2.08	3.04	0.07
	3.90	3.13	3.59	0.09
FeM	4.60	3.88	4.21	0.09
(0.33)	5.10	4.25	4.68	0.09
	6.10	4.63	5.64	0.08
	6.70	4.63	6.24	0.07
	3.25	2.50	3.00	0.08
	3.90	3.54	3.55	0.10
	4.60	4.17	4.18	0.10
HM	5.10	4.47	4.65	0.09
(0.33)	6.10	4.63	5.64	0.08
	6.70	4.63	6.23	0.07
	7.20	4.63	6.74	0.02

process of the reaction. However, linear termination of aqueous acrylamide polymerization by Fe(III) ions was observed long back in 1957 when aqueous Fe(III) perchlorate caused fast termination of x- and γ- ray initiated polymerization of acrylamide with a rate constant of $(1.1 \pm 0.6) \times 10^4$ $L.mol^{-1}.s^{-1}$ (ref. 240). Similar role of other metal oxidants were also observed subsequently. On the other hand, in the presence of mineral mixroenvironment, as the concentration of Fe(III) is increased, R_p as well as X_L tend to decrease

Table - 21

Initing system	[η] ml.g^{-1}	M_v x10^{-5}
Ce(IV) - thiourea (Ref. 164)	—	0.9
Mn(III) - ethoxyacetic acid (Ref. 192)	0.5	0.2
Ce(IV) - ethylenediamine tetraacetic acid (Ref. 241)	133	1.8
Ce(IV) - nitrilotriacetic acid (Ref. 237)	90	1.1
Ce(IV) - nitrilotripropionic acid (Ref. 222)	68	0.8
Ce(IV) - iminodiacetic acid (Ref. 222)	73	0.9

due to transfer to ferric ions. Although R_p and the yield decreased with decreasing TU concentrations, molecular weight of the polymer was higher at lower TU concentrations. In view of the fact that redox initiated polymerization of acrylamide in aqueous medium often yield polymers having not so high molecular weights and intrinsic viscosities because of the fast termination, some M_v and [η] data from recent references are recorded in Table 21. (Table 21 records highest value of [η] and M_v from each of the Ref. 164, 192, 222, 237, 241). The most significant observation of loading Fe(III) ions of the initiating redox couple in the interlayer spaces of montmorillonite lie in achieving polymers with much higher intrinsic viscosity and molecular weight. The [η] value of the polymer formed in homogeneous solution and in the absence of the mineral varied from 14 to 90 ml.g^{-1} under the present experimental condition. In contrast, the [η] displayed by polymers formed in the mineral phase is found to vary from 247 to 600 ml.g^{-1} under identical conditions. The M_v values as calculated from viscosity data of present experiments ranged from 0.62 x 10^6 to 2.5 x 10^6 . However, comparison of M_v with literature values should be done carefully because previous workers applied a different Mark-Houwnik equation. The TU exponent changes from 2 to 1 due to occurrence of the reaction in montmorillonite interlayer space (Figure 10 and 28). In order to measure the metal exponent for the reaction in the mineral phase, R_p's were

plotted as a function of Fe(III) ion concentration in montmorillonite gel phase. The slope of the double logarithmic plot was found to be 0.50 at 50°C (Figure 27). Significant departure from that of homogeneous reaction was also observed in the nature of the above plot. While the linear termination by Fe(III) is prominent in solution phase reaction as is evident from the observed nature of variation of R_p with Fe(III) ion concentration, transfer to Fe(III) ion is almost controlled in the case of reaction in the layered space. Thus, it is evident that the modification achieved with respect to the kinetics and mechanism of the acrylamide polymerization in the montmorillonite phase stems from a number of factors viz., (I) instead of collision between a monomer molecule and an initiating radical, a monomer pair is involved in the initiation step (ii) 'cage effect' is prominent in montmorillonite phase reaction where a pair of TU radicals form a potential barrier to hinder diffusion of the radicals and favours their recombination (iii) rate of linear termination process decreases significantly because transfer to Fe(III) ions is highly restricted for the latter's location in the layered spaces of the mineral and diffusion of the living radical through montmorillonite gel is rather slow. In general, loading of the oxidant, i.e. metal ions, of the redox couple in the interlayer space of clay minerals, i.e. montmorillonite, offers a potential method of achieving very high degree of polymerization for a redox initiated reactions.

Recently EDTA terminated polyacrylamide was obtained by using Ce(IV)/EDTA redox initiator in aqueous acrylamide polymerization[222]. The consumption rate of Ce(IV) depends on a first order reaction on the ceric ion concentration. The compex formation constant (K) and disproportionation constant (k_d) of Ce(IV) – EDTA chelated complex were found to be 1.07×10^4 and 3.77×10^3, respecrtively.[222] The rate dependence of polymerization on monomer and EDTA concentratioins both followed second order reactions in the run of monomer concentrations at 0.2 $mol.L^{-1}$. The complex formation constant (K) as well as the disproportionation constant (k_d) also varied significantly with the kind of reducing agents used. The reducing agent even

influenced and the behaviours of polymerization at the later stages. Further, comparatively low molecular weight polymers were formed because the polymerization mechanism involves fast termination process via transfer to the Ce(V) ions. Present investigation, however, shows that the polymerization mechanism is affected to a great extent if the reaction occurs in the interlayer space of the mineral. Both EDTA and acrylamide molecules, intercalate into the layered space of montmorillonite where Ce(IV) ions react with EDTA to form the initiating primary radicals. The most striking feature is that while the number average molecular weight, M_n, (M_v values are not available), were ranged between 9.7 x 10^4 to 3.1 x 10^5 in case of solution polymerization, montmorillonite mediated polymerization yield polymers having M_v as high as 3.9 x 10^5 to 2.9 x 10^6. The effect of Ce(IV) ion concentration on the R_p is nevertheless interesting. While the previous study on homogeneous polymerization by Ce(IV)/EDTA system showed a steady decrease in R_p with Ce(IV) concentration, present study gives a reverse trend (Table 17). This indicates that the linear termination by Ce(IV) ions is no longer important in the polymerization mechanism of the present system. The adopted technique of trapping the metal oxidant inside the layered space of montmorillonite seems to work well in enhancing chain growth for the Ce(IV) / EDTA system also. The mechanisms of the reactions in the montmorillonite gel have been suggested and rate equations are proposed, which account for the observed experimental results (Section 3.4 & 3.5).

CHAPTER - 4

STUDIES ON COPOLYMERIZATION OF ACRYLAMIDE WITH DIACETONE ACRYLAMIDE AND N-tert-BUTYLACRYLAMIDE BY Fe(III)-TU REDOX COUPLE ON MONTMORILLONITE SURFACE

4.1 INTRODUCTION AND REVIEW OF PREVIOUS WORK

Copolymers of acrylamide have shown a number of properties lending themselves to a variety of industrial applications. Of growing importances are those related to use as water soluble viscofiers and displacement fluids in enhanced oil recovery.[242-247] Two of the critical limitations of polyelectrolytes are, however, loss of viscosity in the presence of mono or multivalent electrolytes (viz. NaCl, $CaCl_2$ etc.) and ion binding to the porous reservoir rock substrates. Copolymers of acrylamide and acrylates can be synthesized by several methods including those of solution[248-259] and emulsion[260-263] polymerizations. The physical properties of the copolymers in some cases, are dependent on the method of preparation. The copolymers of AM with sodium acrylate in aqueous ammonium persulfate solution was conducted at 70° for 60 min. producing a honeylike copolymer which had molecular weight 1.25 x 10^6 as reported by Soltez and co-workers.[248] Cationic free radical copolymers of acrylamide with dimethylaminoethyl methacrylate and dimethylaminoethyl acrylate had been prepared by Baade and Hunkeler[249] with azocyano valeric acid and $K_2S_2O_8$ at 45°-60°C. Lafuma and Durand have found that during random copolymer formation of acrylamide and a quaternary ammonium acrylate monomer, the cleavage of the ester function occurred in mild alkaline medium with a simultaneous inter-chain reaction resulting in imide group formation.[250] Lavrov and co-workers have reported that copolymerization of 2-hydroxy ethyl methacrylate with acrylamide in aqueous solution in the presence of $(NH_4)_2S_2O_8$/ascorbic acid redox catalyst proceeded without the gel effect characteristic of bulk polymerization[251]. The reactivity ratios of the dimethylamino ethyl methacrylate methyl chloride salt with acrylamide at 54° C were 1.54 and 0.30 respectively when redox azo compounds were used as catalyst [252]. The molecular weight of copolymers of auxin-containing monomers with acrylamide was determined to be in the range of 5.5 - 18.0 x 10^4 when a 4 - pyrrolidinopyridine and dicyclohexyl carbodiimide [253] catalysts were used. For AM - Na acrylate copolymer, prepared in aqueous solution at room temperature

and at pH 7.4 - 12.1, the reactivity ratios were 0.9 - 1.18 and 0.32 - 0.48 respectively[254]. McCormick and Salazar have reported that the increasing randomness in the copolymers of acrylamide with Na-3-acrylamido - 3-methybutanoate is observed if prepared in NaCl solution rather than in distilled water[256]. The polyelectrolytes had inherent hydrogen bonding capacity and pseudo plasticity and exhibited large dimension in aqueous solution[257]. In inverse microemulsion copolymerization of AM with methylacrylate initiated with AIBN by Vaskova was a typical "dead - end" polymerization[260]. In inverse emulsion polymerization method, incorporation of high hydrophile - lyophile balance coemulsifier in addition to the water-in-oil type main emulsifier increased the rate of polymerization significantly. Free radical copolymerization of acrylamide with butylacrylamide or isopropyl methacrylate in the presence of AIBN in DMF at 60°C was investigated by Srinivasula, Rao and co-workers[261-262]. The chemical structures of random copolymers of acrylamide with Na - 2 - sulfoethylmethacrylate in dextron were determined by McCormick in roder to gain a more complete understanding of the structure - property relations and performance under simulated field conditions encountered in enhanced oil recovery[263]. The synthesis and characterization of copolymers of acrylamide with N-alkylacrylamide were investigated by McCormick and Nonaka and co-workers in aqueous solution utilizing Na-dodecyl sulfate as a surfactant and $K_2S_2O_8$ as the initiator[264]. A remarkable increase in apparent viscosity was observed at low mol. fractions of N-alkylacrylamide in the copolymer at a critical concentration which is a function of alkyl chain length in the monomer and copolymer molecular weight. The viscosity behaviour is interpreted in terms of a concentration dependent model involving interchain hydrophobic association in aqueous solution[264]. The copolymer microstructures and reactivity ratios of copolymers of acrylamide with N-(1,1-dimethyl-3-oxo-butyl)-N-(n-proply) acrylamide were studied by McCormick and Blackmon and the value of r_1r_2 determined to be 2.20 (ref 265). The copolymer of acrylamide with N-(1,1 - dimethyl 3 - oxo-butyl) acrylamide yielded a r_1r_2 value of 0.75 and the copolymer of AM with N, N-dimethyl acrylamide provided a r_1r_2 value of 0.86 as reported by

McCormick and Chen[266]. Monoazeotropic and non ideal copolymers were prepared during copolymerization of methyl methacrylate with AM, N-methylacrylamide and N,N-dimethylacrylamide in 1,4 Dioxan solution at 65°C using AIBN as initiator[267]. Low molecular weight water soluble copolymers of acrylamide with itaconic acid, methacrylic acid and acrylic acid were prepared in the presence of $K_2S_2O_8$ and thioglycerin by Sumi and co-workers[268]. Granular copolymers of ethylacrylate (EAC) and acrylonitrile (ACN) had been prepared by Thomas with dispersed bentonite when EAC and ACN were dissolved in ethanol and heated under reflux condition with benzoyl peroxide for six hours[269]. The copolymerization of methyl methacrylate with acrylonitrile and methacrylonitrile were studied by Bhattacharyya in the presence of HM/thiourea redox couple[270].

In the present work, attempts have been made to prepare water soluble copolymers of acrylamide with N - (1, 1 - Dimethyl - 3 - oxybutyl) acrylamide (commonly referred to as Diacetone acrylamide, DAAM) and N-t butyl acrylamide (N-t BAM) on the montmorillonite surface by interlayer trapped Fe(III) ions in the presence of TU. Importance of the study lie in the fact that (I) the applied technique provides high molecular weight polymers having high intrinsic viscosities and (II) at least one of the above copolymers has already shown some promises by not losing its solution viscosities in the presence of added electrolytes[11]. The success in copolymerization would result in relatively pure copolymer without subsequent solvent extractions. Moreover, the structure of the clay mineral would, perhaps, control the structure and physico-chemical property of the copolymer. This chapter deals with the studies on copolymerization of AM with DAAM and N-tert BAM and including microstructures and reactivity ratios of the polymers. Copolymerization of vinyl monomers on clay surface have not been studied so far in detail. Attempts have, therefore, been made to use FeM/TU initiating system in the copolymerization reactions.

4.2. EXPERIMENTAL

4.2.1 Materials and purification

Reagents

The purification techniques of acrylamide(reagent grade, Fluka) and thiourea (Merck) were discussed in previous section 3.2. Method of preparation and the characteristics of Fe(III) - montmorillonite (FeM) were similar to those as already described in section 3.2.

N-(1,1-dimethyl-3-oxybutyl) acrylamide(reagent grade, Fluka) was recrystallised twice from methanol and vacuum dried. N-t butyl acrylamide (reagent grade, Fluka) was used as received.

Polymerization

Poly(acrylamide-co-N,N-dimethylacrylamide)

The copolymerization of acrylamide with N, N dimethylacrylamide (DAAM) was conducted in aqueous solution at 50°C using 0.50%(w/v) of FeM and 0.04 M of thiourea as initiator. Table-23 lists reaction parameters for four series of reactions in which the ratio of monomers in the feed and reaction times were varied. A specified amount of DAAM dissolved in distilled water was added to the mixtures of acrylamide and thiourea solutions of known concentrations in 100 ml stoppered pyrex bottles under nitrogen. In another set of bottles, known amounts of aqueous FeM suspensions were degassed and, finally added to the former bottles under nitrogen atmosphere. The pH of the final mixture was adjusted to 2.0 $\pm$ 0.1 by drop-wise addition of 0.01M HCl solution, well shaken and immediately placed in thermostatic bath of appropriate temperature. pH adjustment was necessary to ensure the formation

of adequate amount of the amido-sulfenyl primary radicals to initiate the copolymerization reaction[114]. After the designated reaction intervals, the copolymerization reactions were stopped by diluting the reaction mixtures with chilled water, keeping the reaction vessel in ice bath and FeM was separated by centrifugation(1.5 x 10^4 r. p. m.). AM-DAAM copolymers were precipitated out by the addition of excess acetone. The copolymers and FeM were washed separately by acetone and water respectively. The copolymers and FeM were then dried at 60°C under vacuum for 48 hrs. Conversions were determined gravimetrically.

Poly (acrylamide-co-N-tert-butylacrylamide)

Since N-t-butylacrylamide is insoluble in water, the monomer was dissolved in micellar pseudo-phase of non ionic surfactant Triton-X-100(R). Four series of copolymerization of acrylamide with N-t-butylacrylamide having a total monomer concentration of 0.42M were conducted in aqueous solution at 50°C using 0.50% FeM (w/v) and 0.04M TU as the initiator. Reaction parameters for four series of reactions are given in Table-24. The reaction procedures were same as those described for the preparation of copolymers of AM with DAAM.

Elemental Analysis

Elemental analysis for carbon and nitrogen for the AM-DAAM and AM-N-t BAM in copolymers were conducted by Regional Sophisticated Instrumentation Centre (RSIC), Chandigarh, India (Table 23 and 24). The copolymer compositions were calculated based on C/N ratios because of the variability of absolute values due to the hygroscopic nature of the polymers. Elemental analyses were conducted at polymer conversion levels, i.e. low and high, to assess drift in the copolymer composition.

Viscosity Measurements

A series of copolymer solutions of different concentrations in aqueous 0.1 M NaCl are prepared from the 0.5% stock solution. The intrinsic viscosity measurement technique has already been mentioned in Section 3.2.

4.3 RESULTS AND DISCUSSION

The study of copolymerization involves the calculation of reactivity ratios of the monomers. Present investigation involves the copolymers of DAAM and N-tert BAM with AM. Such monomer conjugates have been chosen because (I) the groups attached to the vinyl groups are electron withdrawing (II) the position occupied by the methyl group in both the monomers (DAAM and N-tert BAM) is similar with respect to the vinyl carbon atom. It is clear from the Table - 22 that, in case of AM-DAAM, the monomer conversion decreases with decreasing AM-DAAM ratios. However, at lower monomer ratios than 4:1, no copolymers were detected. But in presence of Triton X-100 (R), the monomer conversion increases with decreasing monomer composition ratios. The monomer conversion was also increased with decreasing the AM : DAAM ratio when the concentration of Triton X-100(R) was changed from 0.01 mol.L^{-1} to 0.02 mol.L^{-1}. On the other hand, in case of AM-N-t BAM, copolymerization raction proceeds efficiently in presence of surfactant, Triton X-100(R). The monomer conversion increases with decreasing AM-N-tert BAM ratios. High conversion is also observed by FeM/TU initiating system (Table-22).

Table - 22

Copolymerization of 0.4 M AM (0.7108 g) in aqueous medium (25 ml) with DAAM and N-t BAM in presence of 0.04 M TU and 0.50% (w/v) FeM at 50°C (pH 2.01) in presence of varying amounts of DAAM and N-t BAM.

[AM] mol.L^{-1}	[DAAM] mol.L^{-1}	AM]/[DAAM]	Triton-X-100(R) mol.L^{-1}	Conversion[a] %
0.40	0.02	20.0	0.01	11.70
0.40	0.04	10.0	0.01	36.01
0.40	0.06	6.6	0.01	33.30
0.40	0.08	5.0	0.01	32.50
0.40	0.02	20.0	0.02	18.53
0.40	0.04	10.0	0.02	40.30
0.40	0.06	6.6	0.02	34.60
0.40	0.08	5.0	0.02	33.50
0.40	0.02	20.0	_	45.6[b]
0.40	0.04	10.0	_	27.5
0.40	0.06	6.6	_	14.6[b]
0.40	0.08	5.0	_	14.5[b]
0.40	0.09	4.4	_	_[c]
0.40	0.17	2.3	_	_[c]

[AM]	[N-t BAM]	[AM]/N-t BAM]	Conversion[a]
0.40	0.01	41.0	53.8[b]
0.40	0.02	20.0	54.1[b]
0.40	0.03	13.3	59.8[b]
0.40	0.04	10.0	56.6[b]

[a]Copolymer yield after 4.5 hrs, [b]In absence of surfactant, [c]No copolymer formed.

Reactivity Ratios

The variation in feed ratios and the resultant copolymer compositions (Table 23 and 24) as determined from elemental analyses were used to calculate the reactivity ratios for the AM-DAAM and AM-N-t BAM copolymer systems. The Fineman - Ross method[271] and Kelen - Tüdos method[272] were employed to determine the monomer reactivity ratios at low conversion, whereas an integrated form of the Mayo-Lewis equation[273] was used for higher conversion copolymerization data. Figure 52 is the Fineman - Ross plot for acrylamide (M_1) and diacetoneacrylamide (M_2). The reactivity ratios r_1 and r_2 for the monomer pair M_1 and M_2 can be determined by

$$F(f-1)/f = r_1 (F^2/f) - r_2 \qquad (44)$$

Where $f = d(M_1)/d(M_2)$, $F = (M_1)/(M_2)$.

The reactivity ratio r_1 was determined to be 0.69 ± 0.03 from the slope and $r_2 = 0.62 \pm 0.05$ from the intercept. The reactivity ratios are however calculated as 6.18 ± 0.17 and 1.06 ± 0.06 respectively for AM and DAAM on changing the index on monomer as acrylamide (M_2) and diacetone acrylamide (M_1) (Table 26). Similarly, the Kelen - Tüdos approach was applied for evaluation of reactivity ratios for the same monomer pair according to

$$\upsilon = r_1 \xi - r_2 (1 - \xi) / \alpha \qquad (45)$$

where $\upsilon = G/\alpha + H$ and $\xi = H/\alpha + H$.

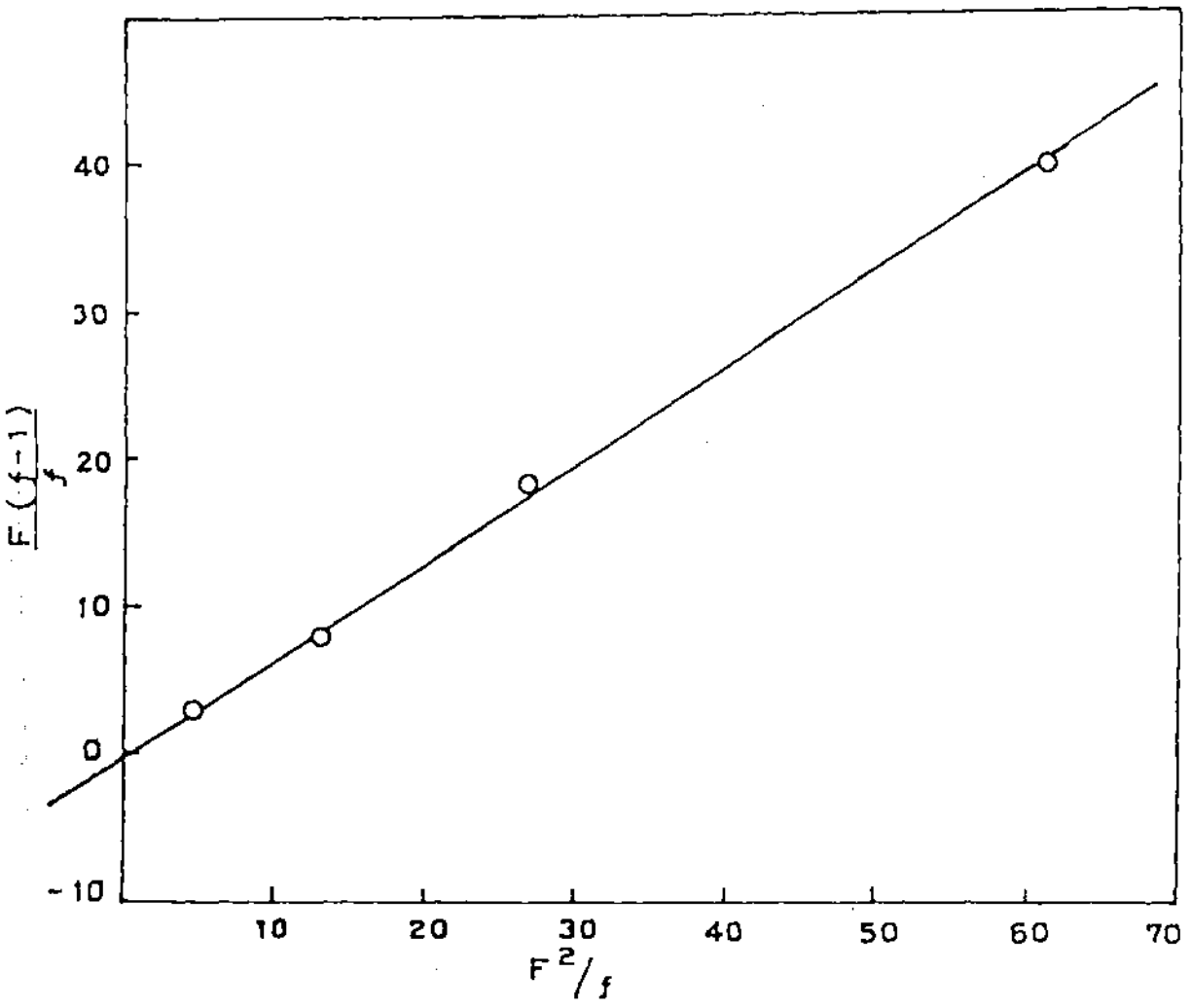

Fig. 52 Determination of reactivity ratios for copolymerization of AM with DAAM by Fineman-Ross method.

Table - 23

Reaction parameters for the copolymerization of AM with DAAM at 50°C in Distilled water (Total Monomer concentration = 0.42 M)

Sample number	Monomer concentration in the feed (M)			Reaction time (min.)	Conversion(%)	Elemental Analysis (wt%)		Mol % DAAM in copolymer	[η] $ml.g^{-1}$
	[AM]	[DAAM]	[AM]/ [DAAM]			C	N		
DAAM-10-1	0.41	0.01	41	90	37.10	41.46	15.03	3.60 ± 0.04	
DAAM-10-2	0.41	0.01	41	150	48.13	41.72	15.15	3.52 ± 0.04	420
DAAM-10-3	0.41	0.01	41	210	54.19	42.62	14.82	5.91 ± 0.04	
DAAM-20-1	0.40	0.02	20	90	23.37	42.08	14.51	6.32 ± 0.08	
DAAM-20-2	0.40	0.02	20	150	31.84	42.03	14.26	7.32 ± 0.09	350
DAAM-20-3	0.40	0.02	20	210	40.54	43.05	14.81	6.54 ± 0.09	
DAAM-30-1	0.38	0.04	9.5	90	6.00	43.47	13.51	12.52 ± 0.20	
DAAM-30-2	0.38	0.04	9.5	150	15.40	43.30	13.52	12.24 ± 0.20	340
DAAM-30-3	0.38	0.04	9.5	210	30.37	44.31	14.11	11.05 ± 0.20	
DAAM-40-1	0.34	0.08	4.25	90	11.10	45.28	12.36	21.22 ± 0.30	
DAAM-40-2	0.34	0.08	4.25	150	6.47	45.25	11.39	27.23 ± 0.40	333
DAAM-40-3	0.34	0.08	4.25	210	7.41	46.23	12.70	20.71 ± 0.30	

Table - 24

Reaction Parameters for the copolymerisation of AM with N-t BAM At 50°C (Total Monomer Concentration = 0.42 M)

Sample number	Monomer concentration in the feed (M)			Reaction time (min.)	Conversion(%)	Elemental Analysis (wt%)		Mol % N-t BAM in copolymer	[η] ml.g^{-1}
	[AM]	[N-t-BAM]	[AM]/ [N-t BAM]			C	N		
N-t-BAM-10-1	0.41	0.01	41	90	27.01	41.16	14.78	6.21 ± 0.08	
N-t-BAM-10-2	0.41	0.01	41	150	35.81	40.32	15.53	1.66 ± 0.04	430
N-t-BAM-10-3	0.41	0.01	41	210	55.61	42.28	15.50	4.57 ± 0.06	
N-t-BAM-20-1	0.40	0.02	20	90	36.27	40.91	15.62	1.31 ± 0.04	
N-t-BAM-20-2	0.40	0.02	20	150	40.78	40.94	15.08	4.15 ± 0.04	415
N-t-BAM-20-3	0.40	0.02	20	210	52.79	42.02	15.07	6.32 ± 0.08	
N-t-BAM-30-1	0.38	0.04	9.5	90	28.58	42.10	14.21	11.42 ± 0.20	
N-t-BAM-30-2	0.38	0.04	9.5	150	31.81	41.11	14.94	5.21 ± 0.05	403
N-t-BAM-30-3	0.38	0.04	9.5	210	34.53	43.58	12.79	24.33± 0.30	
N-t-BAM-40-1	0.34	0.08	4.25	90	28.38	42.35	14.29	11.44 ± 0.20	
N-t-BAM-40-2	0.34	0.08	4.25	150	39.40	41.96	14.30	10.57 ± 0.20	300
N-t-BAM-40-3	0.34	0.08	4.25	210	40.98	43.67	13.10	22.25 ± 0.30	

The transformed variables G and H are given by

$$G = \frac{[M_1]/[M_2]\left[\left(d[M_1]/d[M_2]-1\right)\right]}{d[M_1]/d[M_2]} \quad (46)$$

$$H = \frac{\left([M_1]/[M_2]\right)^2}{d[M_1]/d[M_2]} \quad (47)$$

The parameter α is calculated by taking square root of the product of the lowest and highest values of H for the copolymerization series. A plot of the data according to the Kelen - Tüdos method is shown in Figure 53. Reactivity ratios were determined for AM : DAAM monomer pair as r_1 = 0.71 and r_2= 0.61 respectively. The observed data in the Kelen - Tudos plot are linear, an indication that these copolymerization follow the conventional copolymerization kinetics under a prerequisite that the reactivity of a polymer radical is only determined by the terminal monomer unit[274]. Table - 25 lists the parameters used to statistically determine reactivity ratios from the Mayo-Lewis method at high conversion [equation 48].

$$r_2 = \frac{\log\frac{[M_{2,0}]}{[M_2]} - \frac{1}{p}\log\left(\frac{1-p[M_1]/[M_2]}{1-p[M_{1,0}]/[M_{2,0}]}\right)}{\log\frac{[M_{2,0}]}{[M_2]} + \log\left(\frac{1-p[M_1]/[M_2]}{1-p[M_{1,0}]/[M_{2,0}]}\right)} \quad (48)$$

Where p is an integration constant defined by $(1-r_1)$ / $(1-r_2)$, the initial concentrations of AM and DAAM are represented by $[M_{1,0}]$ and $[M_{2,0}]$ respectively. Values of 0.76 and 0.58 were obtained for r_1 and r_2 respectively (Fig. 54). Closely comparable values of r_1 and r_2 were obtained from Fineman - Ross, Kelen - Tüdos, and Mayo - Lewis treatments for the copolymerization of acrylamide with diacetone acrylamide on montmorillonite surface and are listed

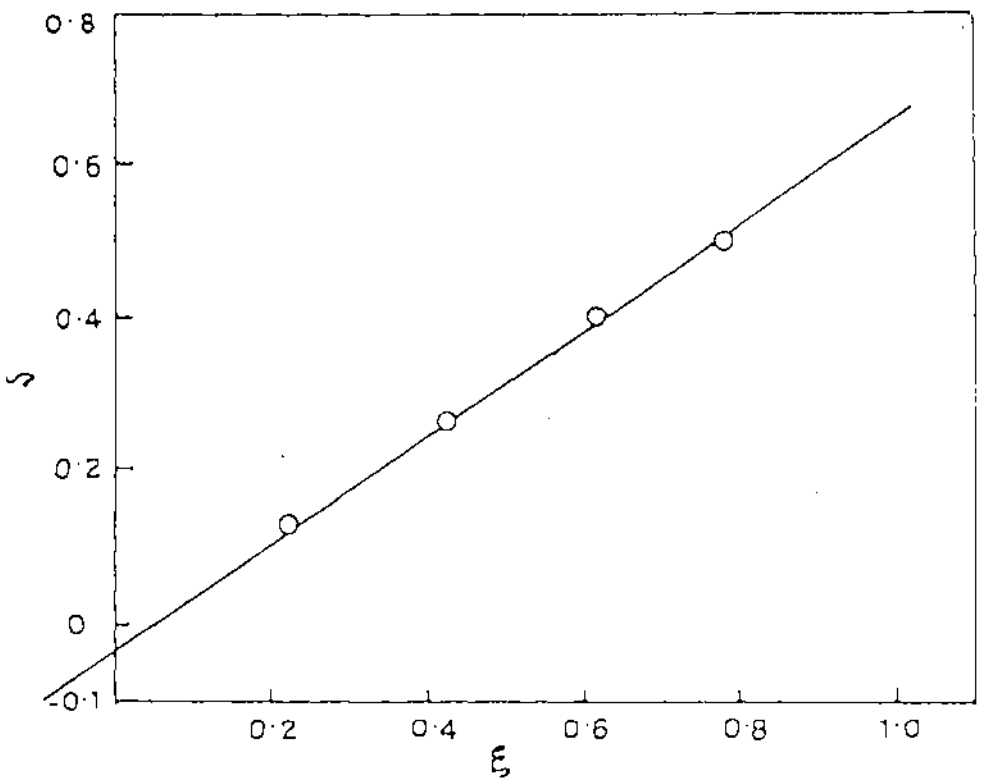

Fig. 53 Determination of reactivity ratios for copolymerization of AM with DAAM by Kelen-Tüdos method.

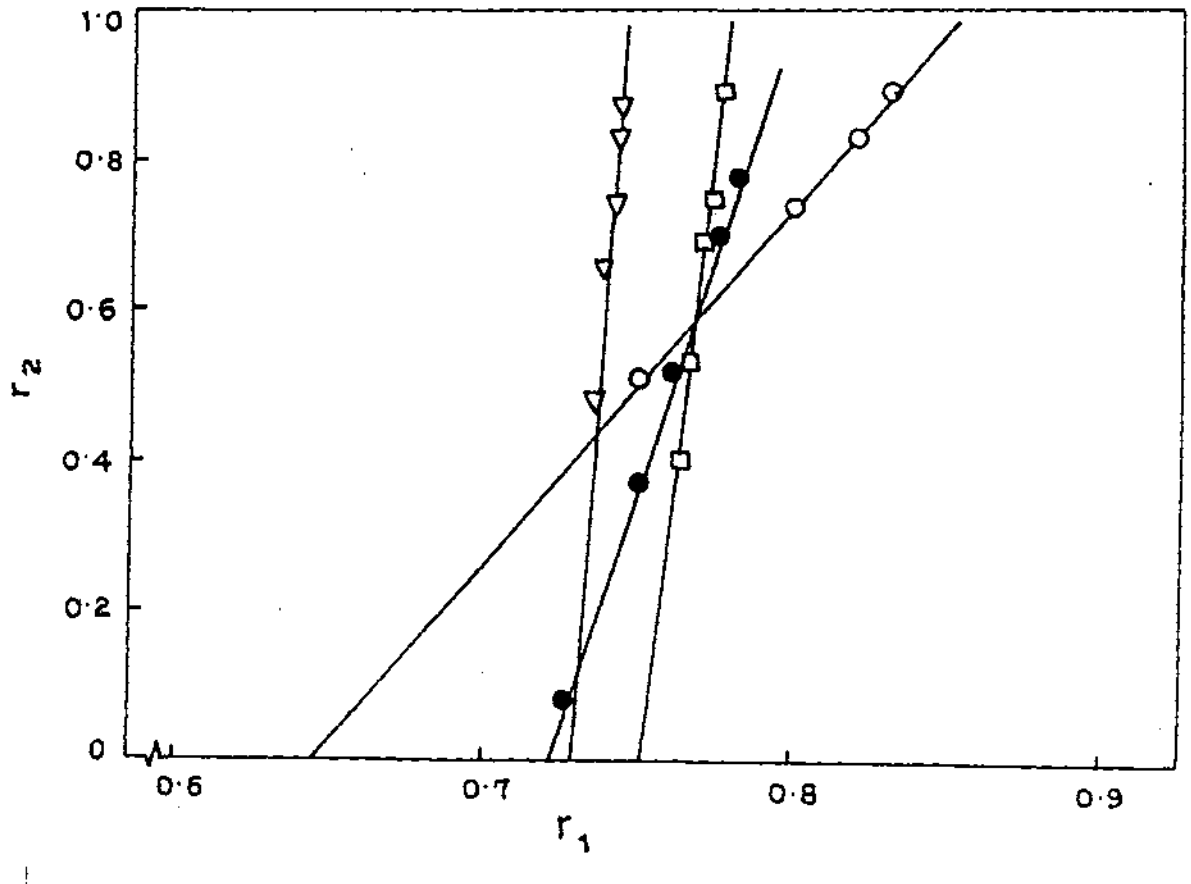

Fig. 54 Mayo-Lewis plot of AM-DAAM coplymer (high conversion).

Table - 25

Variables for the Evaluation of the Reactivity Ratios by the Lewis - Mayo Method

Sample number	$M_{1,0}$	$M_{2,0}$	Q_1	M_1	M_2	Q	F_1	F_2	r_1	r_2
DAAM-10-2	0.41	0.01	41	0.218	0.004	53.17	0.47	0.59	0.76 ± 0.02	0.58 ± 0.04
DAAM-20-3	0.40	0.02	20	0.244	0.011	23.24	0.39	0.47		
DAAM-30-3	0.38	0.04	9.50	0.269	0.026	10.25	0.29	0.34		
DAAM-40-3	0.34	0.08	4.25	0.316	0.074	4.29	0.07	0.08		

$M_{1,0}$ = initial concentration of AM

$M_{2,0}$ = initial concentration of DAAM

$Q_1 = M_{1,0}/M_{2,0}$

M_1 = residual AM in solution

M_2 = residual DAAM in solution

$Q = M_1/M_2$

$F_1 = 1-M_1/M_{1,0}$

$F_2 = 1-M_2/M_{2,0}$

r_1 = reactivity ratio of AM r_2 = reactivity ratio of DAAM

in Table 26.

Reactivity ratio studies were also conducted for the copolymerization of acrylamide (M_1) with N-t-butylacrylamide (M_2) using Fineman-Ross (Figure 55) and Kelen-Tüdos (Figure 56) methods. Mayo-Lewis treatment did not give desirable results. The calculated reactivity ratios are listed in Table 27. Figure 57 shows the composition as a function of the acrylamide in the feed based on the experimentally determined reactivity ratios in the copolymerization of AM with DAAM and with N-t-BAM. The AM-DAAM copolymers with $r_1r_2 = 0.43$ and the AM-N-t BAM copolymers with $r_1r_2 = 0.70$ exhibit an opposite tendency toward alternation. Experimental points on the figure are, however, restricted upto 80 mole % of AM in the feed because no copolymer was formed below that value. Previous study on the copolymerization of AM with DAAM by potassium persulfate initiator showed a variation of r_1 and r_2 values from 0.76 to 0.83 and 0.92 to 0.99 respectively for the three methods applied.[266] These values are, however, higher than those obtained in the present study. Current investigation also shows that r_1 values for the copolymerization of AM with

Table - 26

Reactivity Ratios for copolymerization of AM (r_1) with DAAM (r_2) Method

Method	r_1	r_2
Fineman - Ross[a]	0.69 ± 0.03	0.62 ± 0.05
Fineman - Ross[b]	6.18 ± 0.17	1.06 ± 0.06
Kelen - Tudos	0.70 ± 0.08	0.60 ± 0.09
Mayo - Lewis	0.76 ± 0.02	0.58 ± 0.04

[a]M_1 = AM, M_2 = DAAM; [b]M_1 = DAAM, M_2 = AM

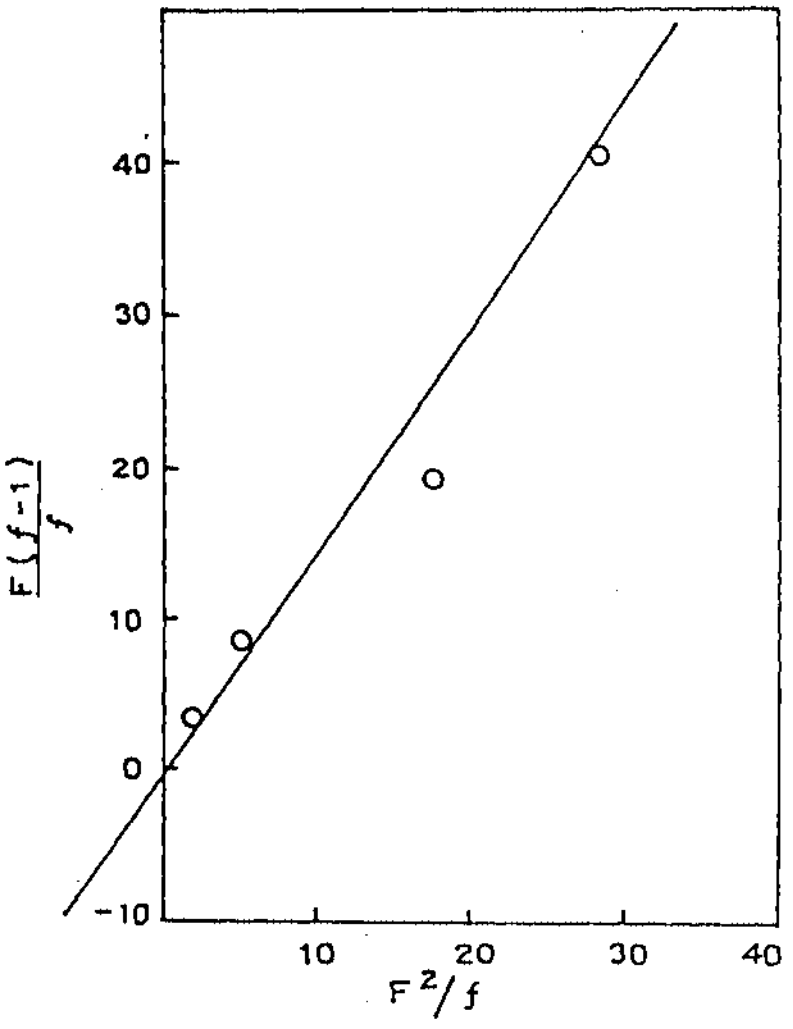

Fig. 55 Determination of reactivity ratios for copolymerization of AM with N-t-BAM by Fineman-Ross method.

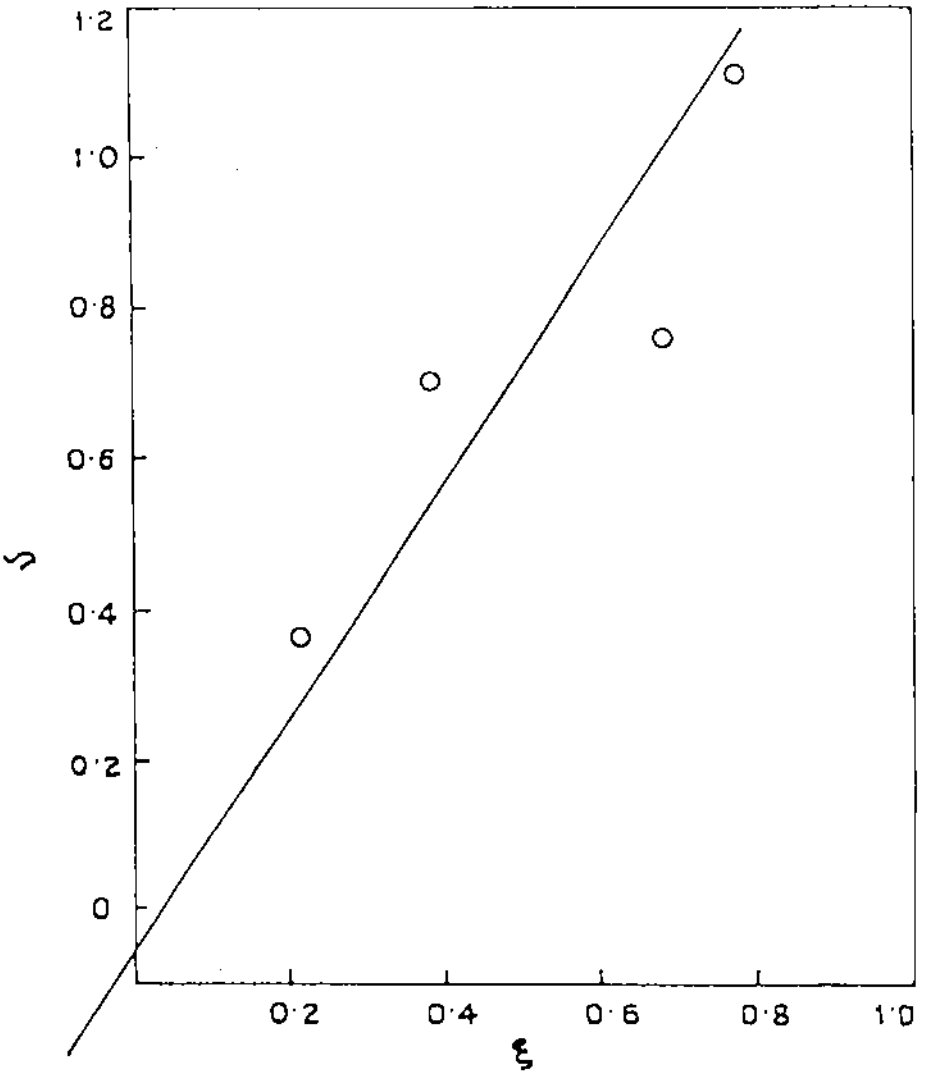

Fig. 56 Determination of reactivity ratios for copolymerization of AM with N-t-BAM by Kelen-Tüdos method.

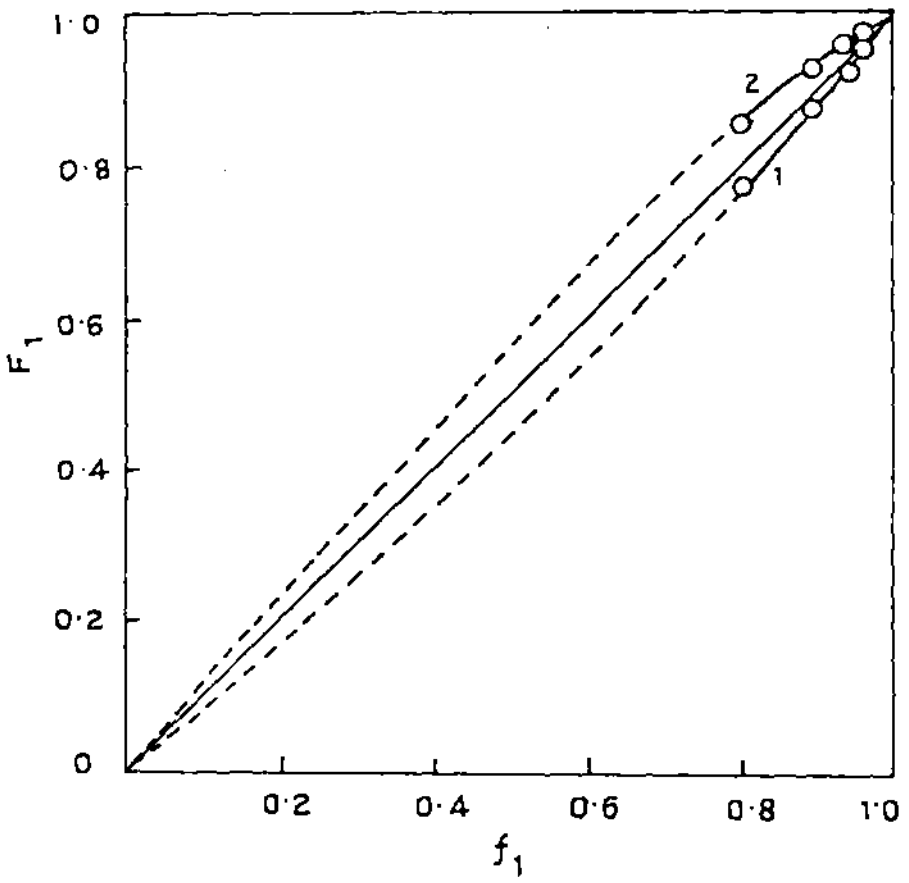

Fig. 57 Copolymer composition as a function of feed composition for the copolymerization of AM with DAAM (curve 1) and AM with N-t-BAM (curve 2).

Table - 27

Reactivity Ratios for copolymerization of AM(r_1) with N-t BAM (r_2)

Method	r_1	r_2
Fineman - Ross[a]	1.50 ± 0.10	0.50 ± 0.04
Fineman - Ross[b]	1.39 ± 0.08	0.75 ± 0.06
Kelen - Tudos	1.50 ± 0.10	0.46 ± 0.04

[a]M_1 = AM, M_2 = N-t-BAM; [b]M_1 = N-t-BAM, M_2 = AM

N-t-BAM is considerably higher than AM-DAAM copolymers, where as, those of r_2 are smaller in the case AM-N-t BAM than that of the other copolymer.

Copolymer microstructure

The microstructures of the AM-DAAM and AM-N-t BAM copolymers are expected to be important in determining the solution properties of copolymers. As mentioned earlier, observed data follow the conventional copolymerisation equation and the adherence of the data to this equation is an important point in establishing the validity of the statistical microstructure analyses. The statistical distribution of monomer sequences, $M_1 - M_1$, $M_2 - M_2$, and $M_1 - M_2$ may be calculated utilizing equations[275-276].

$$X = \phi_1 - 2\phi_1(1 - \phi_1)/\{1 + [(2\phi_1 - 1)^2 + 4r_1r_2\phi_1(1 - \phi_1)]\}^{1/2} \quad (49)$$

$$Y = (1 - \phi_1) - 2\phi_1(1 - \phi_1)/\{1 + [(2\phi_1 - 1)^2 + 4r_1r_2\phi_1(1 - \phi_1)]\}^{1/2} \quad (50)$$

$$Z = 4\phi_1(1 - \phi_1)/\{1 + [(2\phi_1 - 1)^2 + 4r_1r_2\phi_1(1 - \phi_1)]\}^{1/2} \quad (51)$$

The mole fractioins of $M_1 - M_1$, $M_2 - M_2$ and $M_1 - M_2$ sequences in the copolymer are designated by X, Y and Z respectively. The copolymer

composition is ϕ_1 and, r_1 and r_2 are the reactivity ratios, for the respective monomer pairs. Mean sequence lengths, μ_1 and μ_2, can be calculated utilizing equation (52) and (53) with the consideration of compositional drift.[275]

$$\mu_1 = 1 + r_1 [M_1]/M_2] \quad (52)$$

$$\mu_2 = 1 + r_2 [M_2]/M_1] \quad (53)$$

The intermolecular linkage and mean sequence length distributions for the AM-DAAM and the AM-N-t BAM copolymers are listed in Table 28 and 29 respectively. The Kelen - Tüdos values of reactivity ratios were used for sequence distribution calculation. For the series of AM-DAAM copolymers, the mean sequences length of acrylamide, μ_{AM}, varied from 30.03 at an 96.36/3.64 mol ratio of AM/DAAM in the copolymer to 4.01 with a 78.77/21.23 mol ratio. For those compositions, values of μ_{DAAM} were 1.01 and 1.14 respectively. On the other hand, the AM-N-t BAM copolymers had μ_{AM} value of 62.50 and 7.37 at 98.33/1.67 and 89.42/10.58 mol ratios of AM/N-t BAM respectively. Above values for $\mu_{N\text{-}t\ BAM}$ were 1.01 and 1.11 respectively.

Effect of Feed Composition

The effect of feed composition on intrinsic viscosity of copolymers synthesized at high conversion was studied for both AM-DAAM and the AM-N-t BAM copolymers listed in Table 23 and 24 respectively. Figure 58 illustrates the effect of feed composition on the intrinsic viscosity for each copolymer series. The observed decrease in intrinsic viscosity with increasing diacetoneacrylamide or N-tert-butylacrylamide co-monomer concentrations may be explained by increased cross-termination rates of copolymerization as compared to the very low rate of termination observed for acrylamide, resulting in the decrease of the overall molecular weight of the copolymers[278,279].

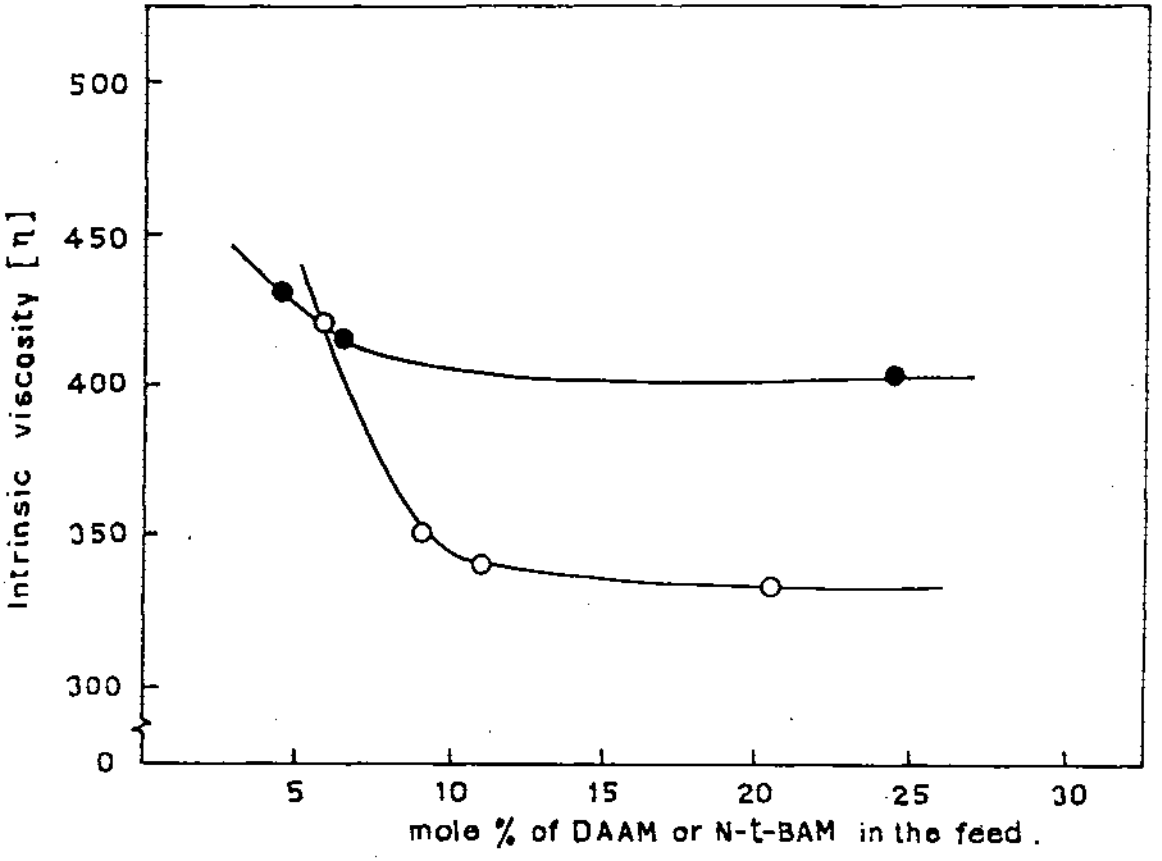

Fig. 58 Effect of feed composition on the intrinsic viscosity of AM-DAAM (o) and AM-N-t-BAM (•) copolymers.

Table- 28

Structural Data for the copolymers of AM with DAAM

Sample Number	Composition[a] (mole%)		Block ness[b] (mole%)		Alternation[b] (mole%)	Mean Sequence length		μ_{AM}/μ_{DAAM}
	AM	DAAM	AM-AM	DAAM-DAAM	AM - DAAM	μ_{AM}	μ_{DAAM}	
DAAM-10-1	96.36	3.64	92.78	0.06	7.16	30.03	1.01	29.58
DAAM-20-1	93.61	6.39	87.41	0.19	12.40	15.16	1.03	14.71
DAAM-30-1	87.44	12.56	75.67	0.79	23.54	7.72	1.06	7.29
DAAM-40-1	78.77	21.23	60.05	2.51	37.43	4.01	1.14	3.51
DAAM-10-2	96.46	3.54	92.97	0.06	6.97	30.03	1.01	29.58
DAAM-20-2	92.69	7.31	85.70	0.32	13.98	15.16	1.03	14.71
DAAM-30-2	87.73	12.27	76.21	0.76	23.03	7.72	1.06	7.29
DAAM--40-2	72.76	27.24	50.00	4.47	45.54	4.01	1.14	3.51
DAAM--10-3	94.08	5.92	88.32	0.16	11.51	30.03	1.01	29.58
DAAM--20-3	93.49	6.51	87.17	0.20	12.62	15.16	1.03	14.71
DAAM-30-3	88.94	11.06	78.48	0.60	20.92	7.72	1.06	7.29
DAAM-40-3	79.22	20.78	60.83	2.40	36.77	4.01	1.14	3.51

[a] Calculated from elemental analysis ; [b] Statistically calculated from the reactivity ratios.

Table- 29

Structural Data for the copolymers of AM with N-t BAM

Sample Number	Composition[a] (mole%)		Block ness[b] (mole%)		Alternation[b] (mole%)	Mean Sequence length		$\mu_{AM}/\mu_{N\text{-}t\,BAM}$
	AM	N-t BAM	AM-AM	N-t BAM-N-t BAM	AM - N-t BAM	μ_{AM}	$\mu_{N\text{-}t\,BAM}$	
N-t-BAM-10-1	93.78	6.22	87.84	0.28	11.87	62.50	1.01	61.80
N-t-BAM-20-1	98.61	1.39	97.23	0.01	2.75	31.00	1.02	30.30
N-t-BAM-30-1	88.59	11.41	78.16	0.98	20.86	15.25	1.05	14.52
N-t-BAM-10-1	88.56	11.44	78.10	0.98	20.91	7.37	1.11	6.64
N-t-BAM-10-2	98.33	1.67	96.68	0.01	3.30	62.50	1.01	61.80
N-t-BAM-20-2	95.82	4.18	91.77	0.12	8.11	31.00	1.02	30.30
N-t-BAM-30-2	94.75	5.25	89.70	0.20	10.10	15.25	1.05	14.52
N-t-BAM-40-2	89.42	10.58	79.68	0.84	19.48	7.37	1.11	6.64
N-t-BAM-10-3	95.44	4.56	91.03	0.46	8.82	62.50	1.01	61.80
N-t-BAM-20-3	93.68	6.32	87.65	0.29	12.06	31.00	1.02	30.30
N-t-BAM-30-3	75.62	24.38	56.05	4.80	39.14	15.25	1.05	14.52
N-t-BAM--40-3	77.77	22.23	3.95	3.95	36.55	7.37	1.11	6.64

[a]Calculated from Elemental Analysis

[b]Statistically calculated from Reactivity Ratios.

CHAPTER - 5

STUDIES ON SOLUTION PROPERTIES OF POLYACRYLAMIDE IN WATER - DIMETHYL SULPHOXIDE MIXTURE

5.1 INTRODUCTION AND REVIEW OF PREVIOUS WORK

In the treatment of the properties of very dilute polymer solutions it is convenient to represent the molecule as a statistical distribution of chain elements, or segments, about the centre of gravity. The average distribution of segments for a chain polymer molecule is approximately Gaussian[280], its breadth depends on the molecular chain length and on the thermodynamic interaction between polymer segments and solvent. According to hydrodynamics, the specific viscosity of a Newtonian liquid containing a small amount of dissolved material should depend in first approximation only upon the volume concentration and the shapes of the suspended particles. By suitable application of such hydrodynamical considerations to solutions of long chain molecules, it is possible in a rough fashion to derive the Staudinger-Kraemer equation, denoting proportionality between specific or intrinsic viscosity and molecular weight.[281] It is an experimental fact, however, that the proportionality constant, K_m, is dependent not only upon the type of polymer concerned, but also upon the temperature and the nature of the solvent. A relationship between intermolecular and intramolecular agglomeration tendency is established. Solutions of polystyrene, rubber and cellulose acetate in the solvent-non solvent systems were investigated by Alfrey and co-workers.[281] They observed that the specific viscosity of a dilute solution of polystyrene or rubber is strongly dependent upon the nature of solvent, the specific viscosity is high in a good solvent and low in a poor solvent or a solvent-non solvent mixture. This has been interpreted as being due to changes in mean molecular shape. The specific viscosities of cellulose acetate solutions are not so sensitive to the nature of solvent. Besides this, the extrapolated specific viscosity at the limit of solubility is in the same range for several different solvent-non solvent systems. The effect of temperature upon intrinsic viscosity should depend strongly upon the nature of solvent. Alfrey and co-workers also noted that the effect of a temperature increase is to lower the specific viscosity of rubber or polystyrene solutions in a good solvent, but to increase the specific viscosity in a mixture of solvent and non-solvent. Unperturbed dimensions of

flexible linear macromolecules can be obtained from intrinsic viscosity-molecular weight data in any solvent, good or poor, if (as is almost always true) the hydrodynamic draining effect is negligible and if an estimate can be made of the viscosity expansion factor α_η, defined by[282]

$$[\eta] = K_\theta M^{1/2} \alpha_\eta^3 \qquad (54)$$

In principle, this can be done graphically from the relation alone if a reliable expression is available for the dependence of α_η on M. In particular, it has been shown from theoretical considerations that the intrinsic viscosity should depend on the molecular weight M, temperature T and solvent type in accordance with the relationships,[283-285]

$$\alpha^5 - \alpha^5 = 2\,\psi_1\, C_M\, (1 - \theta/T) M^{1/2} \qquad (55)$$

where $\theta = k_1 T/\psi_1$

$$K_\theta = \phi_o \left(\overline{r_o^2} / M\right)^{3/2} \qquad (56)$$

$$C_M = 27(2^{5/2} / \pi^{3/2} N)\, (\bar{\upsilon}^2 / v_1)\, (M / \overline{r_o^2})^{3/2}$$

$$= 1.4238 \times 10^{-24}\, (v^2/v_1)\, (\theta_o / K_\theta) \qquad (57)$$

where ψ_1 is entropy parameter, k_1 is the enthalpy parameter, θ is the temperature and K_θ is the unperturbed dimension of the polymer, ϕ_o is the Flory's universal constant. Here, $\bar{\upsilon}$ is the partial specific volume of the polymer and v_1 is the molar volume of the solvent.

Intrinsic viscosities of polyisobutylene fractions ($M=1.8 \times 10^5$ to 1.88×10^6) and polystyrene fractions ($M = 7.0 \times 10^4$ to 1.27×10^7) have been determined in various pure solvents and in several solvent mixtures at several temperatures by Fox and Flory[286,287]. They observed that the parameter K_θ in

---

K *and* k *in this chapter are different from those used in chapter 3.*

the equation (54), is same in different solvents but decreases somewhat with temperature (1.08×10^{-3} at 24° to 0.91×10^{-3} at 105° for polyisobutylene and 8.0×10^{-4} at 34° to 7.3×10^{-4} at 70° for polystyrene). The root-mean square end-to-end distance $(\overline{r_0^2})^{1/2}$, unperturbed by intramolecular interactions (other than hindrance to free rotation) for a polyisobutylene molecule and polystyrene molecule with $M=10^6$ has been calculated to be 795Å and 730Å at 25°C respectively. The solution properties of poly (methyl acrylate) in various solvents by light scattering, osmometry, and viscosity techniques have been investigated by many workers.[288-300] Many empirical and semi empirical methods for the estimation of K_θ from viscometric measurements in good solvents have recently been proposed.[301-314]

The viscosity behaviour of poly (methyl methacrylate) in four solvents was studied within the temperature range of 25° to 60°C and the thermodynamic parameters were evaluated and discussed using Fox-Flory,[285] Burchard Stockmayer-Fixman,[315, 316] Kurata-Stockmayer[317,318] and Berry[319] equations by Lenka and co-workers.[320] On the other hand, for evaluation of K_θ from $[\eta]$ at $T > \theta$ (in good solvent), a number of equations relating $[\eta]$ and M through K_θ (after eliminating linear expansion factor (α), hydrodynamic expansion factor (α_η), lattice co-ordination number (z) etc.) have been suggested. These equations are shown below (where symbols have their usual meanings). Fox and Flory equation[285]:

$$[\eta]^{2/3}/M^{1/3} = K_\theta^{2/3} + K_\theta^{5/3} C_T (M/[\eta]) \qquad (58)$$

Kurata-Stockmayer (K-S) equation[317,318]:

$$[\eta]^{2/3}/M^{1/3} = K_\theta^{2/3} + 0.363\, \phi\, B[g(\alpha_\eta) M^{2/3} / [\eta]^{1/3}] \qquad (59)$$

Burchard-Stockmayer and Fixman (B.S.F) equation[315,316]

$$[\eta]/M^{1/2} = K_\theta + 0.51 \phi\, BM^{1/2} \qquad (60)$$

Berry equation[319]:

$$([\eta]/M^{1/2})^{1/2} = K_\theta^{1/2} + 0.42\, K_\theta^{3/2}\, B\, (\overline{r_0^2}/M)^{3/2}\, (M/[\eta]) \qquad (61)$$

According to these equations, the value of K_θ may be obtained from the intercepts on the ordinates of the plots of the quantity on the left hand side versus a function of M and $[\eta]$ on the right hand side. The unperturbed dimensions for polymethylacrylate, polyethylacrylate, polybutylacrylate, polyacrylonitrile, and polyvinyl pyrrolidine have been calculated by Lenka and co-workers[321] using an expression relating to the cross-over point concentration, C_x, of the polymer in a number of solvents with the unperturbed dimension of polymer molecule $(\overline{r_0^2})^{1/2}$. Assuming Flory's limiting exponent and utilizing the first-order perturbation results for the intrinsic viscosity $[\eta]$ and the friction coefficient (f) of a flexible polymer, Tanaka proposed[322]:

$$([\eta] / M^{1/2})^{5/3} = K_\theta^{5/3} + 0.627\, \phi_o^{5/3}\, (< R^2 >_o/M)\, BM^{1/2} \qquad (62)$$

and Bohdanecky derived the following equation[330]:

$$[\eta]/M^{1/2} = 0.80\, K_\theta + 0.65\, K_\theta K^{0.7} M^{0.35} \qquad (63)$$

The unperturbed dimensions of polystyrene and poly (2-vinylpyridine) have been measured in solvent-precipitant mixtures of various compositions using the Stockmayer-Fixman representation by Dondos and Benoit[323]. They obtained a linear relationship between K_θ and ΔG^E (the excess free enthalpy of mixing of the solvents) if, instead of using the bulk composition of the mixture, one introduces its "local" composition. This composition is calculated from the values of the preferential adsorption coefficient measured by light scattering.

In a resin-solvent system, the change in temperature initiates conformational transition in polymer chains[282] and the process of aggregation

on precipitation is caused by such transitions.[324] Raju and Yaseen reported that the continuous decrease in limiting viscosity number of Nylon-6 in m-cresol at temperatures ranging from 20° to 75°C was due to the contraction of the dimensions of the polymer coil.[325] Quoting the view of other workers they explained that a partial helix-coil type polymer chain transition occurs in polyamide-6 in solution and results in higher value of limiting viscosity number of nylon-6 in m-cresol at lower temperatures which in turn favours the dissolution.[326] They also observed that limiting viscosity number of Nylon-6 in phenol increase with temperature and the system attained a state of optimum dissolution at 55°C and further increase in temperature and had adverse effect. Chatfield reports that solvent power of an alcohol-ether mixture for nitrocellulose increases with lowering of temperature and at –50°C, methyl alcohol alone becomes a solvent for cellulose ethers.[327] Recently, Savas and Zuhal have determined the unperturbed dimensions of anionically polymerized poly (p-tert-butyl-styrene) at various temperatures and found the θ-temperature of the polymer of the order of 31°C and 32.7°C in 1-nitropropane and 2-octanol respectively.[328] Several other workers reported the conformational transition of polymers in solution with change in temperature.[310,329] Coil dimensions of poly (methylacrylate) in the cosolvent medium of CCl_4 and MeOH have been investigated by Maitra and Nandi.[331] They observed that the intrinsic viscosity exhibited a maximum for all fractions of polymer at a composition, ϕ_{CH_3OH} (volume fraction of methanol) = 0.33 and also Huggins constant showed a minimum at the same composition. The unperturbed dimension (K_θ) exhibited a maximum and molecular extension parameter α_n, showed a minimum at ϕ_{CH_3OH} =0.33. The experimental data for the solution properties of poly (N,N-dimethylacrylamide) and poly (N-isopropylacrylamide) show that the hydrodynamic and configurational characteristics of these two N-substituted polyacrylamide, in methanol and water are different, showing a peculiar behaviour in water, which cannot be easily interpreted in terms of random coil molecules.[332,333] Also, the unperturbed dimensions estimated from data in good solvents are found to depend more on the lateral substituent structure

than on its dimensions. Chintore and co-workers found that bahaviour of poly (N-methylacrylamide) molecules in aqueous solution was quite abnormal, as indicated by the values of the second virial coefficients, lower than those measured in methanol solutions by the large difference of estimated unperturbed dimensions.[332,333] Therefore, the hypothesis was made that the solvation of N-substituted poly acrylamides by water would occur with large dipole interaction and/or hydrogen bonding with the structural units of the polymers in such a way as to give a large chain expansion with low chain flexibility, so that the polymer molecules could no more be treated as random coils in aqueous solutions. It has been pointed out that polyacrylamide, in which the lack of N-substituents increases the chances of intramolecular interactions, has the highest unperturbed dimensions.[334] The aqueous solutions of polyacrylamides are suspected to contain fibrous aggregates of very high molecular weight. These aggregates were observed by electronic microscopy[335] and the disaggregation kinetics studied by viscometry.[336,337] This phenomenon is generally attributed to intermolecular hydrogen bonds and is evidenced by an important decrease of viscosity with time. Boyadijian and co-workers have noticed differences of measured molecular weight by light scattering, according to the nature of solvent and have concluded the presence of aggregates broken up by the effect of salts in pure water but not in formamide.[338] However, even for non-hydrolysed polyacrylamide, there is a lack of reliable data in the literature concerning the chain conformation in salt water solutions and its relation to intrinsic viscosity, particularly in the range of molecular weights of interest.[339,240] However, Francois and Sarazin and co-workers were successful in studying molecular weight dependence of radius of gyration, viscosity sedimentation and diffusion on a set of fractions in the same range of molecular weight.[214] It has been shown recently that, the unperturbed dimensions of polyacrylamide could be determined by light scattering measurements in methanol-water system.[340] These authors concluded that the high value of the exponent (0.64) of the molecular weight dependence of the radius of gyration was not related to a great expansion of the macro molecular coil, and the determination of the unperturbed dimensions by extrapolation of viscosity

measurements in good solvents at M $\rightarrow$0 should be possible and works of Okada and Yamaguchi provide such determinations.[341,342] Fundamental parameters of poly (2-acrylamido-2-methyl propane sulfonamide) which is soluble in water and formamide are obtained by light scattering, osmometry and viscometry in these good solvents by Gooda and Huglin[343] and has been analysed by extrapolation procedures to yield the unperturbed dimensions $(r^2_o/M_w)^{½}$, steric factor (σ) and characteristic ratio (C_α) . There was good accord between the values of $(\langle r^2\rangle_o/M_w)^{½}$, σ and C_α thereby obtained directly and those derived indirectly, the mean values being 8.73 x 10^{-9} $cmg^{½}$ $mol^{½}$, 4.07 and 32 respectively. Bohdanecky and Petrus and co-workers investigated the solution of 9 polyacrylamide fractions (molecular weight 3300-800,000) in water at 25°C and in a mixed θ solvent (3.2 volume, H_2O-MeOH) at 20°C by light scattering, sedimentation and viscometry.[344] Measurements in water gave the configuration character ratio C_α = 8.5.

The fundamental parameters of the polyacrylamide obtained previously by viscometry in good solvent i.e. water and in a θ solvents have been analysed by viscosity molecular weight relationship procedures suggested by several workers (Scholtan[339], Newman[345] and Misra[346]). High value of excluded volume exponent, as was observed in some cases, once thought to be the result of great expansion of polyacrylamide in aqueous solution as mentioned above[214,340]. This arose doubts on the applicability of the method of extrapolation of the viscosity data in determining unperturbed dimension of the polymer in water. Further study, however, confirmed that the high value of the exponent of molecular weight dependence of the radius of gyration was not due to a great expansion of the macromolecular coil in water and it is now believed that determination of the unperturbed dimension by extrapolating viscosity data in good solvents is possible.[340] Although some studies on the solution viscosity properties of acrylamide in water are available in the literature, similar studies in other solvents or cosolvent systems are surprisingly little.[340,344] In a binary liquid mixture, it is the interaction between the liquids that governs

the solubility of a polymer in the mixture. Expansion of coil are also occurred due to two main reasons. (I) variation of molecular extension factor (α_n) and (II) change of the unperturbed dimension of the polymer due to interactions of two component liquids.[347,348] In the present chapter, the results of our investigation on unperturbed dimension, interaction parameter and related aspects of unhydrolized polyacrylamide in water-DMSO mixtures have been described. The intrinsic viscosities [η] of the polymer have been measured for different molecular weight fractions of the polymer and also in different compositions (water/DMSO) of the cosolvent mixture. From the [η] – M relation, the unperturbed dimension(K_θ) and molecular extension factor (α_n) have been measured. The Huggins constant value in each case was also determined in order to study the influence of cosolvent system on the aggregation of polymer.[331] While DMSO is a poor solvent for PAM, water-DMSO mixture acts as a cosolvent in all proportions. In the previous chapters, we have reported the technique by which the molecular weight of the polyacrylamide in aqueous solution may be controlled by trapping the initiator component in the interlayer space of montmorillonite. This method has been adopted selectively to prepare polymers of varying molecular weights for the solution property studies as presented in this chapter.

5.2 EXPERIMENTAL

Polymerization

PAM was synthesized from acrylamide monomer (AM) by redox polymerization technique. The polymerization technique of AM, initiated by Ferric-montmorillonite (FeM) - thiourea (TU) redox system has been discussed in Chapter 3 (section 3.2).. To obtain high molecular weight polymers for the present study, a similar technique has been adopted using 0.4 M monomer and 0.04 thiourea in aqueous suspension of 0.50% FeM (W/V) in the temperature range between 70°C and 50°C (already discussed in Chapter 3,

section 3.4.3). Low molecular weight polymers were obtained via polymerization of AM monomers initiated by 1.5×10^{-3} M $FeCl_3$ and 0.04M TU redox system at 50°C in absence of montmorillonite(already discussed in Chapter 3, section 3.3.3). The molecular weights (determined from intrinsic viscosity measurements in water at 30°C) of the polymers used in the present study are listed in Table-30.

Viscosity Measurements

The intrinsic viscosities [η] of the polymers in aqueous solutions were determined by an Ubbelohde viscometer, placed at appropriate temperature in a thermostat, measuring specific viscosities (η_{sp}) and using the Huggin's equation for extrapolation :

$$\eta_{sp}/C = [\eta] + K[\eta]^2C \qquad (64)$$

where C is the concentration of the polymer solution. Molecular weights of the polymer were calculated from the intrinsic viscosity data (already mentioned in section 3.3.3 and 3.4.3). The [η] values of the polymer in various water-DMSO compositions (prepared by volume) were also measured in a similar way.

Table-30

Molecular weights of polyacrylamides

Polyacrylamide types	$M_v \times 10^{-5}$
High Molecular weight (HM)	12.55
Medium Molecular weight (MM)	8.44
Low Molecular weight (LM)	1.33

5.3 RESULTS AND DISCUSSION

Nature of the interaction between the liquids governs the solubility of a polymer in a binary liquid mixture. The changes in the molecular dimensions of the polymers in these systems are manifested in the varied molecular extension parameter (α_η) and the unperturbed dimensions due to the interaction with two component liquid.[347,348] The changes in intrinsic viscosities [η] of various molecular weight fractions of PAM at 30°C and different solution compositions are shown in Figure 59. With increasing DMSO (poor solvent) concentration, the intrinsic viscosity decreases due to contraction of the dimensions of the polymer coil as well as for the degree of intermolecular agglomeration. However, at high value of ϕ_{DMSO} (ϕ being the relative volume composition in the mixture), the [η] value tends to increase again for preferential solvation of the polymer due to high cosolvent effect. It is found that for all the molecular weight fractions, the intrinsic viscosity attains the minimum near ϕ_{DMSO} value between 0.6-0.7 indicating energitically most unfavourable solvent composition for the polymer. The lowest value of [η] around ϕ_{DMSO} = 0.6 - 0.7 indicates the maximum degree of intermolecular aggregation of the polymers at this solvent composition. Similar nature of the variation of [η] on solvent composition is also observed at 40°C temperature (Figure 60). Such changes of the [η] value as a function of solvent composition clearly indicates the flexibility of the PAM molecules in the present solvent systems also. On the other hand, at 50°C temperature the nature of the curves is changed dramatically (Figure 61). Instead of giving a minimum with the variation of solution composition, the [η] reaches a maximum near ϕ_{DMSO} = 0.3, for all the polymer fractions. The maximum intrinsic viscosities for all polymer fractions at this solvent composition indicate preferential solvation of the polymers due to most powerful cosolvent effect.[331] The effect of temperature upon [η] should depend strongly upon the nature of the solvent. In a binary solvent composition where cosolvancy factor is poorer, an increase of temperature should increase the relative importance of entropy factors over energetic factors, and results in

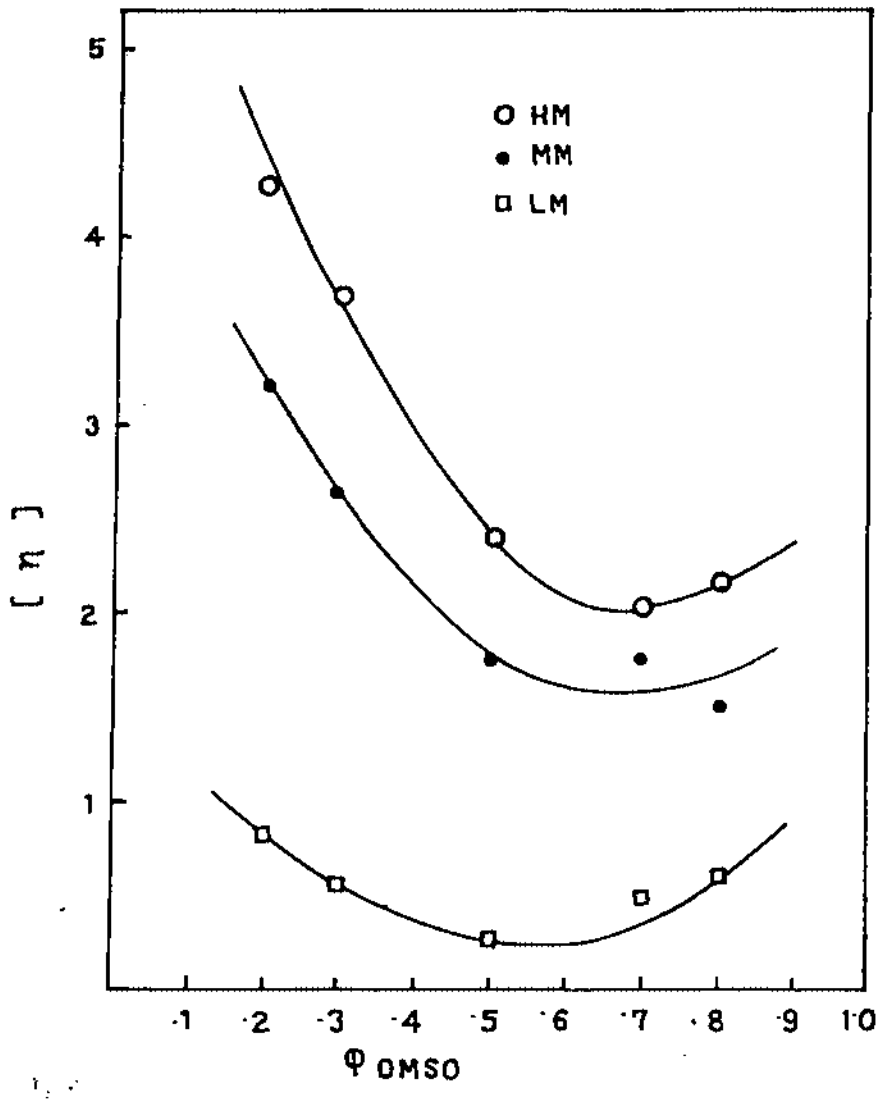

Fig.59 Plot of intrinsic viscosity of PAM fractions at 30°C versus volume fraction of DMSO.

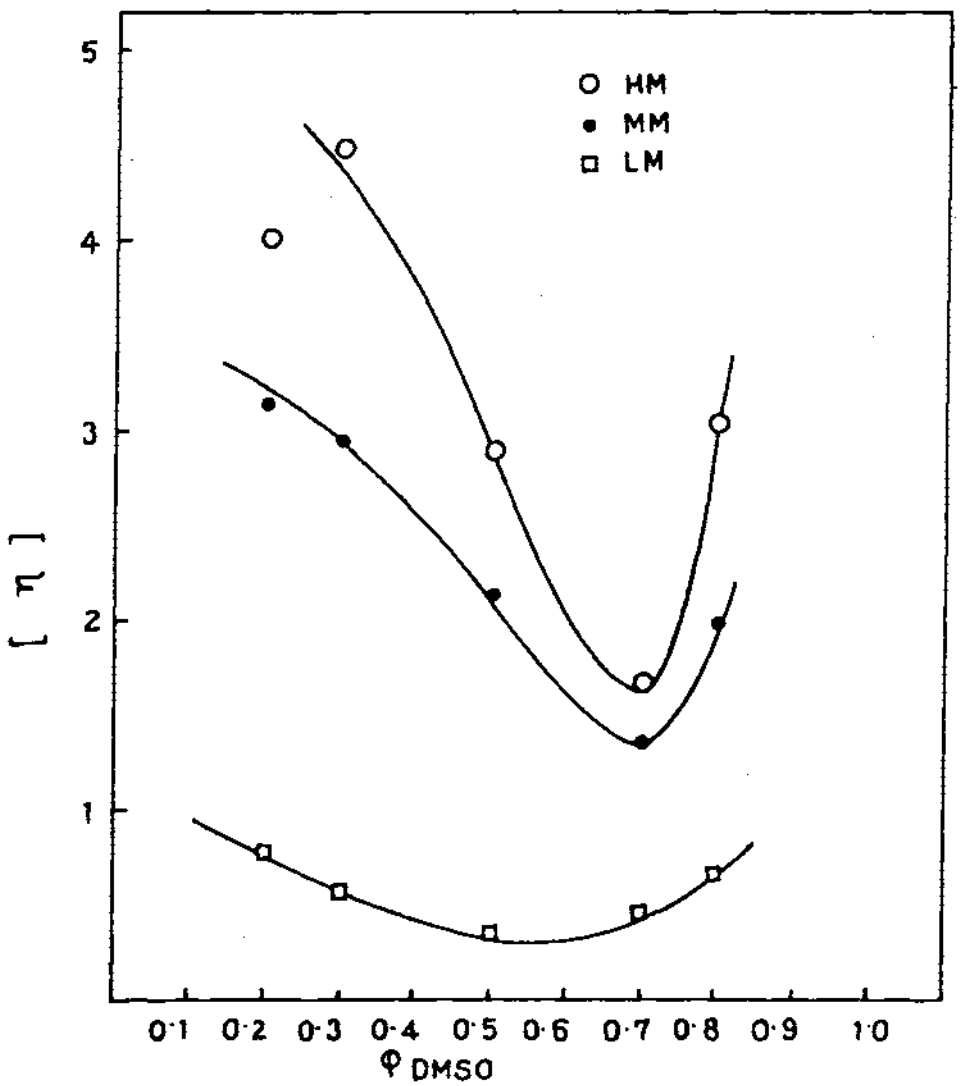

Fig. 60 Plot of intrinsic viscosity of PAM fractions at 40°C versus volume fraction of DMSO.

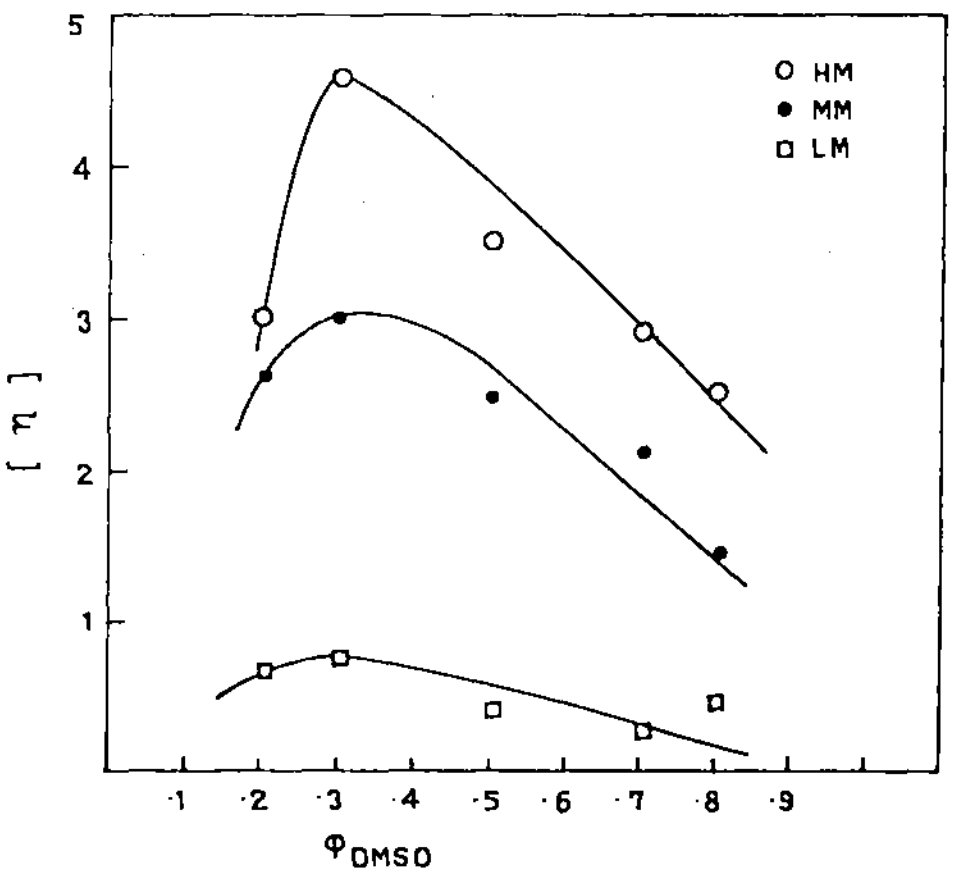

Fig. 61 Plot of intrinsic viscosity of PAM fractions at 50°C versus volume fraction of DMSO.

an uncurling of the molecule.[281] The uncurled configurations will be favoured due to long chain molecule being surrounded by solvated hull which tends to prevent polymer-polymer contacts. In such a solvent, a temperature increase should result in an increase of [η]. On the other hand, at higher cosolvancy condition, the energetic weighting factors favour the more extended configuration; here an increase in temperature should diminish the [η] value. As a result, above maxima in [η] versus ϕ_{DMSO} plots are observed at high temperature for all types of the polymer studied. The cosolvency and the intermolecular interaction of polymers are also manifested in the Huggins constant values when the composition of the solvent system were varied. Plots of Huggins constant as a function of solvent composition are shown in Figures 62-64. The Huggins constants (K) are calculated from the least square slopes of equation (64). It is observed that there is a maximum at solvent composition ϕ_{DMSO} = 0.7 for medium and high molecular weight polymers. This shows that cosolvent effect is apparent above ϕ_{DMSO} value of 0.7. However, at 50°C temperature, although a maximum is obtained at ϕ_{DMSO} ~ 0.7 , the small value of K indicate better cosolvency at this temperature for MM and HM samples. For LM fraction, very high values of K indicate strong aggregation of polymer molecules at all the temperatures studied. Figure 65 shows a plot of Huggins constant against log M_v for three different solvent compositions (upto ϕ_{DMSO} = 0.5) . All the curves show a decrease in the Huggins constant value with the increase in molecular weight indicating higher tendency of intermolecular aggregation for smaller fractions of the polymers in poor cosolvent conditions.

Unperturbed Dimension

The unperturbed dimension of a polymer chain is important in understanding the physical properties of the polymer both in solution as well as in the solid state. It is the dimension of the polymer chain where the volume exclusion due to long range segmental interaction is nullified by its interaction

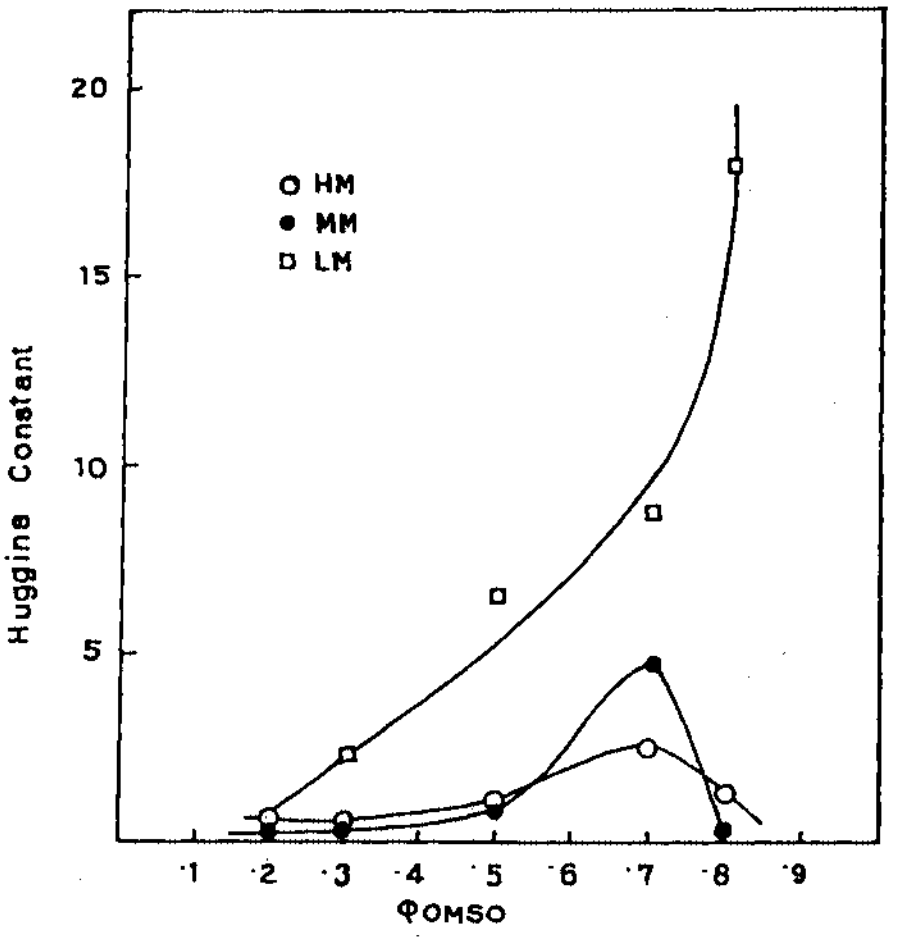

Fig. 62 Plot of Huggins constant of PAM fractions at 30°C versus volume fraction of DMSO.

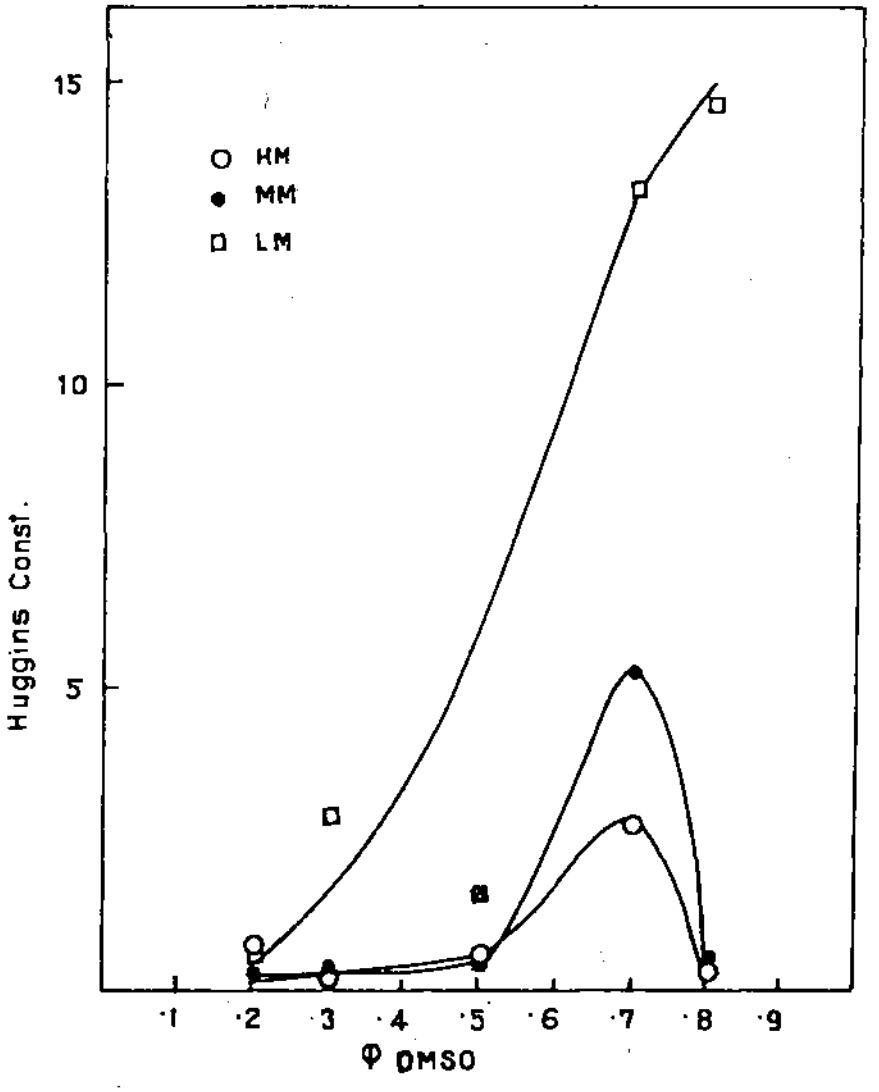

Fig. 63 Plot of Huggins constant of PAM fractions at 40°C versus volume fraction of DMSO.

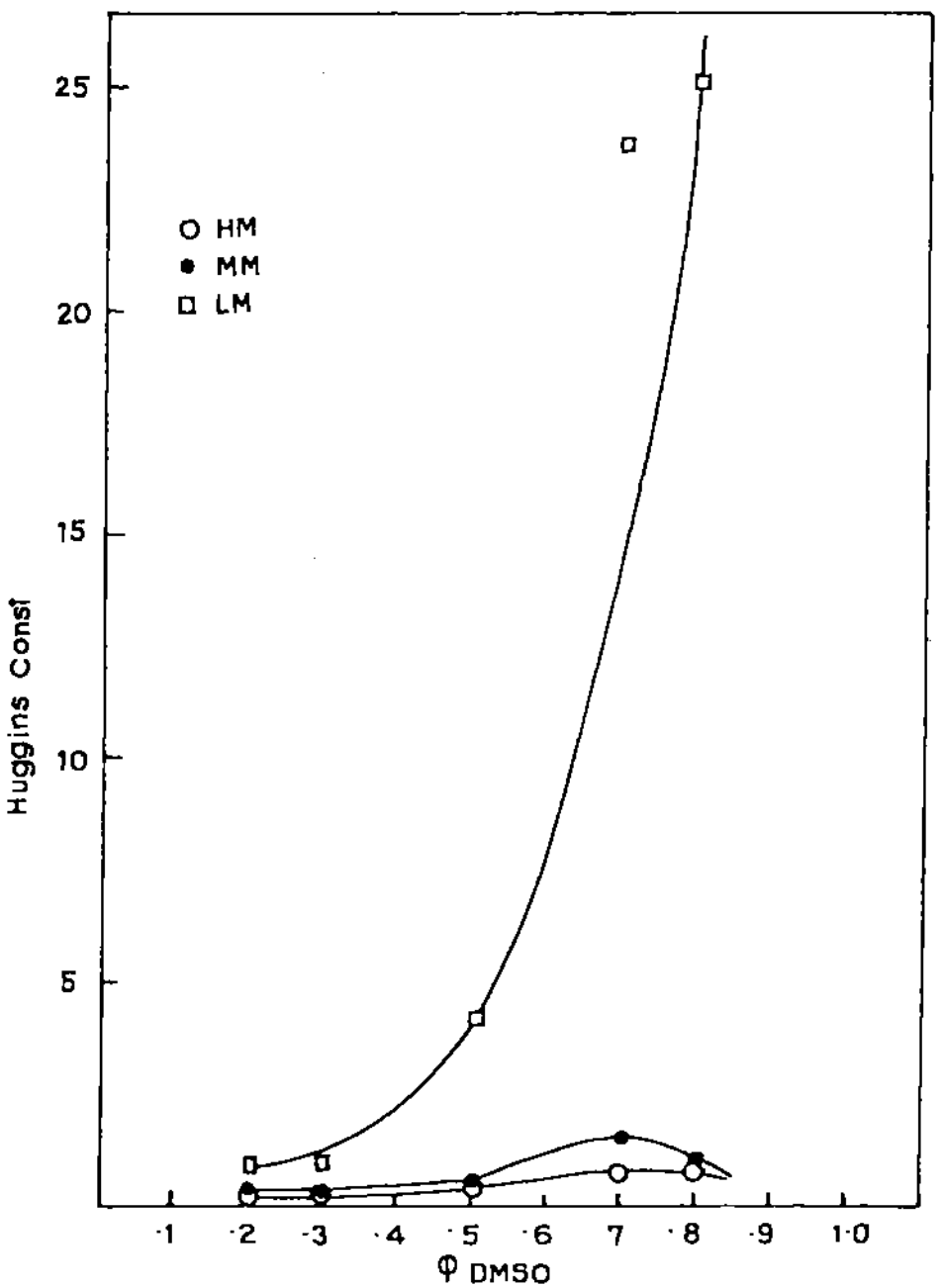

Fig. 64 Plot of Huggins constant of PAM fractions at 50°C versus volume fraction of DMSO.

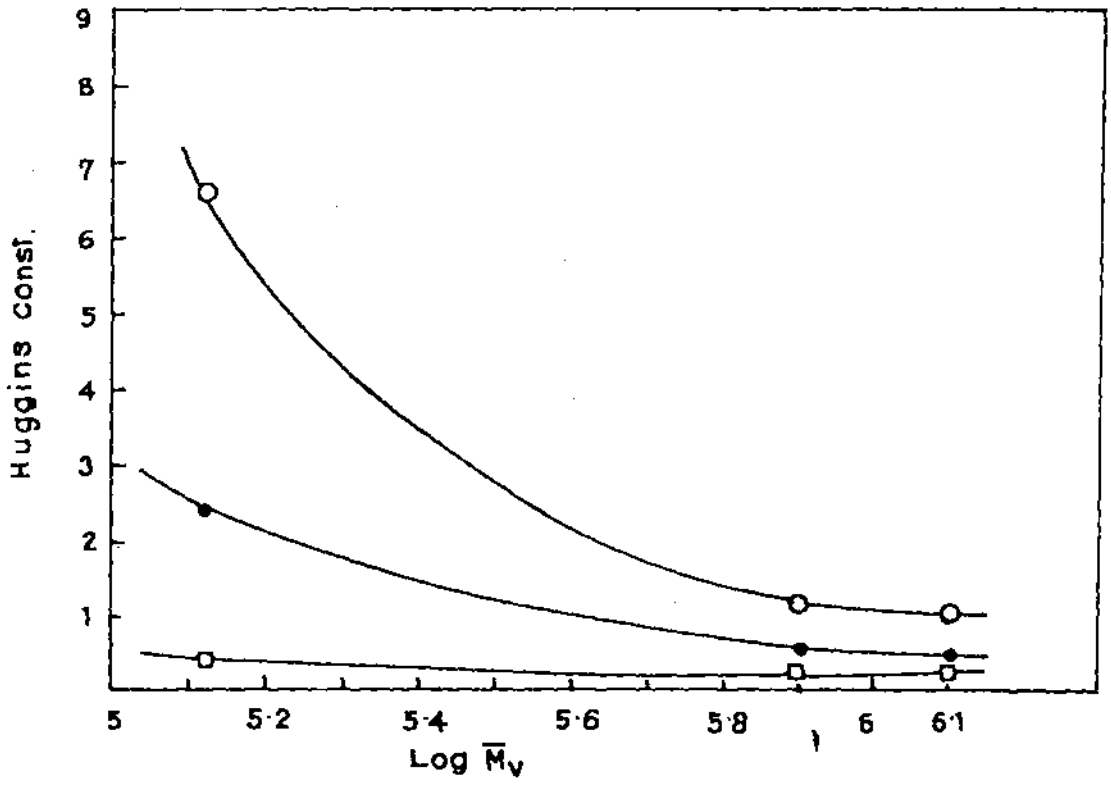

Fig. 65 Plot of Huggins constant versus log(molecular weight) at different solvent composition at 30°C. φ_{DMSO} = 0.5 (o), 0.3 (•), 0.2 (□).

with a definite solvent (θ solvent).[282] The unperturbed dimension (K_θ) is the end-to-end dimension of polymer chain under θ conditions and can be determined from the intrinsic viscosity measurement at this condition.

$$[\eta]_\theta = \phi_o(\overline{r_o^2}/M)^{3/2}M^{1/2} = K_\theta M^{1/2} \quad (65)$$

where ϕ_o is the Flory's universal constant (2.5×10^{23} $mole^{-1}$), M stands for molecular weight and $\overline{r_o^2}$ is the mean square unperturbed dimension. However, in the present study, the Burchard-Stockmayer – Fixman equation (60) has been used for deriving K_θ of PAM in various water – DMSO mixtures under non θ conditions.[315,316] The BSF plots for PAM fractions at various cosolvent compositions at 30°C are shown in Figures 66-67. The K_θ values obtained by plotting $[\eta]/M^{1/2}$ against $M^{1/2}$ from the equation (60) in different cosolvent compositions

$$[\eta] / M^{1/2} = K_\theta + 0.51B\phi_o M^{1/2} \quad (60)$$

(B being the polymer-solvent interaction free energy parameter) are compared with those obtained from other methods of measurement, viz., Kurta-Stockmayer (KS)[317,318], Fox-Flory (FF)[285] , Berry (Be)[319], Tanaka(T)[322] and Bohdanecky(Bo)[330] methods. The results are summarized in Table 31. The values obtained by different methods agree well with each other except in a few composition conditions of the solvent. From the Table 2, it is apparent that at $\phi_{DMSO} = 0.5$ i.e., at the same volume ratio of water and DMSO in the mixture, strong attraction of two solvents, causes the polymers to have the lowest value of unperturbed chain. This observation is independent of the method of measurement with certain exceptions. Effect of temperature is rather interesting. The BSF plots for PAM fractions at various cosolvent compositions at 40°C and 50°C are shown in Figures 68-71. With an increase in temperature, $\overline{r_o^2}$ and hence K_θ, are decreased due to greater freedom to rotation around the skeletal

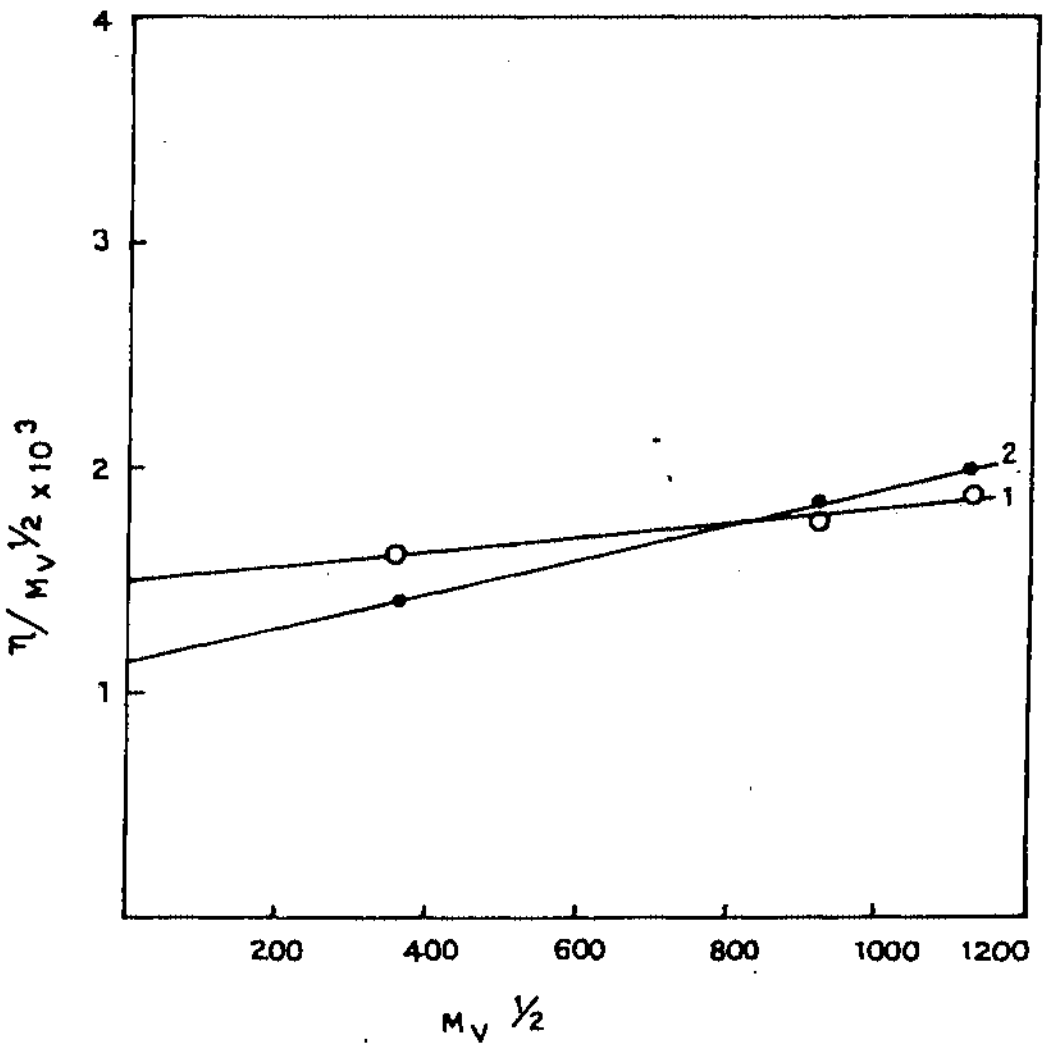

Fig. 66 BSF plots for PAM fractions at various cosolvent compositions at 30°C: φ_{DMSO} = 0.20(1); φ_{DMSO} = 0.30(2).

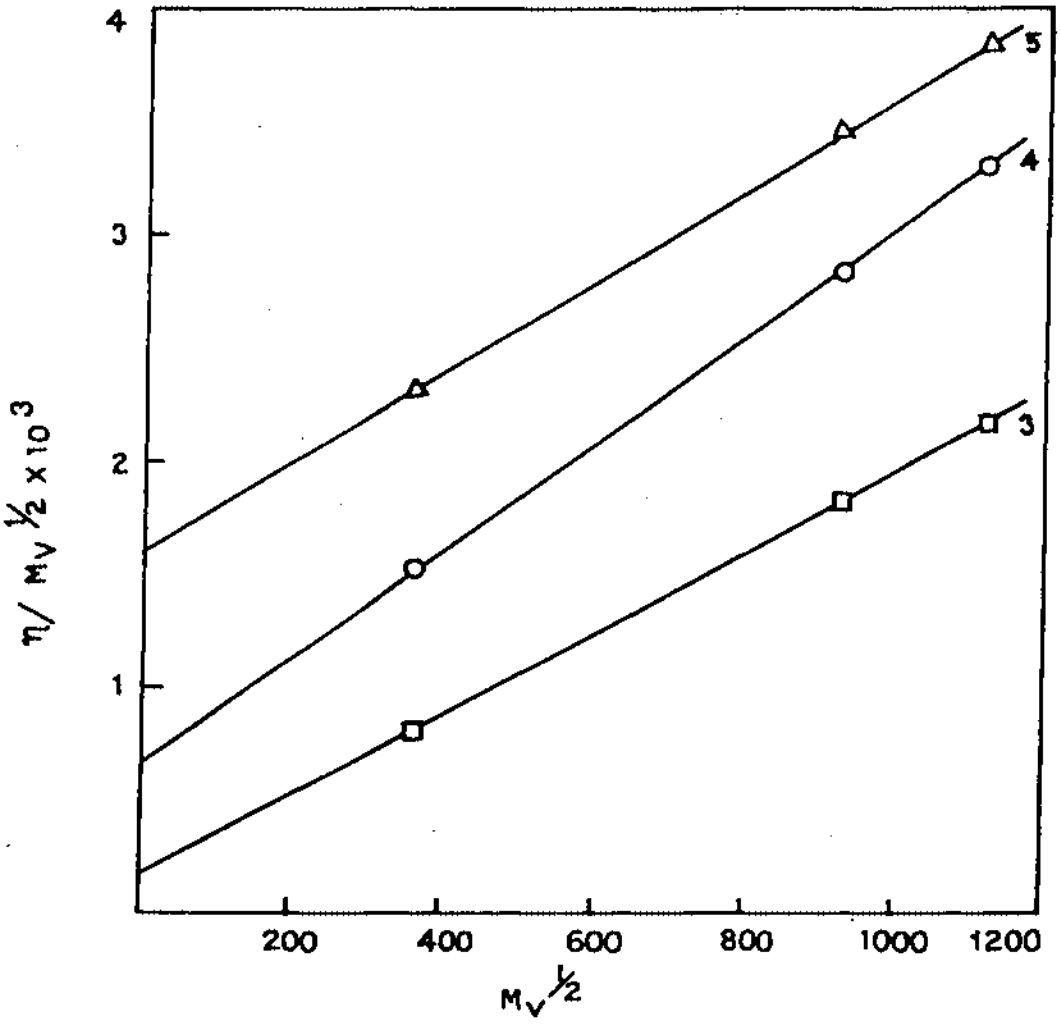

Fig. 67 BSF plots for PAM fractions at various cosolvent compositions at 30°C: φ_{DMSO} = 0.50(3); φ_{DMSO} = 0.70(4); φ_{DMSO} = 0.80(5).

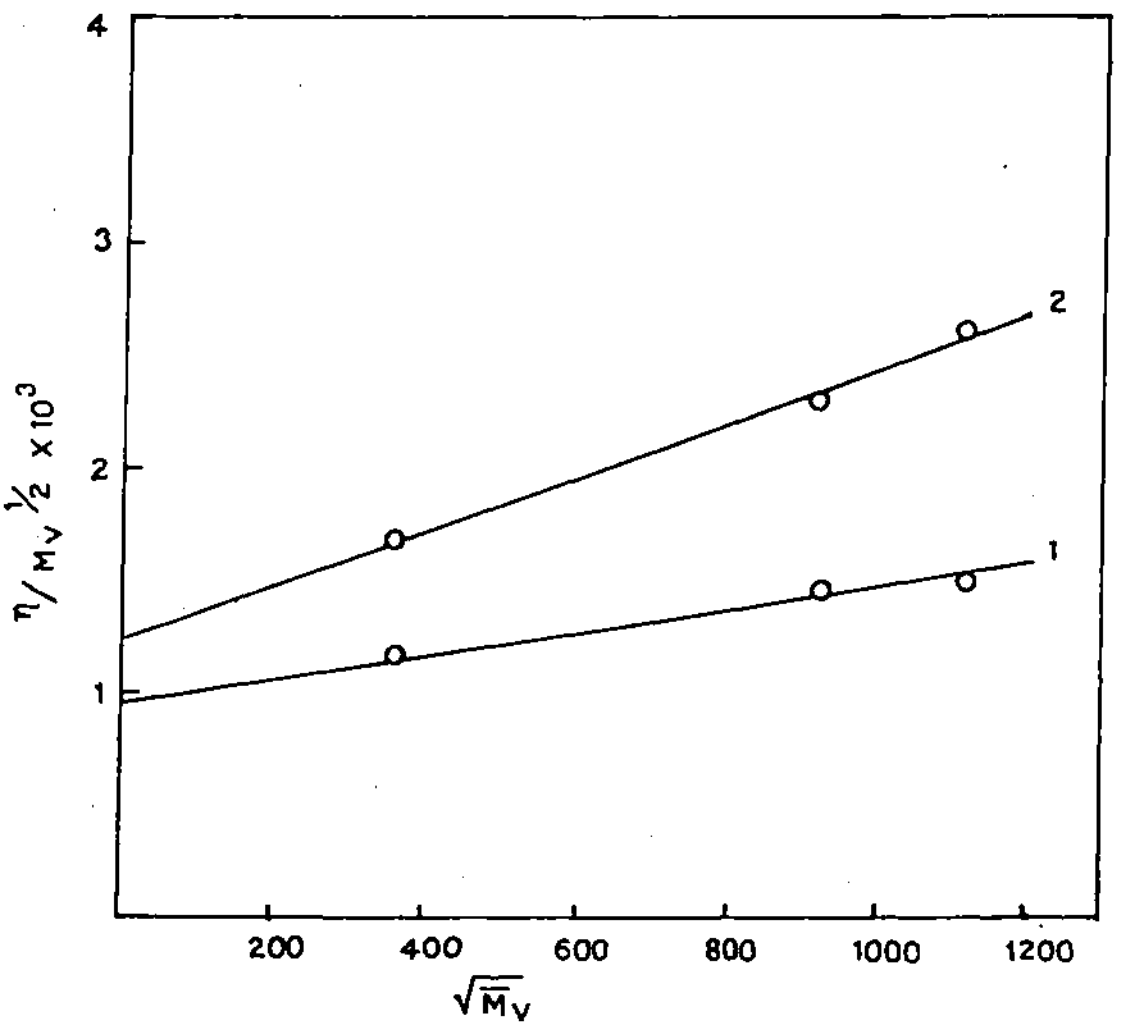

Fig. 68 BSF plots for PAM fractions at various cosolvent compositions at 40°C: φ_{DMSO} = 0.20(1); φ_{DMSO} = 0.30(2).

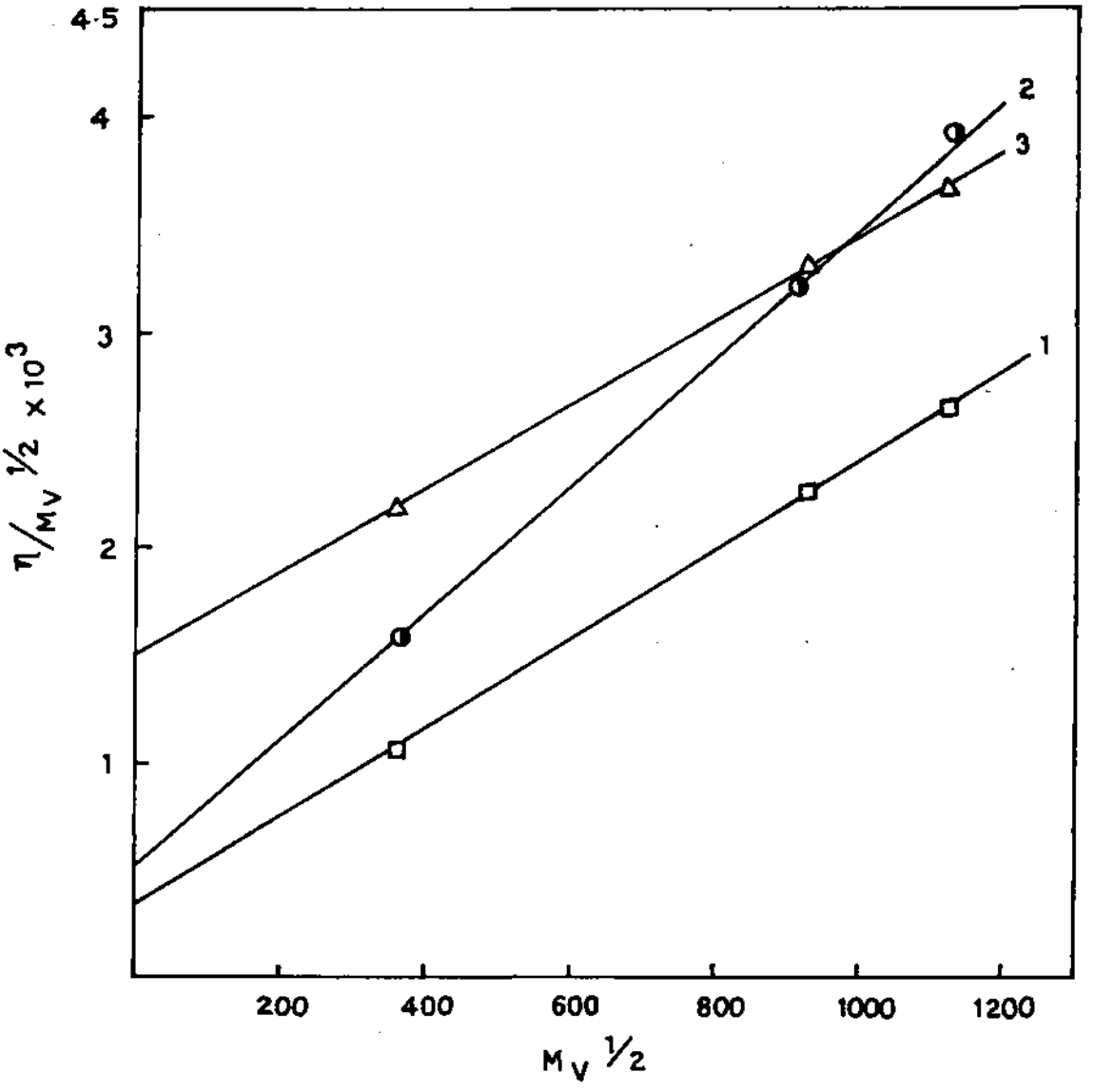

Fig. 69 BSF plots for PAM fractions at various cosolvent compositions at 40°C: φ_{DMSO} = 0.50(1); φ_{DMSO} = 0.70(2); φ_{DMSO} = 0.80(3).

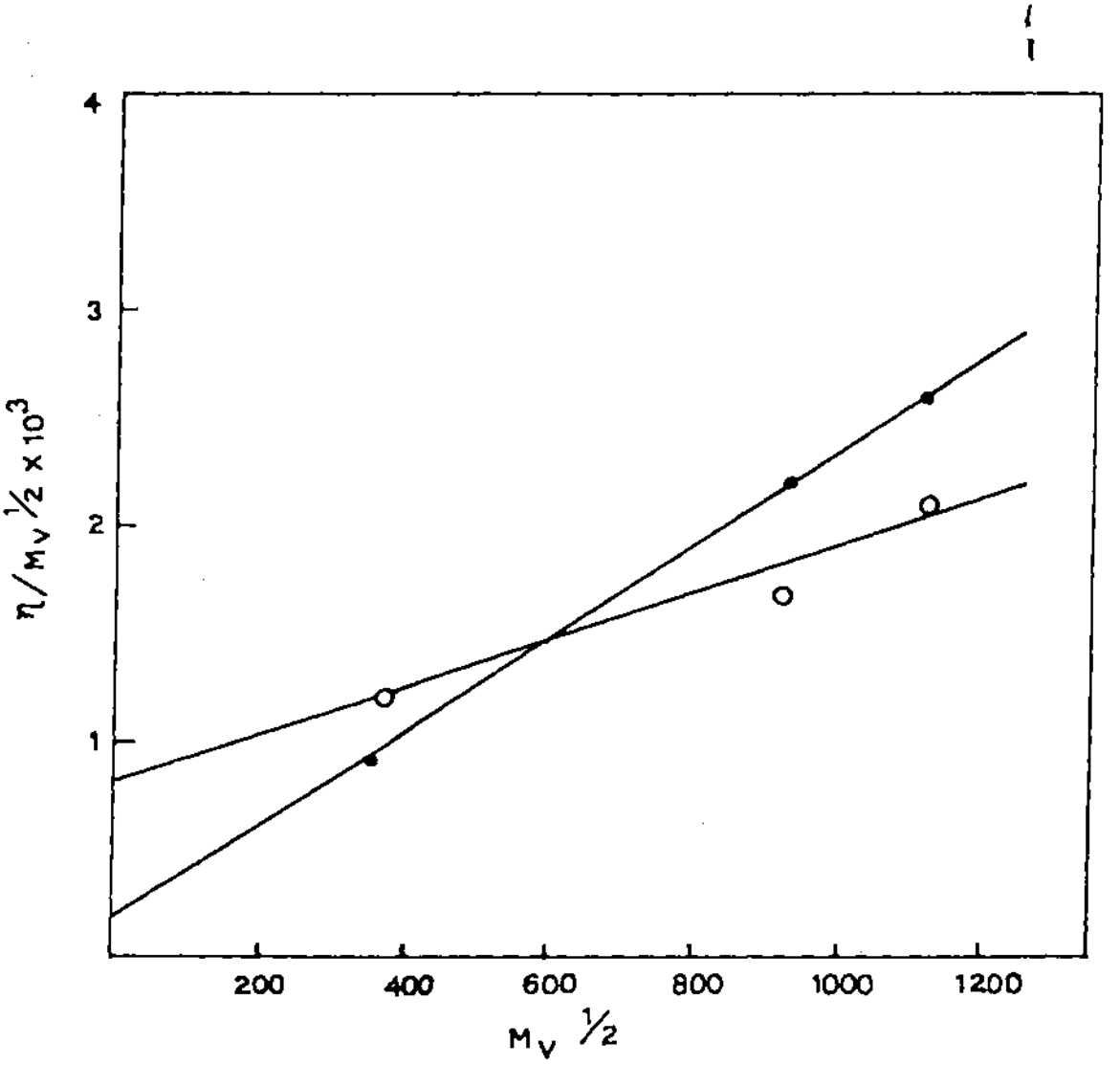

Fig. 70 BSF plots for PAM fractions at various cosolvent compositions at 50°C: φ_{DMSO} = 0.20(1); φ_{DMSO} = 0.30(2).

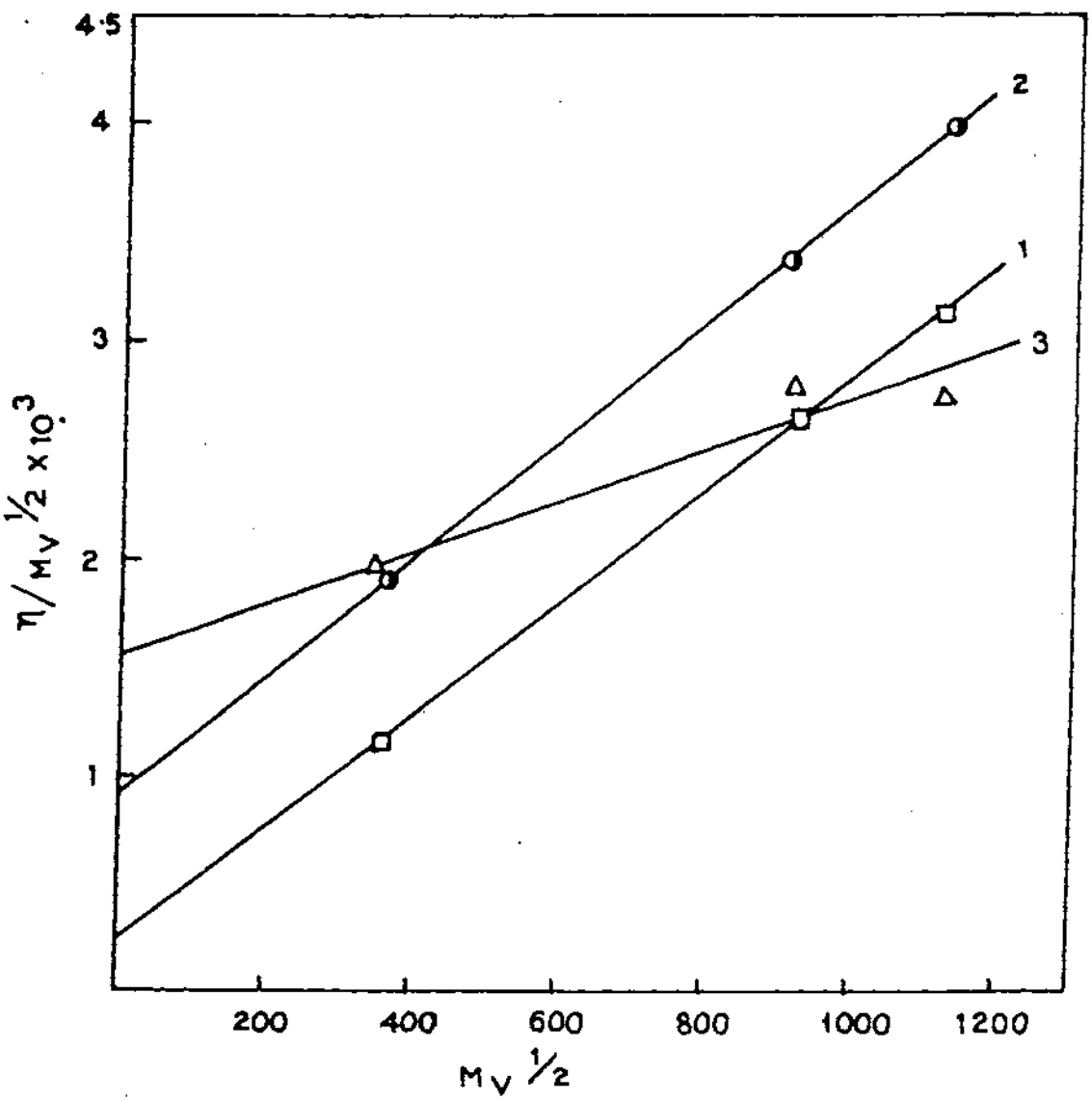

Fig. 71 BSF plots for PAM fractions at various cosolvent compositions at 50°C: φ_{DMSO} = 0.50(1); φ_{DMSO} = 0.70(2); φ_{DMSO} = 0.80(3).

bonds.[282] Such a temperature dependence of unperturbed dimension can be attributed not only to the change in flexibility of macromolecular chains but also to the specific polymer-solvent interaction[349]. The effect may also be correlated to the cohesive energy density of the polymer and the solvent.[323]

Temperature coefficient of unperturbed dimension

K_θ is related to the statistical parameters ($\overline{r_o^2}$) and the unperturbed mean square end-to-end distance by the Flory's Equation (56)

$$K_\theta = \phi_o [\overline{r_0^2} /M]^{3/2} \qquad (56)$$

On differentiating equation (56) with respect to T, the temperature coefficient of unperturbed dimension may be obtained

$$(d \ln K_\theta/dT) = 3/2 [\{d \ln (\overline{r_0^2})\}/dT] = K^l \qquad (66)$$

Here K^l, the temperature coefficient of K_θ, provides information regarding the configuration dependent properties of polymer chain and energies of bond conformations in the molecule.[350] The plots are shown in Figures 72-73 In water – DMSO composition of 2:8, K^l is found to be 0.046 degree^{-1} for acrylamide polymer (Table-32). The value of the temperature co-efficient increases upto 3:7 mixture of the solvent, indicating again that the solvency power increases with the increase in temperature upto above solvent composition.[351] This further shows that the acrylamide polymer molecule expands more in the later solvent composition and reveals the presence of low energy configuration in this solvent mixtures at high temperature. On the otherhand, at 5:5 and 7:3 compositions, the K^l value is negative. The negative coefficient value indicates more compact structure and the existence of high energy configuration of the polymer in these

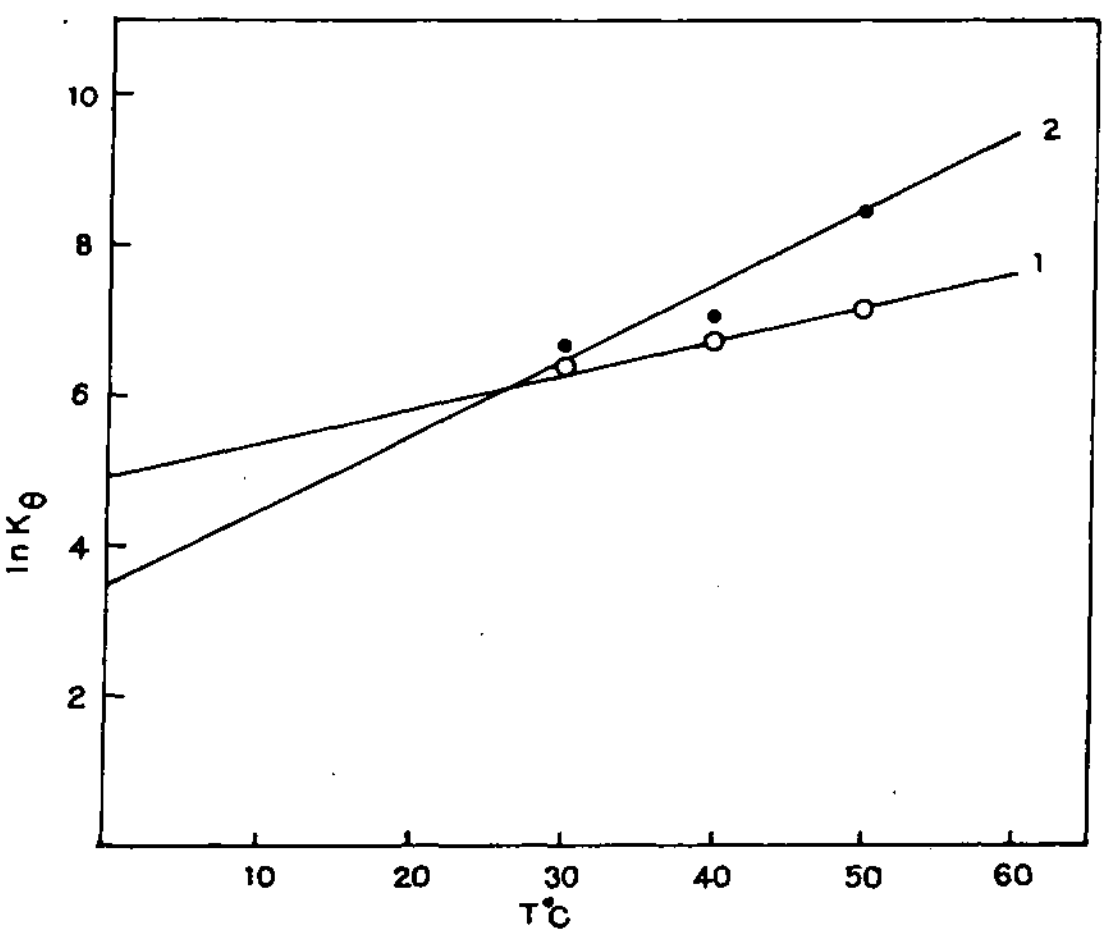

Fig. 72 Dependence of $\ln K_\theta$ on temperature for PAM fractions at various cosolvent compositions: φ_{DMSO} = 0.20(1); φ_{DMSO} = 0.30(2).

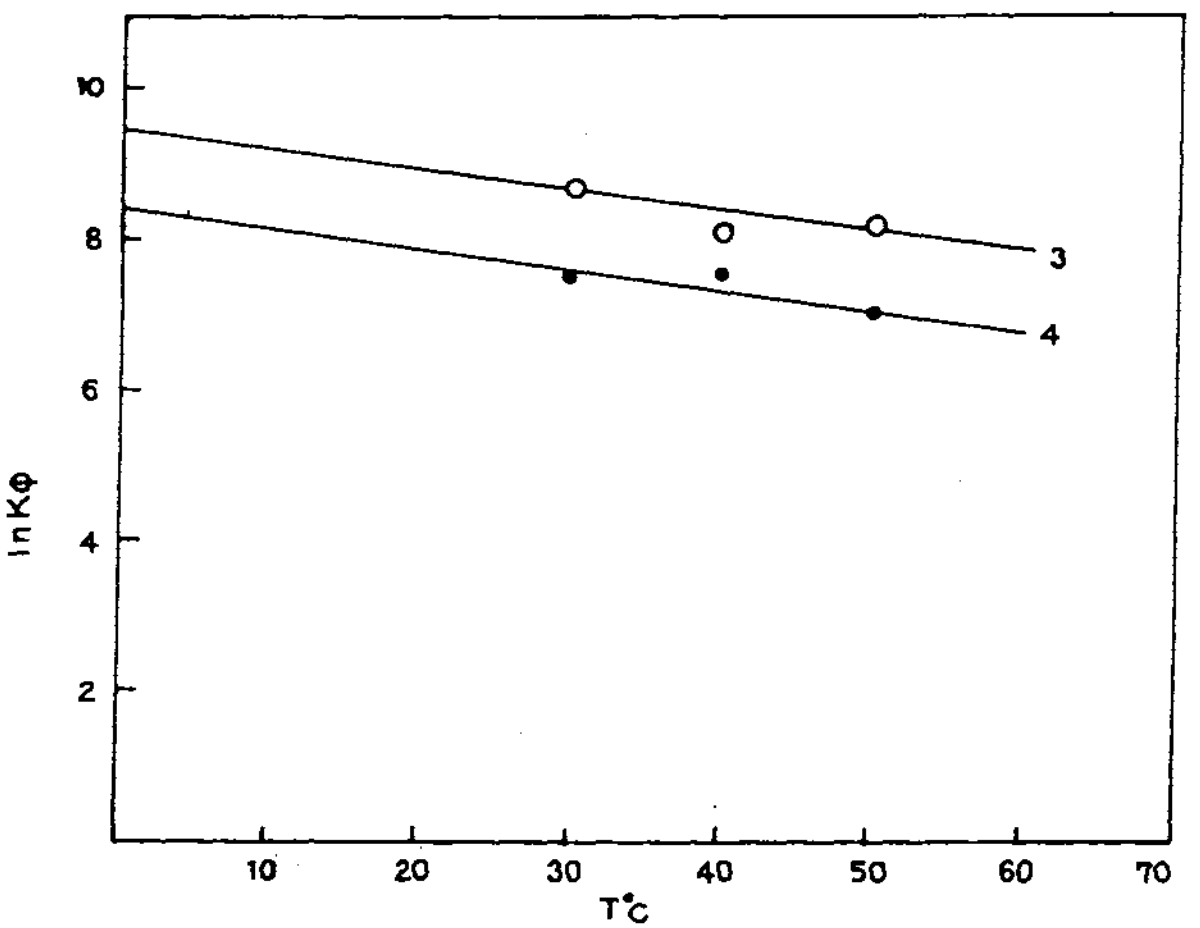

Fig. 73 Dependence of $\ln K_\theta$ on temperature for PAM fractions at various cosolvent compositions: φ_{DMSO} = 0.50(3); φ_{DMSO} = 0.70(4).

compositions of the solvent.[352] However, at 8:2 composition, K^{l} again assumes a positive value showing better cosolvency of the mixture.

Table – 31

Unperturbed dimension of PAM in water + DMSO mixtures at different temperatures determined by different methods.

Temp. °C	ϕ_{DMSO}	K_0 X 10 ($cm^3g^{-3/2}$ $mole^{½}$)					
		BSF[a]	KS[b]	T[c]	Bo[d]	FF[e]	Be[f]
	0.2	1.500	1.480	1.446	1.500	1.440	1.440
	0.3	1.125	1.115	0.910	1.120	1.114	1.123
30	0.5	0.150	0.116	0.110	0.125	0.107	0.086
	0.7	0.650	0.649	0.490	0.375	0.196	0.225
	0.8	1.600	1.570	1.430	1.312	1.250	1.370
	0.2	1.25	1.240	1.070	1.125	1.174	1.123
	0.3	0.95	0.960	0.954	0.968	0.960	0.945
40	0.5	0.35	0.327	0.287	0.187	0.290	0.256
	0.7	0.50	0.465	0.435	0.312	0.164	0.100
	0.8	1.50	1.483	1.300	1.281	1.253	1.225
	0.2	0.825	0.818	0.435	0.812	0.801	0.730
	0.3	0.200	0.125	0.110	0.125	0.098	0.095
50	0.5	0.250	0.241	0.165	0.125	0.218	0.170
	0.7	0.925	0.925	0.807	0.688	0.512	0.484
	0.8	1.550	1.525	1.375	1.343	1.525	1.520

[a] Burchard – Stockmayer – Fixman, [b] Kurata – Stockmayer,

[c] Tanaka, [d] Bohdanecky, [e] Fox-Flory, [f] Berry.

Table – 32

Temperature co-efficients (K^l) of unperturbed dimension at different DMSO compositions.

ϕ_{DMSO}	K^l (degree^{-1})
0.2	0.0460
0.3	0.0947
0.5	-0.0300
0.7	-0.0280
0.8	0.0320

Molecular extension factor (α_n)

The molecular extension factor (α_n) has been calculated from the relation[331] :

$$\alpha_n^3 = [\eta] / K_\theta M^{1/2} \qquad (54)$$

using K_θ from the BSF plot. The actual end–to-end distance, $\alpha_n K_\theta$, of polymer molecule is also computed, which are shown in Table 33. It is observed that at ϕ_{DMSO} = 0.5 , $\alpha_n K_\theta$ attains the lowest value for all the molecular weight fractions of the polymer. However, α_n value is the highest at the above composition. The intermolecular interaction is probably responsible for the high value of α_n at ϕ_{DMSO} = 0.5 because of the small value of the unperturbed dimension at this composition. The molecular weight dependency of α_n is also clear from the table ; α_n increases with the increase in molecular weight of the polymer. As the molecular weight of the polymer increases, the number of segmental interactions of the polymer molecule with solvent molecule increases, resulting in a larger value of α_n.

Chain rigidity

The structural parameters of PAM, viz., the steric factor σ and the characteristic ratio C_∞ are also calculated in the usual manner from the following equations[29] :

$$\sigma = [\langle r^2\rangle_o / M]^{1/2}{}_{of} / [\langle r^2\rangle_{of} / M]^{1/2} \quad (67)$$

$$[\langle r^2\rangle_{of} /M]^{1/2} = [\langle r^2\rangle_{of} / N]^{1/2} [1/M_o]^{1/2} \quad (68)$$

$$C_\infty = (K_\theta/ \phi_o)^{2/3} (M_o / 2L^2) \quad (69)$$

where $\langle r^2\rangle_{of}$ is the unperturbed mean square end-to-end distance for a freely rotating chain, N is the degree of polymerization, M_o is the molecular weight of the monomer unit and L is the backbone bond length (L = 0.154 nm). For vinyl polymers the value of ($(\langle r^2\rangle_{of} /N)^{1/2} = 3.08 \times 10^{-8}$ cm (Ref.353). The computed values of C_∞, σ and $(r^2)_o / M)^{1/2}$ for PAM at different solvent compositions and temperatures are shown in Table 34. Cowie[354] observed that the range of values of σ normally encountered is about 1.5 – 2.5 (Ref. 354). In the present study also the value of σ falls within the above range and it decreases with ϕ_{DMSO} initially and, then increases giving rise to the lowest value at $\phi_{DMSO} = 0.5$. This indicates again that the most rigid structure of the polymer exists at the above solvent composition.

Table-33

Molecular extension factor and coil dimensions of PAM at different temperatures and water + DMSO mixtures.

Temp.		LM		MM		HM	
°C	ϕ_{DMSO}	α_n	$\alpha_n K_\theta$x10	α_n	$\alpha_n K_\theta$ x 10	α_n	$\alpha_n K_\theta$x 10
	0.2	1.031	1.546	1.026	1.539	1.085	1.628
	0.3	1.053	1.185	1.192	1.340	1.176	1.323
30	0.5	1.723	0.258	2.332	0.350	2.426	0.364
	0.7	1.330	0.865	1.640	1.070	1.720	1.117
	0.8	1.133	1.813	1.299	2.080	1.339	2.142
	0.2	1.114	1.392	1.203	1.503	1.296	1.620
	0.3	1.091	1.036	1.170	1.112	1.169	1.110
40	0.5	1.438	0.503	1.890	0.661	1.948	0.682
	0.7	1.470	0.735	1.858	0.929	2.000	1.001
	0.8	1.130	1.695	1.313	1.970	1.338	2.008
	0.2	1.143	0.943	1.235	1.020	1.393	1.150
	0.3	1.580	0.316	2.250	0.450	2.347	0.470
50	0.5	1.663	0.416	2.216	0.554	2.327	0.582
	0.7	1.293	1.196	1.522	1.408	1.650	1.526
	0.8	1.074	1.664	1.222	1.894	1.200	1.860

Table – 34

Unperturbed dimension, steric factor (σ), characteristic ratio (C_∞) as functions of ϕ_{DMSO} and temperature.

Temp. °C	ϕ_{DMSO}	$[\langle r^2 \rangle_o/M]^{1/2} \times 10^9$ (cm.g$^{-1/2}$ mole$^{1/2}$)	C_∞	σ^a
	0.2	8.43	8.85	2.31
	0.3	7.66	7.30	2.10
30	0.5	3.91	1.89	1.07
	0.7	6.38	5.05	1.75
	0.8	8.62	9.24	2.36
	0.2	7.94	7.83	2.17
	0.3	7.24	6.52	1.98
40	0.5	5.19	3.34	1.42
	0.7	5.85	4.24	1.60
	0.8	8.43	8.85	2.31
	0.2	6.91	5.93	1.89
	0.3	4.31	2.30	1.62
50	0.5	4.64	2.67	1.27
	0.7	7.18	6.40	1.97
	0.8	8.52	9.01	2.33

[a] value of $[r^2 >_o/M]^{1/2}$ has been taken as 3.65 X 10^{-9} cm.g$^{-1/2}$ mole$^{1/2}$

Chapter - 6

SUMMARY AND CONCLUSION

In chapter 1, an introduction covering various aspects of the present research scheme on aqueous polymerization of acrylamide has been presented. In view of the increasing industrial applications of water soluble acrylamide polymers in a number of areas including the use of polyacrylamide as water soluble viscofier in enhanced oil recovery, researches in the field have gained momentum in recent days. Research on the intercalation chemistry of phyllosilicates is increasing rapidly to transform these abundant minerals into new class of selective heterogeneous catalysts. In the present study, attempts have been made to prepare acrylamide polymer having high molecular weight and intrinsic viscosity by polymerizing the monomer on montmorillonite surface. A major difficulty of applying redox initiators is fast termination by the oxidant of the redox couple. In an attempt to increase the chain length of polyacrylamide, the potential electron acceptor of the redox couple, (e.g., Fe (III) ions) has been loaded into the interlayer space of montmorillonite (phyllosilicate) prior to the reactions. In the introduction part (chapter 1), a brief review covering all these aspects viz., polymers of acrylamide, structure of the mineral clay montmorillonite, clay-organic interaction and clay catalyst polymerization have been presented.

(page 1-17)

Chapter 2 describes the scope and object of the present investigation. In view of the nature of applications of polyacrylamide, high molecular weight polymers with high intensity viscosities are very important. Redox polymerization technique is a simple efficient technique which yield polymers with high rates. However, one major difficulty of redox technique is the fast termination process via transfer to the oxidant of the redox couple as mentioned above. As a result, low molecular weight polymers are usually formed. The copolymers of acrylamide are used as water soluble viscofiers and displacement fluids in enhanced oil recovery. The critical limitation of homopolyacrylamide is the loss of viscosity in presence of electrolytes. Keeping these in view, a detailed study on redox polymerization of acrylamide has been undertaken by trapping the oxidant of the redox couple (e.g., Fe (III) ions of the

Fe(III)/thiourea (TU) system) in the interlayer space of the montmorillonite. This ensures slow termination due to inability of the growing polymer chain to transfer to the oxidants trapped inside the layered space. As a result, high molecular weight polymers and some industrially important copolymers of acrylamide are found. Studies on the solution properties of polyacrylamide have also been undertaken in view of the fact that the role of the hydrodynamic dimensions on different factors which govern the efficiency of their use is important.

(page 18-21)

In chapter 3, various aspects of the redox initiated polymerization of acrylamide on the surface of mineral clay montmorillonite with a view to control the linear termination process for achieving high molecular weight polymers are presented. A detailed solution phase reaction has also been performed involving the same redox couple (viz., $FeCl_3$ / TU) but in the absence of montmorillonite, to check what modifications pertaining to kinetics and mechanism have been achieved by the mineral phase reactions. Kinetics and mechanism of the reaction under both the conditions have been looked into. The technique of interlayer polymerization for another redox system (viz., Ce(IV)/EDTA) is also incorporated in this chapter, which enables to examine the scope of the proposed technique of controlling the termination process in different systems. In section 3.1 a brief review on this aspect is presented.

(page 22-27)

Methods of preparation and purification of different montmorillonite samples viz., hydrogen montmorillonite, ferric montmorillonite and ceric montmorillonite are presented in section 3.2. The experimental technique for the study of polymerization of acrylamide is also presented in this section.

(page 28-32)

In the first part of the result and discussion, polymerization results under homogeneous conditions are presented and discussed. The polymerization of

acrylamide occurred in presence of ferric chloride and thiourea in solution phase. The conversions are dependent on ferric chloride, acrylamide, thiourea concentrations and the temperature. In the present systems, no induction periods were observed. The initial rate of polymerization, R_p's, were moderately high and ranged between (3-17) x 10^{-5} mole. L^{-1}. s^{-1}. At a fixed TU and AM concentrations, all the parameters viz., R_p, X_L, [η] and M_v were decreased with the increase in Fe(III) concentrations of the initiating redox couple. This clearly shows the involvement of the linear termination process in the present polymerization reaction via transfer to the metal ion. The rate of polymerization, R_p, as well as the polymer yield, X_L decreased from 17.17 x 10^{-5} to 4.16 x 10^{-5} mol. L^{-1}. s^{-1} and 73% to 26% respectively with the increase in the Fe(III) ion concentration in the range of (1.5—8.0) x 10^{-3} mol. L^{-1}. The [η] values are low and found to vary from 14 to 137 ml. g^{-1} under the present reaction conditions. The [η] as well as M_v are increased with increasing monomer and TU concentrations. The R_p and X_L are also increased with increasing polymerization temperature. The overall energy of activation as calculated from Arrhenius plot has been found to be 12.93 kcal / mol within the temperature range 45° to 70° C.

The initial rate is inversely proportional to nearly first power of metal concentrations. Such a dependence is commonly observed in most of the aqueous free radical polymerization reactions. On the other hand, R_p increases with increased concentration of TU. The rate of polymerization shows a nearly second order dependence on the TU concentration as well as AM concentration in the range 0.25 to 0.40 mol.L^{-1} but first order in the higher concentration range of (0.4 — 0.6) mol. L^{-1}.

In the polymerization reactions initiated by redox couple involving TU, a free radical mechanism has already been proposed involving isothiocarbamido radicals (i.e., amido-sulfenyl radicals, NH_2–C–(=NH)S radical), as the primary radical. It is believed that the reaction proceeds via the intermediate complex

$[Fe(SC(NH_2)_2]^{+3}$, the stability constant which is approximately 2.0. The decomposition of the complex involves a second order reactions producing two isothiocarbamido radicals, which dimerize further in the presence of ferric ions. Since the reactive TU radicals are formed as pairs, assumption of 'cage effect' seems to be conceptually appropriate. The 'cage effect' suggests that when an initiator decomposes into two radicals, there is a formation of a potential barrier by the surrounding solvent molecules which prevent their immediate diffusion and favours their destruction by mutual recombination. The initiation step involves collision of acrylamide molecules with caged TU radicals at the wall of the cage and random diffusion of the radicals from the cage and their secondary recombination are less significant. In order to rationalize the results, following reaction steps are assumed to be involved.

$$Fe(III) + TU \underset{}{\overset{K}{\rightleftharpoons}} \underset{\text{complex}}{Fe(III) - TU}$$

$$Fe(III) - TU \xrightarrow{k_d} Fe(II) + (2TU^{\bullet}) + H^{+}$$

Initiation

$$(TU^{\bullet}) + M \xrightarrow{k_i} M_1^{\bullet}$$

Propagation

$$M_1^{\bullet} + M \xrightarrow{k_p} M_2^{\bullet}$$

$$M_{n-1}^{\bullet} + M \xrightarrow{k_p} M_n^{\bullet} \quad \ldots\ldots\ldots \text{ etc.}$$

Termination

$$M_n^{\bullet} + Fe(III) \xrightarrow{k_t} M_n^{\bullet} + Fe(II)$$

$$(TU^{\bullet}) + Fe(III) \xrightarrow{k_t'} TU + Fe(II)$$

$$(2TU^{\bullet}) \xrightarrow{k_t''} TU - TU$$

(caged species are enclosed in brackets)

Assuming that the pseudo steady state approximation holds, following rate law has been established

$$R_p = \frac{k_d k_i k_p K[TU]^2[M]^2}{k_t\left(k_i[M] + k_t'[Fe(III)] + k_t''\right)}$$

(page 33-43)

Section 3.4 concerns the results of the polymerization of acrylamide on montmorillonite surface initiated by $\overline{Fe}$(III)/TU systems. This includes a detail of kinetics and mechanism of the reaction also. Unlike the solution phase reactions, just described, the initial rate of polymerization, R_p, was increased from 4.76×10^{-5} to 6.61×10^{-5} mol. L^{-1}. s^1 as the $\overline{Fe}$(III) concentration increased from 0.60×10^{-3} to 2.07×10^{-3} mol. $L^{-1}.s^{-1}$. Conversion efficiencies were also increased regularly with increasing $\overline{Fe}$(III) ion concentration upto 2.07×10^{-3} mol. L^{-1}. Although R_p and the polymer yield decreased with decreasing TU concentrations, molecular weight of the polymer was higher at lower TU concentrations. Moreover 'gel effect' was observed in the presence of clay mineral apparently for the formation of the high molecular weight polymers due to decrease in linear termination rates. The more significant observation of loading $\overline{Fe}$(III) ions of the initiating redox couple in the interlayer spaces of montmorillonite is that the [η] values of the polymers formed are increased significantly, which vary from 247 to 600 $ml.g^{-1}$ under present reaction conditions. The R_p as well as X_L increase with increasing polymerization temperature. The [η] is also increased with increasing monomer and TU concentrations while it is increased with temperature upto 50°C but decreased at higher temperatures. The activation energy, E_a, of the overall polymerization reaction gives an average value of 14.9 kcal / mole.

(page 44-53)

The effect of pH and use of additives like different solvents and surfactants upon the polymerization process and the properties of the resulting

polymers have also been examined. The protonated form of the amidosulfenyl radical at low pH is more stable than the radical itself and consequently the dimerization process is less favourable. The intensity of the ESR signal of the spin trap-radical adduct was maximum at low pH. It is found that some water miscible organic solvent viz., ethanol, DMSO and DMF depressed the polymer yield. On the other hand, dioxan the increased the polymer yield upto 20% (V/V) but decreased at higher concentrations.

(page 53-57)

The rate of reaction shows a second order dependence on monomer concentration. The dependence of rate on the actual $\overline{Fe}$(III) ion concentration in the montmorillonite gel reveals that the reaction is 0.5 order with respect to $\overline{Fe}$(III) ion concentrations. The dependence of R_p on TU concentrations indicates that the reaction is first order with respect to TU concentration. To rationalize the experimental results and to predict a possible mechanism in the mineral microenvironment, the following assumptions are made (section 3.4.2).

(1) Intercalated TU reacts fast with $\overline{Fe}$(III) ions of montmorillonite layered spaces to form the reactive isothiocarbamido radicals.
(2) In the acidic and metal ion exchanged aqueous montmorillonite system, a fraction of the intercalated acrylamide molecules are present near reacting sites as pairs either through hemisalts formation or/and through weak coordination to the exchanged cations.
(3) Strong 'cage effect' on the initiating TU radicals is operative.

Proposed reaction steps are as follows:

Initiation

$$\overline{Fe}(III) + TU \underset{}{\overset{K}{\rightleftharpoons}} \overline{Fe}(III) - TU$$
complex

$$\overline{Fe}(III) - TU + TU \xrightarrow{k_d} \overline{Fe}(II) + \left(2TU^{\bullet}\right) + H^{+}$$

$$\left(TU^{\bullet}\right) + M_2H^{+} \xrightarrow{k_i} M_1^{\bullet} + M + H^{+}$$

Propagation

$$M_1^{\bullet} + M \xrightarrow{k_p} M_2^{\bullet}$$

$$M_{n-1}^{\bullet} + M \xrightarrow{k_p} M_n^{\bullet} \quad \ldots\ldots\ldots \text{ etc.}$$

Termination

$$M_n^{\bullet} + M_n^{\bullet} \xrightarrow{k_t} M_n - M_n$$

$$\left(TU^{\bullet}\right) + \overline{Fe}(III) \xrightarrow{k_t'} TU + \overline{Fe}(II)$$

$$\left(2TU^{\bullet}\right) \xrightarrow{k_t''} TU - TU$$

(caged species are enclosed in brackets as before and the 'bar' on Fe(III) or Fe(II) indicates their presence in the layered space of montmorillonite).

Assuming the pseudo steady state approximation to hold, rate law has been established as

$$R_p = \frac{k_p\left(k_d k_i K K^1 / k_t k_t''\right)^{1/2} K_{tu}^a \left(K_m^a\right)^2 \left(L_o^a\right)^3 \left[\overline{Fe}(III)\right]^{1/2} [TU]_s [M]_s^2}{\left(1 + K L_o^a K_{tu}^a [TU]_s\right)^{1/2}}$$

(where L_o^a is the total active sites in unit mass of the mineral, K_m^a and K_{tu}^a are the selectivity coefficients and subscript 's' denotes solution)

Under the present condition the above rate equation is however reduced to

$$R_p = k_p\left(k_d k_i K K^1 / k_t' k_t''\right)^{1/2} K_{tu}^a \left(K_m^a\right)^{1/2} \left(L_o^a\right)^3 \left[\overline{Fe}(III)\right]^{1/2} [TU]_s [M]_s^2$$

The effect of mineral microenvironment on the $\overline{Ce}$(IV)– EDTA initiated aqueous polymerization of acrylamide has also been studied with a view to generalize the adopted method for enhancing chain growth. The results are presented in section 3.5.

The molecular weights of the polymer were moderately high and ranged from 3.9×10^5 to 2.9×10^6. The initial rate of polymerization, R_p's, were ranged between (2.1 — 10.6) x 10^{-5} mol. L^{-1}. s^{-1} depending on various reaction parameters. Upto 95% of the polymers were formed at 50°C in the presence of 1.5×10^{-3} mol. L^{-1} of $\overline{Ce}$(IV) ions (EDTA = 0.01 mol. L^{-1} and AM = 0.4 mol. L^{-1}). R_p, X_L and M_v were increased with the increase in AM concentrations. The value of $[\eta]$ was also high and varied from 145 to 650 ml. g^{-1}. On the other hand, R_p increases with increased concentration of EDTA. Previous study on homogeneous polymerization by $\overline{Ce}$(IV)/EDTA system showed a steady decrease in R_p with Ce(IV) concentration. But, present study gives a reverse trend. This indicates that the linear termination by $\overline{Ce}$(IV) ions is no longer important in the present polymerization on the mineral surface. The pseudo - overall activation energy was 19.3 kcal/mole, which is close to that for usual redox systems.

The initial rate is approximately first order with respect to the monomer concentration. The significant departure of monomer exponent from 2.0 (in absence of montmorillonite) to 1.0 in the presence of clay mineral demands that the polymerization mechanism be reconsidered for the present condition. To rationalize the above experimental results and to predict a possible mechanism following assumptions are made.

(1) Intercalated EDTA molecule react fast with $\overline{Ce}$(IV) ions of montmorillonite layered space to form reactive EDTA radicals via an intermediate complex. Due to restricted mobility of $\overline{Ce}$(IV) ions at the exchange sites of montmorillonite, the formation constant of the complex is small.

(2) Polymerization locus is the interlayer space of montmorillonite. The linear termination of growing polymer chain by $\overline{Ce}$(IV) ions is restricted due to the presence of metal ions in the layered space.

(3) The initiation steps involves the collision of acrylamide with EDTA radicals, where monomer pairs (as already mentioned) are entailed. Generation of initiator fragment, propagation and the termination steps may be shows as follows:

Generation of initiator fragment

$$\overline{Ce}(IV) + EDTA(R) \underset{}{\overset{K}{\rightleftharpoons}} (\overline{Ce}(IV) - R)$$
complex

$$(\overline{Ce}(IV) - R) \xrightarrow{k_d} R^{\bullet} + \overline{Ce}(III) + H^{+}$$

$$R^{\bullet} + M_2H^{+} \xrightarrow{k_i} M_1^{\bullet} + M + H^{+}$$

Propagation

$$M_1^{\bullet} + M \xrightarrow{k_p} M_2^{\bullet}$$

$$M_{n-1}^{\bullet} + M \xrightarrow{k_p} M_n^{\bullet} \quad \ldots\ldots\ldots \text{ etc.}$$

Termination

$$M_n^{\bullet} + M_n^{\bullet} \xrightarrow{k_t} M_n - M_n$$

$$R^{\bullet} + \overline{Ce}(IV) \xrightarrow{k_t'} \text{Oxidative product} + \overline{Ce}(III) + H^{+}$$

The rate equation under the present condition has been found to be

$$R_p = k_p K_M^a \left(L_o^a\right)^{3/2} \left(k_d K K_R^a / k_t\right)^{1/2} \left[\overline{Ce}(IV)\right]^{1/2} [R]_s^{1/2} [M]_s$$

Above equation could satisfactorily account for the present behaviour of the $\overline{Ce}$(IV) – EDTA initialized acrylamide polymerization exhibited in the aqueous montmorillonite layered space.

(page 65-74)

The x.r.d, e.s.r. and n.m.r. spectral data are shown in section 3.6. e.s.r. study confirms that lattice substituted $\overline{Fe}$(III) in montmorillonite reacts with TU, but the reaction failed to initiate the polymerization of acrylamide in water. The redox characteristics of $\overline{Fe}$(III) towards TU reductant remains almost unaltered even when $\overline{Fe}$(III) ions are adsorbed by the mineral clay montmorillonite. Propagating radicals were characterised by spin trapping technique. The hyperfine splitting parameters a_N and a_H^β for MNP adduct are 1.45 and 0.31 mT respectively. The polymers as characterise by ^1H and ^{13}C n.m.r. are mostly TU terminated head-to-tail polymers with mixed tacticities where Bernoulli statistics are followed. The acrylamide molecules readily intercalate into both forms of mineral resulting in two-stage intercalation. The first saturation value is nearly 1.25 m.mol.g^{-1} whereas the second one is just nearly double. Unlike acrylamide, the TU leads to the monolayer formation only and maximum capacity is found to be 1.37 m.mol.g^{-1}, which is consistent with that of monolayer of acrylamide. The Langmuir constants are low; they are 12.0 and 9.2 for TU and AM respectively in the case of FeM. Above observation strongly justify the assumptions made in establishing the kinetics and mechanism for acrylamide polymerization on montmorillonite surface.

(page 75-83)

Chapter 4 is concerned with the study of copolymerization of acrylamide (AM) with diacetone acrylamide (DAAM) and N-tert-butylacrylamide (N-t-BAM) on montmorillonite surface. In section 4.1, a brief review on this aspect is presented. Copolymers of acrylamide have shown a number of properties leading to varieties of industrial applications including those as water soluble viscofires and displacement fluid in enhanced oil recovery. Two of the critical

limitations of polyelectrolytes are loss of viscosity in the presence of electrolytes and ion binding to porous reservoir rock substrate. Importance of the present study lie in the fact that (i) the applied technique provides high molecular weight polymers having high intrinsic viscosities (ii) at least one of the above copolymers viz., diacetone acrylamide, has already shown some promises by not losing its solution viscosities in the presence of added electrolytes. The copolymers are found in good yield by $\overline{Fe}$(III) – TU redox initiator when the $\overline{Fe}$(III) were loaded in the interlayer spaces of montmorillonite. Characteristics of the copolymers including the reactivity ratios for the respective monomers are determined and micro structures are predicted.

(page 84-87)

The experimental procedure for the copolymerization reaction is presented in section 4.2.

(page 88-90)

Both Fineman-Ross and the Kelen-Tüdos methods were employed to determine reactivity ratios of the monomer pairs. The reactivity ratios for AM:DAAM monomer were determine as $r_1 = 0.71$ and $r_2 = 0.61$ according to the more reliable Kelen-Tüdos method. For AM:N-t-BAM monomer pair they were as 1.51 and 0.46 respectively. The AM-DAAM copolymers with $r_1r_2 = 0.43$ and the AM–N-t-BAM copolymers with $r_1r_2 = 0.70$ exhibit an opposite tendency towards alternation. The micro-structures of copolymers including mean sequence length distribution is presented for a range of feed compositions through the knowledge of reactivity ratios. For the series of AM-DAAM copolymers, the mean sequence length of acrylamide, μ_{AM}, varied from 30.03 at an 96.36/3.64 mole ratio of AM/DAAM in the copolymer to 4.01 with a 78.77/21.23 mole ratio. For those compositions, values of μ_{DAAM} were 1.01 and 1.14 respectively. On the other hand, the AM-N-t-BAM copolymers had μ_{AM}

value of 62.50 and 7.37 at 98.33/1.67 and 89.42/10.58 mole ratios of AM/N-t-BAM respectively. Above values for $\mu_{N\text{-}t\text{-}BAM}$ were 1.01 and 1.11 respectively.

Due to slower termination rates in the adopted polymerization technique, copolymers with high intrinsic viscosities are formed. The observed decreased in the intrinsic viscosity with increasing DAAM or N-t-BAM comonomer concentrations may be explained by increased cross termination rates of copolymerization.

(page 90-101)

Chapter 5 records the results of the study on solution properties of polyacrylamide in water and water-dimethylsulphoxide mixtures. In view of the use of polyacrylamide in various fields including those as water soluble viscofiers and displacement fluids in secondary oil recovery process, the understanding of the role of charged groups on different factors which govern the efficiency in their use is important. Such studies on the solution properties of the polymer viz., intrinsic viscosity and unperturbed dimension of the polymer, temperature coefficient of unperturbed dimension, molecular extension factor and chain rigidity in different solvents and cosolvent media are important. A brief review on this aspect is presented in section 5.1.

(page 102-110)

In the present study, the intrinsic viscosities [η] of polyacrylamides having different sizes are measured at 30° – 50°C temperature in various mixtures of water (good solvents) and dimethyl sulphoxide (DMSO, poor solvents). The observed result and the Huggins constant values show a significant variation of cosolvency as a function of solvent composition (φ) and temperature. The nature of plots of [η] versus φ_{DMSO} indicates relative importance of entropy factors over energetic factors in determining molecular configuration at high temperature. The unperturbed dimensions (K_θ) of the polymer are determined by various methods, which agree well with each other and exhibit a minimum at

φ = 0.5. The temperature coefficients of the unperturbed dimension (K^l) gives both positive and negative values depending on the solvent composition, which indicates the variation of compactness and the presence of low and high energy configurations as a function of solvent composition. Molecular extension factor (α_n) and the chain rigidity (σ) values are evaluated and the influence of temperature is discussed.

(page 112-120)

REFERENCES

1. P. Moiyeux, Water-soluble synthetic polymers : Update I and II. Macrophile Associates, U.K. (1988).
2. B.K.G. Theng, The Chemistry of clay organic reactions, Adam Hilger, London **111** (1974).
3. B.K.G. Theng, Clay-polymer Interactions : summary and perspectives, clay and clay minerals, **30**, 1 (1982).
4. T.J. Pinnavaia, *Intercalated Clay Catelysts, Science*, **220**, 365 (1983).
5. The Chemistry of Acrylamide : A review with many references, American Cyanamid Company, New York, (1956).
6. E.R. Kolodny and R.B. Booth, Canadian Pat. 616, 976 (1961), (to American Cyanamid Company).
7. AM-9 Chemical Grout, American Cyanamid Company, New York, 1960.
8. Accostrength Paper Resin 2386, American Cyanamid company, New York, 1959.
9. R.L. Mongan and E.R. Kolodny, U.S. Pat. 2, 868, 753 (1959), (to American Chemical Company).
10. E.R. Kolodny, U.S. Pat. 3,002, 960 (1961), (to American Chemical Company).
11. C.L. McCormick and G.S. Chen, *J. Polym. Sci., Polym. Chem. Ed.*, **22**, 3649 (1984).
12. R.M. Christenson and H.A. Vogel, U.S. Pats, 2, 919, 254 (1959), 2, 940, 943 and 2,940, 944 (1960), to (Pittsburgh Plate Glass Company).
13. H.A. Vogel and H.G. Bittle, U.S. Pats. 2,870,116 and 2,870,117 (1959), H.A. Vogel and H.G. Bittle (to Pittsburgh Plate Glass Company).
14. "Thermosetting Acrylic Regins", a Symposium in *Ind. Chem.* **53**, 458, (1961).
15. A.S. Tomcufeik, S.D. Willson, A.W. Vogel and A. Sloboda, *Nature*, **191**, 611 (1961).
16. U. Hofmann, K. Endell and D. Wilm, *Z. Krist*, **86**, 340 (1933).
17. C.E. Marshall, *Z. Krist.*, **91**, 433 (1935).
18. E. Maegdefrau and U. Hofmann, *Z. Krist.*, **98**, 299 (1937).
19. S.B. Hendricks, *J. Geol.*, **50**, 276 (1942).

20. R.C. Mackenzie and B.D. Mitchell, *Clay Mineralogy, Earth Sci.* Rev., **2**, 47 (1966).
21. D.M.C. Macewan, Montmorillonite Minerals, In G. Brown led.). The X-ray identification and crystal structure of Clay Minerals. Mineral Soc., London, pp. 143-207 (1961).
22. R.W. Mooney, A.G. Keenan and L.A. Wood, *J.Am.Chem. Soc.*, **74**, 1367 (1952).
23. K. Norrish, *Disc. Faraday Soc.*, **18**, 120 (1954).
24. N.D. Foster, *Am. Mineralogist*, **38**, 120 (1954).
25. C.H. Edelman and J.C.L. Favejee, *Z. Krist.* **A 102**, 417 (1940).
26. McConnell, *Am. Mineralogist*, **35**, 166 (1950).
27. R.E. Grim and G. Kulbicki, *Am. Mineralogist*, **46**, 1329 (1961).
28. C.R. Smith, *J.Am.Chem.Soc.*, **56**, 1961 (1934).
29. L.E. Ensminger and J.E. Gieseking, *Soil Sci.*, **48**, 467 (1939).
30. L.E. Ensminger and J.E. Gieseking, *Soil Sci.*, **51**, 125 (1941).
31. S.B. Hendricks, *J.Phys. Coll. Chem.*, **45**, 65 (1941).
32. J.W. Jordon, *J. Phys. Coll. Chem.*, **53**, 294 (1949).
33. W.F. Bradley, *J.Am.Chem.Soc.*, **67**, 975 (1945).
34. D.M.C. McEwan, *J.Soc. Ind (London)*, **65**, 298 (1946).
35. R.E. Grim, *Clay Mineralogy*, Academic Press Inc . London (1964).
36. W.Eitel, *Silicate Science*, Academic Press Inc. London (1964).
37. P.J. Greenland and M.H.B. Hayes, 'The Chemistry of Soil Processes', Wiley Interscience, New York (1981).
38. G. Sposito, 'The Surface Chemistry of Soils', Oxford University Press, New York (1984).
39. G.W. Brindley and G. Brown, 'Crystal Structure of Clay Minerals and Their X-ray identification', Mineralogical Society, London (1980).
40. M.M. Mortland, *Adv. Agron.*, **22**, 75 (1970).
41. H.Mukherji. *J. Ind. Soc. Soil, Sci.*, **2**, 99 (1954).
42. H. Mukherji, D. Phil. Thesis, Calcutta University, (1956).
43. S.K. Chakravarti, *Sci. Cult.*, **22**, 170 (1956).
44. S.K. Chakravarti, *J.Ind. Soc. Soil. Sci.*, **5**, 185 (1957).

45. S.K. Chakravarti, *J. Ind. Soc. Soil. Sci.*, **5**, 65 (1957).
46. S.K. Chakravarti, *J.Ind. Soc. Soil. Sci.*, **6**, 239 (1958).
47. S.K. Chakravarti, *J.Ind. Soc. Soil. Sci.*, **7**, 27 (1959).
48. S.K. Chakravarti, D. Phill. Thesis, Calcutta Univ. (1959).
49. S.K. Chakravarti and S.K. Mukherjee, *J.Ind. Chem.Soc.*, **42**, 289 (1965).
50. S.K. Chakravarti and S.K. Mukherjee, *Ind. J. Appl. Chem.*, **34**, 50 (1971).
51. D.K. De, S.K. Chakravarti and S.K. Mukherjee, *J.Ind.Chem.Soc.*, **44**, 743 (1967).
52. D.K. De, S.K. Chakravarti and S.K. Mukherjee, *J.Ind.Chem.Soc.*, **45**, 566 (1968).
53. D.K.De, S.K. Chakravarti and S.K. Mukherjee, *J.Ind.Chem.Soc.*, **46**, 119 (1969).
54. D.K.De, J.L. Das Kanungo and S.K. Chakravarti, *J.Ind.Soc.Soil Sci.*, **21**, 137 (1973).
55. B.K.G. Theng, 'Formation and Properties of Clay-Polymer Complexes', Elsevier Scientific Publishing Co., New York (1979).
56. M.M. Mortland, *J. Molecular Catalysis*, **27**, 153 (1984).
57. S.A. Boyd and M.M. Mortland, *Nature*, London, **316**, 532 (1985).
58. S.A. Boyd and M.M. Mortland, *Experiemntia*, **41**, 1564 (1985).
59. S.A. Boyd and M.M. Mortland, *J. Molecular Catalysis*, **34**, 1 (1986).
60. D.J. Greenland, *Soils Fertilizers*, **28**, 415 (1965).
61. R.W. Hofmann and G.W. Brindley, *Geochim. Cosmochim. Acta.*, **21**, 15 (1960).
62. W.L. German and D.A. Harding, *Clay Minerals*, **8**, 213 (1969).
63. R.W. Doehler and W.A. Young, *clays and Clay Minerals*, **9**, 468 (1962).
64. C.A. Bower, *Soil Sci.*, **95**, 192 (1963).
65. J.H.De Boer and G. Heller, *Physica*, **4**, 1045 (1937).
66. H.C. Mahaker, *Physica*, **4**, 1058 (1937).
67. D.J. Greenland, *J. Colloid Sci.*, **18**, 647 (1963).
68. R.L. Parfilt and D.J. Greenland, *Clay Minerals*, **8**, 305 (1970).
69. D.M.C. McEwan, *Trans, Faraday Soc.*, **44**, 349 (1948).
70. K.K. Bissada, W.D. Johns and F.S. Cheng, *Clay Minerals*, **7**, 155 (1967).

71. S.Tahoun and M.M. Mortland, *Soil Sci.*, **102**, 248 (1966).
72. R.A. Weismiller, *Diss. Abst.*, **30**, 4874B (1970).
73. J. Well-Malherbe and J. Weis, *J. Chem. Soc.*, 2164 (1948).
74. G. Briegleb, Electronen-Donator-Acceptor-Complex, Pringer Verlag, Berlin.
75. D.H. Solomon, B.C. Loft and J.D. Swift, *Clay Minerals*, **7**, 389-408 (1968).
76. Llona Toch, J. Szepvolgyi, J. Emma, P. Szabo and T. Szekey. *Thermochim. Acta*, **170**, 155 (1990).
77. M. Ogawa, K. Kuroda and C.Kato, *Clay Sci.*, **7(4)**, 243 (1989).
78. H. Nagae, K. Kawase, H. Sakami, S. Lida and Hayakawa, *Kiyoshi. Kabunshi Ronbunshu*, **47(8)**, 631 (1990).
79. C.Kemball and J.J. Rooney, *Proc. Roy. Soc. (London)*, 567 (1961).
80. Soconi Mohil Oil Co., INC., Brit. Pat. 896, 864 (1962).
81. Y. Suehiro. M. Kuwabara and V. Ayukawa, *J. Chem. Soc., Japan*, **52**, 43 (1949).
82. F.E. Shephard, J.J. Rooney and C. Kemball, *J. Catalysis*, **1**, 379 (1962).
83. H.Z. Friedlander, *J. Pllym. Sci.*, **C-4**, 1291 (1964).
84. J.A. Bittles, A.K. Chaughuri and S.W. Benson, *J. Polym. Sci.*, **A-2**, 1221 (1964).
85. D.H. Solomon, J.d. Swift and A.J. Murphy, *J. Macromal. Sci.*, **A5(3)**, 587 (1971).
86. P.H. Flesch, 'Cationic Polymerization and Related complexes', Academic Press, New York (1953).
87. D.C. Pepper, *Trans Faraday Soc.*, **45**, 397 (1949).
88. D.C. Pepper, *Trans Faraday Soc.*, **45**, 404 (1949).
89. D.C. Pepper and M.J. Hayes, *Proc. Chem. Soc.*, 228 (1958).
90. A.G. Evans and G.W. Meadows, *Trans. Faraday Soc.*, **46**, 327 (1950).
91. G.F. Endres and C.G. Overberger, *J.Am. Chem. Soc.*, **77**, 2201 (1955).
92. J.P. Kenedy, 'Cationic Polymerization of Oelfins' : A Critical Inventory, Wiley-Interscience, (1975).
93. J.A. Britles, A.K. Choudhuri and S.W. Benson, *J. Polym.Sci.*, **A-2**, 1847 (1964).

94. J.A. Biltles, A.K. Choudhuri and S.W. Benson, *J. Polym. Sci.*, **A-2** 3203 (1964).

95. D.H. Solomon and M.J. Rosser, *J. Polym. Sci.*, **9**, 1261 (1965).

96. T. Matsumoto, I. Sakai and M. Arihara, Chem. High Polymers (Japan), **26**, 378 (1969).

97. M.M. Mortland, Trans. 9th Intern. *Cong. Soil Sci., Adelaide*, **1**, 691 (1968).

98. W. Bodenheimer, L. Heller and S. Yariv, *Proc. Internat. Clay Conf., Jerusalem*, **I**, 251 (1966).

99. A. Blumstein, *J. Polym. Sci.*, **A-3**, 2653 (1965).

100. A. Blumstein and F.W. Billmeyer, Jr., *J. Polym. Sci.*, **A-4**, 465 (1966).

101. A. Blumstein and R. Blumstein, *Polymer Letters*, **5**, 69 (1967).

102. A. Blumstein, S.L. Malhotra and A.C. Waterson, A.C.S., *Polymer Reprints*, 167 April (1968).

103. O.L. Glavati, L.S. Polak and V.I. Shchexin, *Neftekhimiya*, **3**, 905 (1963).

104. H.G.G. Dekking, *J. Appl.Polym. Sci.*, **9**, 1641 (1965).

105. H.G.G. Dekking, *J.Appl. Polym. Sci.*, **11**, 23 (1967).

106. D.H.Solomon and B.C. Loft, *J.Appl.Polym. Sci.*, **12**, 1253 (1968).

107. B.K.G. Theng and G.F. Walker, *Israel J. Chem.*, **8**, 417 (1970).

108. B.K.G. Theng, *Clays and Clay Minerals*, **18**, 357 (1970).

109. I.A. Uskov, Yu. G. Tarasenco, V.P. Solomko, *Vysokomolekhul. Soedin*, **6**, 1768 (1964).

110. S. Talapatra, S.K. Saha, S.K. Chakravarti and S.C. Guhaniyogi, *Polym. Bull.*, **10**, 21 (1983).

111. S. Talapatra, S.C. Guhaniyogi and S.K. Chakravarti, *J. Macromol. Sci. Chem.*, **A22(11)**, 1611 (1985).

112. J. Bhattacharya, S.K. Chakravarti, S. Talapatra, S.K. Saha and S.C. Guhaniyogi, *Journal of polymer Science, Part A : Polymer Chemistry*, **27**, 3977 (1989).

113. J. Bhattacharya, S.K. Saha and S.C. Guhaniyogi, *Journal of Polymer Science, Part A : Polymer Chemistry*, **28**, 2249 (1990).

114. S.K. Saha and D.J. Greenslade, *Bulletin of Chemical Society of Japan*, **65**, 2720 (1992).

115. Jpn. Patent, 58, 28, 313, June 15, 1983, Nilto Chemical Industry Co. Ltd.
116. T. Ono, T. Takahashi, M. Konno and T. Mikawa, Ken Kyu Kiyomiyagi, Kagyo Koto Senmon Gakko, **18**, 57 (1982).
117. F.C. Avagon and N.M. Evole, *An Quin, Ser. B*, **78(1)**, 13 (1982).
118. M. Lazar, J. Rychly and J. Pavlinec., *Chem. Zvesti.*, **30(3)**, 318-27 (1976).
119. Ulagaraj Chandra Singh, S.P. Manickam, and Krishnarao Venkatarao, *Makromol. Chem.*; **180**, 589-94 (1979).
120. P.Ghanasundaram and H. Kothandaraman, *Polym. J.*, **11(1)**, 261-5 (1979).
121. Tsutomu Miyagawa, Takashi Nakata and Motoaki Tanaka, Jpn. Kohai Tokkyo Koho. 79, 133, 583, 17 Oct. 1979, Appl. 78/41, 568, 08 Apr. 1978, 7 pp.
122. S. Sarasvathy and K. Venkatao, *Curr. Sci.*, **49**, 702, (1980).
123. Kesavan Kaliyamurthy, Pivamiah Elayaperumal, Thayikkannu Balakrishnan and Muchi Santappa, *Polym. J.* (Tokyo), **14**, 107 (1982).
124. S. Lenka, P.L. Nayak, S.B. Dash and S. Ray, *Colloid Polym. Sci.*, **261**, 40 (1983).
125. A. Kaim, *J. Polymn. Sci., Polymn, Lett. Ed.*, **22**, 203 (1984).
126. A. Copalan, S. Paulrajan, S. Vaidyanathan, K. Venkatarao and N.R. Subbaratham, *Eur. Polym. J.*, **20**, 971 (1984).
127. T. Balakrishnan and E.K. Kasilingam, *J. Indian. Chem. Soc.*, **60**, 1186 (1983).
128. Jaroslav Barton and Viera Juranicova, Viera Vaskova, *Makromol. Chem.*, **186**, 1935 (1985).
129. Xuanchi Wa and Yujin Peng, *Gaofenzi Tongxun*, **6**, 499 (1984).
130. Sivananda Misra and Gangadhar Sahu, *J.Polym.sci., Polym. Chem. Ed.*, **23**, 2647 (1985).
131. Arun V. Pantar and Mandapati V.R. Rao, *Makromol Chem., Rapid commun.*, **7**, 77 (1986).
132. Maja Cvetkovska and T. Greev, *Hem. Ind.*, **41**, 188 (1987).
133. L.G. Revel'skaya and V.I. Kurlyankina, *Vyosomol. Soedin., Ser. A.* **29**, 1086 (1987).

134. Viera Vaskova, Daniela Oremusova and Jaroslav Barton, *Makromol Chem.*, **189**, 709 (1988).

135. Yinghai Liu, Xingru Song, Homgmei Shi and Lili Xu, *Gaodeng Xuexiao Huaxue Xuebao* **11**, 328 (1990).

136. D. Hundeler and A.E. Hamielec., *Polym. Prepr.* (Am. Chem. Soc. Div. Polym. Chem.), **30(2)**, 346 (1989).

137. Yinghai Lui, Xingru Song, Hongmei Shi and Lili Xu, *Huaxue Shijie* **31**, 159 (1990).

138. Rita Vasishtha and Anil K. Srivastava, *J.Polym. Sci., Part A : Polym. Chem.*, **28**, 1297 (1990).

139. Mitsumi Takahashi, *Nippon Kagaku Kaishi*, **12**, 2070 (1989).

140. L.L. Stupen'kova, T.A. Baiburdov, V.F. Gromov and E.N. Teleshov, *Vysokomol. Soedin, Ser, A.*, **33**, 1498 (1991).

141. D. Hunkeler, *Macromolecules*, **24**, 2160 (1991).

142. V.A. Bhanu and K. Kishore, *J. Polym. Sci. Part A : Polym. Chem.* **28**, 3617 (1990).

143. S.K. Ghosh, M. Nazimuddin, S.N. Bhattacharya and B.N. Mandal, *Polym. Sci.* [symp. Proc. Polym., 91] **1**, 199 (1991).

144. V.F. Kurenkov, E.V. Nurullina and V.A. Mgagchenkov, *Izv, Vyash. Uchebn Zaved, Khim. Khim. Tekhnol.* **32**, 96 (1989).

145. G.S. Misra and J.J. Rebello, *Makromol. Chem.*, **177**, 21 (1976).

146. M.M. Husain and Archana Gupta, S. Misra, *Makromol. Chem.*, **176**, 2861 (1975).

147. G.S. Misra and U.D.N. Bajpai, *J. Macromol. Sci. Chem.*, **13**, 1135 (1979).

148. U.D.N. Bajpai and G.S. Misra, *Vysokomol. Soedin, Ser. A*, **21**, 1720 (1979).

149. G.S. Misra and S.N. Bhattacharya, *J. Marcomol, Sci., Chem.*, **A14**, 907 (1980).

150. U.D.N. Bajpai and A.K. Bajpai, *J. Macromol. Sci. Chem.*, **A19**, 487 (1983).

151. U.D.N. Bajpai and A.K. Bajpai, *J. Polym. Sci. Polym. Chem. Ed.* **22**, 1803 (1984).

152. U.D.N. Bajpai and A.K. Bajpai, *Macromolecules*, **18(11)**, 2113 (1985).

153. K.C. Gupta, M. Verma and K. Behari, *Macromolecules,* **19**, 548 (1986).

154. K. Behari, K.C. Gupta, and M. Verma, *Vysokomol. Soedin, Ser. A.* **28**, 1781 (1986).

155. K. Berhari, K.C. Gupta, G.D. Raja and P. Das, *Acta Polym.* **42**, 206 (1991).

156. U.D.N. Bajpai and Anita Ahi, *J. Appl. Polym. Sci.* **40**, 359 (1990).

157. U.D.N. Bajpai and G.S. Misra, *Vysokomol. Soedin, Ser. B.* **21**, 419 (1979).

158. S.P. Rout, A. Rout, N. Mallick and B.C. Singh, *Makromol Chem.* **178**, 1971 (1977).

159. M.M. Husain and A. Gupta, *J. Macromol.Sci., Chem.*, **A II**, 2177 (1977).

160. G.S. Misra and G.P. Dubey, *Polym. Bull.* **1**, 671 (1979).

161. G.S. Misra and S.N. Bhattacharya, *Colloid. Polym. Sci.* **258**, 954 (1980).

162. G.S. Misra and G.P. Dubey, *J. Macromol. Sci., Chem.* **A16**, 610 (181).

163. D. Pramanik and K. Das, *Indian J.Phys. Nat. Sci.* **1**, 8 (1981).

164. G.S. Misra and S.N. Bhattacharya, *J.Polym.Sci., Polym. Chem. Ed.* **20**, 131 (1982).

165. G.S. Misra, P.S. Bassi and S.L. Abral, *Indian J. Chem. Sect, A.* **22A**, 286 (1983).

166. G.S. Misra and J.I. Khatil, *J. Polym. Sci, Polym. Chem. Ed.* **21**, 1665 (1983).

167. G.S. Misra and A.K. Bajpai, *J. Macromol. Sci. Chem.* **A19**, 487 (1983).

168. D. Pramanick and B. Chakraborty, *Bull. Pure Appl. Sci. Soc.* C. **2**, 1 (1983).

169. K.C. Gupta and K. Behari, *J.Polym. Sci. Part A : Polym. Chem.* **24**, 764 (1986).

170. A.S. Savac, A. Gocmen and B. Basaran, *J. Solution Chem.* **19**. 901 (1990).

171. Kunyuan, Qiu, Wei Wang and Yingfei Yang Xinde Feng, *Chin. Sci. Bull.* **34**, 1348 (1989).

172. W. Wang, Y. Sun, Ye. Song, Kuryan Qiu and Zinde Feng, *Gaofenzie Xuebao*, **2**, 213 (1990).

173. Kinyan Qui, W. Wang, W. Guo, D. Zhang and Xinde Feng, *Gaofenzi Xueba* **4**, 496 (1990).
174. Kinyuan Qiu and W. Wang, *Gaofenzi Xuebao*, **3**, 355 (1989).
175. Xinquiu, Guo, Kinyuan, Qiu, Xinde Feng, Chin. *J.Polm. Sci.*, **7**, 165 (1989).
176. Xinqui Guo, K. Qiu and Xinde Feng, *Makromol, Chem.* **191**, 577 (1990).
177. G.P. Patapov and M.I. Alieva, Izu. Vyash. Vchebn. Zaved., *Khim. Khim. Tekhnal.* **34**, 107 (1991).
178. Gilles Maihot and M. Bolte, *Polyhedron*,, **10**, 237 (1991).
179. Kinyuan Qiu, Yingfei Yang and Xinde Feng, *Gaofenzi Xuebao*, **5**, 593 (1989).
180. V.F. Kuvenkov, T.A. Baiburdov and L.L. Stupen'Kova, *Zh. Prikl. Khim.* **60**, 2311 (1987).
181. V.F. Kurenkov, M.N. Tritonova and V.A. Myagchenkov. *Eur.Polym. J.* **23**, 685 (1987).
182. V.F. Kurenkov, T.A. Baiburdov and L.L. Stupen'Kova, *Vyskomol. Soedin*,, Ser. A, **29**, 348 (1987).
183. R.M. Akopyan, A.M. Kaifadzhyan and N.M. Beileryan, *Arm. Khim. Zh.*, **39**, 471 (1986).
184. R.M. Akopyan, N.M. Beileryan and A.M. Kaifadzhyan, *Arm. Khim. Zh.*, **36**, 139 (1983).
185. L.K. Voronova, N.S. Shaglaeva, A.V. Rzhepka, V.A. Loprev and M.G. Voronkov, *Zh. Prikl. Khim.*
186. Xinqui Guo, Kinyuan Qui and Xinde Feng, *Gaodeng Xuexiao Huaxue Xuelao* **10**, 1068 (1989).
187. Qingpu Liu, Runhua Ha, Hongrong Liu and Jinsheng Hu, *Gaodeng Xuexiao Huaxue Xuelao,* **10**, 673 (1989).
188. C.Y. Chen and J.F. Kuo, *J. Polym. Sci., part A : Polym. Chem.*, **26**, 1115 (1988).
189. M. Cvetkovoka and T. Greev, *Hem. Ind.*, **41**, 188 (1987).
190. R.A. Smith, U.S. 4, 617, 359, 14 Oct. 1986, US Appl. 649, 622, 12 Sep. 1984. 10 pp. Cont-in-Part of U.S. Ser No. 649, 622 abandoned.
191. Xuanchi Wu and Jianqiang He, *Gaofenzi Tongxun* **6**, 402 (1986).

192. T. Balakrishnan and S. Subbu, *J. Polym. Sci., Part A : Polym. Chem.*, **24**, 2771 (1986).

193. Chuh Yung Chen and Jen Feng Kuo, Ch'eng-Kung Ta Hsueh Hsueh Pao, K'ochi, *I.Hsueh Pian*, **20**, 193 (1985).

194. T. Grcev and M. Cvetkovska, Al-Dabas, Imad. *J. Serb. Chem. Soc.*, **51**, 15 (1986).

195. A.V. Pantar and M.V.R. Rao, *Makromol. Chem.*, Rapid Commun., **7**, 77 (1986).

196. Xuanchi Wu and Yujin Peng, *Gaofenzi tongxun*, **6**, 449 (1984).

197. A. Gopalan, S. Paulrajan, S. Vaidyanathan, K. Venkatarao and N. R. Subbaratnam, *Eur. Polym. J.*, **20**, 971 (1984).

198. S. Lenka, P.L. Nayak and S. Roy, *J. Polym. Sci., Polym Chem. Ed.* **22**, 959 (1984).

199. M. Cvetkovska, T. Grcev and G. Petrov, *Makromol Chem.* **185**, 429 (1984).

200. C. Namasivayam, P. Natarajan, Proc, IUPAC, I.U.P.A.C., Macromol. Symp. 28th 1982, 181, Int. Union. Pure Appl. Chem. Oxford, U.K.

201. T.A. Kay, F. Rodriguez, Proc. IUPAC, I.U.P.A.C., Macromol Sym. 28th 1982, 77, Int. Union, Pure Appl. Chem., Oxford, U.K.

202. D.V.P.R. Varaprasad and V. Madadevan, *J. Macromol. Sci., Chem.* **A18**, 1429 (1982).

203. P. Elayaperumal, T. Balakrishnan, M. Santappa and R.W. Lenz, *J. Polym. Sci., Polym. Chem. Ed.* **20**, 3325 (1982).

204. D.V.P.R. Varaprasad and V. Madadevan, *Eur. Polym. J.* **17**, 1185 (1981).

205. P. Elayaperumal. T. Balakrishnan, M. Santappa, R.W. Lenz, *J. Polym. Sci., Polym. Chem. Ed.* **20**, 3325 (1982).

206. G.S. Sur and S.K. Choi, *J. Macromol. Sci., Chem.* **A15**, 671 (1981).

207. Mahadevan Haragopal, A. Jayakrishnan and Venkatanarayana *Mahadevan, Makromol. Chem.* **183**. 657 (1982).

208. P. Ganasundaram and H. Kothandaraman, *Eur. Polym. J.* **15**, 399 (1979).

209. G.S. Sur, *Yongu Pogoyongnam Taehakkyo Kongop Kishl Yonguso*, **7**, 43 (1979).

210. M.M. Husain, S.N. Misra and R.D. Singh, *Makromol. Chem.* **179**, 295 (1978).

211. D.Z. Chshmarityan and N.M. Beileryan, *Arm. Khim. Zh.* **30**, 120 (1977).

212. M.L. Jackson, *Soil Chemical Analysis*, Prentice Hall of India (P) Ltd., New Delhi, 168 (1973).

213. B.S. Ruruiss, A.J. Haknorfod, V. Rogers, P.W.G. Smith and A.R. Tatchell, Vogel Text Book of Practical Organic Chemistry, Longman, London, 169, 279-280.

214. J. Francois, D. Sarazin, T. Schwartz and G. Weill, *Polymer*, **20**, 969 (1979).

215. F.Candau, Y.S. Leong, G. Pouget and S. Candau, *J.Coll. Inf. Sci.*, **101**, 167 (1984).

216. J. Bhattacharya, S. Talapatra and S.K. Saha, *J. Appl. Polym. Sci.*, **39**, 2237 (1990).

217. G.S. Misra, U.D.N. Bajpai and J. Trekoval, *J. Rev. Macromol. Chem. Phys.*, **C24(3)**, 335 (1984).

218. P.L. Nayak, S. Lenka and M.K. Misra, *J. Appl. Polym. Sci.*, **25**, 63 (1980).

219. C.L. McCormick and G.S. Chen, *J.Polym. Sci., Polym. Chem. Ed.*, **22**, 3633 (1984).

220. J.E. Lancaster and M.N.O'Connor, *J.Polymer Sci., Polym. Letts.*, **20**, 547 (1982).

221. N. Pustelnik and R. Soloniewiez, *Chem. Anal. (Warsaw)*, **21**, 503 (1976).

222. C.W. Hsu, J.F. Kuo and C.Y. Chen, *J. Polym. Sci. Part A : Polym. Chem.* **31**, 267 (1993).

223. E.F. Tai, J.A. Caskey and B.D. Allison, *J.Polym. Sci. Part A : Polym. Chem.* **24**, 567 (1986).

224. J.P. Riggs and F. Rodringuez, *J. Polym. Sci,* Part **A1 5**, 3151 (1967).

225. W. Bodenheimer, L. Heller and S. Yariv, *Proc, Internat. Clay Conf., Jerusalem*, **1**, 251 (1966).

226. J.J. Fripiat, Trans. 9th Intern. *Cong. Soil Sci., Adelaide*, **1**, 691 (1968).

227. B.M. Mandal, U.S. Nandi and S.R. Palit, *J.Polym. Sci.* **A1 8**, 67 (1970).

228. U.D.N. Bajpai, A.K. Bajpai and J. Bajpai, *J. appl. Polym. Sci.*, **42(7)**, 2005 (1991).
229. U.D.N. Bajpai and A.K. Bajpai *J. Polym. Sci., Polym. Chem. Ed.* **22**, 1803 (1984).
230. V. Vaskova, D. Oremusova and J. Barton, *Makromol. Chem.*, **189**, 709 (1988).
231. J.H. Fendler and E.J. Fendler, 'Catalysis in Micellar and Macromolecular Chemistry', Academic, New York (1975).
232. P.L. Nayak and M. Santappa, *Ind. J. Appl. Chem.*, **35**, 662 (1976).
233. J.P. Friend and A.E. Alexander, *J.Polym. Sci.* **A1 6**, 1833 (1966).
234. J.A. Marinsky, F.G. Lin and K.S. Chung, *J. Phys. Chem.*, **87**, 3139 (1983).
235. D.D. Perrin, Organic Ligands : IUPAC Chemical Data Series (No. 22), Pergamon Press, New York (1983).
236. A.E. Martell and R.M. Smith, 'Critical Stability Constant (vol.3)', New York (1979).
237. W.C. Hsu, C.Y. Chen, J.F. Kou and E.M.Wu, *Polymer*, **35**, 849 (1994).
238. G.S. Misra and J.I. Khatib, *Colloid Polym. Sci.*, **261**, 188 (1983).
239. J.J. Fripiat, 'Development in Sedimentology', Eisevier, New York, (1982).
240. E. Collison, F.S. Dainton and G.S. McNaughton, *Trans. Faraday Soc.*, **53**, 489 (1957).
241. W.C. Hsu, J.F. Kuo and C.Y. Chen, *Journal of Polymer Science, Part A : Polymer Chemistry*, **30**, 2459 (1992).
242. A.L. Barnes, *J. Pet. Tech.*, 1147 (October 1962).
243. D.J. Pye, *J. Pet. Tech.*, 911 (August 1964).
244. H.L. Chang, *J. Pet. Tech.*, 1113 (August 1978).
245. N.J. Bikales, Ed., 'Water-soluble Polymers Plenum', New York, 105 -126 (1973).
246. C.L. McCormick, Symposium on Polymeric Materials for Basic Energy Needs, Case Western Reverve, 13 (1978).
247. M.T. Szabo, *J. Pet. Tech.*, 553 (May 1979).
248. L. Soltesz, K. Rajnai, M. Gerzson, ErnoGova, G. Halas, J. Balogh, M. Varga, Z. Ferdinand and J. Ratkovszky et al. Ger. Offer. DE 3,801, 736,

27 July 1989, Appl. 21 Jan. 1988.

249. W. Baade, D. Hunkeler and A.E. Hamielec, *J. Appl. Polym. Sci.*, **38(1)** (1989).
250. F. Lafuma and G. Durand, *Polym. Bull.*, **21(3)**, 315 (1989).
251. N.A. Lavrov, A.F. Nikolaev and S.A. Kuzmina, *Zh. Prikl, Khim*, **62(2)**, 429 (1989).
252. Xinyuan Yang, Hui Yu and Yufang Bao, *Shiyan Huagong*, **17(1)**, 21 (1988).
253. C.L. McCormick and K. Khim, *J. Controlled Resease*, **7(2)**, 101 (1988).
254. Hansheng Xu, Xhicheng Zhang and Wei Liu, *Fushe Yanjiu Yu Fushe Gongyi Xuebao*, **3(3)**, 19 (1985).
255. W. Baade, D. Hunkeler and A.E. Hamielec, *Polym. Mater. Sc. Eng*, **57**, 850 (1987).
256. C.L. McCormick and L.C. Salazar, *Polym. Sci. Eng.* **57**, 859 (1987).
257. C.L. McCormick and G.S. Chen, *J. Polym. Sci., Polym. Chem. Ed.* **20(3)**, 817 (1982).
258. Yu. P. Chernenkova, E.N. Zil'berman and G.N. Shvareva, *Vysokomol Soedin*, Ser B., **24(2)**, 119 (1982).
259. M. Georgieva and E. Georgieva, *Angew Makromol. Chem.* **66** 1, (1978).
260. Viera Vaskova, Viera Juranicova and Jaroslav Barton, *Makromol. Chem.* **192(4)**, 989 (1991).
261. B. Srinivasula, P.R. Rao and E.V. Sundaram, *Angew Makromol. Chem.*, **189**, 97 (1991).
262. B. Srinivasula, P.R. Rao, E.V. Sundaram, M. Srinivas and L. Sirdeshmukh, *Eur. Polym. J.* **27(9)**, 979 (1991).
263. C.L. McCormick, L.S. Park, G.S. Chen and H.H. Neidlinger, *Polym. Prepr.* **22(1)**, 138 (1981).
264. C.L. McCormick, T. Nonaka and C.B. Johnson, *Polymer*, **29(4)**, 731 (1988).
265. C.L. McCormick and K.P. Blackmon, *Angew Makromol. Chem.* **144**, 73 (1986).

266. C.L. McCormick and G.S. Chen, *J. Polym. Sci., Polym. Chem. Ed.*, **22(12)**, 3633 (1984).
267. M. Orbay, R. Laible and L. Dulog, *Makormol. Chem.* **183(1)**, 47 (1982).
268. H. Sumi, H. Holta, S. Hiratsuna and A. Yada, Jpn. Kohai Tokyo Koho Jp 61, 126, 104, 13 Jun. 1986, April 84/247, 146, 22 Nov. 5 (1984).
269. Thomas, V.S. Pat. 2, 558, 396, June 26, (1951) (to American Cyanamid Co.)
270. J. Bhattacharya, Ph.D.Thesis, North Bengal University, India (1988).
271. M. Fineman and S.D. Ross, *J. Polym. Sci.*, **5**, 259 (1950).
272. T. Kelen and F. Tudas, *J. Makromol. Sci., Chem.*, **A9**, 1 (1975).
273. F.R. Mayo and F.M. Lewis, *J.Am.Chem.*, **66**, 1594 (1994).
274. S. Iwatsuki, A. Kondo and H. Harshina, *Macromolecules*, **17**, 2473 (1984).
275. S. Igarashi, *J. Polym. Sci., Polym. Lett, Ed.*, **1**, 359 (1963).
276. C.W. Pyun, *J.Polym. Sci., Part A2*, **8**, 1111 (1970).
277. H.J. Harwood, *J.Polym. Sci., Part C*, **25**, 37 (1968).
278. W.M. Thomas, in Encyclopaedia of Polymer science and Technology, Vol. 1, N. Bikales, Ed., Wiley-Interscience, New York, 177 (1964).
279. F.S. Dainton and M. Tordoff, *Trans Faraday Soc.*, **53**, 666 (1957).
280. P. debye and I.M. Krieger (unpublished) have shown that the average distribution of each segment about the centre of gravity is exactly Gaussian for random chain unperturbed by intramolecular interactions.
281. T. Lafrey, A. Bartovics and H. Mark; *J. Am. Chem. Soc.*, **64**, 1557 (1942).
282. P.J. Flory, Principles of Polymer Chemistry, Cornell University Press, Ithaca, N.Y., Chap. XIV, (1953).
283. P.J. Flory, *J. Chem. Phys.*, **17**, 303, (1949).
284. T.G. Fox, Jr., and P.J. Flory, *J. Phys. Colloid Chem.*, **53**, 197 (1949).
285. P.J. Flory and T.G. Fox, Jr., *J.Am.Chem.Soc.*, **73**, 1904 (1951).
286. T.G. Fox, Jr.[2] and P.J. Flory, *J.Am.Chem.Soc.*, **73**, 1909 (1951).
287. P.J. Flory, Jr.[2], and P.J. Flory, *J.Am.Chem.Soc.*, **73**, 1915 (1951).
288. J.M.G. Cowie, *Polymer*, **7**, 487 (1966).
289. T. Brandrup and E. H. Immergut (eds.), Polymer Handbook, Wiley-Interscience, New York, p - 47, (1966).

290. G.V. Schulz and R. Kriste, *Z. Phys, Chem.* (F. furt), **30**, 171 (161).
291. S.N. Chinal and C.W. Bondurant, Jr. *J.Polymer. Sci.*, **22**, 555 (1956).
292. H. Lutje and G. Meyerhoff, *Markromol. Chem.*, **68**, 180 (1963).
293. T.G. Fox, *Polymer*, **3**, 111 (1962).
294. M. Bohdanecky, *Collect. Czech. Chem. Commun.*, **30**, 1576 (1965).
295. H. Inagaki and S. Kawai, *Makromol.Chem.*, **79**, 42 (1964).
296. M. Bohdanecky, *collect, Czech. Chem. Commun.*, **34**, 407 (1969).
297. V.V. Varadaiah and V.S.R. Rao, *J. Sci. Ind. Res.*, **20B**, 280 (1961).
298. S.N. Chinal, J.D. Matlack, A.L. Resnick, and R.S. Samuels, *J.Polym. Sci.*, **17**, 391 (1955).
299. W.R. Moore and R.J.Fort, *J.Polym.Sci.*, **A1**, 929 (1963).
300. S. Gundiah, R.B. Mohite and S.L. Kapur, *Makromol. Chem.*, **123**, 151 (1969).
301. S. Arichi, *Bull. Chem. Soc. Jpn.*, **39**, 439 (1966).
302. U. Bianchi and A. Peterlin, *J. Polym. Sci.*, **A-2**, 6, 1759 (1968).
303. D.W. Van Krevelen and P.J. Hoftyzer, *J. Appl. Polym. Sci.*, **11**, 1409 (1967).
304. D.W. Van Krevelen and P.J. Hoftyzer, *J. Appl. Polym. Sci.*, **10**, 1331 (1968).
305. K. Kanide, Kobunshi Kagaku, 25, 781 (1968); *Chem. Abst.*, **70**, 88348Y (1969).
306. V.S.R. Rao, *J. Polym. Sci.*, **62**, S157 (1962).
307. H.L. Bhatnagar, A.B. Biswas and M.K. Gharpurey, *J. Chem. Phys.*, **23**, 88 (1958).
308. H. Yamakawa, *J. Chem. Phys.*, **34**, 1360 (1961).
309. T. Sakai, *J. Polym. Sci.*, A-2, **6**, 1535 (1968).
310. P. Vasudevan and M. Santappa, *Makromol. Chem.*, **137**, 261 (1970).
311. S. Gundiah, R.B. Mohite, and S.L. Kapur, *Markromol. Chem.*, **123**, 151 (1969).
312. P. Vasudevan and M. Sentappa, Unpublished Result.
313. P.C. Deb and S.R. Chatterjee, *Makromol. Chem.*, **120**, 49 (1968).
314. P.C. Deb and S.R. Chatterjee, *J. Indian Chem., soc.*, **46**, 468 (1969).

315. W. Burchard, *Makromol. Chem.*, **50**, 20 (1960).
316. W.H. Stockmayer and M. Fixman, *J. Polym. Sci.*, **C1**, 137 (1963).
317. M.Kurata, W.H. Stockmayer, *Fortschr, Hochpolym. Forsch.*, **3**, 196 (1963).
318. H. Kurata, W.H. Stockmayer, and A. Roig, *J. Chem. Phys.*, **33**, 151 (1960).
319. G.C. Berry, *J. Chem. Phys.*, **46**, 1338 (1967).
320. S. Lenka, P. Nayak and M. Dash., *J. Macromol. Sci. Chem.*, **A20(4)**, 467 (1983).
321. S. Lenka, P. Nayak and M. Dash., *J. Macromol Sci. Chem.*, **A19(3)**, 321 (1983).
322. G. Tanaka, *Macromolecules*, **15**, 1028 (1982).
323. A. Dondas and H. Benoit, *Macromolecules*, **6(2)**, 242 (1973).
324. I.W. Vanden Berg, G. Vande Ridder, and C.A. Smoldevs, *Eur, Poly.J.*, **17**, 935 (1981).
325. G. Tanaka, K.V.S.N. Raju and M. Yaseen, *J. Appl. Polym. Sci.*, **43**, 1533 (1991).
326. H. Haneczek, E. Turska, *Polymer*, **24**, 1590 (1983).
327. H.W. Chatfield, "Varnish Constituents", Leonard Hill Ltd., London, 412, 419 (1953).
328. K. Savas and K. Zuhal, *Polymer Communications*, **31(1)**, 35 (1990).
329. I. Nishio, S.T. Sun, G. Swislow and T.Tanaka, *Nature*, **281**, 208 (1979).
330. M. Bohdanecky, *J. Polym. Sci.* (B), **3**, 201 (1965).
331. B. Maitra and A.K. Nandi, *Polymer*, **34(6)**, 1260, (1993).
332. O.Chintore, M. Guaita and L. Trossarelli, *Makromol. Chem.*, **180**, 2019 (1979).
333. O. Chintore, M. Guaita, L. Trossarelli, *Makromol. Chem.*, **180**, 969, (1979).
334. M. Kurata, Y. Tsunashima, M. Iwama and K. Kamada, in : "Polymer Handbook", edited by J. Brandrup and E.H. Immergut, 2nd edition, Wiley-Interscience, New York, IV - 36, (1975).
335. J.W. Herr, and W.G. Routson, paper number SPE 5098, 49th Ann. Fall. Metting (1974).
336. W.P. Shyluk and F.S. Stow, Jr, *J. Appl.Polym. Sci.*, **13**, 1023 (1969).
337. N. Narkis and M. Rebhun, *Polymer*, **6**, 507 (1966).

338. R. Boyadjian, G. Seytre, P. Berticat and G. Vallet, *Eur. Polym. J.*, **12**, 401 (1975).
339. W. Scholtan, *Makromol. Chem.*, **14**, 169 (1954).
340. T. Schwartz, J. Sabbadin and J. Francois, *Polymer*, **22**, 609 (1981).
341. C. Okada, K. Kamada, T. Yoshihara, J. Hosoda and A. Fumuro, 'Reports on Progress in Polymer Phymer physics in Japan', XX5, (1977).
342. N. Yamaguchi, N. Onda and Y. Hirai, 'Reports on Progress in Polymer Physics in Japan', XXI, 63, (1978).
343. S.R. Gooda and M.B. Huglin, *Polymer*, **34(9)**, 1913 (1993).
344. M. Bohdanecky, V. Petrus and B. Sadlacek, *Makromol. Chem.*, **184(10)**, 2061 (1983).
345. S. Newman, W.R. Krigbaum, C. Laugier and P.J.Flory, *J.Polym.Sci.*, **14**, 451(1954).
346. G.S. Misra and S.H. Bhattacharya, *Eur. Polym. J.*, **15**, 125 (1979).
347. A. Dondos, P. Rempp and H. Benoit, *J. Polym. Sci.*, **C30**, 9 (1970).
348. A. Dondos and H. Benoit, *Macromolecules*, **4**, 279 (1971).
349. I. Katima and M.T. Garay, *Eur. Polym., J.* **21**, 489 (1985).
350. A.J. Hopdintwe, 'Intermolecular Interactions and Biomolecular Organisation', Wiley, New York, (1977).
351. P. J. Flory, 'Statistical Mechanics of Chain Molecules', Interscience Publishers, New York, Ch. 2 (1969).
352. Y. Izumi and Y. Miyake. *Polym. J.*, **4**, 205 (1973).
353. J. Brandrup and E.H. Immergut (Eds.), 'Polymer Handbook' 3rd Edn., Wiley Interscience, New York, VII - 35 (1989).
354. J.M.G. Cowie, Cpolymers : Chemistry and Physics of Modern Materials' 2nd Edn, Blackie, Glasgow, Ch. 10 (1991).

List of Publications

1. Redox polymerization of acrylamide to high molecular weights: effect of the mineral clay montmorillonite.
   P.Bera and S. K. Saha, *Macromol. Rapid Commun.*, **18**, 261-265 (1997).
   (Based on the works incorporated in chapter 3, section 3.3 and 3.4)

2. Redox polymerization of acrylamide on aqueous montmorillonite surface: Kinetics and mechanism of enhanced chain growth.
   P. Bera and S. K. Saha, *Polymer*, **39**, 1461-1469 (1998).
   (Based on the works incorporated in chapter 3, section 3.4)

3. Selective trapping of the initiator component in the interlayer space of montmorillonite: A novel technique of controlling linear termination in aqueous acrylamide polkymerization.
   P. Bera and S. K. Saha, *Ind. J. Chem. Tech.*, **6**, 24-30 (1999).
   (Based on the works incorporated in chapter 3, section 3.3)

4. Water-soluble copolymers of acrylamide with diacetone acrylamide and N-t-butylacrylamide on aqueous montmorillonite surface: Synthesis and characterisation.
   P. Bera and S. K. Saha, *Eur. Polym. J.*, December, (1999) (in Press).
   (Based on the works incorporated in chapter 4)

5. Molecular dimension and interaction parameters of polyacrylamide in water-dimethylsulphoxide mixtures: Effect of temperature.
   P. Bera and S. K. Saha, *Eur. Polym. J.*, (communicated)
   (Based on the works incorporated in chapter 5)

6. Solid phase polymerization of acrylamide on montmorillonite surface: Kinetics and mechanism.
   P. Bera and S. K. Saha, *J. Ind. Chem. Soc.*, (communicated)
   (Based on the works in corporated in chapter 3, section 3.5)

Redox polymerization of acrylamide to high molecular weights: effect of the mineral clay montmorillonite

*P. Bera, S. K. Saha**

Department of Chemistry, University of North Bengal,
Raja Rammohunpur, PIN-734430 Dt. Darjeeling, West Bengal, India

(Received: September 25, 1996)

SUMMARY:

Polymerization of acrylamide with the redox couple Fe(III)/thiourea in the presence of the mineral clay montmorillonite has been investigated. Polyacrylamide is obtained in good yield having molecular weight (ca. 0.7 2.5 × 10^6) approximately one order of magnitude higher than without clay. Apparently, the locus of polymerization is the interlayer space of the clay.

Introduction

In view of the use of polyacrylamide as water soluble viscofier and displacement fluid in secondary oil recovery, hydrodynamic volume and intrinsic viscosity of the polymer are of fundamental importance. Redox-initiated polymerization of acrylamide often yields polymers having not so high molecular weights and intrinsic viscosities because of the fast termination process via transfer to the oxidant (viz., metal ions at higher oxidation state) of the initiating redox couple[1]. In this communication we report a method of preparing comparatively higher molecular weight polymers of acrylamide with higher intrinsic viscosity, initiated by ferric ion/thiourea (TU) redox couple in presence of montmorillonite. Montmorillonite is a 2:1 type of trimorphic layered phyllosilicate (smectite) in which the central octahedral aluminium is surrounded by two tetrahedral silica sheets[2]. It has strong sorptive properties due to the expandibility of the mineral layers and has been shown to catalyze the polymerization of some unsaturated organic compounds such as styrene and hydroxyethyl methacrylate but yet to inhibit polymer formation from other structurally related monomers such as methyl methacrylate[3]. This behaviour is believed to be due to the electron-accepting or electron-donating sites on the clay minerals. In order to check the linear termination process and to increase the degree of polymerization, we loaded the Fe(III) ions in the interlayer spaces of the mineral and successfully prepared polymers of acrylamide in presence of TU. For the purpose of comparison, same experiments were conducted with Fe(III)/TU redox initiator in absence of the mineral.

Experimental part

Acrylamide (AM, reagent grade, Fluka) and thiourea (TU, Merck) were purified as usual. Montmorrilonite (diameter <2 μm) was purified following methods described elsewhere[2,3]. Fe(III) ions were loaded onto the exchangeable sites of montmorillonite

 CCC 1022-1336/97/$02.50

(Fe(III)) up to maximum saturation (0.9 meq · g^{-1}) by shaking a known amount of the mineral with $FeCl_3$ solution for 5 h, followed by repeated centrifugation (20000 rpm) and washing with double distilled water. Polymerization reactions were carried out in aqueous solution under pure nitrogen in absence of light. Intrinsic viscosities were measured by Ubbelohde viscometer with water flow rate of 2 mL · s^{-1} at 30 °C, and the molecular weights were calculated using the Mark-Houwink relationship[4]:

$$[\eta] = 9.33 \times 10^{-3} \bar{M}^{0.75} \text{ (mL} \cdot \text{g}^{-1}\text{)}$$

Results and discussion

Tab. 1 shows the data pertaining to the initial rates of polymerization (R_p), polymer yields (X_L), intrinsic viscosities ([η]) and molecular weights ($\bar{M}_v$) of the polymers formed as functions of the concentration of Fe(III) ions, TU and monomer concentrations, pH and temperature, in the presence as well as in absence of montmorillonite. In homogeneous reaction conditions (i.e., in absence of clay mineral), R_p decreases with Fe(III) ion concentration, which is consistent with previous reports on similar redox systems and supports linear termination hypothesis by the metal ion[1,5–8]. The rate dependence on the monomer concentration could neither be related to a first-order nor a second-order reaction, and the slope of the R_p vs. [AM] plot is found to be 1.45. Referring to the literature concerned with other redox systems involving metals as oxidants, the above kinetic behaviour supports a similar polymerization mechanism as reported earlier[7]. At low concentration of TU, a first-order reaction with respect to TU is observed. On the other hand, R_p, polymer yield and polymerization mechanism are influenced to a great extent when Fe(III) ions were trapped in the interlayer spaces of montmorillonite. R_p increases linearly with Fe(III) ion concentration, with an exponent of 0.25 and 0.40 at temperatures of 50 and 70 °C, respectively, while the rate dependence on TU concentration remains the same. An appreciable "gel effect" is observed, apparently due to slower termination rates in presence of the mineral[9]. The initial rate of polymerization also increases with increasing monomer concentration. The corresponding monomer exponent is 2.3. Such a high monomer exponent is striking but not totally unusual and may be attributed to the "cage effect" where the montmorillonite microenvironment forms a potential barrier which prevents the initiating TU radicals to diffuse immediately, thus favouring their destruction by mutual recombination[10].

Above all, the polymers formed have much higher intrinsic viscosity and molecular weight than those observed in absence of montmorillonite. The [η] values of polymers formed in homogeneous solution (absence of montmorillonite) varied from 14 to 108 mL · g^{-1} (Tab. 1) under the present experimental conditions. Previous reports show that redox polymerization always displayed low intrinsic viscosities and molecular weights. Tab. 1 records highest values of [η] and $\bar{M}_v$ from each of the references. On the other hand, [η] values of polymers formed in presence of montmorillonite are found to vary from 208 to 595 mL · g^{-1} under identical experimental conditions. The [η] values also increase with increasing monomer and TU concen-

Tab. 1. Results of acrylamide (AM) polymerization with the redox couple Fe(III)/thiourea (TU) in presence and absence of montmorillonite (MO)

[Fe(III)] [a] mmol · L^{-1}	[MO] in %	[TU] mol · L^{-1}	[AM] mol · L^{-1}	pH	Temp. in °C	$R_p \times 10^3$ [b]	X_L [c] in %	$[\eta]$ [d] mL · g^{-1}	$\bar{M}_v \times 10^{-5}$
0.60	0.2	0.04	0.4	2.01	50	2.86	61	340	12.0
0.90	0.3	0.04	0.4	2.01	50	3.33	62	364	12.2
1.50	0.5	0.04	0.4	2.00	50	2.64	76	369	12.5
2.07	0.7	0.04	0.4	2.01	50	3.97	77	284	9.5
2.67	0.9	0.04	0.4	2.01	50	3.90	60	291	9.8
1.5	0.5	0.01	0.4	2.00	50	1.04	42	487	19.5
1.5	0.5	0.02	0.4	2.02	50	2.56	50	595	25.0
1.5	0.5	0.03	0.4	2.01	50	2.60	55	560	23.0
1.5	0.5	0.04	0.3	2.01	50	1.08	63	363	12.2
1.5	0.5	0.04	0.5	2.01	50	3.60	48	397	14.9
1.5	0.5	0.04	0.6	2.01	50	5.56	57	480	19.1
1.5	0.5	0.04	0.4	2.01	45	1.02	66	208	6.2
1.5	0.5	0.04	0.4	2.01	60	3.72	84	432	16.6
1.5	0.5	0.04	0.4	2.00	70	3.98	94	220	6.8
1.5	0.5	0.04	0.4	1.52	50	2.65	63	300	10.0
1.5	0.5	0.04	0.4	2.10	50	3.09	40	369	12.5
1.5	0.5	0.04	0.4	2.87	50	–	–	–	–

Tab. I. Continued

[Fe(III)] [a] mmol · L^{-1}	[MO] in %	[TU] mol · L^{-1}	[AM] mol · L^{-1}	pH	Temp. in °C	$R_p \times 10^3$ [b]	X_1 [c] in %	$[\eta]$ [d] mL · g^{-1}	$\bar{M}_v \times 10^{-5}$
1.5[e]	–	0.04	0.4	2.00	50	4.40	73	64	1.3
3.0[e]	–	0.04	0.4	2.01	50	5.60	56	73	1.5
4.0[e]	–	0.04	0.4	2.01	50	1.02	40	41	0.7
8.0[e]	–	0.04	0.4	2.01	50	2.50	26	45	0.8
1.5[e]	–	0.04	0.3	2.01	50	5.00	62	60	1.2
1.5[e]	–	0.04	0.6	2.01	50	13.00	77	108	2.6
1.5[e]	–	0.01	0.4	2.00	50	1.78	40	14	0.2
Ce(IV)/TU (ref.[5])									0.9
Mn(III)/EAA (ref.[6])								0.5	0.2
Ce(IV)/EDTA (ref.[7])								133	1.8
Ce(IV)/NTA (ref.[8])								90	1.1
Ce(IV)/NPA (ref.[1])								68	0.8
Ce(IV)/IDA (ref.[1])								73	0.9

[a] Interlayer Fe(III).
[b] Initial rate in mol · L^{-1} · s^{-1}.
[c] Yield after 4.5 h.
[d] Intrinsic viscosity.
[e] Fe(III) in solution.

trations, and increase with temperature up to 50 °C and then tend to decrease at higher temperatures. The $\overline{M}_v$ values as calculated from the viscosity data ranged from 0.7×10^6 to 2.5×10^6. Comparison of $\overline{M}_v$ with literature values is to be done carefully because previous workers used a different Mark-Houwink relation.

XRD studies showed that basal spacing of the present montmorillonite sample is 14 Å, and all the species, viz., Fe(III) ions, TU and monomers, are intercalated between the layers of the mineral without expanding the same. Polymerization increases basal spacing up to 15 Å, and glycerol treatment does not have any effect at this stage. It seems apparent that the locus of the polymerization reaction is the interlayer space of the mineral, and the position of Fe(III) ions eventually retards the linear termination process, resulting in the high degree of polymerization. ^{13}C NMR spectra confirm head-to-tail polymers with mixed tacticities in which Bernoulli statistics is followed[11].

Acknowledgement: The authors are thankful to the *C.S.I.R.*, New Delhi, for financial support.

[1] W. C. Hsu, J. F. Kuo, C. Y. Chen, *J. Polym. Sci., Part A: Polym. Chem.* **31**, 267 (1993)
[2] J. Bhattacharya, S. K. Chakravarti, S. Talapatra, S. K. Saha, S. C. Guhaniyogi, *J. Polym. Sci., Part A: Polym. Chem.* **27**, 3977 (1989)
[3] J. Bhattacharya, S. K. Saha, S. C. Guhaniyogi, *J. Polym. Sci., Part A: Polym. Chem.* **28**, 2249 (1990)
[4] J. Francois, D. Sarazin, T. Schwartz, G. Weill, *Polymer* **20**, 969 (1979)
[5] G. S. Misra, S. N. Bhattacharya, *J. Polym. Sci., Polym. Chem. Ed.* **20**, 131 (1982)
[6] T. Balakrishnan, S. Subbu, *J. Polym. Sci., Part A: Polym. Chem.* **24**, 2271 (1986)
[7] W. C. Hsu, J. F. Kuo, C. Y. Chen, *J. Polym. Sci., Part A: Polym. Chem.* **30**, 2459 (1992)
[8] W. C. Hsu, C. Y. Chen, J. F. Kuo, E. M. Wu, *Polymer* **35**, 849 (1994)
[9] J. E. McGrath, *J. Chem. Edu.* **58**, 844 (1981)
[10] J. P. Riggs, F. Rodriguez, *J. Polym. Sci., Part A-1* **5**, 3151 (1967)
[11] J. E. Lancaster, M. N. O'Connor, *J. Polym. Sci., Polym. Lett. Ed.* **20**, 547 (1982)

Polymer Vol. 39 Nos. 6–7, pp. 1461–1469, 1998

0032-3861/97/$17.00+0.00

PII: S0032-3861(97)00359-5

Redox polymerisation of acrylamide on aqueous montmorillonite surface: kinetics and mechanism of enhanced chain growth

P. Bera and S. K. Saha*
Department of Chemistry, University of North Bengal, Darjeeling 734430, India
(Received 15 August 1996; revised 25 March 1997)

Aqueous polymerisation of acrylamide by Fe(III)–thiourea redox couple has been studied in homogeneous conditions as well as by loading Fe(III) ions in the interlayer spaces of montmorillonite. A dramatic effect was observed in the latter case, resulting in a very high degree of polymerisation and yielding polymers having high intrinsic viscosity due to imposed constraint on linear termination process. The technique, in general, demonstrates a promising method of achieving high molecular weight polymers by redox initiators. Polymerisation locus was identified and propagating radicals were characterised by XRD and e.s.r., respectively. The polymers were characterised by ^{1}H and ^{13}C n.m.r. spectroscopy. Kinetics of the polymerisation reaction is investigated and the mechanism of the reaction is discussed. © 1997 Elsevier Science Ltd. All rights reserved.

(Keywords: aqueous polymerisation; acrylamide; montmorillonite)

INTRODUCTION

Ability of clay minerals to intercalate various molecules and their catalytic properties are long known. The clay–polymer interaction has found many and varied applications[1]. Interest in clay–polymer combinations stems from the use of clay minerals as fillers and reinforcers in polymer systems. All things being equal, the efficiency of a filler in improving the physico-chemical properties of a polymer system is primarily determined by the degree of its dispersion in the polymer matrix. The most effective way of achieving such compatibility is to graft a suitable polymer on to filler surface and/or to encapsulate the mineral particles with the former by polymerising monomers directly on filler surfaces[2]. Montmorillonite, a smectite clay has been shown to catalyse the polymerisation of some unsaturated organic compounds such as styrene and hydroxy ethyl methacrylate and yet to inhibit polymer formation from other structurally related monomers such as methyl methacrylate[3]. This behaviour is believed to be due to the electron accepting or electron donating sites on the clay minerals. However, it has been shown recently that montmorillonite can be used in conjunction with organic substances, viz., alchols, thioureas, etc. to polymerise methyl methacrylate in aqueous medium[3,4].

In view of increasing industrial applications of water soluble acrylamide polymers, clay minerals and their combinations in various fields including the use of polyacrylamide as water soluble viscofier in enhanced oil recovery, we undertake the present study with two major objectives: (i) to examine the catalytic activity of montmorillonite on the polymerisation of acrylamide in aqueous medium and, (ii) to prepare acrylamide polymer having large hydrodynamic volume and molecular weights by Fe(III)/thiourea redox initiator in presence of montmorillonite.

*To whom correspondence should be addressed

EXPERIMENTAL

Materials

Acrylamide (AM, reagent grade, Fluka) was purified by recrystallisation from methanol (two times) and dried in vacuum oven at 45°C overnight. Thiourea (TU, E.Merck) was used after recrystallisation three times from distilled water (m.p. 180°C). A suspension of montmorillonite (Mo) having particle size less than 2 μm (diameter) was prepared by sedimentation[3]. Free iron oxides were removed by dithionite–citrate method. Organic matters were removed following method described elsewhere[5]. H^+-montmorillonite (HM) was prepared by shaking the stock of the mineral (3% w/v) in presence of 0.5 M HCl for about 6 h followed by repeated centrifugation (20 000 rpm) and washing with double distilled water. The cation exchange capacity (CEC) of montmorillonite was determined by potentiometric titrations with standard KOH solution under nitrogen atmosphere and was found to be 0.91 meq g^{-1}. Fe(III)-montmorillonite (FeM) was prepared by shaking HM suspension (3% w/v) in presence of 0.5 M $FeCl_3$ (reagent grade) at pH 2.5 for 6 h followed by purification by repeated centrifugation and washing with distilled water until the test of Fe(III) ions in the supernatent was negative. A separate experiment on the sorption of Fe(III) on to montmorillonite shows that the maximum intake of Fe(III) ions by HM samples slightly exceeds the CEC value viz., 0.98 meq g^{-1}.

Polymerisation

Measured quantities of aqueous solutions of AM were added to known amounts of HM or FeM suspension or their various mixtures in well stoppered pyrex bottles under nitrogen atmosphere and were equilibrated at required temperature. Deaerated TU solutions were then added to these solutions and the reactions were allowed to continue for desired time span in absence of any light. Polymerisation reactions were stopped by diluting the mixture with chilled

water keeping the reaction vessels in ice bath. The mixtures were then centrifuged to remove HM/FeM. The polyacrylamide (PAM) was precipitated out by adding excess of acetone, washed repeatedly with acetone and dried in vacuum at 40°C for 48 hours. Molecular weights of the polymer were determined by viscosity measurement in aqueous 0.1 M NaCl solution using a Ubbelohde viscometer and a Mark–Houwink relationship of the type[6,7]:

$$[\eta] = 9.33 \times 10^{-3} \bar{M}^{0.75} \text{ cm}^3/\text{g}$$

E.s.r., n.m.r. and XRD measurements

E.s.r. spectra were recorded at room temperature with a Varian V4502 spectrometer using 100 kHz magnetic field modulation. Instrumental setup and technique were the same as described previously[8]. ^{1}H and ^{13}C n.m.r. spectra were recorded on a Varian XL-300 spectrometer in D_2O. Chemical shifts were measured with reference to dioxane at $\delta = 67.40$ ppm. The X-ray powder diffraction patterns of solid minerals were recorded with a Philips PW 1730 machine using Ni-filtered CuK_α radiation. X-ray generator was operated at 40 kV/20 mA.

RESULTS AND DISCUSSION

Montmorillonite possesses a layered structure and has strong sorptive properties due to expandability of the mineral layers. It is a 2:1 type or trimorphic layered phyllosilicate in which the central octahedral aluminium is surrounded by two tetrahedral silica sheets. Substitution by Fe^{2+}, Fe^{3+} or Mg^{2+} normally occurs in the octahedral position of aluminium. The isomorphous replacement of both bi and trivalent metals from the lattice position to the mineral surface may also take place slowly on standing. The mineral can accept electrons via the aluminium at the crystal edges and the transition metals, such as Fe(III), in the silicate layers. Aluminium in octahedral coordination acts as a Lewis acid if its coordination water molecules are removed by drying. On the other hand, the electron donor sites are transition metals in the reduced state. Iron in the crystal lattice of montmorillonite participates in various chemical reactions in the layered spaces. One of the examples is the well known reaction of montmorillonite with benzidine molecule to form benzidine blue in which the lattice substituted Fe(III) ions are involved[9].

Montmorillonite especially, and other clay minerals in general, give powder e.s.r. spectra containing a multiplicity of lines, which essentially fall into three zones. *Figure 1a* shows e.s.r. spectra of the present montmorillonite sample containing 0.03% and 2.14% (w/w with respect to mineral wt.) iron in exchangeable and lattice positons respectively. Signal near $g = 4.3$ due to paramagnetic Fe^{3+} cations may be attributed to cis and trans octahedral sites, having axial and rhombic symmetry. A very broad signal near $g = 2.2$ arises from exchange interactions between clusters of Fe^{3+} ions which may be present on the surfaces of the smectite as well as due to hydrated Fe^{3+} in the exchangeable sites[10]. A very small but sharp signal at $g = 2.00$ has been assigned to structural defects. *Figure 1b* shows the e.s.r. spectrum that arises from the same montmorillonite sample but pretreated with excess of TU at 50°C for 30 min under nitrogen. Significant decrease of the intensity at $g = 4.3$ signal indicates that TU reacts with lattice Fe(III) and forms non-Kramers species which are e.s.r. silent. Bhattacharya and coworkers put forward chemical and electrochemical evidences to show that isothiocarbamido radicals (I)

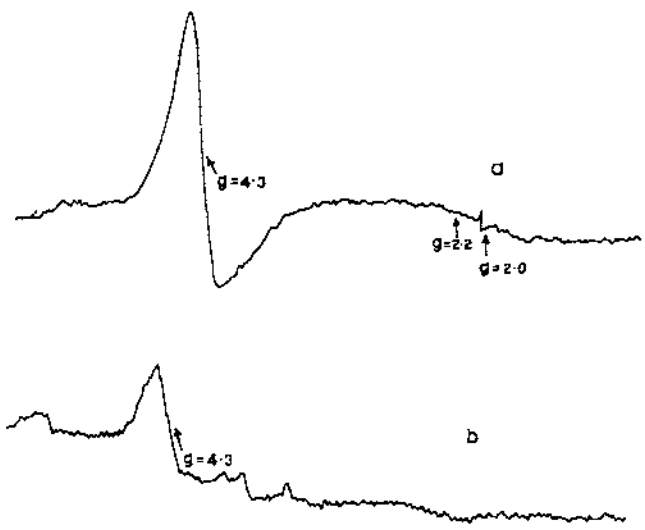

Figure 1 E.s.r. spectra of air dried powder montmorillonite sample at 20°C: (a) H^+ exchanged; (b) pretreated with thiourea at 50°C under N_2

formed in above reaction can activate radical polymerisation of methyl methacrylate in aqueous medium[11].

However, in the present study, attempts to polymerise water soluble acrylamide monomers by lattice-Fe(III)/TU combination were unsuccessful at a wide range of temperature. This is probably due to efficient inhibition of radical polymerisation of acrylamide by montmorillonite via electron transfer from initiating or propagating radicals to the Lewis acid sites. On the other hand, montmorillonite microenvironment seems to have a dramatic effect on the redox polymerisation of acrylamide by Fe(III)–TU combination. In view of the fact that redox initiated polymerisation of acrylamide often yield polymers having not so high molecular weights and intrinsic viscosities primarily because of the fast termination process via transfer to the oxidant (viz., metal ions at higher oxidation state) of the initiating redox couple, we loaded Fe(III) ions in the interlayer spaces of the mineral to control the rate of termination and examined the effect on acrylamide polymerisation in presence of TU[12]. For the purpose of comparison of the results, same experiments were duplicated as controls with Fe(III)/TU redox initiator in absence of the mineral. *Figure 2* shows that the conversion efficiencies are increased dramatically when the Fe(III) ions are loaded in the layered spaces of montmorillonite. Fe(III)/TU redox couple brings about 40% conversion at 45°C (in the absence of any montmorillonite), which is increased slightly with temperature when 4.0×10^{-3} mol l^{-1} $FeCl_3$ is used (TU = 0.04 mol l^{-1}) at pH 2.01. However, 94% conversion is observed for the same concentration of Fe(III) ion when loaded in the interlayer space of montmorillonite ($\overline{Fe}$(III)) under identical conditions (concentration of $\overline{Fe}$(III) being moles of interlayer metal ions per 1000 mL of the reaction mixture). No induction period is observed, however, in either case. At lower $FeCl_3$ concentrations, polymer yield (X_L) as well as the initial rate of reaction (R_p) were increased substantially, indicating slower termination rates in the absence of any mineral clay. On the other hand, in the presence of mineral microenvironment, the initial rate of polymerisation was increased from 2.83×10^{-3} to 3.97×10^{-3} mol l^{-1} min^{-1} as the $\overline{Fe}$(III) concentration increased from 0.60×10^{-3} to 2.07×10^{-3} mol l^{-1}. At a higher concentration of $\overline{Fe}$(III), however, R_p tends to decrease due to transfer to ferric ions. Conversion

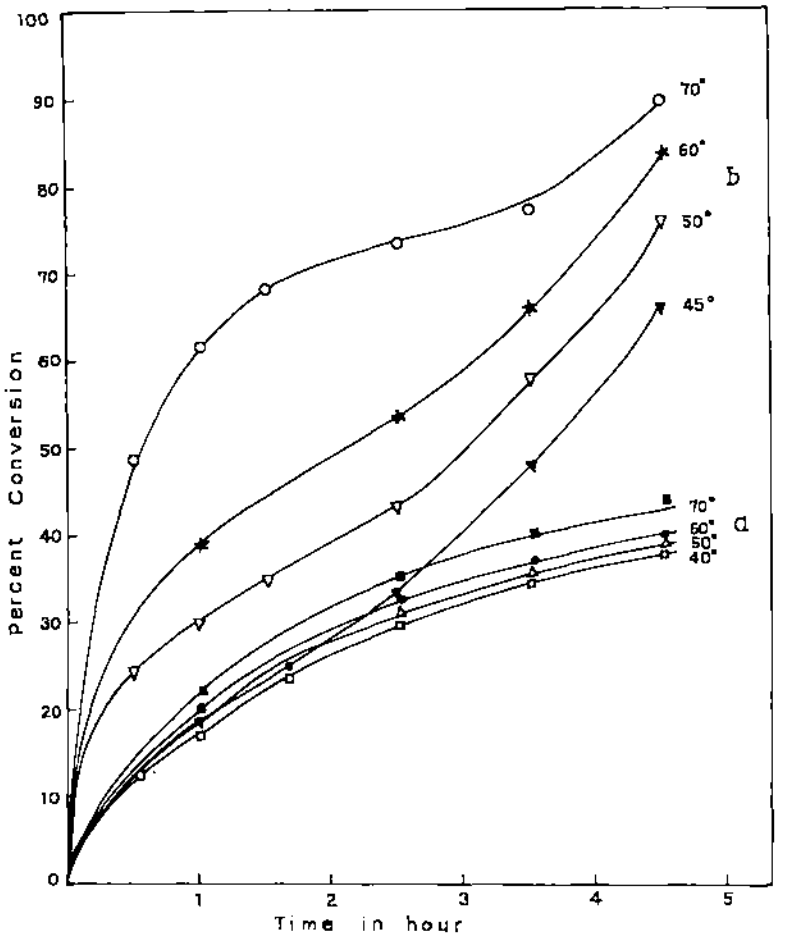

Figure 2 The effect of Fe(III) loading in montmorillonite on the course of polymerisation at various temperatures: (a) [Fe(III)] = 0.004 mol l^{-1}, [Mo] = 0, [TU] = 0.04 mol l^{-1}, [AM] = 0.4 mol l^{-1}, pH 2.01; (b) [Fe(III)] = 0.004 mol l^{-1}, [Mo] = 1.4%, [TU] = 0.04 mol l^{-1}, [AM] = 0.4 mol l^{-1}

efficiencies were also increased regularly with increasing Fe(III) ion concentration up to 2.07×10^{-3} mol l^{-1}. Although R_p and the yield decreased with decreasing TU concentrations, molecular weight of the polymer was higher at lower TU concentrations. Moreover, significant 'gel-effect' was observed in the presence of clay mineral apparently due to decrease in termination rates as mentioned above as well as for comparatively higher viscosity of the medium[13]. 'Gel-effect' was more prominent at lower temparatures than at 70°C. *Table 1* represents the data pertaining to the initial rates of polymerisation (R_p), polymer yeild (X_1), intrinsic viscosity (η) and molecular weight ($\bar{M}_v$) of the polymers formed as functions of the concentration of Fe(III), TU, AM, pH and temperature in the presence as well as in the absence of montmorillonite. The most significant observation of loading Fe(III) ions of the initiating redox couple in the interlayer spaces of montmorillonite is achieving polymers with much higher intrinsic viscosity and molecular weight. The η value of the polymer formed in homogeneous solution and in the absence of the mineral varied from 14 to 90 ml g^{-1} (*Table 1*) under the present experimental condition. Previous reports showed that redox polymerisation always displayed low intrinsic viscosities and molecular weights as are depicted in *Table 2* (which records the highest values of η and $\bar{M}_v$ from each of the References [12,14–17]). On the other hand, η values displayed by polymers formed in presence of montmorillonite were found to vary from 247 to 600 ml g^{-1} under identical experimental conditions. The η is also increased with increasing monomer and TU concentrations while it is increased with temperature up to 50°C but decreased at higher temperatures. The $\bar{M}_v$ values as calculated from viscosity data of present experiments ranged from 0.62×10^6 to 2.5×10^6. However, comparison of $\bar{M}_v$ with literature values should be done carefully because previous workers applied a different Mark–Houwnik equation. The significant role played by montmorillonite probably stems from two factors: (i) polymer initiation in the mineral microenvironment is favoured and (ii) rate of linear termination process decreases significantly because transfer to Fe(III) ions is highly restricted for the latter's location in the layered spaces of the mineral and diffusion of the living radical through montmorillonite gel is rather slow. In general, loading of the oxidant, i.e. metal ions, of the redox couple in the interlayer space of clay minerals, i.e. montmorillonite, offers a potential method of achieving very high degree of polymerisation for a redox initiated reactions.

Generation of primary and propagating free radicals

Previous studies showed that polymerisation of various

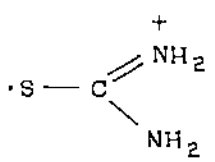

(I)

Table 1 The initial rates of polymerisation, polymer yields, intrinsic viscosities and the molecular weights of Fe(III)–TU initiated polymerisation in the presence and absence of montmorillonite at various conditions

Temp. (°C)	pH	[Mo][a] (g l^{-1})	[$\overline{Fe}$(III)][b] (mmol l^{-1})	[TU] (mol l^{-1})	[AM] (mol l^{-1})	$R_p \times 10^3$ (mol l^{-1} m^{-1})	X_L[c] (%)	η (ml g^{-1})	$\bar{M}_v$ ($\times 10^{-5}$)
		2.0	0.60			2.86	61	340	12.0
		3.0	0.90			3.33	62	364	12.2
50	2.01	5.0	1.50	0.04	0.40	2.64	76	369	12.5
		7.0	2.07			3.97	77	284	9.5
		9.0	2.67			3.90	60	291	9.8
				0.01		1.04	42	487	19.5
50	2.01	5.0	1.50	0.02	0.40	2.56	50	595	25.0
				0.03		2.60	55	560	23.0
					0.30	1.08	63	363	12.2
50	2.01	5.0	1.50	0.04	0.50	3.60	48	397	14.9
					0.60	5.56	57	480	19.1
45						1.02	66	208	6.2
60	2.01	5.0	1.50	0.04	0.40	3.72	84	432	16.6
70						3.98	94	220	6.8
	1.52					2.65	63	300	10.0
50	2.10	5.0	1.50	0.04	0.40	3.09	40	369	12.5
	2.87					–[d]	–	–	–
			0.38 (0.008)			1.23	36	290	9.8
50	2.01	5.0	0.75 (0.015)	0.04	0.40	1.99	43	360	13.0
			1.13 (0.023)			2.22	45	355	12.8
			1.50[e]			4.40	73	64	1.3
50	2.01		3.00[e]	0.04	0.40	5.60	56	73	1.5
			4.00[e]			1.02	40	61	0.7
			8.00[e]			2.50	26	45	0.8
				0.04	0.30	5.0	62	60	1.2
50	2.01		1.5[f]	0.04	0.60	13.00	77	108	2.6
				0.01	0.40	1.78	40	14	0.2

[a]Montmorillonite content
[b]Concentration of interlayer Fe(III) in mmol l^{-1} of the reaction mixture; corresponding concentrations in montmorillonite gel phase is 0.03 mol l^{-1} throughout, except those shown in brackets
[c]Yield after 4.5 hrs. [d]No polymer formed. [e]Concentration of $FeCl_3$ in solution

Figure 3 E.s.r. spectrum of MNP–PAM spin adduct

water insoluble vinyl monomers initiated by redox couples involving TU as the reductant, involved isothiocarbamido primary free radicals (I) in aqueous acid solution[11].

Owing to high 'g' anisotropy and a very short relaxation time, detection of this radical by e.s.r. spectroscopy was not possible until recently, when e.s.r. study of spin adducts of the radical was reported[8]. In the present system also it is believed that the same primary radical (I) is formed and the propagating radicals from acrylamide are trapped by methyl nitroso propane (MNP) spin trap. *Figure 3* shows the e.s.r. spectrum of the MNP spin adduct of the radical (II)

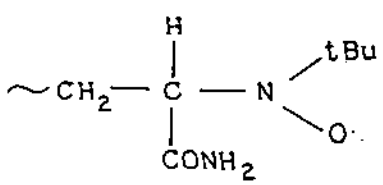

(II)

Table 2 Intrinsic viscosities and molecular weights of acrylamide polymers formed by different redox couples

Initiating system	η (ml g^{-1})	$\bar{M}_v$ ($\times 10^{-5}$)
Ce(IV)–thiourea[14]	–	0.9
Mn(III)–ethoxyacetic acid[15]	0.5	0.2
Ce(IV)–ethylenediamine tetraacetic acid[16]	133	1.8
Ce(IV)–nitrilotriacetic acid[17]	90	1.1
Ce(IV)–nitrilotripropionic acid[12]	68	0.8
Ce(IV)–iminodiacetic acid[12]	73	0.9

The spectrum depicts a 1:1:1 triplet of doublets. The triplet is undoubtedly originated from the nitroxide radical (a_N = 1.45 mT) of MNP and the doublets are generated from H^β splitting (a_H = 0.31 mT). The isothiocarbamido radicals (I) are, however, not trapped by MNP under present condition.

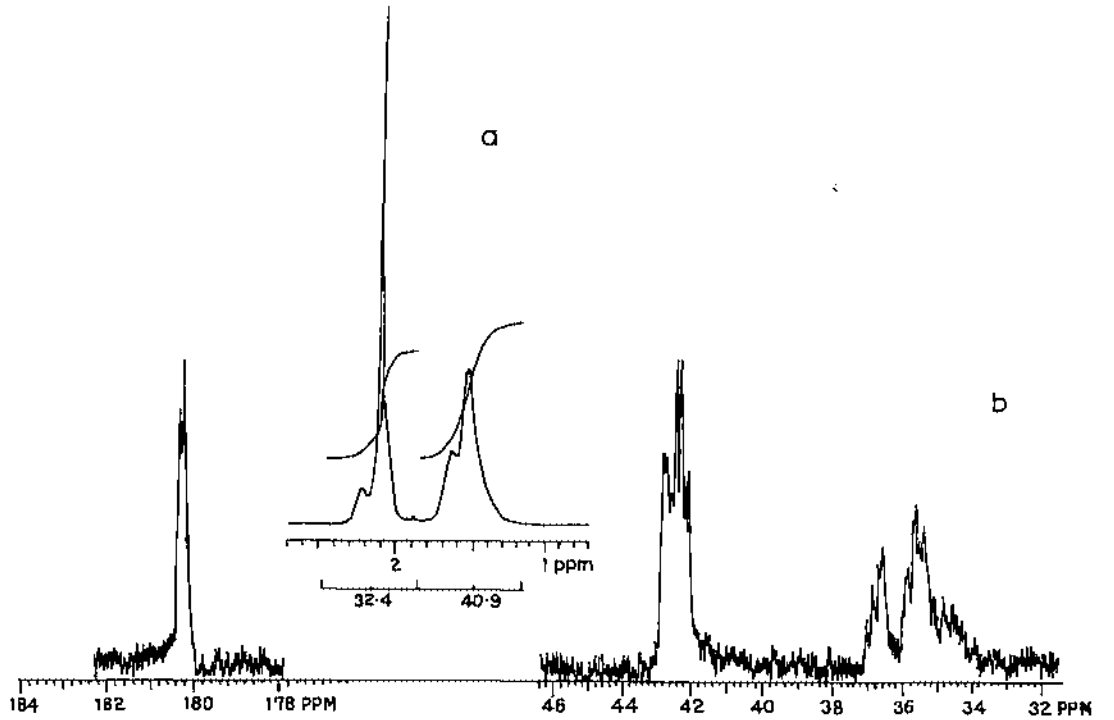

Figure 4 ^{1}H and ^{13}C n.m.r. spectra of thiourea terminated polyacrylamide formed on montmorillonite surfaces: (a) ^{1}H n.m.r. spectrum; (b) ^{13}C n.m.r. spectrum

XRD measurement

Unoriented powder samples of montmorillonite (H^+ and Fe(III) exchanged) before and after polymerisation reaction showed XRD patterns consistent with published results[10]. After the polymerisation reaction, the intensity of peak at $2\theta = 6.25°$ became much lower because of the presence of templates of polymer materials in the interlayer space. On the other hand, intensity of the peak at $2\theta = 9.5$–9.8 is increased due to polymerisation as well as glycerol treatment. Basal spacing of the H^+ and Fe(III) exchanged minerals is increased from 14 to 17 Å due to glycerol treatment for both TU treated and untreated samples. On the other hand, polymerisation increases basal spacing from 14 to 15 Å. Glycerol does not affect basal spacing at this stage. Foregoing results indicate that Fe(III) ions, TU and monomers all are intercalated between layers of the mineral without expanding the same and the locus of the polymerisation reaction is the interlayer spaces of the mineral. The location of Fe(III) ions in the interlayer space eventually retard the termination process, resulting in the higher degree of polymerisation.

^{1}H and ^{13}C n.m.r. spectra of PAM

^{1}H n.m.r. spectrum of PAM is not usually an well resolved spectrum and no special feature is apparent in present spectrum (*Figure 4a*) except that of overlapping of a sharp line with chemical shift of 2.12 ppm near the $-CHCONH_2$ position. This line in all probability represents the hydrogens from the isothiocarbamido end groups of thiourea terminated PAM. The expanded ^{13}C n.m.r. spectrum (*Figure 4b*) showed methylene, methine and carbonyl carbons of head-to-tail polymer of AM. No monomeric acrylamide was seen indicating purity of the polymer sample. The carbonyl carbon (at 180.2 ppm) splittings were small and not as readily interpreted as backbone carbon absorptions. The methine resonance

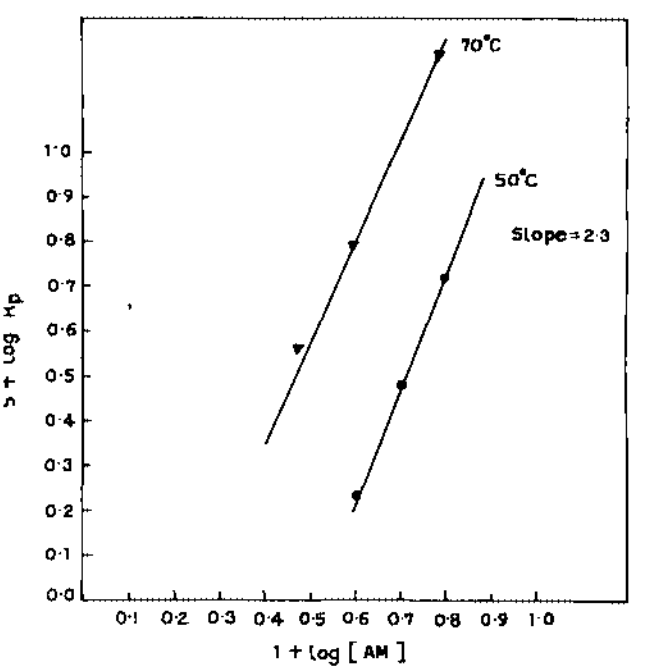

Figure 5 Logarithm plot of R_p *versus* [AM]: [Fe(III)] = 0.0015 mol l^{-1}, [TU] = 0.04 mol l^{-1}

(42.2–43.5 ppm) is a triplet (triad sensitivity) which is further split, showing pentade sensitivity. The low field and high field triplet peaks are assigned to rr (syndiotactic) and mm (isotactic) sequences, respectively. The central peak corresponds to heterotactic sequences (mr + rm). The methylene carbon lines (34–37.4 ppm) fall into three fairly well separated groups with almost all the 20 lines required by hexad sensitivity resolved. The resemblance of the

spectrum to those obtained by Lancaster and Coworker suggests that Bernoulli statistics are followed, which is common in vinyl polymers[20].

Kinetics and mechanism. In homogeneous reaction condition (i.e., in the absence of any clay mineral) R_p is decreased with increased Fe(III) ion concentrations (*Table 1*), which is consistent with previous reports on similar redox systems and supports linear termination hypothesis by the metal ions[12,14–17]. The rate dependence on the monomer (M) concentrations could be related to neither a first order nor a second order reaction and the slope of the logarithm plot of R_p *versus* [AM] was found to be 1.45 (not shown in figure). Referring to the literature concerned with other redox systems involving metals as oxidants, the above kinetic behaviour predicts a polymerisation mechanism similar to that reported earlier[16]. The variation of the initial rate of polymerisation as a function of monomer concentration in the presence of montmorillonite is shown in *Figure 5*. Not all the points fell on a linear line. If it is assumed to be linear, the slope could be estimated as about 2.3. (The proposed mechanism, however, predicts an exponent of 2.0, the error in the experimental data may be introduced from the inherent coarseness in following the kinetics of a heterogeneous system.) The significant change in the monomer exponent due to the occurrence of the reaction on the montmorillonite surface indicates that the polymerisation mechanism is greatly affected by the mineral microenvironment. A rate dependence of second order and above on monomer concentration was also observed earlier in heterogeneous and precipitation polymerisation of acrylamide and various interpretations, including 'cage effect' and 'complex theory', were proposed to account for the significant departure from first order kinetics[18,19]. The 'cage effect' suggests that when an initiator decomposes into two radicals, there is a formation of a potential barrier by the surrounding solvent molecules which prevent their immediate diffusion and favours their destruction by mutual recombination. The 'complex theory' is based on the formation of a complex between the initiator and the monomer, the rate of initiation then being determined by the rate of decomposition of the complex. The 'cage effect' seems to be a good conceptual starting point in explaining the high monomer exponent which has been observed in the present system. To examine the dependence of rate on the montmorillonite content and Fe(III) concentrations, the initial rate of polymerisation is plotted as a function of $\overline{Fe}$(III) ion concentration (*Figure 6*), R_p is increased with the montmorillonite and Fe(III) contents of the reaction mixture but the slope of logarithm plot varied from 0.25 to 0.40 as a result of raising the reaction temperature from 50 to 70°C. However, if the locus of polymerisation is assumed to be the interlayer space of montmorillonite, above slopes can not be regarded as metal ion exponents because increasing addition of Fe(III)-saturated mineral does not increase Fe(III) ion concentration in the mineral phase but, on the contrary, only

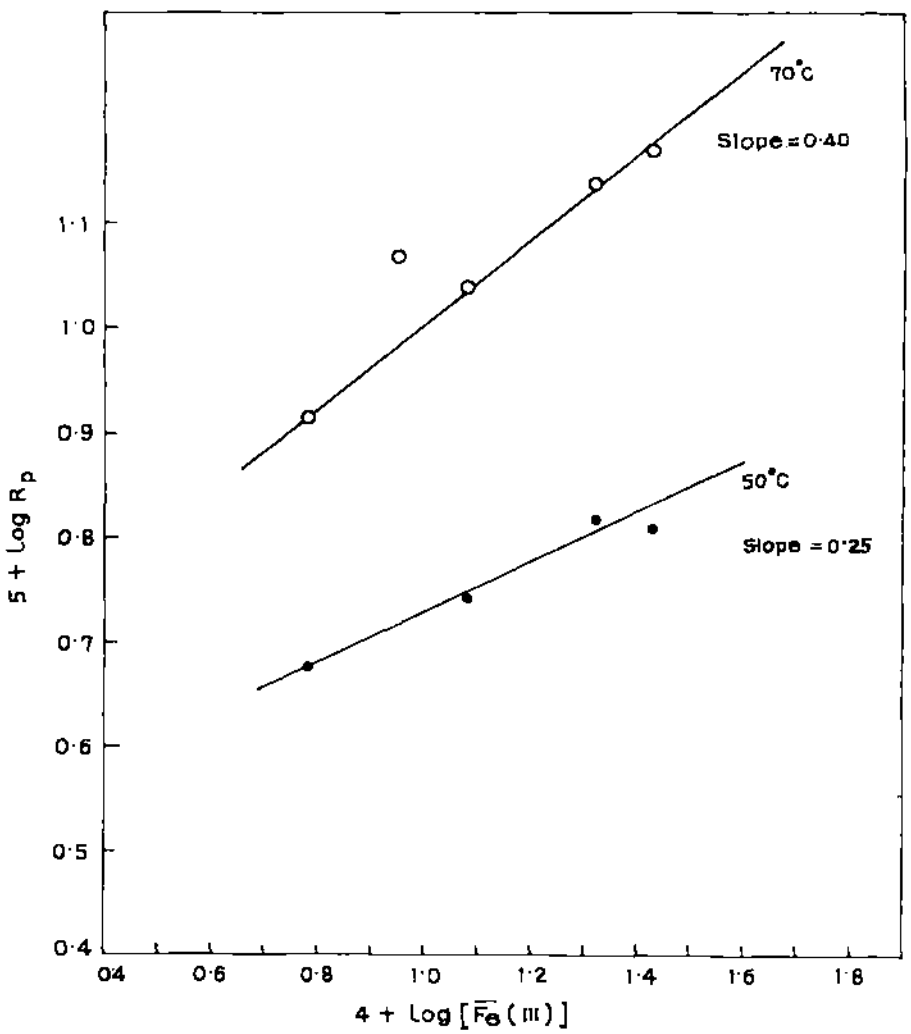

Figure 6 Logarithm plot of R_p *versus* [Fe(III)]: [AM] = 0.4 mol l^{-1}, [TU] = 0.04 mol l^{-1}, [Mo] = 0.5%

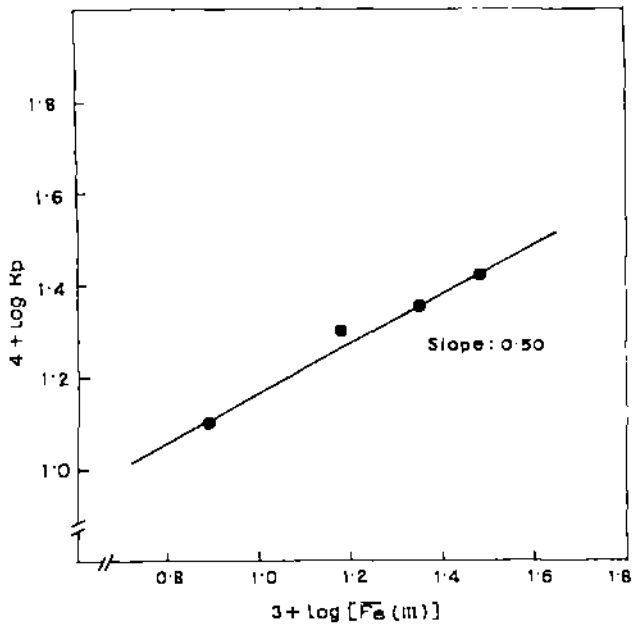

Figure 7 Logarithm plot of R_p *versus* [$\overline{Fe}$(III)]: [AM] = 0.4 mol l^{-1}, [TU] = 0.04 mol l^{-1}, [Mo] = 0.5% ([Fe(III)] in this figure represents moles of ferric ions in the montmorillonite gel phase)

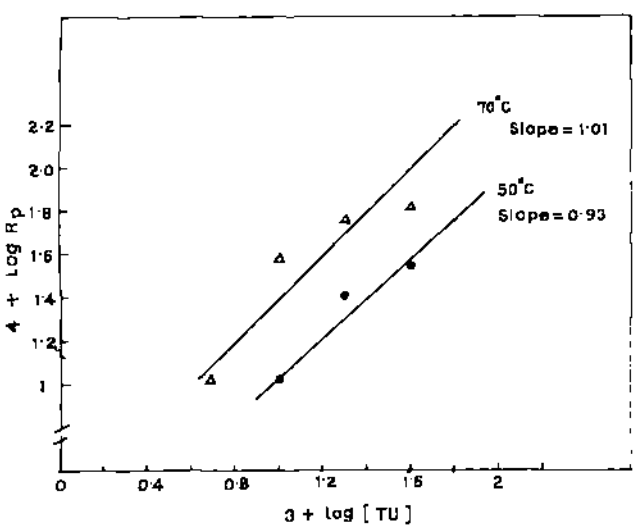

Figure 8 Logarithm plot of R_p *versus* [TU]: [Fe(III)] = 0.0015 mol l^{-1}, [AM] = 0.4 mol l^{-1}, [Mo] = 0.5%

adds to the total metal ion and adsorbent contents of the reaction mixture. This in turn increases monomer and TU contents of the intercalate position, which result in the high rates of polymer yield. In order to measure the actual metal exponent for the reaction in the mineral phase, R_p values were plotted as a function of Fe(III) ion concentration in the montmorillonite gel. The concentrations of Fe(III) in the montmorillonite gel were varied by adding calculated quantities of HM in the reaction mixture. The slope of such a logarithm plot (*Figure 7*) has been estimated as 0.50 at 50°C. (The concentration of Fe(III) now being moles of interlayer Fe(III) ions per 1000 mL montmorillonite gel; the water content of montmorillonite sample was measured following the method described by Marinsky and co-workers and found to be 10 ml g^{-1})[21]. *Figure 8* shows the dependence of R_p on TU concentrations. Since the isothiocarbamido primary radicals (I) have strong tendency to dimerise above 0.05 mol l^{-1}, the present study was confined below that concentration only[8]. Again, not all the points fell on a linear line (in the logarithm plot) owing to the heterogeneous reaction mixture. However, the slopes of the average lines drawn through the points at two different temperatures indicate that the reaction is first order with respect to TU concentrations. To rationalise the above experimental results and to predict a possible mechanism for the seemingly complex polymerisation reaction occurring in the mineral microenvironment, the following assumptions are made[12,22].

(1) Intercalated TU reacts fast with the Fe(III) ions of montmorillonite layered spaces to form the reactive TU (isothiocarbamido (I)) radicals via an intermediate complex. The decomposition of the complex is the rate-controlling step.

(2) In the acidic and metal ion exchanged aqueous montmorillonite system, a fraction of the intercalated acrylamide molecules are present near reacting sites as pairs either through hemisalts formation, where two amide molecules share a proton by means of symmetrical hydrogen bond or/and through weak coordination to the exchanged cations[2]. The protonated as well as the complexed amide pairs are at fast equilibrium with unprotonated and free amide molecules, respectively, which are defined by a protonation constant or a formation constant. In view of high monomer exponent, it is certain that it must have resulted in part from the involvement of monomer in the initiation step, where such monomer pairs are entailed.

(3) Since the reactive TU radicals are formed as pairs, assumption of the 'cage effect' seems to be conceptually appropriate. The initiation step involves collision of the 'amide pairs' with caged TU radicals at the wall of the cage and random diffusion of the radicals from the cage and their secondary recombination are less significant in comparison with the rate of dimerisation of caged radicals or their reaction with acrylamide.

Initiation

$$\overline{Fe}(III) + TU \overset{K}{\rightleftharpoons} \underset{Complex}{\overline{Fe}(III) - TU} \tag{1}$$

$$\overline{Fe}(III) - TU + TU \xrightarrow{k_i} \overline{Fe}(II) + (2TU^{\cdot}) + H^+ \tag{2}$$

$$(TU^{\cdot}) + M_2H^+ \xrightarrow{k_i} M_1^{\cdot} + M + H^+ \tag{3}$$

Propagation

$$M_1^{\cdot} + M \xrightarrow{k_p} M_2^{\cdot}$$

$$M_{n-1}^{\cdot} + M \xrightarrow{k_p} M_n^{\cdot} \ldots \text{etc.} \tag{4}$$

Termination

$$M_n^{\cdot} + M_n^{\cdot} \xrightarrow{k_t} M_n - M_n \tag{5}$$

$$(TU^{\cdot}) + \overline{Fe}(III) \xrightarrow{k_t'} TU + \overline{Fe}(II) \tag{6}$$

$$(2TU^{\cdot}) \xrightarrow{k_t''} TU - TU \tag{7}$$

(caged species are enclosed in brackets)

Using the above scheme and the pseudo-steady-state assumption, we derive the rate expressions as follows:

$$\frac{-\mathrm{d}[\overline{\mathrm{Fe}}(\mathrm{III})]}{\mathrm{d}t} = \frac{k_\mathrm{d}K[\mathrm{TU}]^2[\overline{\mathrm{Fe}}(\mathrm{III})]}{1+K[\mathrm{TU}]} \tag{8}$$

$$R_\mathrm{p} = \frac{(k_\mathrm{d}k_\mathrm{i}KK')^{1/2}k_\mathrm{p}[\overline{\mathrm{Fe}}(\mathrm{III})]^{1/2}[\mathrm{TU}][\mathrm{M}]^2}{k_\mathrm{t}^{1/2}(k_\mathrm{i}K'[\mathrm{M}]^2 + k_\mathrm{i}KK'[\mathrm{M}]^2[\mathrm{TU}] + k_\mathrm{t}'[\overline{\mathrm{Fe}}(\mathrm{III})] + k_\mathrm{t}''(1+K[\mathrm{TU}]))^{1/2}} \tag{9}$$

(K' ($= [\mathrm{M_2H^+}]/[\mathrm{M}]^2$) is the apparent protonation constant at a fixed pH (or a formation constant))

If the oxidative termination (step 6) is assumed to be insignificant in comparison with the dimerisation rate of caged radicals, equation (9) reduces to:

$$R_\mathrm{p} = \frac{(k_\mathrm{d}k_\mathrm{i}KK')^{1/2}k_\mathrm{p}[\overline{\mathrm{Fe}}(\mathrm{III})]^{1/2}[\mathrm{TU}][\mathrm{M}]^2}{k_\mathrm{t}^{1/2}(k_\mathrm{i}K'[\mathrm{M}]^2 + k_\mathrm{i}KK'[\mathrm{M}]^2[\mathrm{TU}] + k_\mathrm{t}''(1+K[\mathrm{TU}]))^{1/2}} \tag{10}$$

The interpretation of high kinetic order of the monomer finally hinges on the dominance of a reaction between caged radicals and those of monomers with the radicals at the cage wall. Although the concentrations of the monomer and TU in solution phase were fixed mostly at 0.40 mol l^{-1} and 0.04 mol l^{-1} respectively, the concentrations of intercalated species must be much lower, specially due to the presence of water molecules in the interlayer spaces.

Thus, while the concentrations, [M] and [TU], in the montmorillonite gel-phase should be

$$[\mathrm{M}] = L_\mathrm{o}^\mathrm{a}\theta_\mathrm{m} = \frac{L_\mathrm{o}^\mathrm{a}K_\mathrm{m}^\mathrm{a}[\mathrm{M}]_\mathrm{s}}{1+K_\mathrm{tu}^\mathrm{a}[\mathrm{TU}]_\mathrm{s}+K_\mathrm{m}^\mathrm{a}[\mathrm{M}]_\mathrm{s}} \tag{11}$$

and,

$$[\mathrm{TU}] = L_\mathrm{o}^\mathrm{a}\theta_\mathrm{tu} = \frac{L_\mathrm{o}^\mathrm{a}K_\mathrm{tu}^\mathrm{a}[\mathrm{TU}]_\mathrm{s}}{1+K_\mathrm{tu}^\mathrm{a}[\mathrm{TU}]_\mathrm{s}+K_\mathrm{m}^\mathrm{a}[\mathrm{M}]_\mathrm{s}} \tag{12}$$

(subscript 's' denotes solution)

(L_o^a and θ are the total active sites in unit mass of montmorillonite and the fraction of total sites occupied by each species respectively; K_m^a and K_tu^a are selectivity coefficients)

the denominators of equations (11) and (12) are nearly unity. By appropriate substitution of [M] and [TU] in equation (10) and considering the dominance of the last term of the denominator over others, the equation becomes

$$R_\mathrm{p} = \frac{k_\mathrm{p}(k_\mathrm{d}k_\mathrm{i}KK'/k_\mathrm{t}k_\mathrm{t}'')^{1/2}K_\mathrm{tu}^\mathrm{a}(K_\mathrm{m}^\mathrm{a})^2(L_\mathrm{o}^\mathrm{a})^3[\overline{\mathrm{Fe}}(\mathrm{III})]^{1/2}[\mathrm{TU}]_\mathrm{s}[\mathrm{M}]_\mathrm{s}^2}{(1+KL_\mathrm{o}^\mathrm{a}K_\mathrm{tu}^\mathrm{a}[\mathrm{TU}]_\mathrm{s})^{1/2}} \tag{13}$$

(Values of K_m^a (or K_tu^a), L_o^a and K are of the order of 10^{-2}, 2 mmol g^{-1} and 2 l mol^{-1}, respectively[22,23]. Small values of above parameters including that of K', ensure that terms involving quadratic and above concentrations are very small in the present conditions[24,25]).

Further inspection of equation (13) shows that the value of $KL_\mathrm{o}^\mathrm{a}K_\mathrm{tu}^\mathrm{a}$ $[\mathrm{TU}]_\mathrm{s}$ in the denominator varies from 10^{-5} to 10^{-6} for the variation of aqueous TU concentration from 0.05 to 0.005 mol l^{-1}. This implies that the rate equation under the present condition is reduced to

$$R_\mathrm{p} = k_\mathrm{p}(k_\mathrm{d}k_\mathrm{i}KK'/k_\mathrm{t}k_\mathrm{t}'')^{1/2}K_\mathrm{tu}^\mathrm{a}(K_\mathrm{m}^\mathrm{a})^2(L_\mathrm{o}^\mathrm{a})^3[\overline{\mathrm{Fe}}(\mathrm{III})]^{1/2}[\mathrm{TU}]_\mathrm{s}[\mathrm{M}]_\mathrm{s}^2 \tag{14}$$

Reviewing the above result, we find that equation (14) could satisfactorily account for the present behaviour of the $\overline{\mathrm{Fe}}$(III)–TU initialised acrylamide polymerisation exhibited in the aqueous montmorillonite layered space.

CONCLUSIONS

Aqueous polymerisation of acrylamide by Fe(III)–thiourea redox couple shows kinetic behaviour and mechanism similar to those of other redox initiated polymerisations of acrylamide. On the other hand, polymerisation initiated by the same redox couple but by loading Fe(III) ions in the interlayer spaces of montmorillonite influences the kinetics as well as the mechanism to a great extent. The latter technique increases the degree of polymerisation and the intrinsic viscosity of the polymers dramatically by decreasing the rate of linear termination process. The method was demonstrated to be a promising technique of achieving high molecular weight polymers for redox initiated reactions, where low molecular weight polymers are often displayed. The maximum values of $\bar{M}_\mathrm{v}$ were found to be 2.6×10^5 and 2.5×10^6 in the absence and presence of montmorillonite respectively, while η values increased from 108 to 595 ml g^{-1} due to the presence of the mineral under identical condition. E.s.r. study confirms that lattice substituted Fe(III) in montmorillonite reacts with thiourea but the reaction failed to initiate polymerisation of acrylamide in water. The locus of the polymerisation was identified by XRD as the interlayer space of the mineral while, the propagating radicals were characterised by spin-trapping technique. The hyperfine splitting parameters a_N and a_H^β for the MNP adduct are 1.45 and 0.31 mT respectively. The polymers, characterised by ^{1}H and ^{13}C n.m.r., were mostly thiourea terminated head-to-tail polymers with mixed tacticities where Bernoulli statistics were followed. The kinetics study showed the monomer, TU and the metal ion exponents to be 2.0, 1.0, and 0.5 respectively, which have been explained by means of a radical mechanism involving 'cage effect' on the initiating TU radical pairs. In view of the presence of acrylamide molecules as hemisalts where two amide molecules share a proton through a symmetrical hydrogen bond in the acidic montmorillonite layered space, the initiation step probably involves collision of caged TU radicals with the monomer pairs at the cage wall.

ACKNOWLEDGEMENTS

Authors are thankful to CSIR, New Delhi for financial support.

REFERENCES

1. Theng, B. K. G., *Clay and Clay Minerals*, 1982, **30**, 1.

2. Theng, B. K. G., *The Chemistry of Clay-organic Reactions*, 1974, Adam-Hilger, London.
3. Bhattacharya, J., Chakravarti, S. K., Talapatra, S., Saha, S. K. and Guhaniyogi, S. C., *Journal of Polymer Science, Part A: Polymer Chemistry*, 1989, **27**, 3977.
4. Talapatra, S., Saha, S. K., Chakravarti, S. K. and Guhaniyogi, S. C., *Polymer Bulletin*, 1983, **10**, 21.
5. Jackson, M. L., *Soil Chemical Analysis*, 1973, Prentice Hall of India(P) Ltd., New Delhi.
6. François, J., Sarazin, D., Schwartz, T. and Weill, G., *Polymer*, 1979, **20**, 969.
7. Candau, F., Leong, Y. S., Pouyet, G. and Candau, S., *Journal of Colloid and Interface Science*, 1984, **101**, 167.
8. Saha, S. K. and Greenslade, D. J., *Bulletin of the Chemical Society of Japan*, 1992, **65**, 2720.
9. Solomon, D. H., Loft, B. C. and Swift, J. C., *Clay Minerals*, 1968, **7**, 389.
10. Fripiat, J. J., *Development in Sedimentology*, 1982, Elsevier, New York.
11. Bhattacharya, J., Saha, S. K. and Guhaniyogi, S. C., *Journal of Polymer Science, Part A: Polymer Chemistry*, 1990, **28**, 2249.
12. Hsu, W. C., Kuo, J. F. and Chen, C. Y., *Journal of Polymer Science, Part A: Polymer Chemistry*, 1993, **31**, 267.
13. McGrath, J. E., *Journal of Chemical Education*, 1981, **58**, 844.
14. Misra, G. S. and Bhattacharya, S. N., *Journal of Polymer Science, Polymer Chemistry Edition*, 1982, **20**, 131.
15. Balakrishnan, T. and Subbu, S., *Journal of Polymer Science, Part A: Polymer Chemistry*, 1986, **24**, 2271.
16. Hsu, W. C., Kuo, J. F. and Chen, C. Y., *Journal of Polymer Science, Part A: Polymer Chemistry*, 1992, **30**, 2459.
17. Hsu, W. C., Chen, C. Y., Kuo, J. F. and Wu, E. M., *Polymer*, 1994, **35**, 849.
18. Tai, E. F., Caskey, J. A. and Allison, B. D., *Journal of Polymer Science, Part A: Polymer Chemistry*, 1986, **24**, 567.
19. Riggs, J. P. and Rodriguez, F., *Journal of Polymer Science, Part A1*, 1967, **5**, 3151.
20. Lancaster, J. E. and O'Connor, M. N., *Journal of Polymer Science, Polymer Letters*, 1982, **20**, 547.
21. Marinsky, J. A., Lin, F. G. and Chung, K. S., *Journal of Physical Chemistry*, 1983, **87**, 3139.
22. Pustelnik, N. and Soloniewiez, R., *Chemia Analityczna (Warsaw)*, 1976, **21**, 503.
23. Bera, P. and Saha, S. K., unpublished results.
24. Perrin, D. D., *Organic Ligands: IUPAC Chemical Data Series (No. 22)*, 1983, Pergamon Press, New York.
25. Martell, A. E. and Smith, R. M., *Critical Stability Constant*, Vol. 3, 1979, Plenum Press, New York.

Indian Journal of Chemical Technology
Vol. 6, January 1999, pp. 24-30

Selective trapping of initiator component in the interlayer space of montmorillonite : A novel technique of controlling linear termination in aqueous acrylamide polymerisation

P Bera & S K Saha

Department of Chemistry, University of North Bengal, Darjeeling 734 430, India

Received 18 August 1998; accepted 11 December 1998

Kinetics and mechanism of aqueous polymerization of acrylamide by $FeCl_3$ -thiourea redox couple are investigated in homogeneous solution with a view to compare results with those observed after trapping metal oxidant in the montmorillonite layered space. The initial rate of polymerization and the intrinsic viscosity are ranged within $(0.3\text{-}2.3) \times 10^4$ mol L^{-1} s^{-1} and (14-137) mLg^{-1} respectively in the former case. Linear termination by metal oxidants is checked in the latter instance resulting in the higher chain growth of the polymers. Formation of the acrylamide pairs in the interlayer positions of acidic montmorillonite, strong 'cage effect' on the initiating thiourea radicals and the delayed termination process are identified as the major causes for the observed mechanistic modification in the montmorillonite gel phase reactions.

Polyacrylamide with high molecular weights and intrinsic viscosities have found applications as water soluble viscofier and displacement fluid in secondary oil recovery[1]. High molecular weight polyacrylamides have such other applications as effective flocculants and chemical grouts. Redox initiated polymerization of acrylamide is one of the most common techniques applied for aqueous polymeri-zation because of the simplicity of technique as well as high yield and reaction rates. Moreover, the above technique is uniquely applied for *in situ* polymerization, where aqueous solutions of the monomer together with a redox catalyst are injected into soil formation. However, one major difficulty of such a technique is the fast termination by oxidant of the redox couple. In an attempt to increase the chain length of polyacrylamide initiated by a redox couple, the potential electron acceptor of the redox couple (e.g., metal ions) is loaded into the interlayer space of montmorillonite[2,3]. This ensures the slow termination due to the inability of a growing polymer chain to transfer to the oxidant trapped inside the layered space. As a result, high molecular weight polymers were formed. However, the effect of montmorillonite micro-environment in the above polymerization was not confined to the lowering of termination rates only but, it affected the mechanism of the reaction also to a great extent. In order to examine various aspects pertaining to such modifications, the kinetics and mechanism of solution polymerization of acrylamide by $FeCl_3$/thiourea system have also been studied. In the present paper, the results of these experiments have been reported and an attempt has been made to identify the pathways through which above modifications are achieved.

Experimental Procedure

Materials

Acrylamide (AM, reagent grade, Fluka) was purified by recrystallization from methanol (two times) and dried in vacuum oven at 45 °C overnight. Thiourea (TU, E.Merck) was used after recrystallization three times from distilled water (m.p. 180°C). A suspension of montmorillonite (MO) having particle size less than 2 micron (diameter) was prepared by sedimentation. Free iron oxides were removed by dithionite-citrate method. Organic matters were removed following method described elsewhere[4]. H^+-montmorillonite (HM) was prepared by shaking the stock of the mineral (3% w/v) in the presence of 0.5 M HCl for about 6 h followed by repeated centrifugation (20,000 rpm) and washing with double distilled water. The cation exchange capacity (CEC) of montmorillonite was determined by potentiometric titration with standard KOH solution under nitrogen atmosphere and was found to be 0.91 meq./g. Fe(III)- montmorillonite (FeM) was prepared by shaking HM suspension (3% w/v) in the presence of 0.5 M $FeCl_3$ (reagent grade) at *p*H 2.5 for 6 h followed by purification by repeated centrifu-

gation and washing with distilled water until the test of Fe(III) ions in the supernatent was negative. A separate experiment on the sorption of Fe(III) on to montmorillonite showed that the maximum intake of Fe(III) ions by HM sample slightly exceeded the CEC value, viz., 0.98 meq/g.

Sorption of TU and AM on montmorillonite

10 mL portions of a 0.5% suspension of HM were placed in a number of pyrex bottles and different amounts of either thiourea or acrylamide were added followed by adjusting the *p*H to 2.0 with dil HCl. The total volume of the suspension was made up to 15 mL in each case by adding the requisite amount of water and were shaken at 30 °C for 4 h to attain equilibrium. The supernatent solutions were then centrifuged (20,000 rpm) and analysed for TU or AM by a Shimadzu UV-vis spectrophotometer at 235 and 195 nm respectively.

Potentiometric measurement

The redox behaviour of Fe(III)-TU and FeM-TU systems were examined by potentiometric titration of either $FeCl_3$ solution or FeM suspension with TU. The electrochemical cells were simple as shown below:

Pt/Fe(III) (or Fe(III)M), Fe(II) (or Fe(II)M)// KCl, $HgCl_2$,Hg/Pt

A stoppered pyrex beaker fitted with nitrogen gas inlet-outlet tubes, Pt-electrode, salt bridge and mechanical stirring arrangements was placed in a thermostat at 50°C. 20 mL $FeCl_3$ solution or FeM suspension was then titrated at *p*H 2.0 with standard thiourea solution under nitrogen atmosphere.

Polymerization

Measured quantities of aqueous solution of AM were added to known amounts of $FeCl_3$ solution or FeM and HM mixtures in well stoppered pyrex bottles under nitrogen atmosphere and were equilibrated at required temperature. Deaerated TU solutions were then added to these solutions and the reactions were allowed to continue for desired time span in absence of any light. Polymerization reactions were stopped by diluting the mixture with chilled water keeping the reaction vessel in ice bath. The mixtures were then centrifuged to remove HM or FeM, if any. The polyacrylamide was precipitated out by adding excess of acetone, washed repeatedly with acetone and dried in vacuum at 40°C for 48 h. Molecular weights of the polymers were determined by viscosity measurement in aqueous 0.1M NaCl solution using a Ubbelohde viscometer and a Mark-Houwink relationship of the type[5,6]:

$[\eta]=9.33\times10^{-3} M^{0.75}$ cc/g.

Results and Discussion

Table 1 shows data pertaining to the aqueous homogeneous polymerization of acrylamide by $FeCl_3$/TU redox initiator. The molecular weight (M_v) of the polymer obtained was ranged between 0.2×10^5–3.6×10^5. The initial rate of polymerization, R_p, was moderately high and ranged between 3×10^{-5}–17×10^{-5} mol $L^{-1}s^{-1}$. At a fixed TU and AM concentrations, all the parameters, viz., R_p, X_L, $[\eta]$ and M_v were decreased with the increase in Fe(III) concentrations of the initiating redox couple. It seems apparent that the Fe(III) ions are not only involved in

Table 1 — The initial rates of polymerization, polymer yields, intrinsic viscosities and the molecular weights of $FeCl_3$/TU initiated polymerization of acrylamide at various conditions

$[FeCl_3]$ mM	[TU] M	[AM] M	*p*H	Temp °C	$R_p\times10^5$ mol $L^{-1}s^{-1}$	X_L [a] %	$[\eta]$ $mL.g^{-1}$	$M_v\times10^5$
1.5					17.2	73	64	1.3
3.0	0.04	0.4	2.01	50	9.4	56	73	1.5
4.0					6.7	40	61	1.2
8.0					4.2	26	45	0.8
	0.01				2.9	40	14	0.2
1.5	0.02	0.4	2.01	50	5.7	53	68	1.4
	0.03				11.9	68	73	1.6
		0.3			8.3	62	60	1.2
1.5	0.04	0.5	2.01	50	20.0	81	96	2.2
		0.6			23.0	77	108	2.6
				45	12.6	68	61	1.2
1.5	0.04	0.4	2.01	60	27.8	75	74	1.6
				70	19.2	86	137	3.6

[a]polymer yield after 4.5 h.

the termination process but also act as retarder in the reaction[7]. Linear termination of aqueous acrylamide polymerization by Fe(III) ions was observed long back in 1957 when aqueous Fe(III) perchlorate caused fast termination of x - and γ-ray initiated polymerization of acrylamide with a rate constant of $1.1\pm0.6\times10^4$ L $mol^{-1}s^{-1}$ (Ref.7). Similar role of other metal oxidants was also observed subsequently.

Effect of AM, TU and Fe(III) concentrations

The rate of polymerization, R_p, as well as the polymer yield (X_L) decrease with the increasing Fe(III) ion concentration in the range of 1.5×10^{-3}–8.0×10^{-3} mol L^{-1}. The value of the metal ion exponent, obtained from the slope of the double logarithmic plot of R_p versus metal concentration is found to be 0.90 (Fig. 3). Thus, the rate is inversely proportional to nearly first power of metal ion concentration. On the other hand, R_p increases with increasing concentration of thiourea. Thiourea alone (in absence of Fe(III) ions) is incapable of initiating polymerization as the control experiment shows. Increasing concentration of the activator (thiourea) in

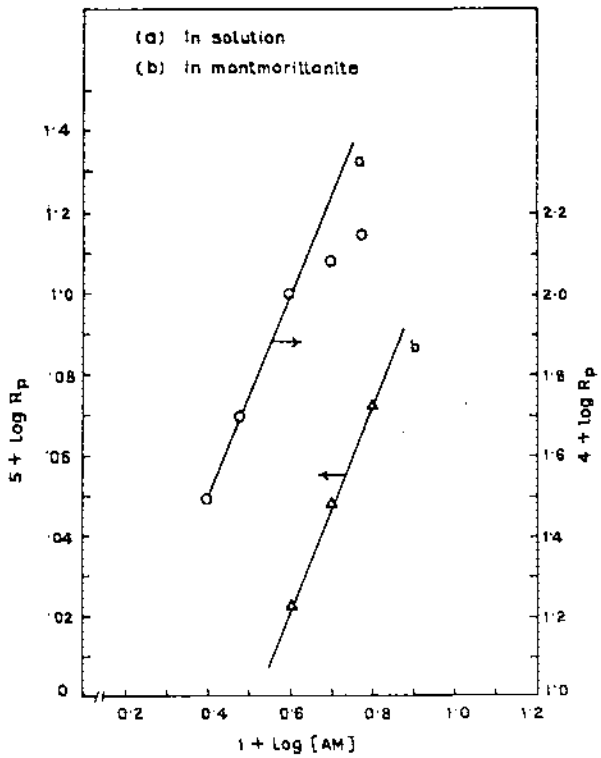

Fig. 1 — Logarithm plots of R_p *versus* [AM] for the polymerization reaction in solution as well as MO phase; $[FeCl_3]=1.5\times10^{-3}$M, [TU]=0.04M and [Fe(III)] $=1.5\times10^{-3}$M.

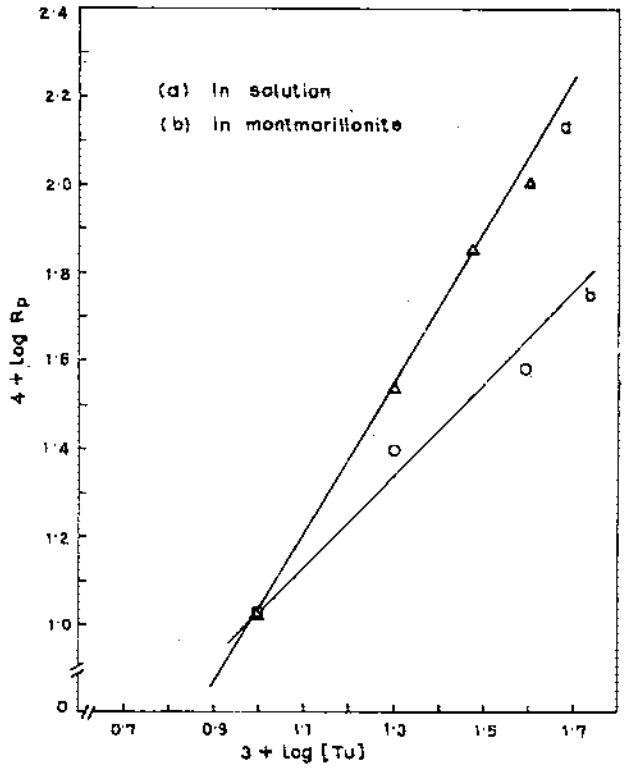

Fig. 2 — Logarithm plots of R_p *versus* [TU] for the polymerization reaction in solution as well as MO phase; $[FeCl_3]=1.5\times10^{-3}$M, [AM]=0.4M and [Fe(III)]$=1.5\times10^{-3}$M.

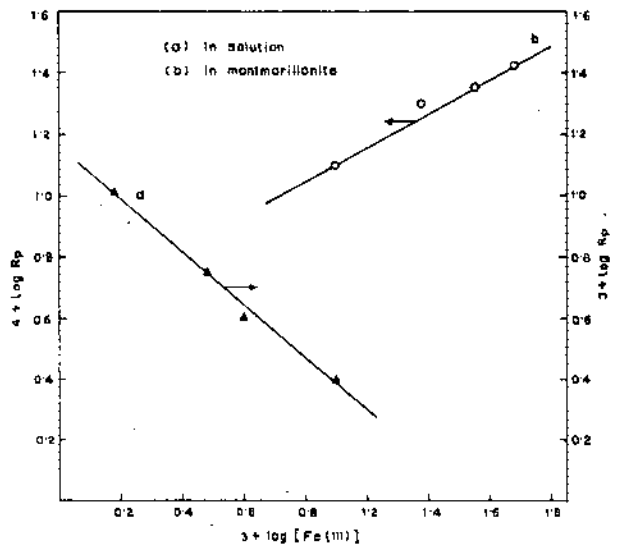

Fig. 3 — Logarithm plots of R_p *versus* [Fe(III)] for the polymerization reaction in solution as well as MO phase; [AM]=0.4M and [TU]=0.04M (for the MO-phase reaction, [Fe(III)] in the figure represents moles of ferric ions in 1000 mL of MO gel).

the presence of Fe(III) ions increases the concentration of the initiating radical and consequently the number of propagating polymer chains and hence the rate of polymerization increases with increasing TU concentration in the range 0.01-0.04 mol L^{-1}. However, at still higher concentrations of TU, R_p as well as X_L tend to decrease considerably due to increase in the rate of termination via dimerization of isothiocarbamido primary radicals (TU)[8]. The value of TU exponent obtained from the slope of the double logarithmic plot of R_p versus TU concentration, is 1.8 (Fig. 2). Thus, the rate of polymerization shows nearly second order dependence on the TU concentration. The dependence of R_p on the monomer concentration is, however, interesting. The initial rate increases with the increase of monomer concentration as expected. The slope of the logarithmic plot of R_p versus concentration of AM is nearly 2.0 (Fig.1) in the range of AM concentration of 0.25-0.40 mol L^{-1}, but tends to decrease (the value becomes 1.0, experimental points shown in Fig.1) in the higher concentration range of (0.4-0.6) mol L^{-1} (explained under kinetics and mechanism). The corresponding plots for the MO gel phase reactions are shown in the Figs 1-3. The data are taken from ref. 3 and reproduced here for comparison.

Effect of temperature

The R_p as well as X_L increase with increasing polymerization temperature. However, the R_p value tend to decrease at temperature above 60°C. The overall energy of activation as calculated from the Arrhenius plot has been found to be 12.4 kcal.mol^{-1} within the temperature range 45-60 °C.

Kinetics and mechanism

In order to rationalize the results, following assumptions are made to predict the mechanism of aqueous homogeneous polymerization of acrylamide by $FeCl_3$/TU system.

1. Isothiocarbamido (TU) primary radicals are formed via an intermediate complex between Fe(III) ions and TU. The decomposition of the complex is the rate-determining step[9,10]

$$\mathrm{Fe(III) + TU} \underset{\text{Complex}}{\overset{K}{\rightleftharpoons}} \mathrm{Fe(III)\text{-}TU} \qquad \ldots (1)$$

$$\mathrm{Fe(III) - TU + TU} \xrightarrow{k_d} \mathrm{Fe(II) + (2TU^{\cdot}) + H^{+}} \qquad \ldots (2)$$

2. Since the reactive TU radicals are formed as pairs, assumption of "cage effect" seems to be conceptually appropriate. The initiation step involves collision of acrylamide molecule with caged TU radicals at the wall of the cage and random diffusion of the radicals from the cage and their secondary recombination are less significant.

Initiation :

$$(\mathrm{TU}^{\cdot}) + \mathrm{M} \xrightarrow{k_i} \mathrm{M}_1^{\cdot} \qquad \ldots (3)$$

Propagation :

$$\mathrm{M}_1^{\cdot} + \mathrm{M} \xrightarrow{k_p} \mathrm{M}_2^{\cdot}$$

$$\mathrm{M}_{n-1}^{\cdot} + \mathrm{M} \xrightarrow{k_p} \mathrm{M}_n^{\cdot} \ldots \ldots \text{etc.} \qquad \ldots (4)$$

Termination :

$$\mathrm{M}_n^{\cdot} + \mathrm{Fe(III)} \xrightarrow{k_t} \mathrm{M}_n + \mathrm{Fe(II)} \qquad \ldots (5)$$

$$(\mathrm{TU}^{\cdot}) + \mathrm{Fe(III)} \xrightarrow{k_t'} \mathrm{TU} + \mathrm{Fe(II)} \qquad \ldots (6)$$

$$(2\mathrm{TU}^{\cdot}) \xrightarrow{k_t''} \mathrm{TU\text{-}TU} \qquad \ldots (7)$$

(Caged species are enclosed in brackets)

Using Eqs (1) and (2), one obtains the consumption rate of Fe(III) concentration as

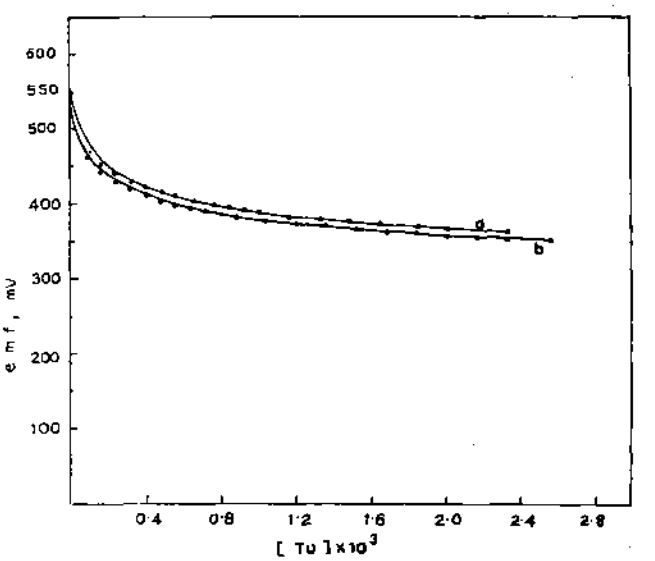

Fig. 4 — Potentiometric titrations of (a) FeM (1.3×10^{-3}M in terms of exchanged Fe(III) per 1000ml of suspension) versus TU; (b) $FeCl_3$ (1.2×10^{-3}M) versus TU.

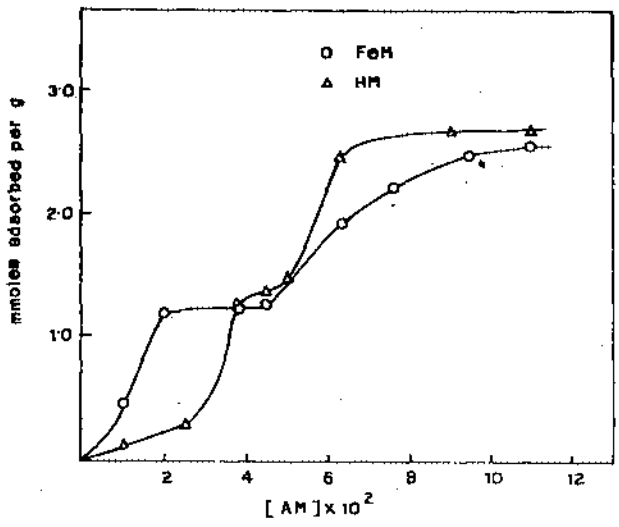

Fig. 5 — Adsorption isotherms of acrylamide on Fe - and H-montmorillonite.

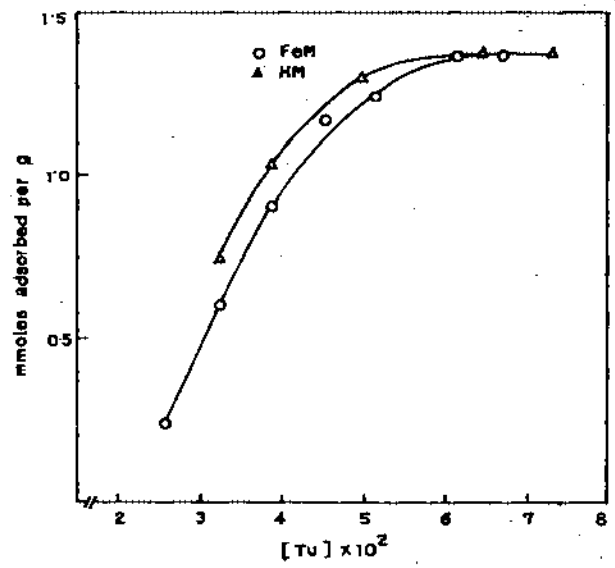

Fig. 6 — Adsorption isotherms of thiourea on Fe- and H-montmorillonite.

Table-2 — The initial rates of polymerization, polymer yields, intrinsic viscosities and the molecular weights of Fe(III)/TU initiated polymerization in montmorillonite phase

Fe(III)[a] mM	[TU] M	[AM] M	*p*H	Temp °C	$R_p \times 10^5$ mol $L^{-1}s^{-1}$	X_L[b] %	$[\eta]$ mL.g^{-1}	$M_v \times 10^5$
1.50	0.04	0.4	2.01	50	4.40	76	369	13.5
2.67	0.04	0.4	2.01	50	6.50	60	291	9.8
1.50	0.01	0.4	2.01	50	1.70	42	487	19.5
1.50	0.04	0.6	2.01	50	9.20	57	480	19.1
1.50	0.04	0.4	2.01	70	6.60	94	220	6.8
1.50	0.04	0.4	2.87[c]	70	—	—	—	—

[a] Concentration of interlayer Fe(III) in mmol. per litre of the reaction mixture (corresponding concentration in MO gel phase is 0.03 mol. per litre of MO gel);
[b] Yield after 4.5h; [c] no polymer formed.

$$-\frac{d[Fe(III)]}{dt} = \frac{k_d K [TU]^2 [Fe(III)]}{1 + K[TU]} \quad \ldots (8)$$

Assuming that the rate of consumption of Fe(III) ions is equal to the rate of formation of TU radicals and a pseudo-steady state approximation to hold, R_p may be shown as follows :

$$R_p = \frac{k_d k_i k_p K [TU]^2 [M]^2}{k_t (k_i[M] + k_t'[Fe(III)] + k'')(1 + K[TU])} \quad \ldots (9)$$

Since the concentration of TU throughout the experiment is low and the value of the equilibrium constant, K is only of the order of 2 L mol^{-1}, the quantity $(1+K[TU])$ in the denominator may approximately be equated to unity. Hence, the Eq (9) is reduced to

$$R_p = \frac{k_d k_i k_p K [TU]^2 [M]^2}{k_t (k_i[M] + K_t'[Fe(III)] + k'')} \quad \ldots (10)$$

Plotting of $[TU]^2[M]^2/R_p$ versus [M] yield a straight line. From the slope and the intercept of the plot the values of $k_t/k_p k_d$ and k_t'/k_i are found as 4.70 and 2.80×10^2 respectively. Reviewing the experimental results it seems apparent that k_t'' in the present homogeneous polymerization is not significant enough in comparison to other terms in the denominator of Eq.(10). Moreover, high value of k_t'/k_i ratio ensures that $k_i[M]$ is also insignificant at low [M] in comparison to the second term in the bracket of the denominator. Thus, Eq. (10) could satisfactorily take account the high monomer exponent as is observed in Fig.1. Deviation of the points from the straight line in the figure as the consequence of high monomer

concentrations is, however, the manifestation of the dominance of first term of the denominator over the other.

Adsorption of AM and TU in MO interlayer space

The adsorption isotherm of Fe(III) ion interaction with montmorillonite exhibit L-type nature, which suggests strong sorbate-sorbent interaction. The maximum saturation corresponds to 0.98 meq/g of the mineral. Most significantly, the redox characteristics of Fe(III) towards TU remains almost unaltered even when Fe(III) ions are adsorbed by the mineral clay montmorillonite. This is evident from the potentiometric titration data of Fe(III) and Fe M by TU solution (Fig. 4). It is thus believed that the same initiating radicals are also involved when Fe(III) ions are trapped between layered spaces of the mineral[3].

Fig.5 shows that the acrylamide molecules readily intercalate from the aqueous solution into the interlayer space of both forms of the mineral, viz., H as well as Fe(III) forms. Both the isotherms are characterized by two plateau regions indicating two-stage intercalation of amide molecules. The first saturation value is nearly 1.25 mmol/g whereas the second one is just nearly double. The bilayer of acrylamide in the internal surface of the mineral seems to play pivotal role in affecting the initiation of polymerization and its mechanism in the layered space as compared to the homogeneous polymerization. In acidic medium, amides may *a priori* accept a proton on either the oxygen or the nitrogen atom. However, both spectroscopic as well as solution studies support the possibility of coming about of the former alternative.[11] Using infrared spectroscopy, Tahoun and Mortland[12] have confirmed that amides predominantly protonate on the oxygen atom in acidic montmorillonite system. In acidic montmorillonite system, hemisalt formation is observed when excess amide is present, i.e., two amide molecules share a proton through a symmetrical hydrogen bond. On the other hand, thiourea is adsorbed in the mineral layer from the aqueous solution giving rise to the isotherm as shown in Fig. 6. The process of removal of water molecules either from the H^+- clay or Fe^{3+} clay to intercalate TU seems almost identical. Unlike acrylamide , the thiourea leads to the monolayer formation only and maximum adsorption capacity is found to be 1.37 mmol/g, which is consistent with that of monolayer of acrylamide.

Polymerization in MO interlayer space

Polymerization mechanism and kinetics both are affected to a great extent due to the occurrence of the reaction in the mineral microenvironment resulting in the significant increase in the molecular weights and intrinsic viscosities of the polymers. Table 2 shows the polymerization data obtained from the reaction under montmorillonite micro-environment. In general, the R_p's are somewhat lower than those obtained in the case of homogeneous polymerization in the absence of any mineral, maintaining the polymer yield (x_L) almost same. The most significant results of loading Fe(III) in the interlayer space of montmorillonite lie in achieving polymers with high molecular weights. The $[\eta]$ value of the polymers formed in the homogeneous conditions ranges between 14-137 $mL.g^{-1}$. In contrast, the $[\eta]$ displayed by polymers formed in the mineral phase is found to vary from 220 to 487 $mL.g^{-1}$ under identical conditions. The M_v as calculated from viscosity data ranged between $(0.68 \times 10^6 - 1.95 \times 10^6$. Unlike homogeneous polymerization, the monomer exponent of R_p remains fixed near 2.3. (Fig. 1, proposed mechanism, however, predicts an exponent of 2.0; the error in experimental data might be due to heterogeneous nature of the reaction mixture[3]). On the other hand, the TU exponent changes from 2 to 1 due to occurrence of the reaction in montmorillonite interlayer space (Fig.2). In order to measure the metal exponent for the reaction in the mineral phase, R_p's were plotted as a function of Fe(III) ion concentration in the montmorillonite gel phase. The slope of the double logarithmic plot was found to be 0.50 at 50°C (Fig. 3). Significant departure from that of homogeneous reaction was also observed in the nature of the above plot. While the linear termination by Fe(III) is prominent in solution phase reaction as is evident from the observed nature of variation of R_p with Fe(III) ion concentration, transfer to Fe(III) is almost controlled in the case of reaction in the layered space. Thus, it is evident that the modification achieved with respect to the kinetics and mechanism of the acrylamide polymerization in the montmorillonite phase stems from a number of factors, viz., (i) instead of collision between a monomer molecule and an initiating radical, a monomer pair is involved in the initiation step (ii) 'cage effect' is prominent in MO phase reaction where the solvent molecules form a potential barrier around the pair of TU radicals to hinder diffusion of

the radicals and favours their recombination (iii) linear termination by Fe(III) is hindered due to location of Fe(III) ions in the interlayer space. Thus, the mechanism of the reaction in the interlayer space of montmorillonite may be shown as follows[3];

Initiation :

$$\overline{\text{Fe(III)}} + \text{TU} \overset{K}{\rightleftharpoons} \underbrace{\overline{\text{Fe(III)}} - \text{TU}}_{\text{Complex}} \quad \ldots(11)$$

$$\overline{\text{Fe(III)}} - \text{TU} + \text{TU} \xrightarrow{k_d} \overline{\text{Fe(II)}} + (2\text{TU}^{\cdot}) + \text{H}^+ \quad \ldots(12)$$

$$(\text{TU}^{\cdot}) + \text{M}_2\text{H}^+ \xrightarrow{k_i} \text{M}_1^{\cdot} + \text{M} + \text{H}^+ \quad \ldots(13)$$

Propagation :

$$\text{M}_1^{\cdot} + \text{M} \xrightarrow{k_p} \text{M}_2^{\cdot}$$

$$\text{M}_{n-1}^{\cdot} + \text{M} \xrightarrow{k_p} \text{M}_n^{\cdot} \quad \ldots \quad \ldots\text{etc.} \quad \ldots(14)$$

Termination :

$$\text{M}_n^{\cdot} + \text{M}_n^{\cdot} \xrightarrow{k_t} \text{M}_n - \text{M}_n \quad \ldots(15)$$

$$(\text{TU}^{\cdot}) + \overline{\text{Fe(III)}} \xrightarrow{k_t'} \text{TU} + \overline{\text{Fe(II)}} \quad \ldots(16)$$

$$(2\text{TU}^{\cdot}) \xrightarrow{k_t''} \text{TU} - \text{TU} \quad \ldots(17)$$

Above scheme of reaction together with psedo-steady state assumption enable one to derive the rate equation as

$$R_p = \frac{k_p (k_d k_i K K' / k_t k_t'')^{1/2} K_{tu}^a (K_m^a)^2 (L_0^a)^3 [\overline{\text{Fe(III)}}]^{1/2} [\text{TU}]_s [\text{M}]_s^2}{(1 + K L_0^a K_{tu}^a [\text{TU}]_s)^{1/2}} \quad \ldots(18)$$

(Subscript 's' refers to solution phase and, k'=apparent protonation constant of AM in MO interlayer space at a fixed pH (or, a formation constant) ; K_{tu}^a=selectivity co-efficient of TU adsorption onto MO; K_m^a=selectivity coefficient of AM adsorption onto MO; L_0^a=total active sites in unit mass of MO)

where the quantity $KL_0^a K_{tu}^a$ $[\text{TU}]_s$ is insignificant compared to unity under present reaction condition and hence can be neglected. The Eq. (18) could satisfactorily explain the behaviour of the Fe(III)-TU initialised acrylamide polymerization exhibited in the aqueous montmorillonite layered space.

Acknowledgement

The authors are thankful to the CSIR., New Delhi, for financial support.

References

1 McCormick C L & Chen G S, *J Polym Sci Polym Chem Ed*, 22 (1984) 3633.
2 Bera P & Saha S K, *Macromol Rapid Commun*, 18(1997) 261.
3 Bera P & Saha S K, *Polymer*, 39(1998) 1461.
4 Jackson M L, *Soil Chemical Analysis* (Prentice Hall of India (P) Ltd., New Delhi), 1973, 168.
5 Francois J, Sarazin D, Schwartz T & Weill G, *Polymer*, 20 (1979) 969.
6 Candau F, Leong Y S, Pouyet G & Candau S, *J Coll Inf Sci*, 101 (1984) 167.
7 Collison E, Dainton F S & McNaughton G S, *Trans Faraday Soc*, 53(1957) 489.
8 Saha S K & Greenslade D J, *Bull Chem Soc Jpn*, 65(1992) 2720.
9 Hsu W C, Kuo J F & Chen C Y, *J Polym Sci Part A Polym Chem*, 31 (1993) 267.
10 Pustelnik N & Soloniewiez, *Chem Anal (Warsaw)*, 21 (1976) 503.
11 Theng B K G, *The Chemistry of Clay-Organic Reactions*, (Adam Hilger, London), 1974, 111.
12 Tahoun S & Mortland M M, *Soil Sci*, 102 (1966) 248.

EUROPEAN POLYMER JOURNAL

Published by Pergamon

An imprint of Elsevier Science Ltd.

Editor-in-Chief
Professor J V Dawkins
Loughborough University
Chemistry Department
Loughborough
Leics LE11 3TU
England
Fax: +44 (0) 1509 223925
E-mail E.PolymerJ@lboro.ac.uk

January 29, 1999

Ref: 196/98

Dr. S.K. Saha,
Department of Chemistry,
University of North Bengal,
Darjeeling - 734430,
INDIA.

Dear Dr. Saha,

I write to follow up my letter dated 6 January 1999 concerning your manuscript entitled:

"Water-Soluble Copolymers of Acrylamide with Diacetone Acrylamide and N-t-Butyl Acrylamide on Aqueous Montmorillonite Surface : Synthesis and Characterisation"

I am pleased to report that this paper is accepted for publication.

Manuscripts, diagrams etc. and proofs are kept in the Editorial Office for a period of one year six months after the above acceptance date. On request we are prepared to return these papers to the author(s) at the end of this period. Thereafter, this material will be destroyed.

Thank you for this contribution to European Polymer Journal.

Could I request that you consider the request on the attached sheet and, if possible, let me have a disk at your earliest convenience.

Yours sincerely,

John Dawkins

Professor J.V. Dawkins

Encs.

Please quote the above reference number in any correspondence

Water-soluble copolymers of acrylamide with diacetone-acrylamide and N-tbutyl acrylamide on aqueous mont-morillonite surface: Synthesis and characterisation.

P. Bera and S.K.Saha
Department of Chemistry
University of North Bengal
Darjeeling-734430, India.

ABSTRACT

The copolymerisation of acrylamide (AM) with N-(1,1-dimethyl-3-oxybutyl) acrylamide (DAAM) and N-t butylacrylamide (N-t BAM) by Fe(III) - thiourea redox initiator has been studied by loading the Fe(III) ions in the interlayer spaces of montmorillonite prior to the polymerisation reaction. The values of $r_1 r_2$ have been determined as 0.43 for the AM : DAAM monomer pair and 0.70 for the AM:N-t BAM pair. The intrinsic viscosities of the copolymers were found to decrease with an increase in the feed composition of DAAM or N-t BAM. The microstructure of copolymers including mean sequence length distribution is predicted for a range of feed compositions through the knowledge of reactivity ratios.

INTRODUCTION

High molecular weight polyacrylamides have found applications as effective flocculants and chemical grouts [1]. Copolymers of acrylamide have shown a number of properties leading to variety of industrial applications including those as water-soluble viscofiers and displacement fluids in enhanced oil recovery [2]. Two of the critical limitations of polyelectrolytes are, however, loss of viscosity in the presence of mono or multivalent electrolytes (viz., NaCl, $CaCl_2$ etc.) and ion binding to the porous reservoir rock substrates. Redox initiated polymerisation is one of the most common method applied in aqueous polymerisation because of simplicity of the technique as well as reasonably high yield and reaction rates. One major difficulty of such a technique is, however, fast termination process via electron transfer to the oxidant of the redox couple. Recently, a novel method has been demonstrated by which the chain growth was enhanced by trapping the metal oxidants in the interlayer space of montmorillonite [3,4]. The later procedure ensures slow termination due to the inability of the growing polymer chain to transfer to the metal oxidant trapped in the layered space.

In the present work, attempts have been made to prepare water soluble copolymers of acrylamide with either N-(1,1-Dimethyl-3-Oxybutyl) acrylamide (commonly referred to as Diacetone acrylamide, DAAM) or N-t butyl acrylamide (N-t BAM) on the montmorillonite surface by interlayer-trapped Fe(III) ions in the presence of thiourea (TU). Importance of the study lie in the fact that (i) the applied technique provides high molecular weight polymer having high intrinsic viscosities and, (ii) atleast one of the above copolymers has already shown some promises by not losing its solution viscosities in the presence of added electrolytes [5]. Characteristics of the copolymers including the reactivity ratios for the respective monomers are determined and the microstructures are predicted.

Experimental Procedures

Materials : Acrylamide (reagent grade, Fluka) was purified by recrystallisation from methanol (two times) and dried in vacuum oven at 45°C for overnight. Thiourea (E.Merck) was used after recrystallisation three times from distilled water (m.p. 180°C). Method of preparation and characteristics of Fe(III)-montmorillonite (FeM) was similar to one as already described [3]. N-(1,1-dimethyl-3-oxybutyl) acrylamide (reagent grade, Fluka) was recrystallised twice from methanol and vacuum dried. N-t butyl acrylamide (reagent grade, Fluka) was used as received.

Polymerisation :

Poly (acrylamide - Co-N-(1,1-Dimethyl-3-oxybutyl) acrylamide

The copolymerisation of AM with DAAM was conducted in aqueous solution at 50°C using 0.5% (W/V) of FeM and 0.04 M of TU couple as initiator. Table-1 lists reaction parameters for four series of reactions in which the ratios of monomers in the feed and reaction times were varied. A specified amount of DAAM dissolved in distilled water was added to the mixture of AM and TU solutions of known concentrations in 100 ml stoppered pyrex bottles under nitrogen. In another set of bottles, known amounts of aqueous FeM suspensions were degassed and, finally added to the former bottles under nitrogen atmosphere. The pH of the final mixture was adjusted at 2.0± 0.1 by dropwise addition of 0.01 M HCl solution, well shaken and immediately placed in thermostatic bath of appropriate temperature. pH adjustment was necessary to ensure the formation of adequate amount of the amido- sulfenyl primary radicals to initiate the copolymerisation reaction [6]. After the designated time interval, the copolymerisation reaction was stopped by diluting the reaction mixture with chilled water, keeping the vessel in the ice-bath and FeM separated by centrifugation (1.5×10^4 r.p.m.). AM-DAAM copolymers was precipitated out by the addition of excess acetone. The copolymers and FeM were washed

separately by acetone and water respectively. The copolymers and FeM were then dried at 60°C under vacuum for 48 hours. Conversions were determined gravimetrically.

Poly (acrylamide-Co-N-tert-butylacrylamide)

Since N-t-butylacrylamide is insoluble in water, the monomer was dissolved in micellar pseudo-phase of nonionic surfactant, Triton-X 100(R). Four series of copolymerisation of acrylamide with N-t-butyl acrylamide with a total monomer concentration of 0.42 M were conducted in aqueous solution at 50°C using 0.50% FeM(w/v) and 0.04M TU as the initiator. Reaction parameters for four series of reactions are given in Table-2. The reaction procedures were the same as those described for the preparation of copolymers of acrylamide with diacetoneacrylamide.

Elemental Analysis

Elemental analyses for carbon and nitrogen of AM-DAAM and AM-N-t BAM copolymers were conducted by RSIC, Chandigarh, India (Table 1,2). The copolymer compositions were calculated based on C/N ratios because of the variability of absolute values due to the hygroscopic nature of the polymers. Elemental analyses were conducted at polymer conversion levels, i.e. low and high, to assess drift in the copolymer composition.

Viscosity Measurements

A series of copolymer solution of different concentrations in aqueous 0.1M NaCl are prepared from the 0.5% stock solution. The time of flow of the solutions and solvent are recorded by Ubbelohde type viscometer placed in thermostatic water bath at 30°C (± 0.2°C) . Specific viscosity (η_{sp}) is calculated from the time of flow data. The intrinsic viscosity (η) value is obtained from the intercept of the plot of η_{sp}/C versus C following the relation,

$[\eta] = \eta_{sp}/C$ Lim C 0 , where C stands for concentration of copolymer solution.

RESULTS AND DISCUSSION

Studies on reactivity ratios : The variation in feed ratios and the resultant copolymer compositions (Table 1 and 2) as determined from elemental analyses were used to calculate the reactivity ratios for the AM-DAAM and AM-N-t BAM copolymer systems. The Fineman - Ross method [7] and Kelen-Tüdos method [8] were employed to determine the monomer reactivity ratios at low conversion polymerisation data. Figure 1 is the Fineman - Ross plot for the copolymer of acrylamide (M_1) and diacetoneacrylamide (M_2). The reactivity ratios r_1 and r_2 for the monomer pair M_1 and M_2 can be determined by

$$F(f-1)/f = r_1(F^2/f) - r_2 \qquad (1)$$

where $f = d(M_1)/d(M_2)$, $F = (M_1)/(M_2)$

The reactivity ratio r_1 was determined to be 0.69 ± 0.03 from the slope and $r_2 = 0.62 \pm 0.05$ from the intercept. However, it is well known that in Fineman-Ross analysis, values of reactivity ratios are dependent on indexing of the monomers. On reversing the indexes of the monomers (i.e., assuming DAAM as M_1 and AM as M_2) the values of reactivity ratios are changed to 6.18 ± 0.17 and 1.06 ± 0.07 for acrylamide and diacetoneacrylamide respectively. Kelen - Tüdos approach was also applied for evaluation of reactivity ratios for the same monomer pair according to

$$\upsilon = r_1\xi - r_2(1-\xi)/\alpha \qquad (2)$$

where $\upsilon = G/\alpha + H$ and $\xi = H/\alpha + H$.

The transformed variables G and H are given by

$$G = \frac{[M_1]/[M_2]\,[(d[M_1]/d[M_2]) - 1]}{d[M_1]/d[M_2]} \qquad (3)$$

$$H = \frac{([M_1]/[M_2])^2}{d[M_1]/d[M_2]} \qquad (4)$$

The parameter α is calculated by taking square root of the product of the lowest and highest values of H for the copolymerisation series. A plot of the data according to the Kelen-Tüdos method is shown in Figure-2. Reactivity ratios were determined for AM : DAAM monomer pair as $r_1 = 0.71$ and $r_2 = 0.61$ respectively. The observed data in the Kelen-Tüdos plot are linear, an indication that these copolymerisation follow the conventional copolymerisation kinetics under a prerequisite that the reactivity of a polymer radical is only determined by the terminal monomer unit [9]. The values of r_1 and r_2 obtained from Fineman-Ross and Kelen-Tüdos treatments for the copolymerisation of acrylamide with diacetone acrylamide on montmorillonite surface are listed in Table 3.

Reactivity ratio studies were also conducted for the copolymerisation of acrylamide with N-t-butylacrylamide using Fineman-Ross (Figure-3) and Kelen-Tüdos (Figure 4) methods. The calculated reactivity ratios are listed in Table 4. Figure 5 shows the composition as a function of the acrylamide in the feed based on the experimentally determined reactivity ratios in the copolymerisation of AM with DAAM and with N-t BAM. The AM-DAAM copolymers with $r_1 r_2 = 0.43$ and the AM-N-t BAM copolymers with $r_1 r_2 = 0.70$ exhibit an opposite tendency toward alternation. Experimental points on the figure are, however, restricted upto 80 mole % of AM in the feed because no copolymer was formed below that value. Previous study on the copolymerisation of AM with DAAM by potassium persulfate[2] initiator showed a variation of r_1 and r_2 values from 0.76 to 0.83 and 0.92 to 0.99 respectively for the different methods applied. The Kelen-Tüdos analysis which is considered more reliable than others, shows that r_1 values for the copolymerisation of AM with N-t BAM are considerably higher than AM-DAAM copolymers, where as, those of r_2 are smaller in the case of AM-N-t BAM than that of the other copolymer.

Copolymer microstructure

The microstructures of the AM-DAAM and AM-N-t BAM copolymers are expected to be important in determining the solution properties of copolymers. As mentioned earlier, observed data follow the conventional coolymerisation equation and the adherence of the data to this equation is an important point in establishing the validity of the statistical microstructure analyses. The statistical distribution of monomer sequences, M_1 - M_1, M_2 - M_2, and M_1 - M_2 may be calculated utilizing equns. (6-8) [10 - 12].

$$X = \phi - 2\phi_1 (1-\phi_1)/\{1+[(2\phi_1 - 1)^2 + 4r_1r_2\phi_1(1-\phi_1)]\}^{1/2} \quad (6)$$

$$Y = (1-\phi_1) - 2\phi_1 (1-\phi_1)/\{1+[(2\phi_1 - 1)^2 + 4r_1r_2\phi_1(1-\phi_1)]\}^{1/2} \quad (7)$$

$$Z = 4\phi_1 (1-\phi_1)/\{1+[(2\phi_1 - 1)^2 + 4r_1r_2\phi_1(1-\phi_1)]\}^{1/2} \quad (8)$$

The mole fractions of M_1 - M_1, M_2 - M_2, and M_1 - M_2 sequences in the copolymer are designated by X, Y and Z respectively. The copolymer composition is ϕ_1 and, r_1 and r_2 are the reactivity ratios, for the respective monomer pairs. Mean sequence lengths, μ_1 and μ_2, can be calculated utilizing equation (9) and (10) with the consideration of compositional drift (10).

$$\mu_1 = 1 + r_1[M_1]/[M_2] \quad (9)$$

$$\mu_2 = 1 + r_2 [M_2]/[M_1] \quad (10)$$

The intermolecular linkage and mean sequence length distributions for the AM-DAAM and the AM-N-t BAM copolymers are listed in Table 5 and 6 respectively (Kelen-Tüdos values of reactivity ratios were used for the calculations). For the series of AM-DAAM copolymers, the mean sequence length of acrylamide, μ_{AM}, varied from 30.03 at an 96.36/3.64 mol ratio of AM/DAAM in the copolymer to 4.01 with a 78.77/21.23 mol ratio. For those compositions, values of μ_{DAAM} were 1.01 and 1.14 respectively. On the other hand, the

AM-N-t BAM copolymers had μ_{AM} value of 62.50 and 7.37 at 98.33/1.67 and 89.42/ 10.58 mol ratios of AM/N-t-BAM respectively. Above values for $\mu_{N\text{-}t\,BAM}$ were 1.01 and 1.11 respectively.

Effect of Feed Composition

The effect of feed composition on intrinsic viscosity of copolymers synthesized at high conversion was studied for both AM-DAAM and the AM-N-t BAM copolymers listed in Table 1 and 2 respectively. Figure 7 illustrates the effect of feed composition on the intrinsic viscosity for each copolymer series. The observed decrease in intrinsic viscosity with increasing diacetoneacrylamide or N-tert-butylacrylamide co-monomer concentrations may be explained by increased crosstermination rates of copolymerisation as compared to the very low rate of termination observed for acrylamide, resulting in the decrease of the overall molecular weight of the copolymers [13, 14].

ACKNOWLEDGEMENT

Authors are thankful to CSIR, New Delhi for financial support.

REFERENCES

1. P.Molyneux. *Water-Soluble Synthetic Polymers: Up date I and II*, Microphile Associates, U.K. (1988).

2. C.L.McCormick and G.S.Chen. *J.Polym. Sci. Polym. Chem.* **22**, 3633 (1984).

3. P. Bera and S.K.Saha. *Macromol.* Rapid Commun. **18**, 261 (1997)

4. P. Bera and S.K.Saha, *Polymer* **39**, 1461 (1998).

5. C.L.McCormick and G.S.Chen. *J.Polym. Sci. Polym. Chem.* **22**, 3649 (1984).

6. S.K.Saha and D.J.Greenslade. *Bull. Chem. Soc. Jpn.* **65**, 2720 (1992).

7. M. Fineman and S.D.Ross, *J. Polym. Sci.* **5**, 259 (1950).

8. T.Kelen and F. Tüdos. *J. Macromol. Sci. Chem.* **A9**, 1 (1975)

9. S.Iwatsuki, A. Kondo and H. Harashina. *Macromolecules* **17**, 2473 (1984).

10. S.Igarashi, *J. Polym. Sci. Polym. Lett.* **1**, 359 (1963).

11. C.W.Pyun. *J. Polym. Sci.* Part A2. **8**, III (1970).

12. H.J.Harwood, *J. Polym. Sci.* Part C. **25**, 37 (1968)

13. W.M.Thomas, in *Encyclopedia of Polymer Science and Technology*, Vol. I, N. Bikales, Ed. Wiley-Interscience, New York, 177 (1964).

14. F.S.Dainton and M. Tordoff. *Trans. Faraday Soc.* **53**, 666 (1957).

Ligends of figures

Fig. 1 Determination of reactivity ratios for copolymerisation of AM(M_1) with DAAM (M_2) by Fineman-Ross method.

Fig. 2 Kelen-Tüdos plot for the determination of reactivity ratios for copolymerisation of AM with DAAM.

Fig. 3 Determination of reactivity ratios for copolymerisation of AM(M_1) with N-t BAM(M_2) by Fineman-Ross method.

Fig.4 Determination of reactivity ratios for copolymerisation of AM with N-t BAM by Kelen-Tüdos method.

Fig. 5 Copolymer composition as a function of feed composition for the copolymerisation of AM with DAAM (curve 1) and AM with N-t BAM (curve 2).

Fig. 6 Effect of feed composition on the intrinsic viscosity of AM-DAAM(O) and AM-N-t BAM (●) copolymers.

Table - I

Reaction parameters for the copolymerization of AM with DAAM at 50°C in Distilled water (Total Monomer concentration = 0.42 M)

Sample number	Monomer concentration in the feed (M)			Reaction time (min.)	Conversion(%)	Elemental Analysis (wt%)		Mol % DAAM in copolymer	[η] $ml.g^{-1}$
	[AM]	[DAAM]	[AM]/ [DAAM]			C	N -		
DAAM-10-1	0.41	0.01	41	90	37.10	41.46	15.03	3.60 ± 0.04	
DAAM-10-2	0.41	0.01	41	150	48.13	41.72	15.15	3.52 ± 0.04	420
DAAM-10-3	0.41	0.01	41	210	54.19	42.62	14.82	5.91 ± 0.04	
DAAM-20-1	0.40	0.02	20	90	23.37	42.08	14.51	6.32 ± 0.08	
DAAM-20-2	0.40	0.02	20	150	31.84	42.03	14.26	7.32 ± 0.09	350
DAAM-20-3	0.40	0.02	20	210	40.54	43.05	14.81	6.54 ± 0.09	
DAAM-30-1	0.38	0.04	9.5	90	6.00	43.47	13.51	12.52 ± 0.20	
DAAM-30-2	0.38	0.04	9.5	150	15.40	43.30	13.52	12.24 ± 0.20	340
DAAM-30-3	0.38	0.04	9.5	210	30.37	44.31	14.11	11.05 ± 0.20	
DAAM-40-1	0.34	0.08	4.25	90	11.10	45.28	12.36	21.22 ± 0.30	
DAAM-40-2	0.34	0.08	4.25	150	6.47	45.25	11.39	27.23 ± 0.40	333
DAAM-40-3	0.34	0.08	4.25	210	7.41	46.23	12.70	20.71 ± 0.30	

Table - 2

Reaction Parameters for the copolymerisation of AM with N-t BAM At 50°C (Total Monomer Concentration = 0.42 M)

Sample number	Monomer concentration in the feed (M)			Reaction time (min.)	Conversion(%)	Elemental Analysis (wt%)		Mol % N-t BAM in copolymer	[η] ml.g^{-1}
	[AM]	[N-t-BAM]	[AM]/ [N-t BAM]			C	N		
N-t-BAM-10-1	0.41	0.01	41	90	27.01	41.16	14.78	6.21 ± 0.08	
N-t-BAM-10-2	0.41	0.01	41	150	35.81	40.32	15.53	1.66 ± 0.04	430
N-t-BAM-10-3	0.41	0.01	41	210	55.61	42.28	15.50	4.57 ± 0.06	
N-t-BAM-20-1	0.40	0.02	20	90	36.27	40.91	15.62	1.31 ± 0.04	
N-t-BAM-20-2	0.40	0.02	20	150	40.78	40.94	15.08	4.15 ± 0.04	415
N-t-BAM-20-3	0.40	0.02	20	210	52.79	42.02	15.07	6.32 ± 0.08	
N-t-BAM-30-1	0.38	0.04	9.5	90	28.58	42.10	14.21	11.42 ± 0.20	
N-t-BAM-30-2	0.38	0.04	9.5	150	31.81	41.11	14.94	5.21 ± 0.05	403
N-t-BAM-30-3	0.38	0.04	9.5	210	34.53	43.58	12.79	24.33± 0.30	
N-t-BAM-40-1	0.34	0.08	4.25	90	28.38	42.35	14.29	11.44 ± 0.20	
N-t-BAM-40-2	0.34	0.08	4.25	150	39.40	41.96	14.30	10.57 ± 0.20	300
N-t-BAM-40-3	0.34	0.08	4.25	210	40.98	43.67	13.10	22.25 ± 0.30	

Table-3

Reactivity Ratios for copolymerisation of AM(r_1) with DAAM (r_2)

Method	r_1	r_2
Fineman-Ross[a]	0.69±0.03	0.62 ± 0.05
Fineman-Ross[b]	6.18 ±0.17	1.06 ± 0.06
Kelen-Tüdos	0.70 ± 0.08	0.60 ± 0.09

[a]M_1 = AM, M_2 = DAAM ; [b]M_1 = DAAM, M_2 = AM

Table-4

Reactivity Ratios for copolymerisation of AM(r_1) with N-t BAM(r_2)

Method	r_1	r_2
Fineman-Ross[a]	1.50 ± 0.10	0.50 ± 0.04
Fineman-Ross[b]	1.39 ± 0.08	0.75 ± 0.06
Kelen-Tüdos	1.50 ± 0.10	0.46 ± 0.04

[a]M_1=AM, M_2=N-t BAM ; [b]M_1=N-t BAM, M_2=AM

Table-5

Structural Data for the copolymers of AM with DAAM

Sample Number	Composition[a] (mole%)		Blockiness[b] (mole%)		Alternation[b] (mole%)	Mean Sequence length		μ_{AM}/μ_{DAAM}
	AM	DAAM	AM-AM	DAAM-DAAM	AM - DAAM	μ_{AM}	μ_{DAAM}	
DAAM-10-1	96.36	3.64	92.78	0.06	7.16	30.03	1.01	29.58
DAAM-20-1	93.61	6.39	87.41	0.19	12.40	15.16	1.03	14.71
DAAM-30-1	87.44	12.56	75.67	0.79	23.54	7.72	1.06	7.29
DAAM-40-1	78.77	21.23	60.05	2.51	37.43	4.01	1.14	3.51
DAAM-10-2	96.46	3.54	92.97	0.06	6.97	30.03	1.01	29.58
DAAM-20-2	92.69	7.31	85.70	0.32	13.98	15.16	1.03	14.71
DAAM-30-2	87.73	12.27	76.21	0.76	23.03	7.72	1.06	7.29
DAAM--40-2	72.76	27.24	50.00	4.47	45.54	4.01	1.14	3.51
DAAM--10-3	94.08	5.92	88.32	0.16	11.51	30.03	1.01	29.58
DAAM--20-3	93.49	6.51	87.17	0.20	12.62	15.16	1.03	14.71
DAAM-30-3	88.94	11.06	78.48	0.60	20.92	7.72	1.06	7.29
DAAM-40-3	79.22	20.78	60.83	2.40	36.77	4.01	1.14	3.51

[a] Calculated from elemental analysis ; [b] Statistically calculated from the reactivity ratios.

Table-6

Structural Data for the copolymers of AM with N-t BAM

Sample Number	Composition[a] (mole%)		Blockiness[b] (mole%)		Alternation[b] (mole%)	Mean Sequence length		$\mu_{AM}/\mu_{N\text{-}t\,BAM}$
	AM	N-t BAM	AM-AM	N-t BAM-N-t BAM	AM - N-t BAM	μ_{AM}	$\mu_{N\text{-}t\,BAM}$	
N-t-BAM-10-1	93.78	6.22	87.84	0.28	11.87	62.50	1.01	61.80
N-t-BAM-20-1	98.61	1.39	97.23	0.01	2.75	31.00	1.02	30.30
N-t-BAM-30-1	88.59	11.41	78.16	0.98	20.86	15.25	1.05	14.52
N-t-BAM-10-1	88.56	11.44	78.10	0.98	20.91	7.37	1.11	6.64
N-t-BAM-10-2	98.33	1.67	96.68	0.01	3.30	62.50	1.01	61.80
N-t-BAM-20-2	95.82	4.18	91.77	0.12	8.11	31.00	1.02	30.30
N-t-BAM-30-2	94.75	5.25	89.70	0.20	10.10	15.25	1.05	14.52
N-t-BAM-40-2	89.42	10.58	79.68	0.84	19.48	7.37	1.11	6.64
N-t-BAM-10-3	95.44	4.56	91.03	0.46	8.82	62.50	1.01	61.80
N-t-BAM-20-3	93.68	6.32	87.65	0.29	12.06	31.00	1.02	30.30
N-t-BAM-30-3	75.62	24.38	56.05	4.80	39.14	15.25	1.05	14.52
N-t-BAM--40-3	77.77	22.23	3.95	3.95	36.55	7.37	1.11	6.64

[a]Calculated from Elemental Analysis

[b]Statistically calculated from Reactivity Ratios.

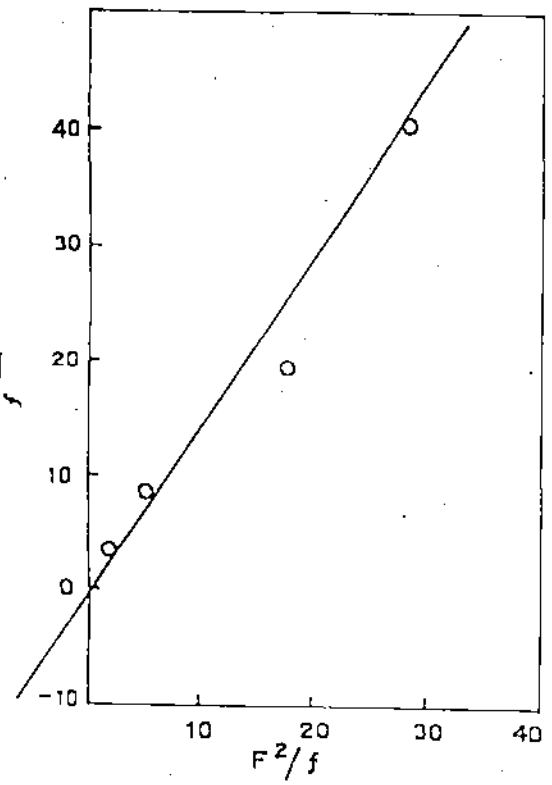

Fig. 3

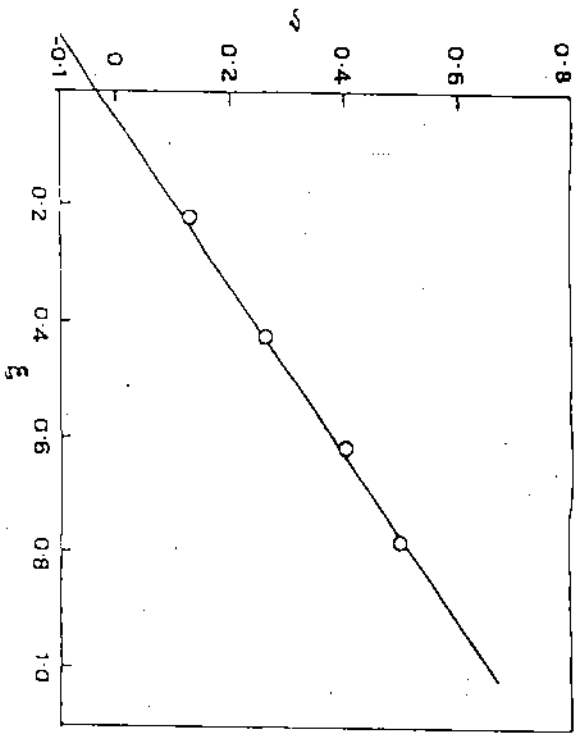

Fig. 2.

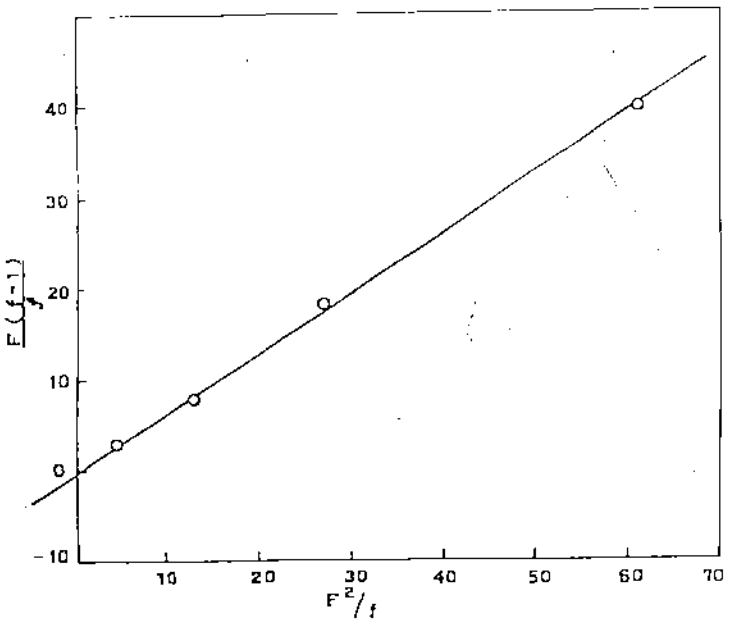

Fig. 1.

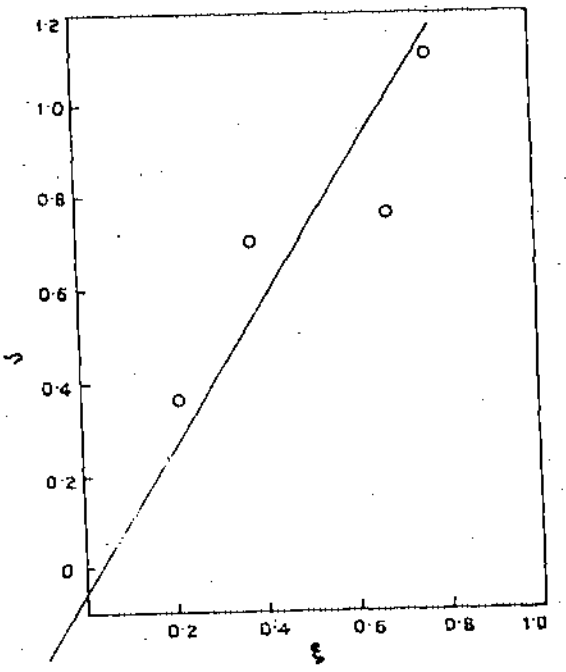

Fig. 4

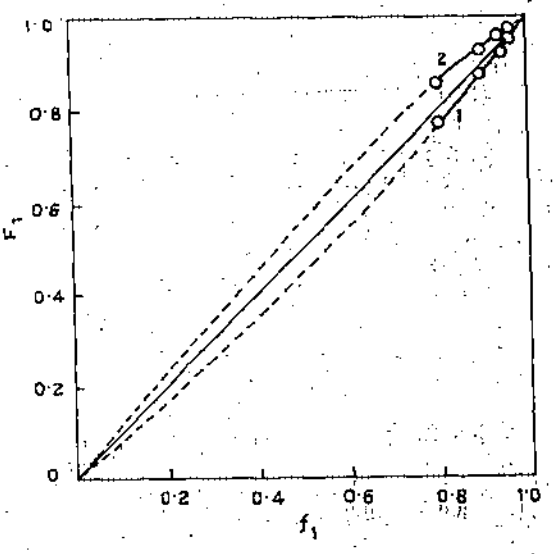

Fig. 5

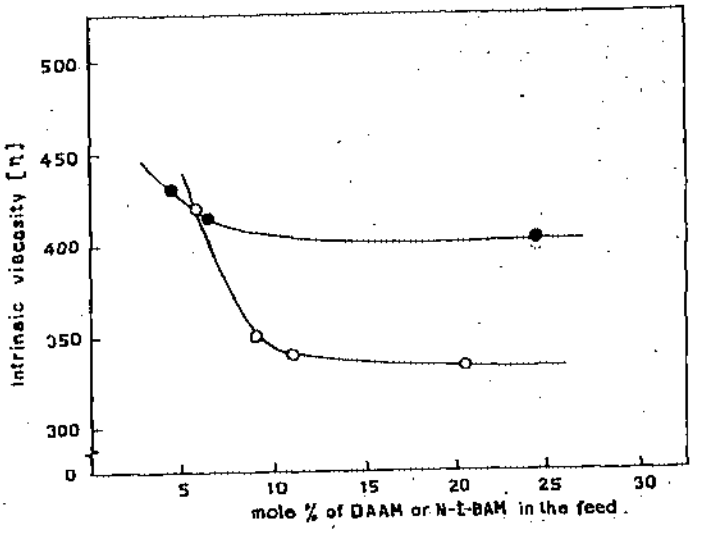

Fig. 6